The role of STAT3 during the Human papillomavirus (HPV) life cycle and in HPV-associated cervical cancer

Ethan Luc Morgan

Submitted in accordance with the requirements for the degree of

Doctor of Philosophy

Astbury Centre for Structural Molecular Biology

School of Molecular and Cellular Biology

The University of Leeds

September, 2018

The candidate confirms that the work submitted is her own and that appropriate credit has been given where reference has been made to the work of others.

Acknowledgement

'Just keep swimming'

Dory, *Finding Nemo*

First and foremost, I would like to give my upmost respect and gratitude to my supervisor, Dr Andrew Macdonald for his continued support throughout my PhD. He has given me the freedom to pursue my own research interests and offered his advice and guidance. His supervision has allowed me to grow as a researcher and his support has given me the best opportunity possible in order to have a successful career in academia.

I also wish to thank my second supervisor, Prof Neil Ranson, who did not end up being involved in my research, for his support in my pursuit of research fellowships towards the end of my PhD.

Many thanks to all of the people who have passed through Garstang 8.53/8.54 over the past four years for making the lab an enjoyable place to work. A big thanks to all members of the Macdonald lab over the years of PhD, with a particular thanks to David Kealy, Gemma Swinscoe, Michaella Antoni and Margarita-Maria Panou for may useful scientific discussion and for making the group what it is. A special mention to Dr Chris Wasson for essentially teaching me science and how to do research – most appreciated!

I would additionally like to thank my Wellcome Trust cohort – Dan Hurdiss, Hugh Smith, Janne Darrell, Anna Higgins and Ieva Drulyte. You guys made the first year bearable!

Finally, I would like to thank my family for all their support over the years. Particularly to my parents, Dean and Jackie Morgan, for their unrelenting support, both emotionally and financially, over the past 8 years. I would not be who I am or where I am without it and I truly appreciate everything you do and have done. I love you both dearly.

To Cate Kendall, for being everything for the past two and half years and making it all worth it. I look forward to my life with you and Frank.

Abstract

Human papillomaviruses (HPV) activate a number of host factors to control their differentiation-dependent life cycles. The manipulation of these host cell signalling pathways can result in the developement of cancer and HPV is responsible for around 5% of all cancers worldwide. Gaining a better understanding of these virus: host interactions is critical for the development of treatments for HPV infection and associated cancers. The transcription factor signal transducer and activator of transcription (STAT)-3 is important for cell cycle progression and cell survival in response to cytokines and growth factors. STAT3 requires phosphorylation on Ser727, in addition to phosphorylation on Tyr705 to be transcriptionally active. Although STAT3 has been shown to be hyperactive in many cancers, including cervical cancer, there is a paucity of information on the role of STAT3 during the productive HPV life cycle and HPV-associated cancers. Utilising a primary keratinocyte system to study the full HPV life cycle, this study demonstrates that STAT3 is essential for the HPV18 life cycle in both undifferentiated and differentiated keratinocytes. Furthermore, the HPV E6 oncoprotein is identified to be sufficient to induce the dual phosphorylation of STAT3 at Ser727 and Tyr705 by a mechanism requiring Janus kinases and members of the MAPK family. Importantly, silencing of STAT3 protein expression by siRNA or inhibition of STAT3 activation by small molecule inhibitors, or by expression of dominant negative STAT3 phosphorylation site mutants, results in blockade of cell cycle progression. Organotypic raft cultures of HPV18 containing keratinocytes expressing a phosphorylation site STAT3 mutant display a profound reduction in suprabasal hyperplasia, which correlates with a loss of cyclin B1 expression and increased differentiation. Finally, increased STAT3 expression and phosphorylation is

observed in HPV positive cervical disease biopsies compared to normal cervical tissue, highlighting a role for STAT3 activation in cervical carcinogenesis. In confirmation of this, STAT3 phosphorylation was demonstrated to be in increased in HPV+ cervical cancer cells when compared to HPV- cervical cancer cells. Detailed mechanistic study identified that this was due to an increase in IL-6 auto/paracrine signalling induce by HPV E6 in an NFκ-dependent manner. Finally, STAT3 was demonstrated to essential for the proliferation, migration and invasion of HPV+ cervical cancer cells. Utilisation of a clinically available inhibitor of JAK2, an upstream kinase for STAT3, also resulted in a similar impairment of proliferation, migration and invasion.

In summary, our data provides evidence of a critical role for STAT3 in the HPV18 life cycle and in HPV+ cervical cancer cells. This suggests a possible therapeutic target for both HPV infection and in the treatment HPV+ cervical cancer

List of Figures

Abbreviations

°C	degrees Celsius
µ	micro
16K	16 kDa subunit of the vacuolar H^+ - ATPase
18E5	human papillomavirus type 18 E5 oncoprotein
18E6	human papillomavirus type 18 E6 oncoprotein
18E7	human papillomavirus type 18 E7 oncoprotein
3'	three prime
3T3 J2	murine fibroblast cell line
4NQO	4-nitroquinolonie 1-oxide
5'	five prime
A or a	adenine
ADAM	disintegrin and metalloproteinase domain containing protein
ADP	adenosine diphosphate
APS	ammonium persulphate
AOM	azoxyymethane
ARS	age standardised rate
ATM	ataxia-telangiectasia mutated
ATR	ataxia telangiectasia and Rad3-related
ATP	adenosine triphosphate
AU	arbitrary units
B-All	B-cell acute lymphoblastic leukaemia
Bap31	B-cell receptor-associated protein 31
BCA	bicinchoninic acid
BCL3	B-Cell Lymphoma 3
bps	base pairs
BPV	bovine papillomavirus
BRCA	breast cancer gene
BRD4	bromodomain-containing 4
C or c	cytosine
c-Cbl	c-Casitas B-lineage Lymphoma
CD151	cluster of differentiation 151
CDK	cyclin-dependent kinase
cDNA	complementary deoxyribonucleic acid
cdt1	chromatin licensing and DNA replication factor 1
CIN	cervical intraepithelial neoplasia
COX-2	cyclooxygenase-2
CR1	conserved region 1
CR2	conserved region 2
CR3	conserved region 3
CRC	colorectal cancer
C-terminus	carboxyl-terminus
CYLD	cylindromatosis
DAPI	4',6-diamidino-2-phenylindole
DBD	DNA-binding domain
ddH_2O	double-distilled water
DMEM	Dulbecco's modified Eagle's medium
DMSO	dimethyl sulphoxide
DNA	deoxyribonucleic acid
DSS	dextran sodium sulphate
DTT	dithiothreitol
DUSP	dual specificity protein phosphatse
DYRK1A	dual-specificity tyrosine phosphorylation-regulated kinase 1A
E	early
e.g.	exempli gratia
E2BS	E2 binding site
E4	E1^E4

E6AP	E6 associated protein
EBV	Epstein Barr Virus
EBNA2	Epstein Barr nuclear antigen 2
ECL	enhance chemoluminescence
EDTA	ethylenediaminetetraacetic acid
EGF	epidermal growth factor
eGFP	enhanced green fluorescent protein
EGFR	epidermal growth factor receptor
EMT	epithelial-mesenchymal transition
ER	endoplasmatic reticulum
ErbB2	epidermal growth factor receptor-related protein 2
ErbB3	epidermal growth factor receptor-related protein 3
ErbB4	epidermal growth factor receptor-related protein 4
ERK 1/2	extracellular signal-regulated kinase ½
EOC	epithelial ovarian cancer
ESCC	oesophageal squamous cell carcinoma
EV	epidermodysplasia verruciformis
EVER1	epidermodysplasia verruciformis protein 1
EVER2	epidermodysplasia verruciformis protein 2
FACS	fluorescence-activated cell sorting
FADD	fas-associaded protein with death domain
FLAG	octapeptide DYKDDDDK
g	gram
μg	microgram
G or g	guanine
GAPDH	glyceraldehyde 3-phosphate dehydrogenase
GFP	green fluorescent protein
GM-CSF	granulocyte macrophage colony stimulating factor
Golgi	Golgi apparatus
Gp130	glycoprotein 130
GSK3	glycogen synthase kinase 3
h	hour(s)
H&E	haematoxylin and eosin
HBV	hepatitis B virus
HCMV	human cytomegalovirus
HCV	hepatitis C virus
HIES	hyper immunoglobulin E syndrome
HEK293TT	Human embryonic kidney 293 TT antigen cells
HEPES	N-2-hydroxyethylpiperazine-N'-2-ethanesulfonic acid
HLA	human leukocyte antigen
HNC	head and neck cancers
HNSCC	head and neck squamous-cell carcinoma
HPV	human papillomavirus
HSIL	high-grade squamous intra-epithelial lesion
IFN	interferon
IgG	immunoglobulin G
IHC	immuno-histochemistry
IL	interleukin
IL-6R	IL-6 receptor
IFN	interferon
IFNAR	interferon-α receptor
IRF	interferon regulatory factor
ISG	interferon stimulated gene
ISGF3	interferon-stimulated gene factor 3
ISRE	interferon sensitive response element
JAK	janus kinase
JH	JAK homology domain
JNK	Jun N-terminal kinase
k	kilo

K_+	potassium ion
kDa	kilo Dalton
KGFR	keratinocyte growth factor receptor
KLF13	Krüpple-like factor 13
KO	knock out
KSHV	Kaposi sarcoma associated herpesvirus
L	litre
LB	Luria-Bertani
LCL	lymphoblastoid cell lines
LCR	long control region
LGL	largw granular lymphocytic leukaemia
LMP1	latent membrane protein 1
log	logarithmic
LSIL	low-grade squamous intra-epithelial lesion
M	molar concentration
m	milli
MAML1 or 3	mastermind-like protein 1 or 3
MAP	mitogen-activated protein
MAVS	mitochondrial antiviral-signalling protein
MEK	mitogen-activated protein kinase kinase
mg	milligram(s)
MHC	major histocompatibility complex
min	minute(s)
miRNA	microRNA
μL	microlitre(s)
mL	millilitre(s)
mM	millimolar
mRNA	messenger ribonucleic acid
mTOR	mammalian target of rapamycin
MS	mass spectrometry
n/a	not applicable
NCOR2	nuclear receptor co-repressor 2
ND	not determined
NES	nuclear export signal
NF-κB	nuclear factor of kappa light polypeptide gene enhancer in B-cells
ng	nanogramme
NHK	normal human keratinocytes
NK	natural killer
NLS	nuclear localisation signal
nm	nanometre
No.	number
nRTK	non-recptor tyrosine kinase
NS1	non-structural 1
NSCLC	non-small cell lung carcinoma
N-terminus	amino-terminus
o/n	overnight
ORF	open reading frame
OSM	oncostatin M
ori	origin of replication
OSCC	oropharyngeal squamous-cell carcinoma
p	probability
PAE	early polyadenylation site
PAL	late polyadenylation site
Pap smear	Papanicolaou smear test
PBS	phosphate buffered saline
PCBP2	poly(rC)-binding protein 2
PCR	polymerase chain reaction
PDGFβ-R	platelet-derived growth factor receptor beta
PDK1	3-phosphoionositide-dependent protein kinase1

PDLIM2	PDZ and LIM containing protein 2
PDZ	post synaptic density protein, Drosophila disc large tumor suppressor, zonula occludens-1 protein
PEI	polyethylenimine
PFA	paraformaldehyde
pH	-log10 concentration of hydrogen ions
PI	propidium iodide
PIAS	protein inhibitor of STAT
PI3K	phosphoinositide-3 kinase
PIN	penile intraepithelial neoplasia
PKC	protein kinase C
PTEN	phosphatase and tensin homologue
PTPR	protein phosphatase receptor-type tyrosine-protein phosphatase
pRB	retinoblastoma-associated protein
PV	papillomavirus
qPCR	quantitative real-time polymerase chain reaction
Ref	reference
rel.	relative
RIG-I	retinoic acid-inducible gen I
RNA	ribonucleic acid
RRP	recurrent respiratory papillomatosis
RT	room temperature
RTK	receptor tyrosine kinase
SCC	squamous-cell carcinoma
SDS	sodium dodecyl sulphate
SDS-PAGE	sodium dodecyl sulphate polyacrylamide gel electrophoresis
sec	second(s)
SFK	SRC family kinase
SH2	SRC homology 2
sIL-6R	soluble IL-6 receptor
siRNA	small interfering RNA
SMAD2	mothers against decapentaplegic homolog 2
SMAD3	mothers against decapentaplegic homolog 3
SOCS	suppressor of cytokine signalling
STAT	signal transducer and activator of transcription
STING	stimulator of interferon genes
SV40	simian vacuolating virus 40
T or t	thymine
TAD	transactivation domain
TBK1	TANK-binding protein 1
TAE	Tris-Acetic acid-EDTA buffer
TAP	transporter associated with antigen processing
TBS	Tris buffered saline
TBST	Tris buffered saline containing Tween-20
TCR	T-cell receptor
TEMED	tetramethylethylenediamine
TGF	transforming growth factor
TLR9	toll-like receptor 9
TRIM	tripartite motif-containing protein
TopBP1	topoisomerase IIβ-binding protein 1
UK	United Kingdom
URR	upstream regulatory region
USA	United States of America
USP	ubiquitin specific protease
UV	ultraviolet radiation
UV B	ultraviolet B radiation
vDNA	viral deoxyribonucleic acid
VEGF	vascular endothelial growth factor
v/v	volume per volume

v-ATPase	vacuolar ATPase
VLP	virus-like particle
w/v	weight per volume
WT	wildtype

Table of Contents

Chapter 1. Introduction

1.1 Papillomaviridae

The *Papillomavirdae* (PV) are an ancient taxonomic family of double stranded DNA viruses that infect almost all mammals and other amniotes such as birds, fish and reptiles (1). A distinctive feature of the PV is their genotype-specific tropism, which is host restrictive, and the preference for certain PV types to infect specific anatomical regions (2). The first papillomavirus was isolated in 1933 in cottontail rabbits (3), with the latest identified from a cervical swab in 2018 (4). Over 300 types of papillomaviruses, including 225 types of human papillomaviruses (HPVs), have been identified to date, and these are arranged in 52 different genera. The classification system used is by the Reference Centre for Papillomaviruses initiated in Heidelberg (5) in 1985, but now managed from the Karolinska Institute. Papillomavirus classification is based on the nucleotide sequence of the gene coding for the L1 capsid protein; HPV that belong to different genera have less than 60% similarity. The most common HPV genera are α-, β-, γ-, μ-genera, with the α- genera having the highest clinical significance (Fig 1.1).

There are currently 5 genera of HPV, split into individual species that share between 60 and 70% similarity (6). Each species comprises of several HPV types that have similar biological properties. The αPV-9 species includes HPV16, 31, 33, 35, 52, 58 and 67. These viruses infect the mucosal epithelium and are associated with malignancies (7) and are therefore often referred to as 'high-risk' HPV types. Infection with the 'low-risk' HPV types, such as HPV6 and 11 of the αPV-10 species, leads to the development of benign legions in the mucosal epithelium. Collectively, these species of HPV are called 'mucosal' PVs, as they infect the mucosal epithelium. PVs that cause legions of the skin, such as HPV49 of the βPV-3 species, are called 'cutaneous' PVs. Although these viruses are mostly linked with the development of

warts (flat, plantar or genital), growing evidence suggests they may also contribute to skin carcinogenesis as a co-factor together with UV irradiation (8,9).

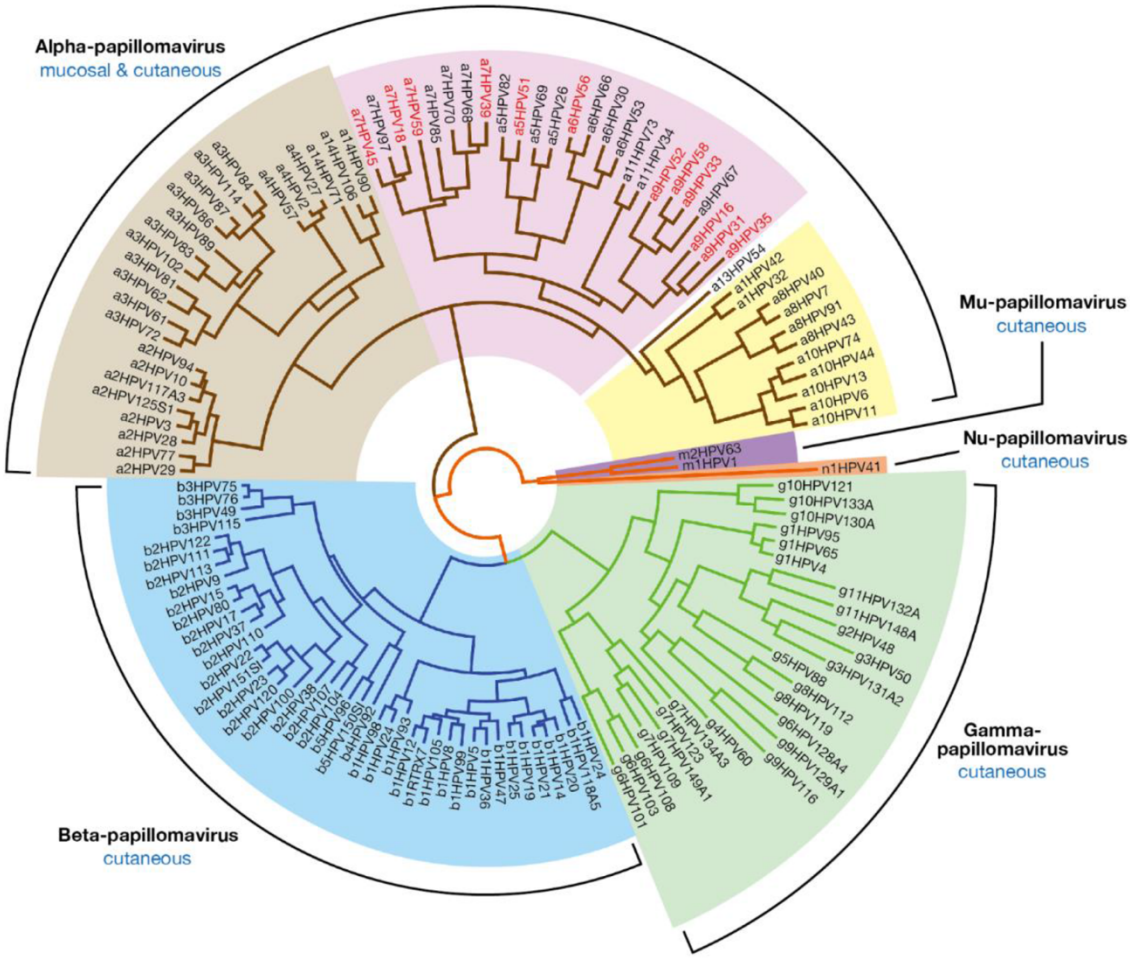

Figure 1.1. Evolutionary Relationship between Human Papillomaviruses. The human papillomaviruses types found in humans; α-, β-, γ-, μ- and ν-. HPV types from the α-PV genus are often classified as low-risk cutaneous (light brown); low-risk mucosal (yellow); or high-risk (pink) according to their association with malignancies. The 'high-risk' types highlighted with red text are confirmed as "human carcinogens" on the basis of epidemiological data. The remaining high-risk types are probable carcinogens.

1.2 HPV Transmission

HPV is the most commonly sexually transmitted disease in the world (10). Infection occurs through micro abrasions in the epidermis of the recipient, most commonly through direct contact with an infected person. Mucosal HPV types are transferred horizontally (i.e. through sexual contact) or vertically (i.e. from other to child), with the primary infection route being sexual contact (11). HPV can also be transmitted *in utero*; the virus can spread through the placenta, amniotic fluid or during delivery (12).

Cutaneous HPVs that cause warts are often spread in children due to the increased frequency of person to person contact and the tendency to have mouth to contaminated surface contact (13). Despite the high rate of infant infection, these are generally cleared with a year.

1.3 HPV associated disease

1.3.1 Cutaneous lesions

The most well studied HPV types that infect the cutaneous epithelia are those of the β-genus (8). These viruses are most commonly associated with the development of planta warts (HPV1, 2 and 4) and flat warts (HPV3, 10 and 49) (14). These warts are characterised by the hyperkeratosis throughout the dermis. Although these viruses establish a persistent infection, the warts are benign and cause relatively minor discomfort to patients, with 80% of cutaneous warts spontaneously resolving.

A rare disorder called Epidermodysplasia verruciformis (EV), which is characterised by an impaired innate immune system due to homozygous mutations in *EVER* genes, results in an increased susceptibility to β-HPV infection (15). This leads to the development of skin lesions and often to squamous cell carcinomas induced by HPV5 and 8 (16). Recent studies have demonstrated that the loss of the *EVER2* gene allows constitutive Protein Kinase C (PKC)α-dependent c-Jun phosphorylation and

this drives HPV5 long coding region (LCR) activation and viral replication (17). This can lead to viral persistence and the potential to develop skin cancer.

Despite little research into the role of the cutaneous HPVs in skin cancer development, the contribution of other HPV species in the β-genus to cancer formation has been demonstrated(8). The E6 and E7 proteins encoded by HPV 49, a β-3 species, have been shown to have similar functionality to the 'high-risk' mucosal HPV types, with co-expression of both HPV49 E6 and E7 able to induce the immortalisation of primary human keratinocytes (18). Furthermore, HPV49 E6 and E7 expressing transgenic mice were highly susceptible to upper digestive tract carcinogenesis upon initiation with 4-nitroquinoline 1-oxide (4NQO) (19). Additionally, expression of HPV 38 E6 and E7 in a transgenic mouse model makes them more susceptible to UV-induced skin carcinogenesis and induces the accumulation of UV-induced DNA mutations (20).

1.3.2 Mucosal lesions

Infections caused by the α-HPV types are much more common than those of the cutaneous HPVs; however, many of these infections are symptomless. The most common anatomical site of symptomatic α-HPV types is the genital mucosa and the oropharyngeal tract; HPV6 and 11 are the most common cause of genital warts (21). However, many of these warts regress and spontaneously resolve within 6 months. Additionally, HPV6 and 11 can also cause Recurrent Respiratory Papillomatosis if they infect the laryngeal mucosa (22). This is a rare medical condition that causes the appearance of benign tumours called papillomas in the aerodigestive tract and this may cause a narrowing of the airways. Although the development of Recurrent Respiratory Papillomatosis is often easily treated; however, in very rare cases the benign legions can turn malignant (23).

HPV13 and 32 are strongly associated with development of focal epithelial hyperplasia or Heck's disease, a rare benign legion of the oral mucosa (24). This is often characterised by multiple whitish or normal coloured papules in the oral cavity and primarily occurs in children, with most cases spontaneously regressing over time.

The 'high-risk' HPV types are the cause of several malignant cancers of different anatomical sites, the most common being anogenital sites and head and neck cancers (2). HPV infection of the mucosal epithelia has been shown to be a contributing factor for cancers of the uterine cervix, penis, vagina, vulva, anus and the oropharynx. The role of HPV in the development of cervical cancer has been the most studied HPV cancer to date, with Professor Harold Zu Hausen winning the Nobel prize for his work in identifying the association of HPV with cervical cancer (25). Currently, there are 13 'high-risk' HPV types associated with cervical cancer – HPV16, 18, 31, 33, 35, 39, 45, 51, 52, 56, 58, 59 and 68 – although HPV16 and 18 account for almost 70% of all cases (2). Most HPV infections of the cervix resolve on their own and pre-cancerous legions often spontaneously revert to normal; however, persistent HPV infections can develop further in to cervical intraepithelial neoplasia (CIN). Although symptomless, progression through the CIN grades from CIN I, abnormal cells of the cervix, to CIN 3, all cells of the cervix are highly abnormal, can result in the progression to invasive carcinoma (2). Cervical cancers are characterised from the anatomical site in which they arise. Cancers that start in the transformation zone of the cervix are squamous cell carcinoma (SCCs), with the other cervical cancer being adenocarcinomas (26).

HPV was first identified as a causal agent in head and neck cancers (HNCs) in 1983 (27)and over the past 15 years, the number of HPV+ HNC has rapidly increased, reaching epidemic levels in the western world (28). HNC are a diverse group of tumours and the role of HPV in HNC is sub-type specific; whilst around 25% of HNC is attributed to HPV infection, 60% of oropharyngeal cancers are associated with HPV infection, in

certain geographical locations. The overwhelming majority of HPV+ HNC are caused by HPV16, with HPV18, 31, 33 and 35 playing a minor role (29).

HPV is also associated with rarer cancers of the anogenital regions; it accounts for approximately 50% of penile cancers, 66% of vaginal cancers, 35% of vulvar cancers and 90% of anal cancers (29). Again, the most commonly associated HPV type in these cancers is HPV16 (29).

1.4 Epidemiology of Papillomaviridae

HPV associated disease has a high impact worldwide, with HPV associated cancers accounting for ~ 5% of all cancers worldwide and having a significant level of morbidity and economic burden, particularly in developing countries (30). The prevalence rate of HPV infection is high, with 80-90% of female adults likely to contract HPV during their life time (31). However, the risk of contracting HPV is much greater for women in Africa and Central American when compared with Europe (32). Furthermore, despite the fact that the burden of HPV-associated cancers is higher in developing countries, the prevalence of HPV infection with 'high-risk' types does not differ greatly.

1.4.1. Epidemiology of HPV malignancies

Cervical cancer is the fourth most common cause of female cancer death worldwide (33). Developing countries account for 85% of all cancer cases (Fig 1.2), with around 50% leading to death. Almost 100% of cervical cancer cases are attributed to HPV infection, with 54% caused by HPV16 and 16.5% by HPV18 (26). HPV infection also accounts for a larger proportion of other female cancers, with ~ 35% of vulvar and 66% of vaginal cancers caused by HPV infection. Additionally, HPV is responsible for over 90/% of anal cancers in both men and women (34). Again, these cancers are much more prevalent in developing countries, likely due to the lack

of contraceptive use and inadequate vaccine programmes (35). Penile cancer is a rare cancer, accounting for only 0.5% of cancers in men. HPV accounts for 50% of all penile cancers. The rates of penile cancer worldwide correlate with cervical cancer and are therefore higher in developing countries (36).

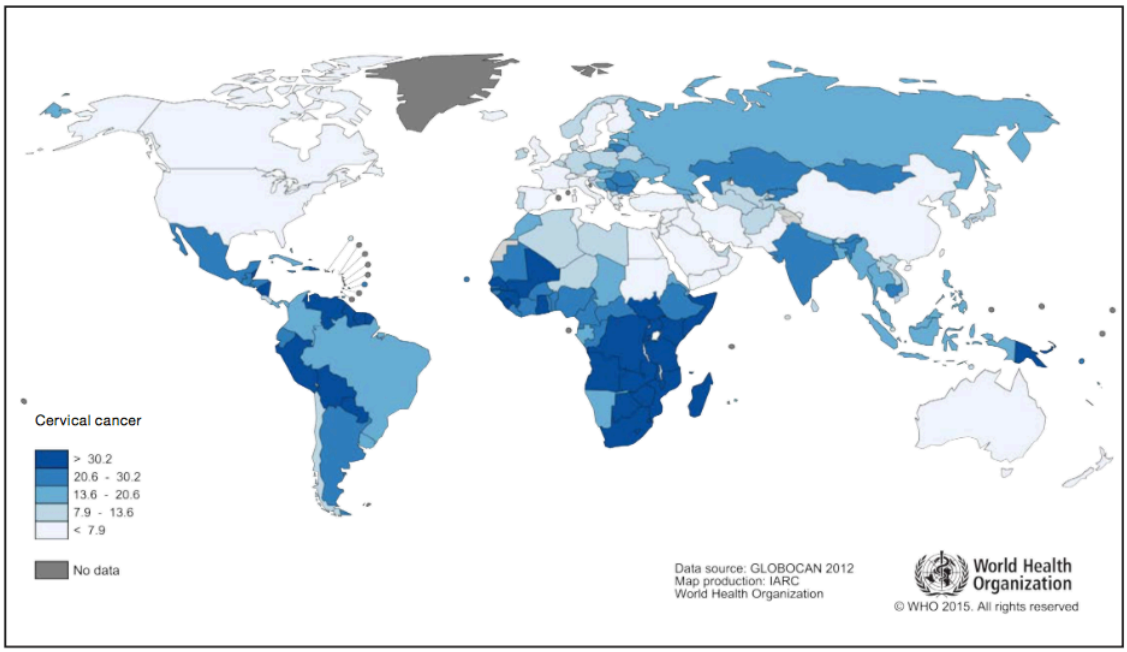

Figure 1.2. Age standardised rate of cervical cancer worldwide. Age standardised rates (ARS) indicated are per 100, 000 women per year. Adapted from WHO and ICO, 2012.

Head and neck squamous cell carcinoma (HNSCC) is the 6th most common cancer worldwide and has been on the rise in the past 20 years (29). HPV- HNSCC are most commonly caused by excessive smoking and drinking, or poor dental hygiene (37). The prevalence of HPV- HNSCC is higher is Asian countries such as China and India, whereas in Europe and the US, HPV+ HNSCC is currently undergoing an

epidemic. In the 1980's, around 20% of HNSCC were associated with HPV infection, whereas today, around 70% are positive for HPV (38).

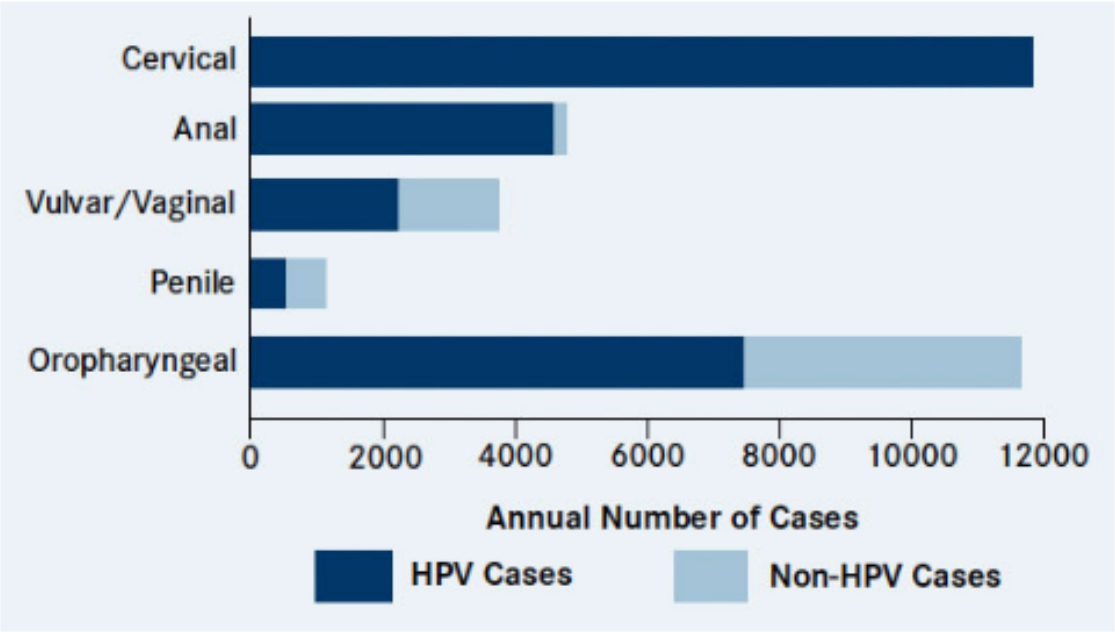

Figure 1.3. The distribution and incidences of HPV and Non-HPV cases in selected HPV associated cancers. The HPV associated cancer cases (dark blue) are contrasted with non-HPV cancer cases (light blue).

1.5 Prevention and treatment of HPV associated disease

There are currently three approved prophylactic vaccines against HPV; all of these vaccines are composed of self-assembled, recombinant L1 major capsid protein as virus-like particles (39). The three vaccines offer protection against different HPV types; Ceravix (GlaxoSmithKline, UK) is a bivalent vaccine and offers protection against the most common HPV types associated with malignancy, HPV16 and 18. Gardasil (Merck, USA), a quadrivalent vaccine, also offers protection against these HPV types but offers additional protection against the 'low-risk' HPV types 6 and 11, the most common cause of genital warts. The most recently developed vaccine, Gardasil 9

(Merck) offers the same protection as Gardasil, but also protects against HPV31, 33, 45, 52 and 58, which account for around 20% of cervical cancers (40).

Since the development of these vaccines, many governments have installed vaccination programmes for young females (41). In the UK, girls aged between 12-13 years old receive the vaccine through secondary education programmes. In July 2018, it was announced that, in the UK, boys in the same age bracket will also receive the vaccine (42). This is likely due to the increase in HPV+ oropharyngeal cancer cases worldwide.

Despite the efficacy of these vaccines, there are several limitations. Firstly, the high cost of these vaccines means that it is difficult to initiate successful vaccination programmes in poorer, developing countries, where cases of HPV infection and associated cancers are highest (43).

Another limitation of these vaccines is that they are not therapeutic and thus are not a treatment option for people already infected with the virus. Currently, there are no specific anti-viral compounds targeting PVs. This means that current treatments for HPV associated disease rely on non-specific approaches that results in many side effect (44). For patients with CIN lesions, clinicians treat the symptoms and not the virus; these include cryotherapy, loop electrosurgical excision and cone biopsies (45). For invasive cervical cancers, hysterectomy or generic chemoradiotherapy treatments are the only options (46). In some HPV associated cancers, such as HNSCC, surgery combined with chemoradiotherapy is also an option (47). In the benign HPV induced lesions, such as genital warts, generic anti-virals such as cidofovir are often used (48). Additionally, genital warts can be treated with cryotherapy (49).

Cervical cancers have shown a steady decline worldwide over the past 30 years (50). This is due to the introduction of cervical screening programmes in many countries.

These screening assays often involve a cytology-based Papanicolaou (Pap) smear test, which detects abnormalities in patients' cells to identify the presence of CIN. If CIN is identified, a small biopsy is taken to check for HPV DNA or RNA (51). These programmes are still not widely used in developing countries; this is mostly due to the cost of initiating country wide programmes and is likely why cervical cancer risk is much greater in these countries (52). Therefore, the current treatment options for HPV infection and associated disease are non-specific and expensive, limiting their used to developed countries. Basic research is still required to identify novel therapeutic targets for HPV infection and malignancies to reduce the burden of these cancers in the developing world.

1.6 Papillomavirus Virology

1.6.1 Genome organisation

Papillomaviruses are small, non-enveloped, double-stranded DNA viruses with a circular genome of approximately 8000 bp packaged into an icosahedral capsid of around 60 nm (7). The genome is comprised of three regions; the early region encodes 6 open reading frames (ORFs) for the E1, E2, E4, E5, E6 and E7 proteins (some papillomavirus types, such as HPV31 and BPV, also encode for an E8 protein (53)) (Fig 1.44A). The late region encodes for the major structural protein L1 and the minor structural protein L2. The upstream regulatory region (URR) or long control region (LCR) contains the origin of replication (*ori*) and binding sites for a number of host transcription factors and several early proteins responsible for the control of viral replication (Fig 1.4A). The HPV18 genome also contains two promoter regions; p105 (p97 in HPV16 and 31), contained upstream of the E6 open reading frame (ORF) in the URR, that facilitates early gene expression, and a differentiation dependant promoter at p811, p765 or p829 (p670 in HPV16 and p742 in HPV31) that is contained within the E7 ORF and this is active during productive viral replication (54).

1.6.2 Papillomavirus life cycle

Productive viral infection requires the proliferation and differentiation of the basal epithelial host cell, the keratinocyte (55); infected cells must remain active in the cell cycle upon cellular differentiation for proficient virus production. Infection requires entry of HPV into the basal epithelial cell layer via microlesions to the skin or mucosa; the tropism of HPV is biased towards keratinocytes in the basal layer of the stratified squamous epithelia (56).

HPV entry is mediated via interactions with a range of putative host cell surface receptors including heparan sulphate proteoglycans and α-6 integrins (57-59) and

the viral major capsid protein L1. Binding of L1 to these receptors leads to exposure of the N-terminus of the L2 protein; L2 is then cleaved by the host protease furin, further exposing a segment of L1 to interact with an unidentified cell receptor (60,61).

The virus can then enter the cell via a range of endocytic routes depending on the specific papillomavirus (62). These include clathrin-mediated or caveolin-mediated endocytosis; however, the 'high-risk' HPV types enter via an endocytic pathway that is clathrin, caveolin, lipid raft, and dynamin independent and instead depends on highly regulated actin dynamics and an association with CD151-containing tetraspanin-enriched microdomains (63,64). Disassembly of the viral capsid is initiated by the acidic endosomal lumen, and L1, L2, and viral DNA traffic via retrograde pathways to the Golgi apparatus and endoplasmic reticulum prior to nuclear entry (65). This trafficking is mediated by direct binding of the retromer complex to L2 (66).

Delivery of the viral genome to the nucleus allows it to be expressed as an autonomous replicating episomal element. Upon nuclear entry, the viral genome is rapidly replicated to between 100-200 copies per cell (2). After initial viral replication, one daughter cell remains in the basal layer to serve as an episome reservoir, while the other daughter cell migrates to the suprabasal layers of the epithelium, where HPV prevents the cell from exiting from the cell cycle. In the suprabasal layers, early viral gene (E5, E6, E7) expression (Fig 1.4B) allows the infected cell to remain in an active cell cycle. This induces viral DNA replication and genome amplification; as the progeny move up the epithelial layer, E4 is expressed alongside the late genes (L1, L2) and capsid proteins are formed in the upper layers of the suprabasal epithelium. The E2 protein recruits the viral genome to sites of virion assembly and this is directed by the L2 minor capsid protein (67,68). This is

followed by viral capsid assembly and virion release, allowing infection of surrounding cells.

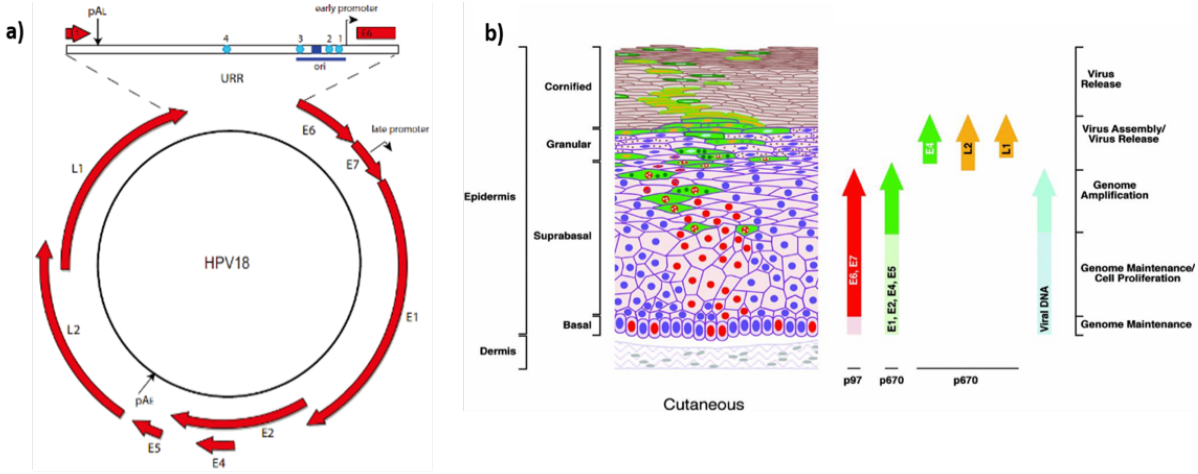

Figure 1.4. HPV genome organization and viral life cycle. A) Organisation of the HPV18 genome, showing the relative positions of the six early genes (E1, E2, E4, E5, E6, E7), the two late genes (L1 and L2) and the upstream regulatory region (URR). Additionally, the early and late promoter regions are shown, as are the E2 (cyan circles) and E1 (blue rectangle) binding sites in the URR (image adapted from (69)). **B)** Schematic of the skin architecture and HPV viral gene expression. Stages of the viral life cycle and viral gene expression at these stages are outlined (70).

1.7 Papillomavirus proteins

1.7.1 E1 and E2 regulatory proteins

The papillomavirus E1 protein is the most conserved viral protein and forms a homo-hexameric DNA helicase (71). It is the only viral protein with enzymatic function and they are highly modulated by the host cell, through phosphorylation, SUMOylation and caspase-dependent cleavage (72). The E1 proteins are highly unstable and are degraded by the ubiquitin-proteasome pathway; the formation of the hexameric structure increases the stability of the protein (73). The E1 ORF is expressed from the early viral promoter (71).

The E1 protein consists of three distinct regions; the regulatory domain at the N-terminus control the nuclear import/export of E1 through a nuclear localisation signal (NLS), which is essential for the control of viral replication (74). Phosphorylation of the NLS by the host kinase cyclin dependent kinase 2 (CDK2) and prevents nuclear translocation of E1 and subsequent DNA replication (75). E1 phosphorylation by mitogen-activated protein kinases (MAPK) Extracellular signal-Related Kinase (ERK) and Jun N-terminal Kinase (JNK) promotes nuclear translocation and thus viral replication (76). The DNA-binding domain (DBD) is adjacent to the N-terminal domain and recognises the viral *ori* site on the LCR(77). The DBD also facilitates the dimerization of E1 proteins (77). Finally, the C-terminal domain contains the helicase domain, consisting of three sub-domains; the adenosine triphosphate (ATP)-binding domain, the oligomerisation domain and the brace domain, which stabilises the homo-hexamer during DNA unwinding (78). E1 helicase activity is required for the establishment of viral genome episome pools upon infection and to promote genome amplification during the later stages of infection. Host modulation of E1 by caspase-dependent cleavage promotes E1-dependent amplification of the viral genome (79).

The E2 protein is an essential viral protein that forms stable homo-dimers in the nucleus (80). Like the E1 protein, E2 proteins contain an NLS and are inherently unstable. Their stability is regulated by phosphorylation and SUMOylation (81). Unusually, the E2 ORF is expressed from both the early and late promoter, depending on the stage of the virus life cycle (82). As E2 is essential for the productive stages of the life cycle, E2 expression from the late promoter results in a higher level of E2 protein expression (83).

The E2 proteins contain three domains; the N-terminal transactivation domain (TAD) plays essential roles in genome replication and the control of viral transcription (82). The C-terminal domain is the dimerization domain and the DBD, which recognises the consensus sequence $ACCN_6GGT$. These two domains are linked by an unstructured, poorly conserved hinge region and this controls nuclear localisation (84).

E2 proteins interact with viral and host cell proteins to establish successful infection and promote viral replication. E2 binding to the minor capsid protein L2 is required to establish initial viral replication (85). E2 also plays the major role in controlling the transcription of viral genes by recruiting the cellular transcriptional machinery to both activate or supress gene transcription. An important role of E2 is the tethering of the viral episomes to mitotic chromosomes to ensure the episomes remain in daughter cells upon cell division; this requires he binding of E2 to bomodomain-containing 4 (BRD4) (86-89). E2 is loaded on to mitotic chromosome by binding to the host cell protein ChlR1 (90). These processes are essential for the maintenance of viral genomes.

Importantly, the E2 ORF is often lost or disrupted during viral genome integration into the host genome. This removes the control of viral transcription by E2, resulting in the

uncontrolled expression of HPV E6 and E7, promoting tumourigenesis (91).

Both the E1 and E2 regulatory proteins are essential for the initiation and maintenance of viral replication upon infection. The viral *ori* site contains palindromic binding sites for E1 and 2-3 E2 binding sites (92); these allow the correct assembly of the E1 hexamer in the correct orientation on the DNA. To initiate replication, the E2 protein first recruits E1 to the *ori* site, forming a ternary complex (72). Conformational changes then result in the ATP-dependant melting of the DNA at the *ori* site (77). The resultant single stranded DNA allows the formation of two E1 hexamers to bind and further unwind the DNA. This allows for the recruitment and binding of host cell DNA replication machinery to the viral DNA, including topoisomerase I {Clower:2006en}.

1.7.2 L1 and L2 structural proteins

The papillomavirus capsid consists of two proteins, the major capsid protein L1 and the minor capsid protein L2 (93). In the mature virion, 360 L1 proteins are arranged into 72 pentameric capsomers alongside an unknown number of L2 proteins, however this may be up to 72 (93). The L1 pentameric capsomers are connected by di-sulphide linkages between cysteine residues; these are highly conserved between HPV types (94).

The entire surface of the virion consists of the L1 protein, with the N- and C-termini facing into the lumen of the virus. This results in the L1 protein facilitating the entry of virions into the host cell via the interaction with heparin sulphate proteoglycans (59,95). This receptor binding induces conformational changes in the virion capsid, exposing the L2 protein and allowing its cleavage by the host protease furin (60,61). Further conformational changes results in the binding of the virion to an as of yet unidentified receptor (96).

After cell entry, the virus traffics through the endocytic pathway, first entering early and then late endosomes (97). Disassembly of the viral capsid is initiated by the acidic endosomal lumen, mediated by L2 (98) and the L2/viral DNA (vDNA) traffics via retrograde pathways to the Golgi apparatus and endoplasmic reticulum prior to nuclear entry. Entry of the virus to the *trans*-golgi network requires the previous cleavage of L2 by furin (61). The trafficking is mediated by direct binding of the retromer complex to L2 (66). The L2/vDNA complex is then trafficked to the nucleus by interacting with the motor protein dynein (99) and entry to the nucleus requires breakdown of the nuclear envelope during mitosis (100,101). Recently, a central region of the L2 protein has been demonstrated to be essential for the tethering of the viral genome and mitotic nuclear entry (101).

Both the L1 and L2 proteins are transcribed from the late viral protein during the productive stages of the virus life cycle(102). Upon the completion of the life cycle, the proteins are expressed in the cytoplasm and L1 is pre-assembled into pentameric capsomers (94). These capsomers, along with L2, are then imported into the nucleus via NLS sequences, and viral assembly occurs.

1.7.3 E4 proteins

The papillomavirus E4 proteins are not well conserved among papillomavirus types and their functions are relatively poorly understood (103). The E4 protein of most papillomaviruses localise to the cytoplasm where, during the late, productive stages of the virus life cycle, they bind to cytokeratins and form fibrous, amyloid-like structures (104). The E4 ORF is part of the early region of the viral genome within the E2 ORF; however, E4 is expressed from the late viral promoter (102). The E4 protein is expressed as a

spliced transcript, containing the initiating codon of the E1 ORF and the whole E4 ORF. The protein, therefore, is also termed E1^E4 (termed E4 here) (105). The functions of E4 are regulated by post translation modification by host cell kinases and proteases (103). Phosphorylation of E4 by the MAP kinase ERK results in the stabilisation of E4 and enhances binding to cytokeratins (106). E4 has also been demonstrated to induce cell cycle arrest in the G2 phase of the cell cycle, promoting viral amplification (107). E4 has recently been shown to enhance E1 nuclear localisation and replication efficiency; this is in a HPV type-dependent manner, with HPV16 being more dependent on E4 functions than HPV18 (108). Additionally, E4 enhances the activation of the MAP kinases p38, ERK and JNK, further enhancing genome amplification (108). The production of infections virions only occurs in cell expressing E4, demonstrating its role in virion production (109).

1.7.4 Papillomavirus oncoproteins E5, E6 and E7

1.7.4.1 E5 oncoprotein

The E5 oncoprotein is the least well understood oncoprotein in human papillomaviruses. Not all papillomaviruses encode an E5 protein: it is, however, expressed in all clinically relevant α– genus HPV types and is the main transforming protein of the carcinogenic Bovine papillomaviruses (BPV) (110). The E5 ORF is located at the 3' end of the early region of the viral genome; however, it is the second ORF present on transcripts from the late viral promoter, suggesting it may play important roles in the differentiation-dependent stages of the viral life cycle (111).

The most studied E5 proteins are from the 'high-risk' HPV types 16 and 31 (112,113) and BPV E5 (110). E5 proteins are integral membrane proteins that localise to the endoplasmic reticulum and Golgi apparatus (114,115). These proteins can induce anchorage independent growth in fibroblasts and are weakly transforming in keratinocytes, suggesting a role in transformation (116). Furthermore, mouse studies have demonstrated that E5 expression results in epithelia hyperplasia and the spontaneous development of tumours (117).

As E5 has no enzymatic activity, it manipulates the host cell through binding to several proteins and modulating their functions (111). A key pathway targeted by E5 is the epidermal growth factor receptor (EGFR) signalling pathway. Mouse studies have demonstrated that the oncogenic potential of E5 is minimised upon inhibition of EGFR (117). The mechanism E5 uses to modulate EGFR and downstream mitogenic signalling is controversial. The initial hypothesis was that the binding of E5 to the 16K subunit of the vacuolar H^+-ATPase inhibited the acidification of endosomes, resulting in reduced EGFR

degradation. However, some groups have demonstrated that the amount of E5 bound to the 16K subunit of the vacuolar H^+-ATPase is insufficient to account for the increased EGFR signalling observed (118). Alternative theories have arisen through the discovery of novel E5 functions. E5 can inhibit the interaction of EGFR with the ubiquitin ligase c-Casitas B-lineage Lymphoma (c-Cbl), resulting in increased receptor cycling to the membrane and prolonged mitogenic signalling (119). E5 expression can also regulate mitogenic signalling independent of the EGFR; E5 expression promotes PKC expression at the cell membrane, resulting in EGF-independent MAPK activation (120).

Additionally, the 'high-risk' HPV E5 proteins have been demonstrated to have channel forming potential and thus can be classified as viroporins (121). The viroporin function of E5 is required for the activation of the mitogenic signalling induced by E5 expression. E5 activity can been inhibited with alkyl-imino sugars and classic ion channel inhibitors such as rimantadine (122); therefore, E5 may be a potential therapeutic target for HPV infection and associated cancer.

Another major function of E5 that contributes to its oncogenic potential is the manipulation of the immune response. A number of E5 proteins have been demonstrated to induce the down regulation of Major histocompatibility class I (MHC I), a key mediator of the adaptive immune response (123,124). This regulation is highly specific as only certain MHC class I alleles, such as HLA-A and -B are targeted. The mechanism E5 uses for the down regulation of MHC I is not fully understood but may involve the retention of MHC class I in the Golgi apparatus (125). This could additionally involve the binding of E5 to B-cell receptor-associated protein 31 (BAP31) and its binding partner A4 (126,127).

In contrast to Human papillomaviruses, E5 is the major transforming protein in BPV (110). The main transforming function of BPV E5 is through modulation of the platelet-derived

growth factor β receptor (PDGFβ-R). BPV E5 dimerises and binds to two PDGFβ receptors, inducing receptor dimerisation and activation. The activation of the receptor is ligand independent and results in the activation of downstream mitogenic signalling (128).

As E5 is not expressed by all papillomaviruses, it is assumed to not be essential for viral infection. During the virus life cycle, E5 is not required by the virus in undifferentiated cells, with no difference in the early maintenance of genome copy number noted upon loss of E5 expression (112,113). However, loss of HPV31 E5 led to a reduced expression of E4 and a reduction in viral transcription from the late promoter and genome amplification in differentiating cells (113), with a subtler effect seen in HPV16 (112). Recently, it has been shown that HPV18 E5 supports cell cycle progression and impairs keratinocyte differentiation by enhancing EGFR signalling, whilst suppressing keratinocyte growth factor receptor (KGFR) signalling (129). Additionally, the viroporin function of E5 is required for the expression of cyclin B1, a key cell cycle protein required for maintenance of the cell cycle in suprabasal keratinocytes, which is essential for viral genome amplification (122). Further studies on the role of E5 during the productive virus life cycle are required to understand the molecular mechanisms involved.

1.7.4.2 E7 oncoprotein

The E7 protein of the 'high-risk' HPV types is the major virus coded transforming protein (130); however, not all papillomaviruses encode an E7 protein. E7 localises primarily to the nucleus of infected keratinocytes but often shuttles between the nucleus and cytoplasm (131). E7 proteins have a flexible N-terminus and a structured C terminus (132); the N- terminus share characteristics of other well known viral oncogenes, simian vacuolating virus 40 (SV40) Large T antigen and the adenovirus E1A

through two conserved regions, CR1 and CR2(133). E7 has also been shown to share some characteristics with polyomavirus small t antigen and can compensate for small t loss in transformation assays when co expressed with Large T (134). The CR2 region contains the LXCXE motif that harbours an essential function of E7; this motif mediates binding to the pocket proteins pRb, p107 or p130 (135). However, residues in CR3 are also required for optimal binding of the pocket proteins (136). The binding of pRb facilitates the release of the transcription factor E2F, which then constitutively activates DNA synthesis and cell proliferation(137). Rb normally binds E2F and inactivates it; 'high-risk' E7 induces the destabilisation and proteasomal degradation of Rb. The 'low-risk' E7 proteins bind pRb with much lower affinity than 'high-risk' E7 proteins as determined by radiolabelled co-immunoprecipitation experiements and this may contribute to their lack of transforming ability {Munger:1989un}. E7 proteins are also phosphorylated at serine residues by casein kinase II in the CR2 domain (138); the binding of Rb and the phosphorylation of E7 by CKII are critical for S phase entry. An additional phosphorylation of E7 by dual-specificity tyrosine phosphorylation-regulated kinase 1A (DYRK1A) at threonine 5 and 7 increases the stability of E7 and thus its transforming potential (139). 'High-risk" E7 can also inactivate the cyclin dependent kinase (Cdk) inhibitors, $p21^{Cip1}$ and $p27^{Kip1}$ (140,141).

Other key transforming activities of E7 include activation of the ataxia-telangiectasia mutated (ATM) protein DNA damage response pathway via STAT5 activation {Hong:2013fh} and this can lead to an increase in genome instability that might promote transformation. Induction of DNA damage can cause an increase in apoptosis; E7 can counteract anoikis, or apoptosis due to lack of cell attachment, by interacting with p600 – this also increases anchorage dependant growth and

contributes to malignant progression (142). E7 also induces chromosomal instability by several mechanisms. Recent work demonstrated that E7 enhances the expression of Chromatin licensing and DNA replication 1 (Cdt1), a DNA replication initiation factor (143). This induces an arrest in the cell cycle at the G2 phase and host cell replication in the absence of mitosis, which induces genomic instability and promotion of viral genome integration.

E7 proteins are also involved in immune evasion strategies employed by HPV. E7 induces the down regulation of the innate immune sensor toll-like receptor 9 (TLR9) through epigenetic regulation (144). Furthermore, E7 binds to the Interferon Regulatory Factor 9 (IRF9), the DNA-binding region of the IFN-stimulated gene factor 3 (ISGF3) complex, disrupting IFN-α signalling (145). E7 can also bind to IRF1, inhibiting IRF-1 mediated activation of the IFN-β promoter (146). In addition to the E5 oncoprotein, E7 can down regulate MHC class I from the cell surface, therefore modulating both the innate and adaptive immune response against HPV (147).

E7 proteins also play a key role during the productive virus life cycle. E7 contributes to the inhibition of keratinocyte differentiation and the maintenance of the cell cycle in suprabasal keratinocytes (148). In addition, E7 inhibits STAT1 phosphorylation and increases STAT5 phosphorylation; these two activities of E7 are required for viral genome amplification upon epithelial differentiation (149,150).

1.7.4.2 E6 oncoprotein

1.7.4.2.1 α-genus E6 proteins

As with the E7 proteins, E6 proteins from the α-genus papillomaviruses are major contributors to transformation (151). The E6 ORF is expressed from the early viral promoter in all papillomaviruses and the protein remains at low levels upon initial infection. The localisation of E6 protein is dependent on the papillomavirus type; 'high-risk' E6 proteins are localised throughout the cytoplasm and nucleus, with 'low-risk' E6 proteins primarily localised to the nucleus (152). The E6 proteins consist of N-terminal and C-terminal zinc binding domains and a helix linker (153). E6 proteins from the 'high-risk' HPV types also contain an eight amino acid PDZ (post synaptic density protein, Drosophila disc large tumour suppressor, zonula occludens-1 protein) binding ligand motif at the C-terminus. The sequence of this PDZ binding motif differs between HPV types and this results in a different affinity of HPV types towards different PDZ containing host proteins (154).

The E6 proteins are only moderately transforming alone; the transforming ability of E6 proteins is greatly enhanced in the presence of E7 (18). Indeed, transgenic mice expressing E6 alone does not result in tumour formation (155). E6 proteins from both mucosal and cutaneous HPV genera recognise and bind host cell proteins containing an acidic leucine rich motif (LXXLL) (156). Recently, a structural study has demonstrated that the LXXLL motif binds to a conserved pocket of E6 (157). One major target of this interaction by the 'high risk' HPV types is the tumour suppressor p53. E6 binds the LXXLL of the host cell E3 ubiquitin ligase E6AP and the subsequent E6/E6AP heterodimer induces the proteasomal degradation of p53 (158). Recent structural work has demonstrated that the binding of the LXXLL motif on E6AP renders the conformation of

E6 able to interact with p53, which is essential for p53 degradation (153). This function of E6 is especially important give that the down regulation of pRb by HPV E7 leads to an increase in apoptosis in infected cells due to reduced growth and an increase in p53 levels. As a further mechanism of p53 functional inhibition, E6 proteins also bind directly to p53 and lead to a block in p53-dependant transcriptional activity by interfering with its DNA-binding activity (159). The 'low risk' HPV types can also interact with E6AP and activate its ubiquitin ligase activity; however, this does not result in the degradation of p53. 'Low risk' HPV type E6 proteins can, however, relocate p53 to the cytoplasm (160). These proteins interact with p300, reducing p53 acetylation and inhibiting p53-dependent apoptosis in response to DNA damage (161). E6 binds to p53 through two distinct E6 binding sites of p53 (162). The binding of E6 proteins to the core of p53 is required for p53 degradation; however, the primary site of E6 is in the C terminus of p53 and is bound by most E6 proteins and thus has no role in p53 degradation. Instead, the 'low risk' HPV type E6 proteins inhibit p53 acetylation, resulting in a reduction in p53 dependent transcription and the induction of pro-apoptotic genes (161). E6 has also been shown to degrade p53 in an E6AP independent manner (163). E6AP deficient mice can still induce the degradation of p53 in the presence of E6, suggesting an E6AP independent mechanism of E6 mediated p53 degradation through an unknown mechanism.

The degradation of p53 results in a deregulation of the cell cycle in infected cells and the promotion of cell proliferation. The 'high risk' HPV E6 proteins can also use other mechanisms to promote cell cycle progression and proliferation; E6 prolongs EGFR signalling by enhancing receptor internalisation, driving downstream mitogenic signalling (164). E6 proteins can also induce eIF4E transcription in order to promote proliferation (165). E6, as with E7, can also inhibit anoikis, in this instance by increasing activation

of the tyrosine kinase FAK, causing phosphorylation and activation of its downstream target paxillin, resulting in cytoskeletal rearrangements that allow proliferation in the absence of cell adherence to the extracellular matrix (166). Another primary function of some 'high risk' HPV E6 proteins is to increase telomerase activity, resulting in increased cell proliferation and survival(167).The mechanism employed by E6 to induce telomerase activation is not fully understood; it occurs independently of p53 degradation and E6AP binding, and interactions with the transcription factor Myc and the transcription factor NFX1-91 are thought to play key roles (168).

The 'low risk' E6 proteins are weak transforming proteins; this is primarily due to their poor efficiency in down regulating p53 function, and the fact that 'low risk' E6 proteins cannot activate telomerase {Klingelhutz:1996js}.

Additionally, E6 proteins from 'high-risk' HPV types that have lost their ability to degrade p53 can still immortalize cells through their interactions with host proteins containing PDZ domains including the putative tumour suppressor proteins Dlg and Scribble (169). Mutation of the residues in E6 necessary for binding to PDZ binding domains within the context of a whole HPV genome leads to reduced host cell growth and loss of viral episomes (170). Recently, a study has demonstrated a striking link between the number of PDZ proteins bound by E6 and the oncogenic potential of the HPV type (154), with the interaction of the host protein Scribble directly correlating with oncogenic potential. Moreover, transgenic mice expressing these E6 mutants are no longer able to develop tumours (170). 'Low risk' HPV E6 proteins do not contain the PDZ binding motif found in the 'high risk' E6 proteins, preventing them from binding to this group of proteins.

E6 proteins also play a role in the inhibition of cell apoptosis. E6 proteins from both 'high risk' and 'low risk', as well as β papillomaviruses, can bind the pro-apoptotic protein Bak; this leads to the degradation of Bak (171). Furthermore, E6 proteins can interact with Fas-associated protein with death domain (FADD) and procaspase 8, preventing downstream apoptotic signalling (172). E6 proteins are also able to modulate the NFκB pathway to promote cell survival and transformation; this is regulated by the ability of E6 to induce the degradation of the deubiquitinase Cylindromatosis (CYLD) in a proteasome dependent manner and is heightened under hypoxic conditions (173). E6 proteins also activate mammalian target of rapamycin (mTOR) (164); this kinase controls cell proliferation in the absence of nutrients and growth signalling. The promotion of mTOR activity by E6 drives downstream signalling through the kinases AKT and 3-phosphoionositide-dependent protein kinase1 (PDK1) to allow continued cell proliferation. Furthermore, the NFκB and B-Cell lymphoma 3 (BCL3) target gene KIAA1199 promotes cell survival through the stabilisation of EGFR and the maintenance of EGFR signalling (174).

In addition to E5 and E7, E6 proteins also play a role in immune evasion; E6 binds to IRF3, inhibiting its transactivation and preventing the transcription of IFN-β (175). E6 proteins also bind to the non-receptor tyrosine kinase TYK2, inhibiting the phosphorylation of TYK2 and the subsequent activation of STAT1 and STAT2 (176). HPV E6 proteins can also bind to Ubiquitin Specific Protease 15 (USP15), a deubiquitinase that is involved in the regulation of tripartite motif-containing protein 25 (TRIM25), an E3 ubiquitin ligase. TRIM25 is important in the activation of retinoic acid-inducible gene I (RIG-I), a pattern recognition receptor (PRR) that sense viral RNA(177). E6 binds to USP15 and TRIM25, increasing TRIM25 ubiquitination and degradation. This results in the suppression of RIG-

I mediated IFN-β induction and the induction of IFN-stimulated genes (ISGs) (177).

E6 proteins are also important during the productive life cycle of HPV. E6 is required for efficient viral genome amplification, as mutant E6 that are deficient in destabilising p53 show a reduction in productive virion production due to a defect in viral genome assembly (170). Additionally, the PDZ binding function of E6 proteins is required for mitotic stability of HPV infected cells and the maintenance of stable viral episomes (178).

1.7.4.2.2 β-genus E6 proteins

The E6 proteins of the cutaneous HPV types of the β-genus share many characteristics with the α-genus E6 proteins, but several key differences do exist. In general, these E6 proteins do not degrade p53. However, HPV38 E6 can supress the transactivation ability of p53. HPV38 E6 increases p53 expression but attenuates its activity through promoting the transcription of the p53 suppressor Δp73 (179,180). Additionally, HPV38 E6 can inhibit p21 induction, a key p53 responsive gene (181). Furthermore, E6 proteins from HPV5, 8 and 38 are able to block p53 stabilisation in the presence of mitotic errors, resulting in continued cell proliferation and an accumulation of cells with polyploidy and aneuploidy, a hallmark of cell transformation (182).

These E6 proteins primarily bind to the LXXLL motif on the transcription co-activator proteins mastermind-like 1 and 3 (MAML1 and 3) of the Notch signalling pathway (183,184). HPV8 E6 also binds to the mothers against decapentaplegic homolog 2 (SMAD2)/SMAD3 transcriptional cofactors of the TGF-β signalling pathway (184). These interactions result in the inhibition of these tumour suppressor pathways and the induction of papilloma formation in infected mice.

The β HPV E6 proteins can enhance the UVB induced carcinogenesis by promoting

p300 degradation, thus reducing ataxia telangiectasia and Rad3-related (ATR) protein expression, which leads to increased thymine dimer persistence and increased UVB induced double stranded DNA breaks (182,185). This degradation of p300 also results in the reduction of Breast Cancer 1 and 2 (BRCA1 and 2), resulting in the attenuation of homology-dependent repair of these double stranded DNA breaks.

In summary, the 'high risk' E6 proteins from the α-genus HPV types are essential proteins that are able to drive cell proliferation, whilst inhibiting detection of the virus by the immune system and inhibiting apoptosis of infected cell induced by expression of the HPV E7 protein. However, various studies have demonstrated that the functions of E6 identified so far cannot account for all of the phenotypes induced by E6 and thus further research is required to identify other mechanism of E6 induced cell proliferation and transformation.

1.8 The STAT Family

The Signal Transducer and Activator of Transcription (STAT) family of proteins were first recognised as ligand induced transcription factors in IFN treated cells (186). Seven family members have currently been identified; STAT1, STAT2, STAT3, STAT4, STAT5a, STAT5b and STAT6. STAT1 and STAT4 map to chromosome 2, bands q12 to q33; STAT3, STAT5a and b map to chromosome 12, bands q13 to q14 and STAT2 and STAT6 map to chromosome 17, bands q11-1 to q22 (187).

The STAT proteins range in size from 750 amino acids to 850 amino acids, but they all share a common domain structure (188). The N-terminal domain mediates the interaction between STAT dimers, leading to the formation of STAT tetramers (189). Adjacent to the N-terminus is a coiled coil domain which is involved in the interaction with other transcription factors and regulatory proteins(189). STAT proteins contain a central DNA binding region which bins the consensus sequence TT(N_{4-6})AA (190). The SRC-homology-2 (SH2) domain binds to the phosphotyrosine of other STAT proteins to mediate dimer formation. The transactivation domain is involved in the transcriptional activation of STAT target genes. This carboxy-terminal domain contains a serine phosphorylation site that enhances transcriptional activity in some STAT proteins (191).

The STAT proteins share a common mechanism of activation through receptor signalling, although the different STATs are activated by different receptors (Fig 1.5). STAT activation was originally identified as being downstream of cytokine signalling, specifically IFN and Interleukin-6 (IL-6) signalling (186). Unlike growth factor receptors, cytokine receptors do not possess kinase activity; therefore, STAT proteins engage with non-receptor tyrosine kinases (nRTKs) bound to activated receptors. The most common nRTKS that are

associated with STAT activation are the Janus Kinase (JAKs) family and the SRC family kinases (SFKs) (192,193). This leads to phosphorylation of the cytoplasmic tail of the cytokine receptors by the nRTKs, presenting a phosphotyrosine site for STAT monomers to bind through their SH2 domains (194). This results in STAT tyrosine phosphorylation by the nRTK, binding of another STAT monomer and STAT dimerisation.

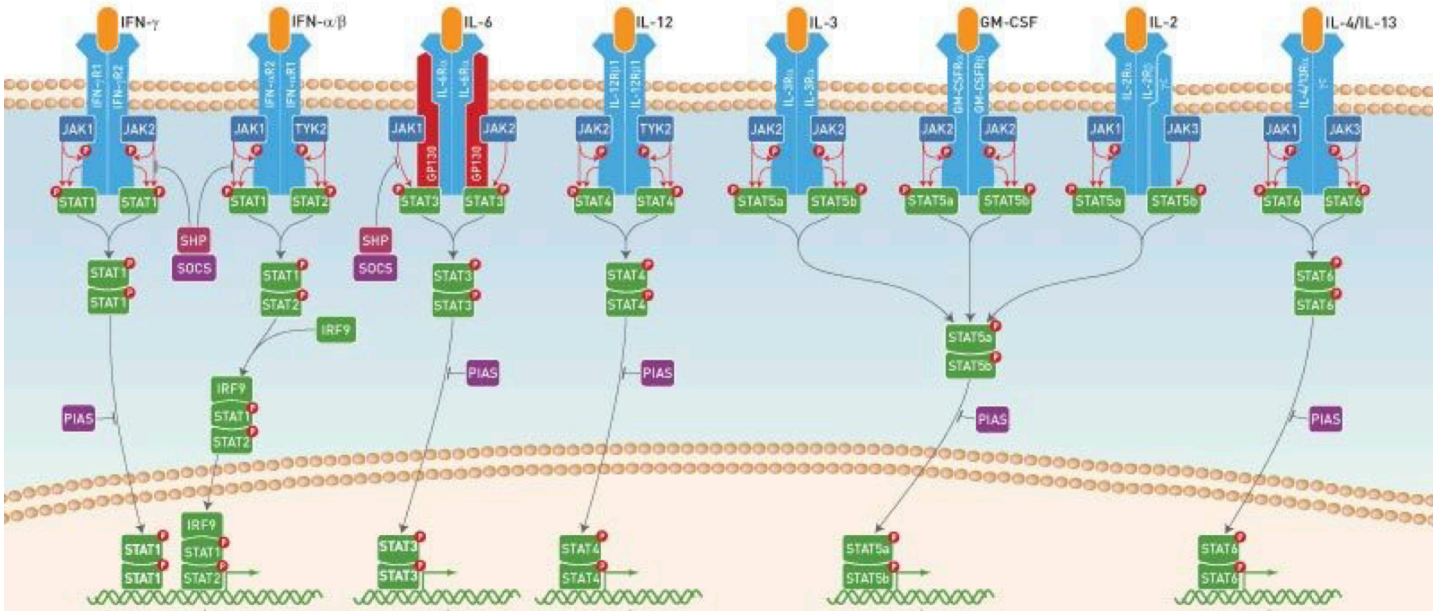

Figure 1.5. STAT activation by cytokine signalling. A) Schematic representation of STAT protein activation by cytokine signalling pathways. The preference for certain STAT proteins for certain cytokine signalling is demonstrated. Adapted from Life Technologies™.

STAT proteins can also be activated by growth factor signalling, in particular EGFR and PDGFR signalling (195,196). In this case, the receptors may also recruit nRTKs and co-operate with them in the phosphorylation of STATs.

1.8.1 STAT1

The STAT1 transcription factor exists in two isoforms; a longer STAT1α and a shorter STAT1β (197). The shorter STAT1 isoform, therefore, contains a shorter transactivation domain and lacks the serine phosphorylation site. The major role of STAT1 is in the IFN-signalling pathway (198); however, STAT1 can also be activated by IL-4, IL-6 and IL-27 (199,200). STAT1 exists as a monomer in the cytoplasm. Upon IFN signalling, STAT1 can homo-dimerise (mostly in response to IFNγ) or hetero-dimerise with STAT2 (mostly in response to IFNα/β) (201). These STAT1 homo-dimers then translocate to the nucleus where they bind to Interferon Gamma Activated Sequence (GAS) promoter elements and drive the expression of key genes involved in the innate immune response, such as IRF1 (202).

STAT1 has many pleiotropic roles other than its canonical function in innate immunity; for example, many studies have demonstrated opposing role in cancer development(203). As a tumour suppressor, STAT1 can promote the expression of pro-apoptotic genes through the activation of p53 dependent apoptosis (204). Additionally, STAT1 promotes the surface expression of Fas/FasL in colorectal carcinoma(205). STAT1 also directly controls the expression of the MHC class I components LMP2 and 7, to promote immunosurveillance in cancer cells (202).

However, several studies have also demonstrated a pro-oncogenic role for STAT1. The activation of STAT1 by IFN results in the expression of pro-inflammatory cytokines and the induction of an inflammatory state (206). The link between inflammation and cancer progression has been clearly demonstrated and STAT1 may contribute to this as many of these processes are STAT1-dependent (203).

Despite the conflicting data on the role of STAT1 in cancer, current data from several

cancers demonstrates that STAT1 activation is inhibited or STAT1 expression is lost (203,207). STAT1 is ubiquitinated and degraded in oesophageal squamous cell carcinoma (ESCC) due to constitutive ERK signalling (208). Furthermore, the STAT1 promoter is often methylated in HNSCC (207). The upregulation of negative regulators of STAT1 is also increased in some cancers; Src homology region 2 domain-containing protein 2 (SHP2) expression is increased in HNSCC and loss of SHP2 expression results an increase in cytotoxic T lymphocyte recognition (209,210). Another mechanism of STAT1 inhibition in cancer is the aberrant activation of STAT3. STAT1 DNA binding can be directly inhibited by active STAT3 as they bind to similar GAS binding sites. Conversely, activated STAT1 has been shown to increase apoptosis by inhibiting STAT3 function in HNSCC (211). These data suggest a reciprocal relationship between these two STAT proteins that may have consequences in cancer biology.

1.8.2 STAT2

The STAT2 transcription factor is only activated by type 1 IFN isoforms (IFN-α, -β, -τ and -ω) (212). STAT2 hetero-dimerises with STAT1 upon activation by IFN signalling (197); the role of STAT1-independent, STAT2-dependent signalling is not clear, but STAT1 deficient mice showed that STAT2 still supported the induction of ISG expression (213). STAT1/STAT2 hetero-dimers then bind to IRF9, forming the IFN Stimulated Gene Factor 3 (ISGF3) complex (214). ISGF3 complexes then translocate into the nucleus where they bind to the promoter of ISGs through an IFN Sensitive Response Element (ISRE), with DNA binding mediated by STAT1 and IRF9 (215). STAT2 is responsible for the recruitment of co-activators, such as p300 and pp32, through its TAD (216,217).

STAT2 is essential for the function of type I IFN signalling: STAT2 deficient mice had a compromised anti-viral response and were vulnerable to viral infection (218). A

recent study also demonstrated that STAT2 deficiency resulted in vaccine-derived measles dissemination in a child (219).

The role of STAT2 in tumourigenesis is poorly understood. STAT2 deficient mice expressing an IFN-α transgene died prematurely with neuroblastoma development and over expressed IFN-γ (220). Additionally, STAT2 loss in an azoxymethane (AOM) / dextran sodium sulphate (DSS) colorectal carcinogenesis mouse model resulted in increased survival and less chronic inflammation (221). This was likely due to the decrease in pro-inflammatory cytokine production, such as IL-6 and CCL2, resulting in decreased STAT3 activation.

1.8.3 STAT4

Unlike most STAT proteins, which are ubiquitously expressed, STAT4 expression appears to be limited to lymphoid, myeloid and testis tissue (222). The most well characterised function of STAT4 proteins are as key regulators of T cell function in the adaptive immune response (223) STAT4 is most prominently activated by IL-12 signalling but can also be activated by IL-23 and type I interferons, resulting in homo-dimerisation (222). STAT4 is essential for IL-12 function; STAT4 knock out mouse fail to induce IFN-γ or enhance natural killer (NK) cell cytolytic function, a key function of IL-12 signalling (224). Additionally, IL-12 is essential for the correct development of T_h1 cells and a T_h1 immune response; STAT4 is also essential for this function of IL-12 (223). This leads to an increased number of parasitic infections, as a functional T_h1 response is essential to combat these infections (225). STAT4 also plays a role in the production of IFN-γ in response to viral infection, which works in concert with the generation of cytotoxic T cell to control the infection (226). Due to the defect in the immune response upon STAT4 loss, many autoimmune diseases are associated with STAT4. Polymorphisms in STAT4 have been demonstrated to be

associated with the development of both rheumatoid arthritis and systemic lupus erythematosus (227,228). Recently, STAT4 has been implicated in cancer development (229,230). In epithelial ovarian cancer (EOC), STAT4 is essential for the induction of metastasis and epithelial-mesenchymal transition (EMT) and is required for the induction of Wnt signalling (229).

1.8.4 STAT5a and STAT5b

STAT5 exists as two separate proteins, STAT5a and STAT5b, transcribed from two different genes, unlike STAT1, which is two isoforms. These proteins share 94% homology but are transcribed from different genes (231). STAT5b is a smaller protein, with 20 fewer amino acids in the TAD. The STAT5 proteins are most commonly activated through JAK2 phosphorylation in response to IL-2, IL-3 and Granulocyte Macrophage Colony-Stimulating Factor (GM-CSF) signalling (232). This results in the formation of STAT5 homo-dimers. Occasionally, STAT5:STAT3 heterodimers form, particularly in repose to GM-CSF signalling, and these are required for the binding of particular consensus sequences (233).

The mechanism of STAT5 transcriptional activation is poorly understood. The STAT5 TAD binds to several co-activators such as p300 (234); however, STAT5 can also bind to transcriptional co-repressors such as Nuclear Receptor Co-repressor 2 (NCOR2) (235). Like STAT4 and STAT6, much of the information on the biological functions of STAT5 have come from studies in immune cells. Mice in which both STAT5 genes were knocked out produced defects in both T and B cells (236). Furthermore, the T cell proliferative response to T cell receptor (TCR) activation was lost and responses to IL-2 were also abrogated (237). Additionally, mice that expressed constitutively active STAT5b through

T cell and B cell development exhibited increased number of pro-B cells, $CD4^+$ regulatory T cells and $CD8^+$ memory T cells (238). Therefore, expression of a constitutively active STAT5b was not the polar opposite of the STAT5a and b knockout mouse. STAT5 also plays a key role in T_h2 development; over expression of active STAT5 skews the differentiation toward T_h2 development (239).

STAT5 also plays a role in the anti-viral response; mice in which STAT5 cannot form higher order tetramers suggests that the formation of these tetramers is essential to mount a robust increase in the proliferation of $CD8^+$ T cells and thus clear viral infections(240,241).

Constitutive STAT5 activation has been identified in several cancers, particularly in haematopoietic cancers(242). A constitutively active mutant of STAT5a was able to efficiently transform haematopoietic cell lines (243). Further, STAT5a activation in myeloma and lymphoma is required for the oncogenicity of the TEL/JAK2 fusion oncogene(244). STAT5 mediates the transforming ability of the Bcr-Abl fusion gene (245). Additionally, STAT5 may play a role in the tumourigenesis of solid cancers, such as HNSCC (246) and prostate cancer (247). Recently, EMT has been shown to be a determinant of EGFR inhibitor sensitivity in HNSCC. STAT5 activation correlates with the expression of certain EMT markers in these cancers and subsequently HNSCC cell with high levels of STAT5 activity are also less sensitive to EGFR inhibition (248)

1.8.5 STAT6

Like STAT4, most of the work to date on STAT6 has derived from its involvement in immune cell responses, having been first identified in B cells (249). STAT6 can exist as one of three isoforms – STAT6a, STAT6b and STAT6c. STAT6a and b have been

demonstrated to have similar biological properties; STAT6c acts as a dominant negative for of STAT6 due to a disrupted SH2 domain (250).

Classic STAT6 activation is mediated by IL-4 and IL-13 signalling (251). Activation of STAT6 results in homo-dimerisation and nuclear translocation. Additionally, STAT6 can be activated by IL-3; however, this only occurs in IL-3 dependent cells (252). Furthermore, IL-15, known for its ability to perform some IL-2 related functions in T cells and NK cells, can induce STAT6 tyrosine phosphorylation through TYK2 activation, although less potently than IL-4 (253).

The transactivation function of STAT6 requires its ability to bind to several co-activators, including p300, C/EBPβ and p100 (234,254,255). The main role of STAT6 is mediating the biological functions of IL-4 and IL-13. IL-4 is the predominant determinant of T cell differentiation to T_h2 cells; this almost exclusively occurs via STAT6 (256). STAT6 is additionally a key regulator of MHC class II induction by IL-4 (257).

More recently, STAT6 has been demonstrated to be essential for the anti-viral innate immune response. Virus induced STAT6 activation occurs through the adaptor protein Stimulator of Interferon Genes (STING) and TANK-binding protein1 (TBK1) upon DNA virus stimulation, or Mitochondrial antiviral-signalling protein (MAVS) upon RNA virus stimulation; STAT6 knockout mice are much more susceptible to viral infection (258) The role of STAT6 in cancer development is currently poorly understood. However, studies have shown that STAT6 is over expressed in both prostate cancer (259) as well as a number of blood cancers (260,261).

1.8.6 STAT proteins in HPV infection and associated disease

Several of the STAT family members are modulated by HPV, either during the virus life cycle or in HPV associated disease. STAT1, as an essential part of IFN signalling in the

anti-viral response, is targeted by HPV in order to evade the immune response (262). Early work demonstrated that the presence of the HPV31 genome in keratinocytes resulted in the downregulation of STAT1 protein expression and IFNα or IFNγ failed to induce STAT1 expression in HPV31 containing keratinocytes (149). Further studies demonstrated that the HPV16 E6 protein downregulates STAT1 protein expression and its binding to ISREs through modulating its nuclear translocation (263).

During the productive viral life cycle, HPV16 and 31 also reduce the expression of STAT1, but not STAT2; this is due to transcriptional down regulation of STAT1 mRNA expression (149). Re-introduction of STAT1 in HPV containing keratinocytes inhibits viral genome amplification and stable expression of STAT1 reduces episome maintenance (149).

HPV18 E6 is also able to inhibit the activation of ISGF3 by binding to the nRTK TYK2; the binding of HPV18 E6 to TYK2 impairs its ability to bind to the IFN-α receptor 1 (IFNAR1), resulting in the reduction of STAT1 and 2 phosphorylation and activation of ISGF3 (176). Interestingly, the 'low risk' HPV11 E6 does not share this function and the effect of HPV18 E6 is specific to IFN-α as signalling after treatment with IFN-γ is not affected (176).

The STAT5 proteins have been extensively studied during the HPV productive life cycle and have essential roles in viral genome amplification (150). STAT5 was first identified as being necessary for the induction of the ATM DNA damage pathway. The ATM pathway was previously identified as being essential for genome amplification (150); STAT5b phosphorylation is induced by the HPV31 E7 protein and this is required for the activation of ATM activity. Importantly, the authors showed that inhibition of STAT5 using the specific small molecule inhibitor pimozide resulted in a reduction in viral genome amplification, suggesting a potential therapeutic target for viral infection. Further work demonstrated that STAT5 was also required for activation of the ATR pathway during the HPV life cycle; this

was through the regulation of Topoisomerase IIβ-binding protein 1 (TopBP1) transcription (264). Recently, the transcription factor Krüppel-like factor 13 (KLF13) was demonstrated to be essential for the phosphorylation of STAT5 and activation of the ATM pathway in HPV31 containing keratinocytes (265). These studies demonstrate the essential role of STAT5 during the productive HPV life cycle; however, the role of STAT5 in HPV mediated cancers remains poorly understood. The chemokine CCL17 has been identified as a regulator of cervical cancer cell proliferation and this is partially dependent on STAT5 activity(266). Furthermore, treatment of cervical cancer cells with IL-2 stimulates their proliferation and this may be attributed to increased STAT5 phosphorylation (267). However, more studies are required to confirm a role for STAT5 in HPV associated cancer.

1.9 STAT3

1.9.1 STAT3 structure

STAT3 was first discovered as an IL-6 responsive factor with DNA-binding activity in hepatocytes (268). Structurally, STAT3 is similar to the other STAT proteins and the crystal structure of various forms of STAT3 have been identified (Fig 1.6) (189,269,270). STAT3 exists as two isoforms, STAT3α and STAT3β, that occur due to different splicing of the *stat3* gene (271). These isoforms differ in their TAD, with STAT3β containing a smaller TAD; the functional difference between these isoforms remains controversial and remains poorly characterised, but STAT3β may act as a dominant negative isoform (271).

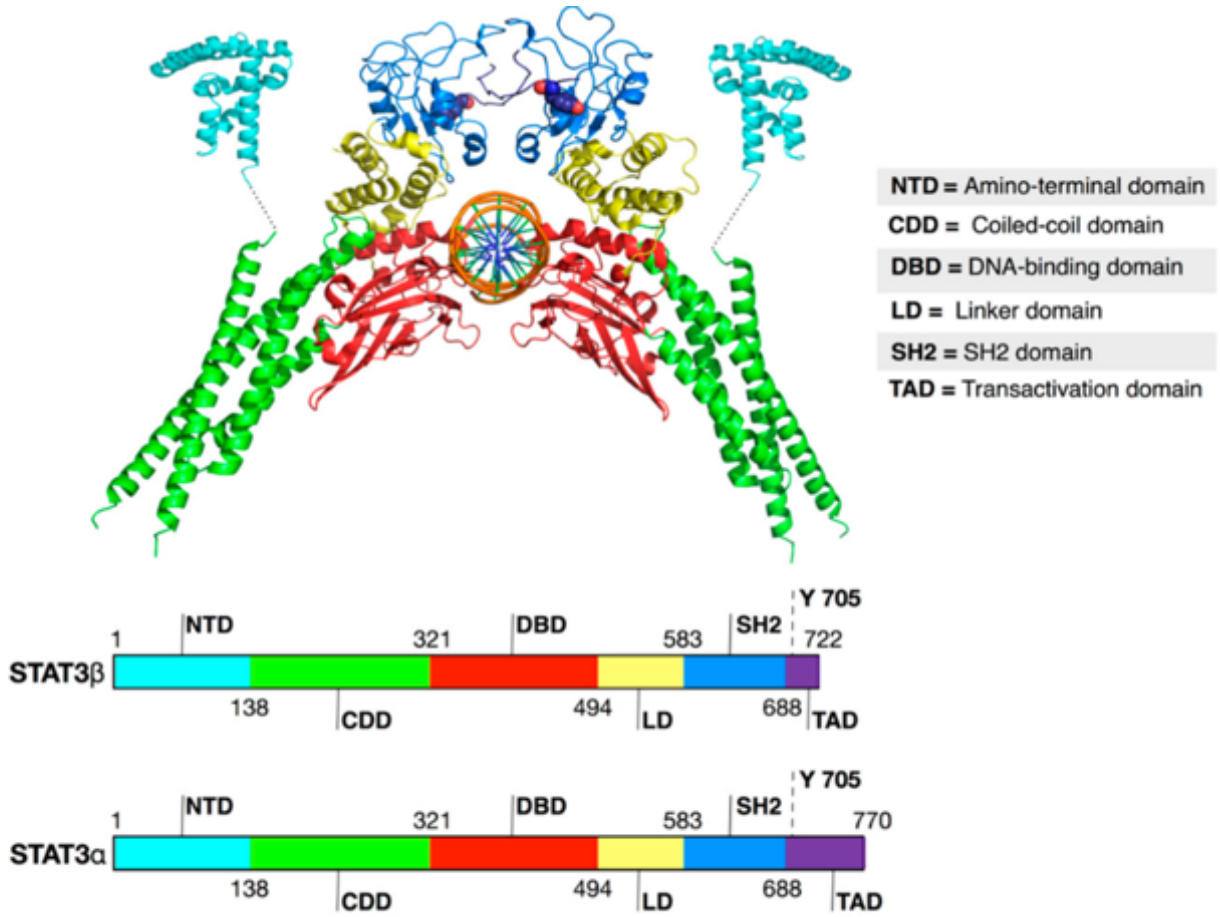

Figure 1.6. Crystal structure and domain organisation of STAT3. Cartoon representation of the unphosphorylated STAT3 crystal structure (PDB ID; 4ZIA for the N-termini and 4E68 for the remain structure). Domain organisation of the two STAT3 isoforms (bottom). Cyan = N-terminal domain; Green = Coiled-coil domain; Red = DNA-binding domain; Yellow = Linker domain; Blue = SH2 domain; Purple = Transactivation domain.

1.9.2 STAT3 activation

Of all the members of the STAT transcription factor family, STAT3 has the strongest link with the promotion of tumour growth and is classified as a *bona fide* oncogene (272). It is additionally the only STAT family member whose genetic deletion results in embryonic lethality, suggesting it has other, essential roles in development (273).

Similar to the other STAT family members, STAT3 exists as a monomer in the cytoplasm. The most well studied inducers of STAT3 activation are EGF, through the EGFR, and the IL-6 family of cytokines, with IL-6 being the most well studied to date. IL-6 mediated activation of STAT3 occurs through the IL-6 receptor (IL-6R) and the co-receptor glycoprotein 130 (gp130) (194). This homo receptor exists as a part of a hetero-hexameric signalling complex, comprising of a gp130 homodimer plus two IL-6R homodimers bound to two IL-6 ligands. The formation of this complex result in the activation of receptor bound JAK proteins, which subsequently phosphorylate gp130, leading to the recruitment of STAT3 (246). Other IL-6 family members include leukaemia inhibitory factor (LIF), oncostatin M (OSM) and IL-11, which all utilise the gp130 co-receptor for receptor activation (274).

IL-6 signalling occurs in two forms; classic and trans-signalling. In classic IL-6 signalling, IL-6 binds to the membrane bound IL-6R, inducing formation of the hetero-hexameric complex and subsequent downstream signalling (194). As well as the activation of JAK/STAT3 signalling, IL-6 can also signal through the PI3K/AKT and RAS/RAF/MEK/ERK signalling pathways (275). IL-6 trans signalling was discovered due to the detection of soluble IL-6R (sIL-6R) in patient samples (276). Subsequent studies identified that the IL-6R can be cleaved from the membrane by the disintegrin and metalloproteinase domain-containing protein 10 (ADAM10) or ADAM17 proteases or by alternative splicing (277). Binding of IL-6 to sIL-6R extracellularly induces the

dimerisation of gp130 monomers and the activation of downstream signalling. Alternative splicing can also result in the expression of secreted forms of gp130 (sgp130). Sgp130 can bind to the IL-6/sIL-6R complex and inhibit IL-6 trans signalling (278).

The nRTK JAK proteins are key components of STAT3 activation through IL-6 signalling. There are four isoforms of JAK proteins: JAK1, JAK2, JAK3 and TYK2 (279). These proteins contain a JAK homology (JH) 1 domain, which is enzymatically functional, and a pseudokinase domain, JH2, which retains JH1 in an inactive state(194). Upon stimulation, formation of the gp130/IL-6/IL-6R complex results in the selective activation of JAK1, JAK2 or TYK2 via binding to gp130. This binding initiates a conformational change in the JAK proteins, removing the inhibition of JH2 on JH1 (279).

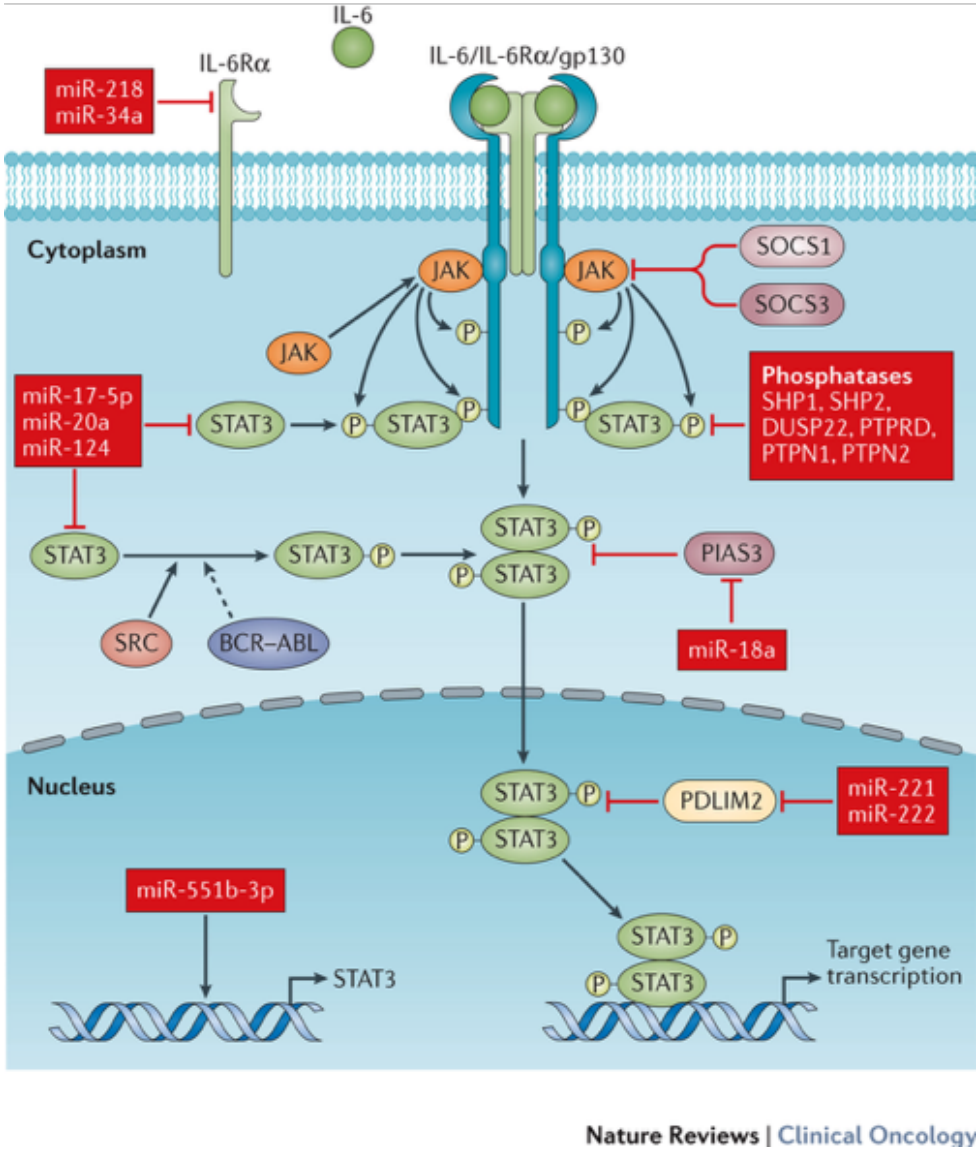

Figure 1.7. The IL-6 signalling pathway. Schematic diagram of IL-6/IL-6R/gp130 complex signalling. Details are in the main text. Key regulators are identified and are described in the main text. Image taken from (194).

STAT3 is the prominent mediator of IL-6 signalling in normal cell processes and in cancer formation. Activation of IL-6 signalling results in STAT3 recruitment via its SH2 domain to phosphotyrosine sites on gp130; this brings STAT3 in close proximity to JAK proteins, resulting in STAT3 tyrosine phosphorylation at Y705. This allows the head-to-tail dimerisation of STAT3 and its nuclear translocation. In the nucleus, STAT3 binds to GAS promoter elements and mediates the expression of genes involving key regulators of cell proliferation (cyclin D1, MYC), cell survival (Survivn, Bcl xL), angiogenesis (vascular endothelial growth factor (VEGF)) and inflammation (IL-6, COX-2) (280).

1.9.3 STAT3 post-translational modifications

The tyrosine phosphorylation of STAT3 was thought for a long time to be essential for STAT3 nuclear translocation; however, many studies have now demonstrated that STAT3 nuclear translocation is independent of tyrosine phosphorylation and is instead dependent on importin β1 and α3 (281). Indeed, unphosphorylated STAT3 has been demonstrated to control a distinct subset of genes that are not activated by phosphorylated STAT3 dimers (282).

Despite this, tyrosine phosphorylated STAT3 is mostly associated with STAT3 activation and is mostly commonly associated with malignancy (283). In addition to the JAK proteins, several other protein kinases have been demonstrated to induce STAT3 tyrosine phosphorylation at Y705 in response to diverse stimuli, including c-Src and Bcr-Abl (193,284). Tyrosine 705 is with the SH2 domain of the STAT3 protein; STAT3 can also be phosphorylated at tyrosine 640 in the SH2 domain by TYK2. The function of this phosphorylation site is poorly understood but reports suggest it may be involved in the negative regulation of STAT3 transcriptional activity (285).

As another layer of regulation, STAT3 is also phosphorylated at serine 727. The function

of this phosphorylation site is controversial and has been shown to induce the maximal transcriptional activity of STAT3 (286) and to inhibit STAT3 tyrosine phosphorylation (287). Furthermore, this serine residue can be phosphorylated by a number of host kinases, including MAP kinase(287-289), PKC(290,291), mTOR(292) and CDK5(293). Therefore, it is likely that the function and mechanism of this phosphorylation is highly dependent on cell type. Additionally, a novel dual phosphorylation event, occurring on residues threonine 714 and serine 727 and induced by Glycogen Synthase Kinase 3α/β (GSK3α/β), has been demonstrated to be essential for STAT3-dependent gene expression in renal cell carcinoma (294).

Other post-translational modifications have been identified that regulate STAT3 activation. STAT3 acetylation is essential in maintaining the stability of STAT3 dimers in response to cytokine treatment. This acetylation occurs at Lysine 685 and is mediated by the p300 histone acetyltransferase (295). STAT3 can also methylated at Lysine 49; this methylation occurs following phosphorylation of tyrosine 705 and is mediated by Enhancer of zeste homolog 2 (EHZ2). This methylation event positively regulates STAT3 transcriptional activity in response to IL-6 signalling (296).

STAT3 is also modulated by ubiquitination; Lysine 97 in the N-terminal domain of STAT3 is the major conjugation site of mono-ubiquitin (297). This ubiquitination event regulates STAT3 interactions with BRD4 and regulates STAT3 mediated transcription. STAT3 can also be deubiquitinated by CYLD; this results in the inhibition of STAT3 nuclear translocation (298). Finally, STAT3 can be SUMOylated at Lysine 451; de-SUMOlyation of this residue by the protease SENP3 results in an increase in STAT3 transcriptional activity (299).

1.9.4 STAT3 regulation

As STAT3 regulates a number of genes that are important in proliferation, survival and inflammation, STAT3 signalling is itself negatively regulated by many cellular proteins to avoid aberrant signalling. As mentioned above (1.9.3), several post translational modifications are able to inhibit STAT3 transcriptional active, switching off STAT3 signalling. A major class of proteins that regulate STAT3 activity are protein phosphatases, including the SHP1 and SHP2, protein phosphatase receptor-type tyrosine-protein phosphatase C (PTPRC), PTPRD, PTPRT, and dual specificity protein phosphatase 22 (DUSP22); these proteins induce the dephosphorylation of STAT3 or upstream kinases (300-303). The Suppressor of Cytokine Signalling 3 (SOCS3) protein impairs STAT3 activation by preventing the phosphorylation of STAT3 (304) and the protein inhibitor of activated STAT3 (PIAS3) protein prevents the STAT3 dimer from binding DNA (305). PDZ and LIM domain protein 2 (PDLIM2), an E3 ligase, promotes the polyubiquitination and degradation of STAT3 (305) and TRIM28 binds the coiled-coil and DNA binding domain of STAT3, negatively regulating the serine phosphorylation of STAT3 (306).

STAT3 is also regulated by many microRNAs (miRNAs) that directly target *stat3* mRNA, including miR-29b and miR-124 (307,308). Let-7a can also directly target *stat3* miRNA and indirectly inhibits STAT3 by promoting SOCS3 expression (309,310). The miRNA miR-34a and miR-218 also supresses STAT3 signalling by targeting *il6* mRNA (311,312). miRNAs can also promote STAT3 signalling by downregulating the expression of negative regulators of STAT3. For example, miR-18a targets the E3 SUMO ligase PIAS3 (313), while miR-221 and -222 supress expression of PDLIM2 (314).

1.9.5 Biological functions of STAT3

As genetic deletion of STAT3 results in embryonic lethality (273), STAT3 plays essential functions in normal biological functions. The development of STAT3-deficient mice that have tissue specific genetic deletions of the *stat3* gene has revealed some of the essential functions of STAT3. For example, in keratinocytes, loss of STAT3 results in a migration defect, resulting in a defective wound healing response (315).

The major functions currently attributed to STAT3 are in the correct functioning of the immune system; however, STAT3 has been demonstrated to both enhance and inhibit the immune response to pathogens (316). In T cells, STAT3 is essential for IL-6 dependent survival and proliferation and for the correct expression of CD25, a component of the IL-2 receptor (IL-2~R), an essential mediator of T cell function (317). Furthermore, STAT3 loss in monocytes and neutrophils results in an enhanced inflammatory response, suggesting STAT3 may play a role in dampening the inflammatory response (317).

In addition to genetic studies in mice, several naturally occurring mutations of STAT3 have identified its important role in normal cell function and how this relates to disease. Autosomal dominant STAT3 inactivating mutations are frequently observed in the human immunodeficiency condition Hyper Immunoglobulin E syndrome (HIES) (318). The mutation observed in HIES includes disruptions in the SH2 domain and the TAD (319). The features of this disease are recurring bacterial infections of the skin and oral fungal infections (318). This is likely due to an altered cytokine response due to defective STAT3 signalling. Further evidence for the role of STAT3 as an essential mediator of the immune response came from studies in keratinocytes; these cells require the activity of cytokines from STAT3 dependent T_h17 cells and pro-inflammatory cytokines to mount an appropriate immune response through the generation of antibacterial mediators and neutrophil chemoattractants (320).

In line with the role of STAT3 in promoting a robust immune response, STAT3 hyperactivation has been demonstrated to play a key role in autoimmune disease. Recently, *de novo* gain of function mutations, located within the DNA binding or SH2 domains, were identified in patients with early-onset, multi-organ autoimmunity and lymphoproliferative disease (321). These mutations result in constitutive STAT3 DNA binding without STAT3 tyrosine phosphorylation. Patients with these gain of function mutations show a decreased number of T regulatory cells, suggesting STAT3 is important for their development.

Another key function of STAT3 in regulating the immune response is in the control of the immunosuppressive cytokine IL-10 (322). In HIES, the elevation of pro-inflammatory cytokine production coincides with the loss of anti-inflammatory IL-10 expression, both attributed to the loss of function mutations in STAT3 (319).

1.9.6 STAT3 in viral infection

As STAT3 has essential roles in the immune response, STAT3 also plays important roles in viral infection. Therefore, many viruses have developed strategies to manipulate STAT3. The hepatitis B virus (HBV) promotes the formation of STAT3 dimers to bind enhancer regions in the viral genome and drive viral replication (323). This is partially mediated by the HBx protein, which drives JAK1 mediated tyrosine phosphorylation of STAT3 (324). HBx also inhibits the expression of the miRNA Let-7a, a negative regulator of *stat3* mRNA expression (325). Furthermore, HBV epigenetically silences *SOCS3* mRNA expression through upregulation of SNAIL1 expression (326).

Another clinical important hepatitis virus, hepatitis C virus (HCV), manipulates STAT3

signalling in several was to its own benefit. HCV drive STAT3 activity by the direct interaction between the HCV core protein and STAT3 (327). HCV also stimulates STAT3 activity through co-opting JAK1 by HCV NS5A activity (328).

Viruses of the *Herpesviridae* can also modulate STAT3 activity. Human cytomegalovirus (HCMV) induces the tyrosine phosphorylation of STAT3 via the viral US28 protein and the expression of viral IL-10 expression (329,330). Similarly, Epstein Barr Virus (EBV) induces STAT3 dual phosphorylation via the latent membrane protein 1 (LMP1) (331) and increases the DNA binding and transcriptional activity of STAT3 via Epstein Barr Nuclear Antigen 2 (EBNA2) expression. This drives expression of poly(rC)-binding protein2 (PCBP2), limiting the response of latent cells to lytic signals, promoting viral persistence (332). Kaposi Sarcoma Herpesvirus (KSHV) infection also drives the dual phosphorylation of STAT3 (333,334), potentially via the expression of a viral IL-6 homologue (335). KSHV mediated activation of STAT3 persists due to sustained serine phosphorylation induced by the kaposin B protein via the negative regulation of TRIM28 by the p38/MK2 pathway (334). As with EBV, the activation of STAT3 by KSHV lead to the persistence of viral latency through the repression of the viral protein R Transactivator (RTA).

Many of these viruses utilise the ability of STAT3 to dampen the effect of the inflammatory response. However, suppression of STAT3 can also reduce the host's ability to respond to inflammatory cytokines in the acute phase. This counterintuitive response of inhibiting STAT3, therefore, needs to be analysed in a virus-dependent manner. In contrast to the ability of HCMV to induce STAT3 tyrosine phosphorylation, in certain circumstances, HCMV can inhibits STAT3 activation by sequestering unphosphorylated STAT3 in the nucleus (336). Additionally, KSHV can reduce *STAT3* mRNA levels via the virally encoded miRNAs miR-K6-5 and miR-K8 (337). This results in the down regulation of ISGs,

including ISG15, IFITM1 and OAS2. Whether or not the ability of HCMV and KSHV to induce STAT3 activation outweighs the negative regulation of STAT3 by these viruses is unknown.

Influenza A virus (IAV) induces STAT3 activation during early infection, but this decreases during infection in correlation to the pathogenicity of the viral strain (338). This may be due to the ability of the viral protein non-structural protein 1 (NS1) to induce *SOCS3* mRNA (339). The Mumps virus V protein induces the degradation of STAT3 by promoting the formation of STAT3-K49 ubiquitin complexes (340).

1.9.7 STAT3 in cancer biology

STAT3 is *bona fide* oncogene; overexpression of a constitutively active STAT3 resulted in the induction of anchorage-independent growth and increased tumourigenic potential of fibroblasts (272). STAT3 is aberrantly activated in an estimated 70% of human cancers (341). This includes a number of haemopoietic cancers (342,343), multiple myeloma (344), and cancers of the breast, brain, colon, prostate and pancreas to name a few (345-347). In many of these cancers, STAT3 activity and phosphorylation correlates with poor clinical prognosis (348,349).

The mechanism of STAT3 oncogenicity is an intense area of study as it is an interesting therapeutic target in several cancers (350); this is particularly true for cancers that are resistant to conventional chemo or radiotherapies, or more targeted therapies such as EGFR inhibitors. In these resistant cancers, STAT3 is often aberrantly expressed, and thus the combination of standard cancer therapies with STAT3 inhibitors may be beneficial.

STAT3 contributes to the expression of several genes that regulate key processes in cancer cells, including cell proliferation and metabolism, cell survival and cell metastasis

(280). STAT3 induces the expression of cyclin D1, an oncogene upregulated in most cancers that is a key regulator of cell cycle progression (351). STAT3 also regulates the expression of Bcl xL and survivin, proteins involved in pro-survival pathways, often over expressed in cancers. Furthermore, STAT3 regulates the expression of VEGF and several MMP proteins, key regulators of angiogenesis and cell migration and metastasis.

STAT3 has also been demonstrated to control the expression of IL-6, resulting in a positive feed-forward loop, maintaining oncogenic STAT3 signalling. The combined upregulation of both IL-6 and VEGF by STAT3 also results in a potent immunosuppressive environment, which may facilitate the immune evasion of tumour cells harbouring STAT3 activity (352).

STAT3 mutations are rare in cancer and are mostly commonly found in haematological cancers (353). Most common are mutations in the SH2 domain of STAT3, found in a number of patients with large granular lymphocytic (LGL) leukaemia (354). As mutations in STAT3 that contribute to cancer development are rare, other mechanisms are the predominant causes of hyperactivation of STAT3 in malignant tissue. A common cause of STAT3 activation in cancer is the increased expression and autocrine/paracrine signalling of IL-6. This induces the activation of the IL-6R and subsequent JAK/STAT3 signalling. Serum IL-6 levels are increased in several cancers, including HNSCC (355), ovarian (356) and renal carcinoma (357). Aberrant IL-6 signalling, mediated through STAT3, is involved in many of the hallmarks of cancer, including the induction of EMT in breast cancer and HNSCC (358,359).

Despite the aberrant activity of IL-6/IL-6R/gp130 in many cancers, no genomic alterations in this pathway have been found in cancer genome databases. However, gp130 activating mutations are found in some cancers, such as hepatocellular adenomas (360). Furthermore, a point mutation in the *IL6* promoter results in an increased expression in IL-

6 (361).

Downstream of IL-6/IL-6R/gp130, the JAK proteins also play a role in cancer development, most commonly in haematological cancers. A common JAK2 mutation, $JAK2^{V617F}$, is found in around 95% of patients with the myeloproliferative disorder polycythaemia vera (362); this mutation results in a constitutively active JAK2 protein independent of cytokine signalling. Additionally, JAK2 mutations occur in other haematological cancers including B cell acute lymphoblastic leukaemia (B-ALL) and B cell lymphoma (363,364).

Additionally, the autocrine activation of growth factor receptor signalling is often activated is cancer; over expression of EGFR in cancers such as NSCLC, can result in the downstream activation of STAT3 (365).

STAT3 activation in cancer also occurs due to the inhibition or loss of negative regulators of STAT3 through a multitude of mechanisms. Loss of SOCS3, most commonly due to transcriptional regulation by promoter methylation, occurs in several cancers, including colon and pancreatic (366,367). Additionally, SHP1 and SHP2 can be inactivated due to loss of function mutations (368); mutations in PTPRT and PTPRD occurs at around 5.6% and 3.7%, respectively, in HNSCC (300).

1.9.8 STAT3 in HPV infection and associated disease

The role of STAT3 during the productive HPV life cycle has not been studied to date; however, the involvement of STAT3 in HPV associated disease has been demonstrated. The aberrant phosphorylation of STAT3, at both tyrosine and serine residues, has been demonstrated to be associated with both HPV16 and 18+ cervical cancers (369). STAT3 phosphorylation and DNA binding activity has also been shown to correlate with cervical disease progression, from pre-cancerous legions to invasive carcinoma. Other studies have shown that the increase in STAT3 phosphorylation may

be due to ‘high risk’ HPV E6 expression (370) and that abolishing STAT3 phosphorylation, by using inhibitors of upstream effectors such as JAK2, inhibits HPV16 E6 and E7 express and restores p53 and pRb expression (370). Conversely, STAT3 has been demonstrated to be down regulated in papilloma tissue due to increased expression of phosphatase and tensin homologue (PTEN), a well characterised tumour suppressor (371).

Despite the fact that a number of studies have suggested that STAT3 may be deregulated by HPV in cancer development, there is a currently no data regarding a role for STAT3 during the HPV productive life cycle. STAT3 expression has been shown to be required for the differentiation of a normal human stratified squamous epithelium, which is deregulated upon HPV infection, and expression of a constitutively active STAT3 expressed at physiological levels can induce immortalisation of keratinocytes in a knock-in mouse model (372). However, whether HPV infection can alter STAT3 signalling to drive keratinocyte proliferation is unknown.

1.10 Aims of the Project

Despite the availability of vaccines that target the small number of HPV types most commonly associated with cancer development, the long term effectiveness of these remains to be seen. Additionally, there is no currently available directly acting antiviral for HPV, and thus a better understanding of the complex interactions of the virus with the host cell is required for the development of anti-virals or cancer therapies. Furthermore, a greater understanding of the mechanisms used by HPV to disable epithelial homeostasis may provide novel insight into fundamental cellular processes. Recent work in the Macdonald group identified a link between the presence of HPV18 in primary keratinocytes and the activation of STAT3 signalling. Therefore, the aims of this PhD project are to investigate the role of STAT3 during the productive virus life cycle and to assess the effect of STAT3 inhibition in HPV+ cervical cancer. Specifically, the objectives of the project are:

1. Investigate the role of STAT3 signalling during the HPV18 viral life cycle using a primary keratinocyte and organotypic raft culture model system

2. Examine the upstream signalling pathway leading to the activation of STAT3 by HPV in HPV+ cervical cancers

3. Investigate the importance of STAT3 in key cancer phenotypes such as proliferation, migration and epithelia-mesenchymal transition (EMT) in HPV+ cervical cancers

Chapter 2. Methods and Materials

2.1 Bacterial cell culture

2.1.1 Bacteria growth and storage

The *Escherichia coli* strain DH5α (New England BioLabs (NEB), USA) was used for the amplification of plasmid DNA vectors. *E. coli* were grown on semisolid medium (agar in Luri-Bertani (LB) Medium) and in liquid shaking cultures (LB medium: 10 g/L tryptone soya broth, 10 g/L NaCl, 5 g/L yeast extract), respectively, overnight (o/n) at 37°C. Appropriate antibiotics were added for selection (50 µg/µL Kanamycin, 100 µg/µL Ampicillin). For long-term storage, cells were frozen at -80°C in freezing medium (50% glycerol in liquid o/n culture).

2.1.2 Transformation of chemically competent bacteria with plasmid DNA

For the transformation of DH5α cells, plasmid DNA (1 µL) was added to 50 µL of chemically-competent DH5α (2.1.2) cells and incubated on ice for 20 mins. Cells then underwent heat shock treatment at 42°C for 45 sec. Cultures were incubated on ice for 5 min followed by the addition of 949 µL of LB medium and an 1 h incubation at 37°C shaking at 180 rpm. The cultures were streaked out onto selective semisolid medium (2.1.1). For a list of plasmids used in this thesis, see Table 1 in Appendix.

2.1.3 Preparation of plasmid DNA

To purify plasmid DNA on a small scale, 20 ml of selective LB medium were inoculated with a single colony previously grown on semisolid medium. The culture was shaken

o/n at 37°C. Cells were harvested by centrifugation of 20 mL of culture for 30 min at 4000 x g. The plasmid DNA was purified using the sodium dodecyl sulphate (SDS)-alkaline denaturation method employed by the Wizard® Plus SV Minipreps DNA Purification System (Promega, UK). Purification was conducted according to the manufacturer's protocol. DNA was eluted from the Wizard® SV Minicolumns with 100 µL dd$H_2$0.

To purify plasmid DNA on a larger scale, a starter culture was prepared by inoculating 20 mL of selective LB medium with a single colony grown on semisolid medium. The culture was shaken for 8 h at 37°C and added to 80 mL of LB medium. This large-scale culture was shaken o/n at 37°C. Cells were harvested by centrifugation at 4000 x g for 30 min at 4°C. The plasmid DNA was purified using the Plasmid Maxikit (Qiagen, Germany) according to the manufacturer's protocol. Plasmid DNA was resuspended in 200 µL – 600 µL ddH_2O.

The concentration of the plasmid DNA was determined using a Nanodrop spectrophotometer (Thermo Fisher Scientific, USA).

2.2 Protein Biochemistry

2.2.1 Bicinchoninic acid assay for protein concentration determination

Protein concentrations of mammalian cell lysates were determined with a bicinchoninic acid (BCA) protein assay kit (Thermo Fisher Scientific, USA) according to the manufacturer's protocol for microplates. After 10 min incubation at RT, the absorbance at 562 nm was determined on a PowerWave XS2 Microplate Spectrophotometer (BioTek, UK). A standard curve was generated using the

accompanying software (Gen5 1.07.5, BioTek, UK) to determine the samples' total protein concentration considering the dilution factor.

2.2.2 SDS polyacrylamide gel electrophoresis (SDS-PAGE)

Proteins were separated according to molecular weight using a minigel system (BioRAD, USA). 8%, 12.5% and 15% SDS-polyacrylamide gels were prepared according to protein resolution required. Protein samples with lithium dodecyl sulphate (LDS) sample buffer (Invitrogen, USA) and 0.1% 2-mercaptoethanol, were loaded alongside 4 µL SeeBlue prestained protein marker (Invitrogen, USA) or ColorPlus Prestained Protein Marker (NEB, USA). Electrophoresis was carried out at 120-180 V in 1 x SDS running buffer (34.7 mM SDS, 250 mM Tris Base, 1.92 M Glycine) until the desired protein resolution was achieved.

2.2.3 Western blot analysis

Separated proteins were transferred from the SDS-polyacrylamide gels to HybondTM-C Extra mixed ester nitrocellulose membranes (Amersham BioSciences, UK) using a Bio-Rad Trans-blot® Turbo™ transfer system (Bio-Rad). Nitrocellulose membranes were then blocked in blocking solution (5% w/v dried skimmed milk powder in TBS-T (TBS: 25 mM Tris/Cl, pH 7.5; 138 mM NaCl and 0.1% Tween-20)) for 1 hr at RT. Primary antibody diluted in blocking solution to the appropriate dilution (Table 3 in Appendix) was added to the membrane and incubated o/n at 4˚C on a shaking platform. Membranes were then washed 4 x 5 min in TBS-T at RT. The secondary antibody, which is conjugated to horseradish peroxidase (Table 3 in Appendix), was diluted in blocking solution (1:5000) and incubated for 1 hr at RT. The membranes were washed 4 x 5 min in TBS-T at RT. To detect the chemiluminescent

signal, membranes were briefly incubated in Pierce™ ECL western blotting solution (Pierce). Membranes were then placed in a protective sleeve with film (CL-Xposure™ Film, Thermo) placed on top and developed for an appropriate length of time. The film was automatically using a Xograph Compact 4 machine.

2.2.4 Densitometry analysis of Western blots

Western blot films (2.3.3) were digitalised by scanning. Protein levels were quantified using ImageJ (National Institutes of Health, USA). For this, the protein bands were selected with a square. The same square surface was selected for every protein band. Band intensity was determined with the 'measure' function. Areas of the film with no protein bands were measured and deducted as background. The resulting data was entered into Excel (Microsoft, USA) and analysed using a Two-tailed Student T-Test.

2.3 Mammalian cell culture

2.3.1 Cell lines and their maintenance

Mammalian cell lines (Table 4 in Appendix) were maintained in Dulbecco's modified Eagle medium (DMEM; Lonza, Switzerland) supplemented with 10% foetal bovine serum (FBS; GIBCO, UK), 1% Non-essential amino acids (GIBCO, UK) and 50 U/ml penicillin and streptomycin (Lonza, Switzerland), respectively. All cell lines were typically kept in 75 cm^3 flasks (Sarstedt, Germany) and grown in a humidified incubator (Sanyo, USA) at 37°C and 5% CO_2. All cell culture work was conducted in an Airstream Class II Biological Safety Cabinet (ESCO, UK).

2.3.2 Passaging of cell lines

Cells were passaged upon reaching 80% - 90% confluence. For passaging, medium

was aspirated, and cells were washed once with sterile phosphate buffered saline (PBS). To detach cells from the culture flask, 1 x trypsin was added and incubated at 37°C, 5% CO_2 until cells were detached. Trypsin was inactivated by addition of complete DMEM. Cells were then re-seeded in T75 flask at a 1:8 ratio, cell suspension: fresh DMEM, or seeded into the appropriate dishes at the required density for each experiment.

2.3.3 Transient transfections with polyethylenimine

For transfection of HEK293TT cells, cells were seeded into 6 well or 12 well cell culture plates (Corning, USA) at a density of 1 x 10^6 or 0.5 x 10^6 cells/mL, respectively, and incubated overnight at the aforementioned conditions. The required amount of plasmid DNA was added to 200 µL of 1 x Opti-MEM Reduced Serum Medium (Opti-MEM; GIBCO, UK). After 5 min incubation at RT, the chemical transfection reagent polyethylenimine (PEI; 23966, Polyscience Inc.) was added at a ratio of 4:1 PEI:DNA. The PEI:DNA mix was incubated for a further 20 min at RT. For co-transfections of two plasmids, equal amounts of each plasmid were added. Complete DMEM in culture dishes was replaced with Opti-MEM I Reduced Serum Medium and the DNA-PEI mixture was added dropwise. Cells were incubated for overnight as described. The mixtures were removed and fresh DMEM was added to each well of the culture plate and cells were incubated as described for the appropriate length of time.

2.3.4 Transient transfections with Lipofectamine 2000

For transfection of primary keratinocytes, HeLa, CaSKi and C33A cells, cells were seeded into 6 well or 12 well cell culture plates (Corning, USA) at a density of 1 x

10^6 or 0.5 x 10^6 cells/mL, respectively, and incubated overnight at the aforementioned conditions. The required amount of plasmid DNA was added to 200 µL of 1 x Opti-MEM (GIBCO, UK)). In a separate eppendorf, the appropriate amount of Lipofectamine® 2000 to make a 2.5:1 Lipofectamine® 2000:DNA was added to 200 µL of 1 x Opti-MEM (GIBCO, UK). After 5 min incubation at RT, the Lipofectamine® 2000 mix was added to the DNA mix and this was incubated for a further 20 at RT. For co-transfections of two plasmids, equal amounts of each plasmid were added. Complete DMEM in culture dishes was replaced with Opti-MEM I Reduced Serum Medium and the Lipofectamine® 2000:DNA mixture was added dropwise. Cells were incubated overnight. The mixtures were removed and fresh DMEM was added to each well of the culture plate and cells were incubated for the appropriate length of time.

2.3.5 Transfection of siRNA with Lipofectamine 2000

For transfection of siRNA, the required cells were plated into 6-well dishes at a density of 1 x 10^6 cells/mL. The siRNA at the appropriate concentration was added to 200 µL of 1 x Opti-MEM (GIBCO, UK). In a separate eppendorf tube, the appropriate amount of Lipofectamine® 2000 was added to 200 µL of 1 x Opti-MEM (GIBCO, UK). After 5 mins, the Lipofectamine® 2000 mix was added to the siRNA mix and this was incubated for 20 mins at room temp. Complete DMEM in culture dishes was replaced with Opti-MEM and the siRNA mixture was added dropwise. Cells were incubated for overnight. The mixtures were removed and fresh DMEM was added to each well of the culture plate and cells were incubated for the appropriate length of time.

2.3.6 Harvesting of cells and lysis

For preparation of cell lysate, media was aspirated from cells in culture plates and washed once in PBS. Leeds lysis buffer (10 mM Tris/Cl, pH7.5; 150 mM NaCl, 0.5 mM EDTA, 0.5% NP40, 1 x Protease inhibitor cocktail, EDTA-free (Roche, Switzerland)) was added to each well and cells were scrapped into the lysis buffer. Cell lysate was transferred to an eppendorf tube and incubated on ice for 20 mins. Lysate was then centrifuged at 17,000 x g at 4°C for 10 mins.

2.3.7 Normal human keratinocytes (NHKs)

Primary NHKs isolated from neonate foreskin tissues (ethical approval no. 06/Q1702/45) were obtained from Dr Sally Roberts, University of Birmingham, UK. The transfection of NHK with the wild type HPV genome was performed in S. Roberts' laboratory as described previously (129). Briefly, plasmids containing the HPV18 genome were digested with *Eco*RI to release the genome, which was then re-circularised with T4 DNA ligase. The genomes were co-transfected with a plasmid encoding resistance to neomycin into low passage NHK. After 24 hours, the cells were harvested and seeded onto a layer of γ-irradiated J2-3T3 fibroblasts and selected with G418 in complete E media containing foetal calf serum (FCS, Lonza) and epidermal growth factor (EGF, BD BioSciences) for 8 days. Cell colonies were pooled and expanded on γ-irradiated J2-3T3 fibroblasts. After selection, NHKs stably expressed episomal wild type HPV18 genomes.

2.3.8 Maintaining and passaging untransfected NHKs

NHKs were maintained in serum free medium (SFM; GIBCO, UK) supplemented with 25 μg/mL bovine pituitary extract (GIBCO, UK) and 0.2 ng/mL recombinant EGF

(GIBCO, UK). The medium was replaced with every 2 days. Cells were only grown to a confluency of ≤ 80% in 10 cm dishes. The incubation conditions were the same as described for established cell lines (2.3.1).

To passage, the medium was aspirated, and cell were washed once with PBS. After the PBS was removed, trypsin was added and left to incubate for 5 min - 10 min until cells detached. Trypsin was inhibited by the addition of SFM supplemented with 1% Trypsin inhibitor (GIBCO, UK). NHKs were then re-seeded a density of 2 x 10^5 cells per dish in serum free media.

2.3.9 Maintaining and passaging NHKs with HPV18 genomes

The HPV18 containing NHK cell lines of both donors were maintained in 10 cm dishes with 3T3 J2 fibroblasts as feeder cells in E-medium supplemented with 2 mM L-glutamine (Lonza, Switzerland) and 5 ng/ml EGF (BD Biosciences, UK). 3T3 J2 fibroblasts were pre-treated with 8 µg/mL mitomycin-C (Roche, Switzerland) in DMEM for 4 h and 2 x 10^6 cells were seeded in E-medium in 10 cm dishes 24 h prior to addition of transfected NHKs. NHKs containing the HPV18 WT were passaged as described (2.5.1) and seeded into the dishes containing the mitomycin-C treated 3T3 J2 fibroblasts.

One litre of E-medium was prepared as follows: 600 ml of DMEM Hepes (Sigma, USA) were mixed with 320 ml Hams-F-12 (GIBCO, UK), 20 mL Penicillin/Streptomycin (GIBCO, UK), 5% FBS, 10 µg Cholera Toxin (Sigma, USA), 1 x hydrocortisone (Sigma, USA) and 1 x cocktail. 100 mL of 100 x cocktail was prepared by mixing 10 mL of 0.18 M Adenine (Sigma, USA), 10 ml of 5 mg/mL Insulin (Invitrogen, USA), 10 mL 5 mg/ml transferrin (Sigma, USA), 10 mL 2 x 10-8 M 3,3`,5-Triiodo-L-thyronine (T3) (Sigma,

USA) in PBS. The E-medium was sterile-filtered prior to use.

2.3.10 Monolayer differentiation assays

For calcium differentiation of NHKs and HPV18 containing NHKs, cells were grown in 6 well plates until 80% confluent. The medium was then removed and replaced with SFM without supplements (SFM, Invitrogen) containing 1.8 mM calcium chloride. Cells were maintained in this media for 48-72 hours before lysis (2.3.6) and analysis.

For methylcellulose differentiation of NHKs and HPV18 containing NHKs, cells were grown in 6 well plates until 80% confluency. Cells were then detached and resuspended in E-media containing 1.5% methylcellulose and cultured for between 24 and 120 hours before lysis (2.3.6) and analysis.

2.3.11 Organotypic raft cultures

NHKs or HPV18 containing NHKs were grown on a matrix of 8 mg/ml rat tail collagen (BD Biosciences, UK) and 2 x 10^6 3T3 J2 fibroblasts in E-medium supplemented with 2 mM L-glutamine and 5 ng/mL EGF. After 4 days, the matrix and keratinocytes were transferred onto a sterile wire mesh at an air-liquid interface created by addition of E-medium without EGF. The organotypic raft cultures were grown for 10 - 14 days at 37°C and 5% CO_2 with media changes every two day. Rafts were fixed by flooding in 4% paraformaldehyde (PFA; 4% PFA in PBS, pH 7.4). Rafts were embedded in paraffin and sectioned into 5 µm slices by Propath, UK. Haematoxylin and eosin (H&E) staining of the sections was also carried out by Propath, UK. Raft cultures of NHK and WT HPV18 containing NHKs were prepared and H&E samples imaged by Dr Christopher Wasson, University of Leeds, UK. Raft cultures of HPV18 E6ΔPDZ containing NHKs were prepared and H&E samples imaged by Dr Sally Roberts,

University of Birmingham, UK.

2.3.12 Immunohistochemistry of organotypic rafts

For the analysis of the paraffin embedded organotypic raft cultures slices or pathological sections (kindly provided by Prof Sheila Graham, University of Glasgow, UK), sections were analysed by immunohistochemistry (IHC). Paraffin was removed by submersing in Histo-Clear® (GENEFLOW LTD, UK) for 3 x 5 min. Rehydration of samples occurred by incubation for 1 min in 100% ethanol, followed by 1 min in 90% ethanol and 1 min in 70% ethanol, followed by 5 min incubation in ddH_2O. Antigen retrieval was achieved by boiling in sodium citrate buffer for 15 min (10 mM Tri-sodium citrate, pH 6; 0.05% Tween-20). Samples were washed in ddH_2O followed by blocking in 10% normal goat serum (NGS) in PBS for 1h at RT. The primary antibody (Table 3 in Appendix) was incubated for 1h at RT in 1% NGS buffer. Slides were washed 5 x in PBS prior to incubation with AlexaFluor labelled secondary antibody (Table 3 in Appendix) for 1h in 1% NGS buffer. Slides were washed 5 x in PBS and the samples were mounted using ProLong Gold Antifade Reagent with 4',6-diamidino-2-phenylindole (DAPI) (Molecular Probes, UK). Dr Chris Wasson performed IHC for NHK and WT HPV18 containing NHKs and Dr Sally Roberts performed IHC for HPV18 E6ΔPDZ containing NHKs.

2.4 Viral Gene Transduction

2.4.1 Production of lentiviruses for gene transduction

For the preparation of lentiviruses for gene transduction, HEK293TT cells (Table 4 in Appendix) were seeded into 10 cm cell culture plates (Corning, USA) at a density of 1 x 10^7 cells/mL and incubated overnight at the aforementioned conditions. The

required amount of plasmid DNA for the gene of interest (GOI) was added to 500 µL of 1 x Opti-MEM (GIBCO, UK). In addition the packaging vectors pUMVC3-gag-pol and the envelope vector pCMV-VSV-G were added so that the final plasmid ratio was GOI:GAG/POL:VSV was 2.4:1:1. In a separate eppendorf tube, the appropriate amount of Lipofectamine® 2000 to make a 2:1 Lipofectamine® 2000:DNA was added to 500 µL of 1 x Opti-MEM (GIBCO, UK). After 5 min incubation at RT the Lipofectamine® 2000 mix was added to the DNA mix and this was incubated for a further 20 mins at RT. The Lipofectamine® 2000:DNA mixture was added dropwise to the cells. After 48 hours, the cell supernatant was harvested and was at centrifuged at 3000 x g at 4°C for 10 mins to remove cell debris. The cell supernatant was then concentrated 10-fold in a 10k molecular weight cutoff (MWCO) concentrator (Spin-X^{R} UF20, 10k MSCO, 20mL; 431488, Corning®).

2.4.2 Virus transduction

For the transduction of lentiviruses, target cells were seeded at 1 x 10^6 cells/mL in 6 well plates and incubated overnight at the aforementioned conditions. Before addition of concentrated virus, culture medium was removed and the cells were washed once with PBS. The concentrated virus was then added for 3 hours (NHKs and HPV containing NHKs) or overnight (HeLa and CaSKi). The virus was then removed, cells were washed once in PBS and the cells were incubated for the appropriate length of time.

2.5 Small Molecule Inhibitors

The STAT3 inhibitor S3I-201 was purchased from AdooQ BioSciences and used at a final concentration of 10 µM. This cell permeable compound binds to the STAT3 SH2

domain to prevent phosphorylation and activation. Cryptotanshinone was purchased from LKT Laboratories to inhibit STAT3 dimerisation and activation. The STAT5 inhibitor Pimozide was purchased from Calbiochem and used at a final concentration of 10 μM. UO126 is a selective MEK1/2 inhibitor, and is used to inhibit activation of ERK1/2 and was used at a final concentration of 20 μM and purchased from Calbiochem. VX-702 was purchased from Tocris and used to inhibit p38 kinase activity and was used at a final concentration in cells of 10 μM. The JNK1/2 inhibitor JNK-IN-8 was purchased from Cambridge BioSciences and used at a final concentration of 3 μM in cells. SB-747651 was used to inhibit MSK1/2 and used at a final concentration of 5 μM in cells. The JAK1/2 inhibitor Ruxolitinib, and JAK2 inhibitor Fedratinib were kindly provided by Dr Edwin Chen, University of Leeds. IKK-16 is a selective inhibitor of the IκB kinase IKKα and IKKβ and was purchased from Calbiochem. All compounds were used at concentrations required to minimise potential off-target activity.

2.6 Quantitative Real-time PCR

2.6.1 RNA extraction

For extraction of total RNA from cells, TRK lysis buffer was added to cells and the lysate was processed with the E.Z.N.A. Total RNA Kit I (Omega Bio- Tek) according to the manufacture's protocol. RNA yield was determined using a Nanodrop spectrophotometer (Thermo Fisher Scientific, USA).

2.6.2 Reverse transcription

One μg of total RNA was DNase treated following the RQ1 RNase-Free DNase protocol (Promega) and then reverse transcribed with a mixture of random primers

and oligo(dT) primers using the qScript cDNA SuperMix (Quanta Biosciences) according to instructions.

2.6.3 Quantitative Real-time PCR

The quantitative real-time PCR (qPCR) reaction was conducted using the QuantiFast® SYBR® Green PCR kit (Qiagen, Germany) and a Corbett Rotor-Gene 6000 (Qiagen, Germany). Briefly, 2.5 µl of RT-reaction mix (2.10.2) (equals 62.5 ng of cDNA) and 1 µM of each forward and reverse primer (Table 2.4) were added to the 2 x QuantiFast SYBR Green PCR Master Mix. The PCR reaction was conducted as follows: initial activation step for 10 min at 95°C and a two-step cycle of denaturation (10 sec at 95°C) and combined annealing and extension (15 sec at 60°C) which was repeated 40 times. The data obtained was analysed according to the ΔΔCt method using the Rotor-Gene 6000 software. Specific primers were used for each gene analysed (Table 6 in Appendix). U6 served as normaliser gene.

2.7 Immunofluorescent Microscope

2.7.1 Cell growth on coverslips

Immunofluorescence staining was conducted in 12-well dishes (130185, Thermo). Cells were seeded into wells containing circular cover slips (400-08-26; glass coverslips, Dia. 19. Academy Science, UK) at a density of 5 x 10^4 cells/mL. Cells were taken forward for staining (2.6.2, 2.6.3) when approximately 80% confluent.

2.7.2 Fixation and permeabilisation of cells

At the appropriate time, culture medium was removed and the cells on coverslips were washed once with PBS. Cells were then fixed by incubation in 4%

paraformaldehyde (PFA) in PBS at RT for 10 min. Cells were washed again in PBS and permeabilised in Triton X-100 (0.1% Triton X-100 in PBS) for 15 min at RT.

2.7.3 Immuno-labelling

After permeabilisation, coverslips were incubated in blocking buffer (4% BSA in PBS) for 1 hour at RT. After a washing step in PBS, the primary antibody (Table 3) was diluted in antibody solution (4% BSA in PBS) and incubated at 4°C overnight. Following by 4 washing steps with PBS, the secondary antibody (Table 3) was diluted in antibody solution and incubated for 2h at RT. The coverslips were then washed 4 times in PBS and the coverslips were mounted onto glass slides (0.8 - 1.0 mm thick: VWR, USA) using the mounting agent ProLong Gold Antifade Reagent with DAPI (Molecular Probes, UK). Edges of coverslips were sealed with nail varnish and slides were stored at 4°C until viewing.

2.7.4 Microscopy

Samples were imaged with a Zeiss laser scanning confocal microscope (LSM700 inverted; Zeiss, Germany) under an oil-immersion 63 x objective lens. Representative images were processed using the Zen 2011 software (Zeiss, Germany).

2.8 Cell cycle analysis by flow cytometry

After incubation of cells as required per experiment, cells were harvested and fixed in 70% ethanol at -20°C overnight. The ethanol was removed, and cells were washed twice in with PBS containing 0.5% BSA. Cells were stained with PBS containing 0.5% BSA, 50 µg/mL propidium iodide (Sigma) and 5 µg/mL RNase (Sigma) and incubated

in this solution for 30 minutes at room temperature. Samples were processed on an LSRFortessa^{TM} cell analyzer (BD) and the PI histograms analysed on modifit software.

2.9 Conditioned Media

For the collection of HeLa and CaSKi conditioned media, 5 x 10^6 cells/mL were seeded in 10 cm dishes. When the cells reached 90% confluency, the cell supernatant was harvested and was centrifuged at 3000 x g at 4°C for 10 mins to remove cell debris. The cell supernatant was then concentrated 10-fold in a 10k molecular weight cutoff (MWCO) concentrator (Spin-X^R UF20, 10k MSCO, 20mL; 431488, Corning®).

For conditioned media experiments, C33A cells were seeded at a density of 1 x 10^6 cells/mL were serum starved in DMEM without FBS addition for 24 hours. After serum starvation, concentrated media from HeLa or CaSKi cells was added for the indicated time points for each experiment. For neutralization assays, IL-6 neutralising antibody (ab6672; Abcam) or gp130 neutralising antibody (28105; R&D system, USA) was added 4 hours before cell lysis, with conditioned media added 2 hours before cell lysis.

2.10 Cytokine and neutralization assays

For cytokine treatments, recombinant human Interleukin-6 (rhIL-6) was purchased from R&D Systems and re-suspended in PBS. For treatments, HeLa, C33A or CaSKi cells were seeded in 6 or 12 well plates at a density of 1 x 10^5 or 5 x 10^4 cells/mL, respectively. The cells were then serum starved in DMEM without FBS addition for 24

hrs. After serum starvation, IL-6 was added at 20 ng/mL for the indicated time points for each experiment, or for the doses indicated.

For pre-treatments with small molecule inhibitors, the required inhibitor was added 4 hours before cell lysis, with rhIL-6 added 30 mins before cell lysis. For neutralization assays, IL-6 neutralising antibody (ab6672; Abcam) or gp130 neutralising antibody (28105; R&D system, USA) was added 4 hours before cell lysis.

2.11 ELISA

Human interleukin-6 (IL-6) levels were detected in the cell supernatants using the DuoSet® ELISA kit according to the manufacturer's instructions (R&D Systems).

2.12 Luciferase reporter assays

C33A cells were seeded in 12 well plates at a density of 1 x 10^5 cells/mL and were transfected by using polyethyleneimine (PEI) with expression plasmids in combination with a reporter plasmid expressing *firefly* luciferase under the control of the *β-casein* or Pom^C promoter, which contain tandem repeats of a STAT-response element (373,374)A constitutively expressing *Renilla* luciferase plasmid was used to assess transfection efficiency. Transfected cells were then lysed and assayed for luciferase activities using Dual-Luciferase Stop and Glo reagent (Promega) and a luminometer (EG&G Berthold). Fold promoter activity was calculated by dividing the relative luciferase activity of stimulated cells by that of mock-treated cells.

2.13 Proliferation assays

2.13.1 Cell growth assay

For the measurement of cell proliferation, cells were seeded in 6 well plates at a density of 1 x 10^6 cells/mL and were treated as required per experiment. At the experiment end point, cells were trypsinised and 50,000 cells were re-plated in a 6 well plate. Cells were then harvested daily and counted manual using a haemocytometer.

2.13.2 Colony formation assay

For the measurement of anchorage dependent cell proliferation, cells were seeded in 6 well plates at a density of 1 x 10^6 cells/mL and were treated as required per experiment. At the experiment end point, cells were trypsinised and 500 cells were re-plated in a 6 well plate. Cells were analysed daily by microscopy until visible colonies were noted (14 - 21 days). At this point, culture medium was removed and colonies were stained in crystal violet staining solution (1% crystal violet (CHE1680; Science Laboratory Support SLS, UK), 25% methanol) for 15 mins at RT. Colonies were then thoroughly washed in water and photographed. Colonies were counted manually.

2.13.3 Soft Agar assay

For the measurement of anchorage independent cell proliferation, cells were seeded in 6 well plates at a density of 1 x 10^6 cells/mL and were treated as required per experiment. In parallel, 60 mm dishes were coated with a layer of 1% agarose (ThermoFischer Scientific, USA) in 2X DMEM (ThermoFischer Scientific, USA) supplemented with 20 % FBS. At the experiment end point, cells were trypsinised and 1000 cells/mL were added to 0.7 % agarose in 2X DMEM (ThermoFischer Scientific, USA) supplemented with 20 % FBS. Once set, DMEM supplemented with 10 % FBS and 50 U/mL penicillin

was added. The plates were then incubated for 14 - 21 days. Colonies were counted manually.

2.14 Migration assays

2.14.1 Wound healing assay

Cells were seeded in 6 well plates at a density of 1 x 10^6 cells/mL cells. Cells were grown to full confluency and then serum starved for 24 hours. Cells were then wounded with a P200 pipette tip. Images were taken immediately after initiation of the wound and at 24 hours post wounding. For siRNA treatment, cells were transfected with STAT3 specific siRNA and incubated in serum free media. After 16 hours, the media was replaced with normal DMEM with 10% FBS. 48 hours post transfection, cells were wounded using a P200 pipette tip. Images were then taken as for inhibitor treatment. All images were analysed using Image J (NIH).

2.14.2 Transwell® migration and Invasion assays

Cells were seeded in 6 well plates at a density of 1 x 10^6 cells/mL and were treated as required per experiment. Cells were then serum starved for 26 hours in serum free medium. Cells were then trypsinised and 5 x 10^4 cells were replated onto the upper chamber of a Transwell® filter with 8 µm pores (Falcon®, Corning, USA) coated with (invasion) or without (migration) 200 µg/mL Matrigel® Matrix (Corning). DMEM containing 10% FBS was used as the chemoattractant. After 24 hours, non-migrated cells on the upper side of the filter were removed with a cotton swab, and cells on the underside of the filter were stained with 1% crystal violet in 25% methanol. For each experiment, the number of cells in five random fields on the underside of the filter was counted, and three independent filters were analysed.

2.15 Apoptosis assays

2.15.1 Annexin V assay

Annexin V apoptosis assay (TACS® Annexin V kit; 4830-250-K) was performed as indicated on the product datasheet. Briefly, cells were seeded in 6 well plates at a density of 1 x 10^6 cells/mL and were treated as required per experiment. Cells were then trypsinised and cell were collected by centrifugation at 700 x g for 5 mins. Cells were then washed in cold PBS and re-centrifuged. 1x10^6 cells were then incubated in 100 µL Annexin V reagent (10 µL 10X binding buffer, 10 µL propidium iodide, 1 µL Annexin V-FITC (diluted 1 in 500), 880 µL ddH_2O) for 15 mins, RT in the dark. 400 µL of 1X binding buffer was then added before analysis by flow cytometry. Samples were processed on an LSRFortessa™ cell analyzer (BD) and the PI histograms analysed on modifit software.

2.15.2 DNA Condensation assay

DNA condensation was analysed using the Vybrant® DyeCycle™ Violet/SYTOX® AADvanced™ Apoptosis Kit (TermoFischer; A35135) and was performed as indicated on the product datasheet. Briefly, cells were seeded in 6 well plates at a density of 1 x 10^6 cells/mL and were treated as required per experiment. Cells were then trypsinised and cell were collected by centrifugation at 700 x g for 5 mins. 1x10^6 cells were then washed in cold Hank's Balanced Salt Solution (HBSS) and re-centrifuged. Cells were then resuspended in 1 mL HBSS and 1 µL of 1 µM Vybrant® DyeCycle™ Samples were then incubated on ice in the dark for 30 min and immediately analysed by flow cytometry. Samples were processed on an LSRFortessa™ cell analyzer (BD) and the PI histograms analysed on modifit software.

Chapter 3. The role of STAT3 during the differentiation-dependent HPV18 life cycle

3.1 Introduction

As an obligate intracellular parasite, HPV replication is critically dependent on host factors, which are mainly controlled by the activities of the virus encoded E5, E6 and E7 proteins (375). HPV E5 can reregulated EGFR signalling, promoting the proliferative abilities of infected keratinocytes (129,376). HPV E7 proteins promote S phase re-entry in the differentiated keratinocytes via an ability to bind and inactivate the pocket family proteins pRb, p107 and p130 (137,377). HPV E6 recruits the cellular ubiquitin ligase E6-associated protein (E6AP) into a protein complex with the tumour suppressor protein p53, resulting in the degradation of p53 (158). In addition, high-risk E6 proteins bind and modulate a select group of PDZ domain containing proteins (169,170). Despite our increased understanding of the role of E5, E6 and E7 during the HPV life cycle, there is still a clear need to better understand HPV-host cell interactions in order to develop novel strategies to treat HPV infections.

As a member of the signal transducer and activator (STAT) family of transcription factors, STAT3 is activated by cytokine and growth factor signalling, which typically involves phosphorylation of a tyrosine (Y705) residue (280). Tyrosine phosphorylated STAT3 molecules form activated dimers and translocate to the nucleus where they initiate a programme of gene expression controlling fundamental biological processes including proliferation, immune regulation and differentiation (283). STAT3 is also subject to stimulus- and tissue-dependent phosphorylation of a serine (S727) residue in its transactivation domain (191). The function of this additional phosphorylation

event remains controversial, as the modification has been reported to both enhance and suppress STAT3 transcriptional activity (286).

In stratified epithelia, STAT3 functions to drive proliferation and is required to maintain cells in an undifferentiated state by impairing differentiation (372). Over expression of constitutively active STAT3 in the epithelia of mice results in hyperplasia, reduced keratinocyte differentiation and an increase in inflammatory cytokine secretion (372). Despite the fact that STAT3 activation is critical for keratinocyte proliferation and disrupting keratinocyte differentiation, it is not known whether STAT3 contributes to the productive infectious HPV life cycle. This is surprising given the important role of STAT3 in maintaining an undifferentiated phenotype in keratinocytes.

The aim of this chapter is to assess the activation status of STAT3 in HPV-containing keratinocytes compared with normal keratinocytes and to identify the role of STAT3 during the productive HPV life cycle.

3.2 Results

3.2.1 HPV18 enhances STAT3 phosphorylation in primary human keratinocytes

To investigate the role of STAT3 in the HPV18 life cycle, stable cell lines harbouring HPV18 episomes were generated from two primary foreskin keratinocyte donors. To exclude donor effects, all experiments were performed using both donor lines and representative data are presented. Levels of STAT3 phosphorylation were measured in normal human keratinocytes (NHK) and HPV18-containing cells by western blotting. In undifferentiated cells, phosphorylation of the tyrosine (Y705) and serine (S727) residues was significantly enhanced in HPV18-containing keratinocytes compared to NHK donor controls (Fig 3.1A, compare lanes 1 and 4, Fig 3.1B, showing combined data from two donors; N = 8 $p<0.05$). To ascertain whether STAT3 phosphorylation was modulated during keratinocyte differentiation, monolayer cultures of NHK and HPV18-containing cells were cultured in high calcium media for 72 hours. Keratinocyte differentiation was confirmed by increased involucrin expression (Fig 3.1A). In HPV containing keratinocytes, enhanced STAT3 phosphorylation was maintained at upon differentiation (Fig 3.1A, compare lanes 2 and 5, 3 and 6). In contrast, HPV18 had no effect upon the total levels of STAT3 protein in the primary keratinocytes (Fig 3.1A).

Next, an organotypic raft culture system, in which NHK and HPV18-containing cells were stratified for 14 days, was used to confirm our findings; this method recapitulates all stages of the HPV life cycle (378). Raft sections were stained with antibodies detecting the total and phosphorylated forms of STAT3 (representative sections shown in Fig 3.1C and 1D). Staining of total STAT3 protein was comparable between the donor-matched NHK and HPV18-containing rafts. Efforts to detect tyrosine

phosphorylated STAT3 by immunofluorescence proved unsuccessful. However, serine phosphorylated STAT3 was evident in both the basal and suprabasal layers of the NHK and HPV18 containing rafts. However, the level of the S727 phosphorylated form of STAT3 was elevated in the presence of HPV18 (Fig 3.1C and 3.1D), in line with our monolayer culture data. Our data clearly demonstrate that primary keratinocytes harbouring HPV18 genomes exhibit increased STAT3 phosphorylation.

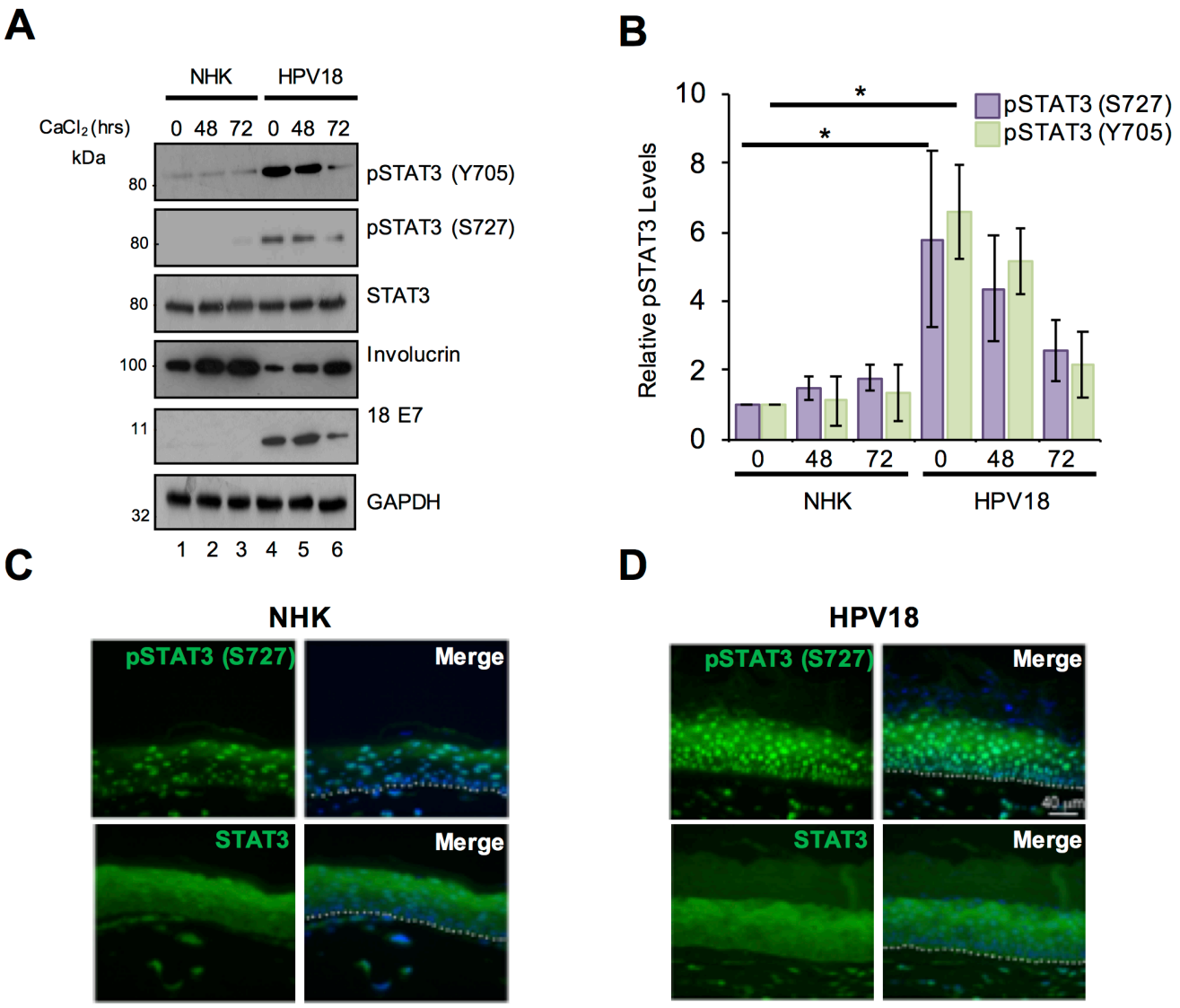

Figure 3.1. HPV18 induces the activation of STAT3 in primary human keratinocytes. A) Representative western blots of normal human keratinocytes (NHK) and HPV18 containing keratinocytes subjected to high calcium differentiation and analysed for Tyrosine 705 and Serine 727 STAT3 phosphorylation and total STAT3. Involucrin expression is a marker of differentiation and E7 demonstrates the presence of HPV18. GAPDH serves as a loading control. **B)** Quantification of the protein band intensities in **A)** standardised to GAPDH levels. Bars represent the means ± standard deviation from 4 independent biological repeats using 2 donor cell lines. *P<0.05 (Student's t-test). Representative sections of organotypic raft cultures

from **C)** NHK and **D)** HPV18 containing keratinocytes stained with antibodies specific for pS727 STAT3 and total STAT3 (green) and counterstained with DAPI to highlight the nuclei (blue in the merged panels). Images were acquired using identical exposure times. Scale bar, 40 μm. White dotted lines indicate the basal cell layer.

3.2.2 HPV18 E6 is necessary and sufficient for the dual phosphorylation and activation of STAT3

The HPV oncoproteins (E5, E6 and E7) are critical in modulating the host cell environment in order to favour viral replication. Thus, one of the HPV oncoproteins may be responsible for the promotion of the STAT3 phosphorylation observed in the HPV18 life cycle model. For this, we expressed GFP-tagged HPV18 oncoproteins in C33A cells (an HPV-negative cervical carcinoma cell line) and measured the levels of STAT3 phosphorylation by western blot analysis (Fig 3.2A). Interestingly, all three oncoproteins increased Y705 STAT3 phosphorylation compared to cells expressing GFP alone (compare lanes 1 with 2, 3 and 4); E5 by average of 3 fold ($p<0.05$), E6 by an average of 4.1 fold ($p<0.05$) and E7 by an average of 3.6 fold ($p<0.05$). In contrast, however, only HPV18 E6 expression increased S727 STAT3 phosphorylation significantly, by an average of 5.6 fold ($p<0.01$) (Fig 3.2A, lane 3). In agreement with our observations from primary keratinocytes, the presence of the HPV oncoproteins did not alter the level of total STAT3 protein.

Next, it was important to investigate whether the viral oncoproteins are responsible for the increased STAT3 phosphorylation observed in HPV18-containing keratinocytes. For this, E6 expression was silenced in the HPV18-containing keratinocytes using a pool of E6-specific siRNA and the levels of phosphorylated STAT3 compared to those in cells transfected with a scrambled control siRNA (Fig 3.2B). Treatment with the E6-siRNA resulted in a loss of E6 protein expression coupled to an increase in levels of the E6 target p53 (Fig 3.2B). Importantly, the loss of E6 also correlated with a significant reduction in both Y705 and S727 STAT3 phosphorylation ($p<0.001$). The depletion of HPV E6 also resulted in decreased E7 expression (average of 55%) (Fig 3.2B). To rule out any contributory role for this oncoprotein, the effects of HPV E7

expression on STAT3 phosphorylation was also assessed. Treatment of HPV18 containing cells with E7-specific siRNA reduced E7 protein expression by approximately 60% without impacting on either E6 expression or STAT3 phosphorylation (Fig 3.2C). To test the contribution of the E5 oncoprotein, a recently generated primary keratinocyte line from our lab containing an E5 knockout HPV18 genome was used {Wasson:2017ju}. In this system, the loss of E5 did not reduce STAT3 phosphorylation in either monolayer cultures differentiated in high calcium media or organotypic raft cultures (Fig 3.2D and E) In summary, these data indicate that E6 is the protein predominantly responsible for increasing STAT3 phosphorylation in HPV18-containing keratinocytes.

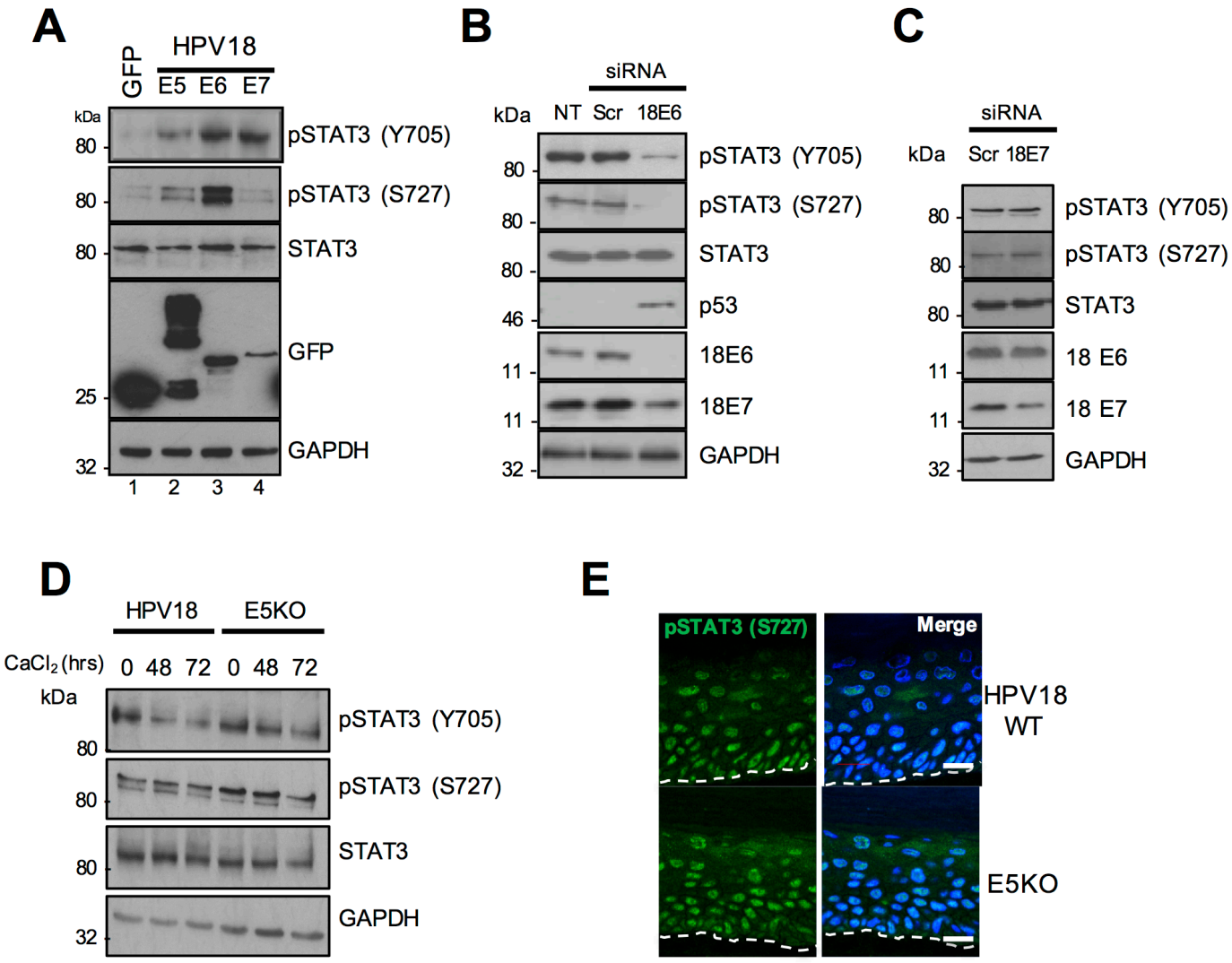

Figure 3.2. HPV E6 is necessary and sufficient for the dual phosphorylation STAT3. A) Representative western blot of C33A cells transfected with GFP tagged HPV18 oncoproteins E5, E6 or E7 and analyzed for STAT3 activation using specific antibodies detecting phosphorylated and total STAT3. Expression of HPV oncoproteins was confirmed using a GFP antibody. GAPDH served as a loading control. A) Representative western blot of HPV18 containing keratinocytes transfected with a two HPV18 E6 specific siRNA and analysed for phosphorylated and total STAT3, HPV18 E6 and E7 and p53. GAPDH expression was used as a loading control. **B)** Representative western blots of HPV18 containing keratinocytes

transfected with HPV18 E7 specific siRNA and analysed for phosphorylated and total STAT3, HPV18 E6 and E7. GAPDH expression was used as a loading control. **C**) Representative western blots of HPV18-containing keratinocytes and HPV18 E5KO containing keratinocytes subjected to high calcium differentiation and analysed for phosphorylated and total STAT3. GAPDH serves as a loading control. **D)** Representative sections of organotypic raft cultures from HPV18 wild type and HPV18 E5KO-containing keratinocytes stained with antibodies specific for pS727 STAT3 and counterstained with DAPI to highlight the nuclei (blue in the merged panels). Images were acquired using identical exposure times. Scale bar, 20 μm. White dotted lines indicate the basal cell layer.

To address whether increased STAT3 phosphorylation correlated with enhanced STAT3 transactivation, the activity of two STAT3-dependent luciferase reporter plasmids was measured. C33A cells were co-transfected with isolated HPV18 oncoproteins and reporter plasmids driving firefly luciferase from the *β-casein* (373) and pro-opiomelanocortin (*Pom*^{C}) (374) promoters. Expression of HPV18 E5 and E7 did not significantly increase STAT3-dependent luciferase expression. Conversely, expression of HPV18 E6 led to an average 8-fold increase in β-casein promoter-driven luciferase ($p<0.01$) and a 5.5-fold increase in Pom^{C}-driven luciferase ($p<0.01$) (Fig 3.3A). Whilst these reporter constructs have been widely used to monitor the activation of STAT3, they can also be responsive to other members of the STAT family of transcription factors {Kitamura:2006hl, Macdonald:2004gn}. In this regard, a recent study identified that HPV31 activates STAT5, which is necessary for HPV31 genome amplification {Hong:2013fh}. To exclude the possibility that the increase in luciferase expression was a result of STAT5 activation, we used small molecule inhibitor molecules to specifically block the activation of STAT3 and STAT5 (Fig 3B). Transfected C33A cells were treated with the STAT5 inhibitor pimozide (150) or two chemically distinct STAT3 inhibitors, cryptotanshinone and S3I-201. Cells treated with pimozide showed no reduction in luciferase expression, whereas treatment with the two STAT3 inhibitors resulted in a significant ($p<0.01$) reduction in β-casein-driven luciferase expression (Fig 3.3B).

Next, the impact of HPV E6 on the expression of endogenous STAT3-dependent gene products was assessed. Expression of HPV18 E6 in C33A cells led to increased expression of cyclin D1 and Bcl-$_{X}$L, two well characterised STAT3-dependent gene products (Fig 3.3C). To confirm that the induction of cyclin D1 and Bcl-xL was STAT3-dependent, E6 expressing cells were treated with cryptotanshinone and S3I-201.

Treatment with either inhibitor reduced STAT3 phosphorylation at both tyrosine and serine residues and also reduced cyclin D1 and Bcl-xL expression to control levels (Fig 3.3C). To understand if this was at the level of gene transcription, qRT-PCR analysis was performed. The data showed E6-dependent increases in cyclin D1(*ccnd1*) and Bcl-$_X$L (*bcl2l1*) mRNA transcripts, and these increases were sensitive to treatment with STAT3 inhibitors (*ccnd1* plus crypto $p<0.01$ and *bcl2l1* plus crypto $p<0.05$) (Fig 3.3D and E). Additional STAT3-dependent genes, including HIF1α and Survivin (*birc5*), were up-regulated by E6 in a STAT3-dependent manner (*hif1*α plus crypto $p<0.05$ and *birc5* plus crypto $p<0.001$) (Fig 3.3F and G). Taken together, these data suggest HPV E6 increases the transcription of STAT3-dependent genes.

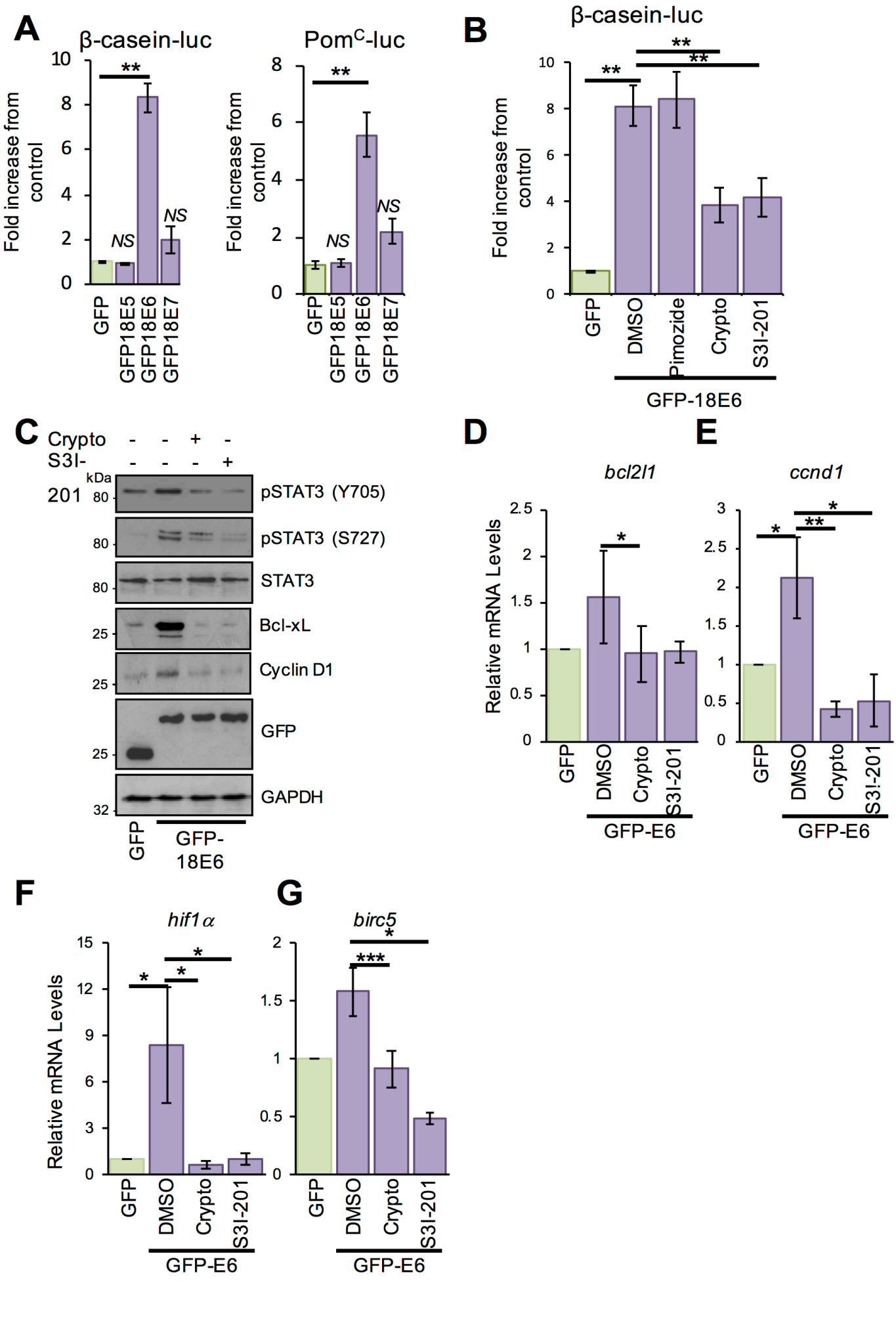
A
β-casein-luc
Pom^C-luc
Fold increase from control
NS
**
GFP
GFP18E5
GFP18E6
GFP18E7
B
β-casein-luc
Fold increase from control
**
GFP
DMSO
Pimozide
Crypto
S3I-201
GFP-18E6
C
Crypto
S3I-201
kDa
pSTAT3 (Y705)
pSTAT3 (S727)
STAT3
Bcl-xL
Cyclin D1
GFP
GAPDH
GFP
GFP-18E6
D
bcl2l1
Relative mRNA Levels
*
GFP
DMSO
Crypto
S3I-201
GFP-E6
E
ccnd1
*
**
GFP
DMSO
Crypto
S3I-201
GFP-E6
F
hif1α
Relative mRNA Levels
*
GFP
DMSO
Crypto
S3I-201
GFP-E6
G
birc5
*
***
GFP
DMSO
Crypto
S3I-201
GFP-E6

Figure 3.3. HPV E6 promotes STAT3 activation and STAT3-dependent gene expression. A) Representative luciferase reporter assays from C33A cells co-transfected with GFP tagged HPV18 oncoproteins E5, E6 or E7 and either a β-casein promoter reporter plasmid (left) or a Pom^C reporter plasmid (right), which contain STAT3 binding sites, and promoter activity measured using a dual-luciferase system. Data are presented as relative to the GFP transfected control cells. Bars represent the means ± standard deviation from at least three independent biological repeats. *P<0.05, *NS* = not significant (Student's t-test). **B)** Representative luciferase reporter assay from C33A cells co-transfected with GFP-E6 and a β-casein promoter reporter plasmid treated with the STAT3 inhibitors cryptotanshinone and S3I-201, and the STAT5 inhibitor pimozide. Promoter activity was measured using a dual-luciferase system. Data are presented as relative to the GFP transfected control. Bars represent the means ± standard deviation from at least three independent biological repeats. *P<0.05, **P<0.01 (Student's t-test). **C)** Representative western blot of C33A cells transfected with GFP or GFP-18E6, untreated or treated with the STAT3 inhibitors as above and analysed for the expression of the STAT3 dependent genes cyclin D1 and Bcl-xL. GAPDH expression was used as a loading control. Data shown are representative of at least three biological repeats. **D-G)** C33A cells were transiently transfected with GFP or GFP-18E6 and left untreated or treated with the STAT3 inhibitors as above and RNA was extracted for qRT-PCR analysis of the indicated STAT3 dependent genes. Samples were normalized against U6 mRNA levels. Representative data are relative to the GFP transfected control. Bars are the means ± standard deviation from at least three biological repeats. *P<0.05, **P<0.01, ***P<0.001 (Student's t-test).

3.2.3 STAT3 is phosphorylated in cells expressing E6 mutants defective for E6AP binding, p53 degradation and PDZ domain-binding

HPV E6 proteins lack intrinsic enzymatic activities; therefore, to manipulate the host cell environment, high-risk E6 proteins have evolved the ability to interact with key cellular partners including E6AP, p53 and a number of PDZ-domain containing proteins to modulate cellular functions (154,158,169). To test if these well-studied partners of E6 are required for E6-dependent STAT3 phosphorylation, the levels of STAT3 phosphorylation were measured in cells transfected with wild type and mutant HPV18 E6 proteins deficient in their ability to bind p53, E6AP or PDZ domains. Valine substitution of phenylalanine at amino acid position four (F4V) generates an E6 protein incapable of destabilizing p53 (379). Whilst deficient for inhibiting p53 destabilization, the E6 F4V mutant enhanced STAT3 phosphorylation to levels comparable with wild type E6 (Fig 3.4A; compare lanes 2 and 4). Expression of an E6 mutant unable to interact with E6AP (L52A) (380), an interaction required for p53 degradation, impaired p53 degradation as expected, but retained the ability to enhance STAT3 phosphorylation (Fig 3.4A; lane 5). Finally, the requirement for HPV E6 interaction with PDZ proteins in E6 mediated STAT3 phosphorylation was assessed by engineering a HPV18 E6 ΔPDZ, which lacks the C-terminal four amino acid PDZ-binding motif and cannot bind to PDZ domains (381). When expressed in C33A cells, this mutant protein induced STAT3 phosphorylation to wild type E6 levels (Fig 3.4A; compare lanes 2 and 3). Additionally, organotypic raft cultures were generated from NHK harbouring wild type and ΔPDZ HPV18 genomes (381). STAT3 S727 phosphorylation was observed throughout the basal and suprabasal layers of the HPV18 wild type and ΔPDZ containing rafts (Fig 3.4B), together suggesting that E6 promotes STAT3 phosphorylation through a p53 and PDZ independent manner.

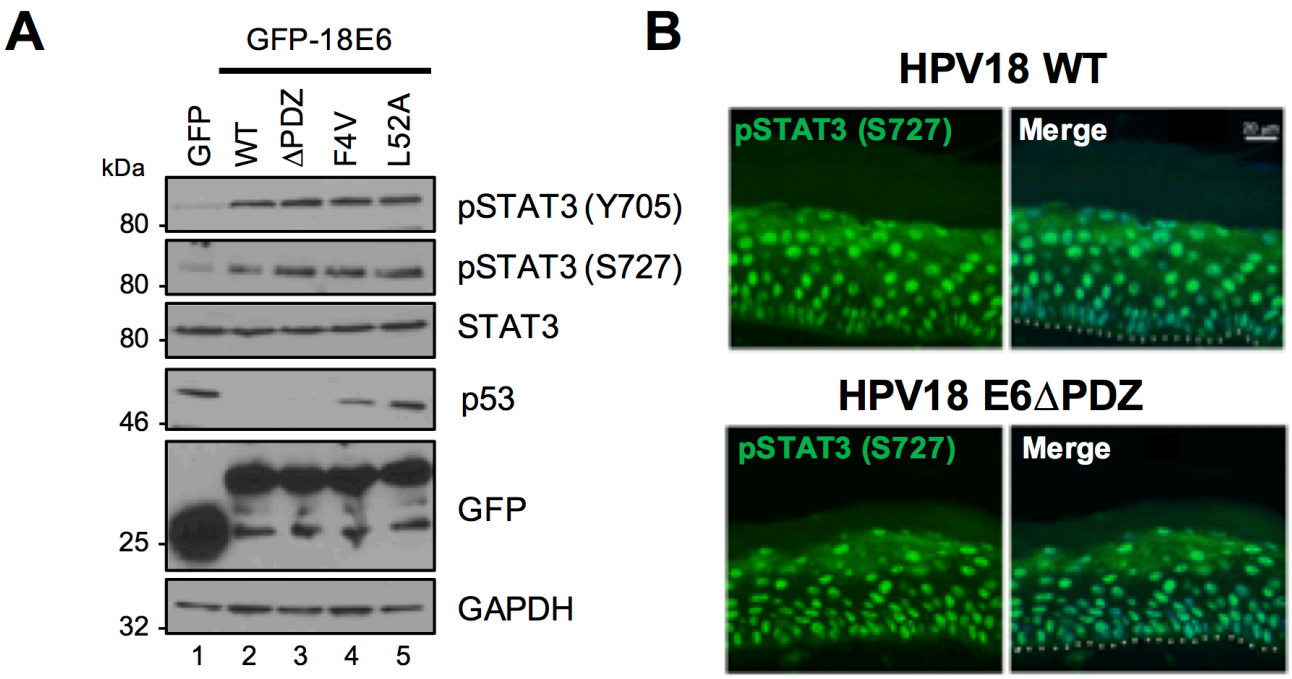

Figure 3.4. STAT3 is phosphorylated in cells expressing E6 defective for p53 degradation and PDZ domain binding. **A)** Representative western blot of C33A cells transfected with GFP or GFP tagged HPV18 E6 wild type, E6 ΔPDZ, E6 F4V or L52A and analyzed using antibodies detecting phosphorylated and total STAT3 and p53. GAPDH expression was used as a loading control and GFP confirmed expression of the E6 proteins. Data presented are representative of at least three independent experiments. **B)** Organotypic raft sections were stained with an antibody specifically detecting STAT3 pS727 (green) and counterstained with DAPI to highlight the nuclei (blue – in merged panels). Images were acquired with identical exposure times. The dotted line indicates the basal cell layer. Scale bar, 20 μm.

3.2.4 Janus kinases (JAK) are responsible for STAT3 Y705 phosphorylation in HPV18 containing keratinocytes

Janus family receptor-associated tyrosine kinases are the most common kinases responsible for mediating STAT3 Y705 phosphorylation, which is deemed necessary for STAT3 activation (283). Previously, it has been shown that the non-specific JAK inhibitor AG490 prevented STAT3 tyrosine phosphorylation in HPV16-positive cervical cancer cells (370). To discover if JAKs played a role in HPV mediated STAT3 phosphorylation during the viral life cycle, activation of JAK2 was assessed in HPV containing keratinocytes. Levels of phosphorylated JAK2 were higher in HPV18-containing keratinocytes compared to NHK controls, and this phosphorylation was retained during differentiation (Fig 3.5A). Next, levels of JAK2 phosphorylation were assessed in cells overexpressing GFP HPV18 E6. Western blot analysis showed increased JAK2 tyrosine phosphorylation in C33A cells expressing GFP-18E6 compared to GFP control (Fig 3.5B; compare lanes 1 and 2). Finally, in order to identify if JAK kinase activity was required for HPV-mediated STAT3 phosphorylation, HPV18-containing keratinocytes were treated with the clinically available JAK1/2 inhibitor Ruxolitinib (382), or the JAK2 inhibitor Fedratinib (383). Treatment with either inhibitor led to a marked reduction in STAT3 Y705 phosphorylation without affecting S727 phosphorylation (Fig 3.5C; compare lane 1 to 2 and 3). These results indicate that JAK2 is the major mediator of the STAT3 Y705 phosphorylation observed in HPV18-containing primary keratinocytes.

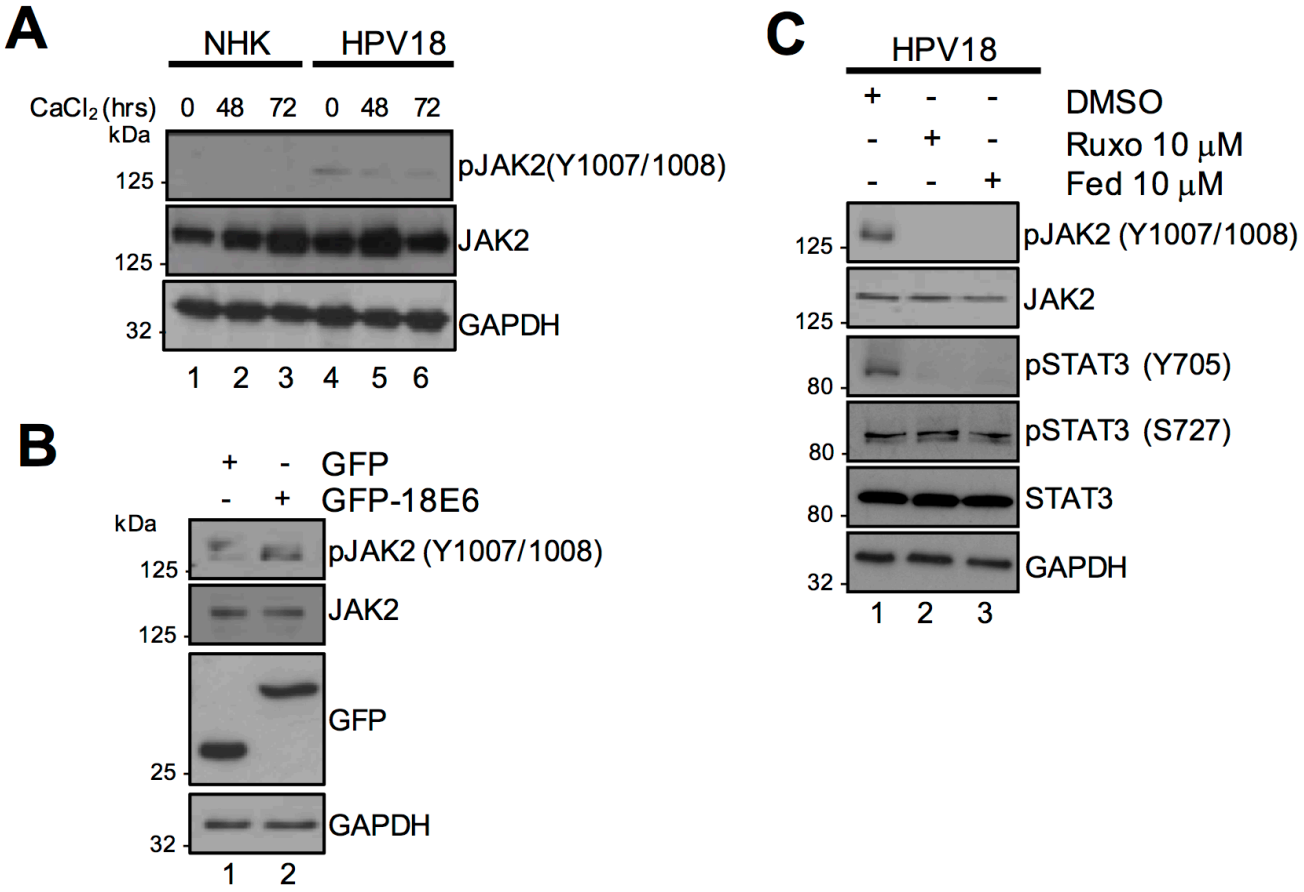

Figure 3.5. JAK2 is responsible for tyrosine phosphorylation of STAT3 in HPV18 containing keratinocytes. A) Representative western blot of normal human keratinocytes (NHK) and HPV18 containing keratinocytes subjected to high calcium differentiation and analysed for phosphorylated and total JAK2. GAPDH serves as a loading control. **B)** Representative western blot of C33A cells transfected with GFP or GFP-18E6 analysed for phosphorylated and total JAK2. GAPDH expression was used as a loading control and GFP confirmed expression of the E6 proteins. **C)** Representative western blot of HPV18 containing keratinocytes incubated with the JAK1/2 inhibitor Ruxolitinib or JAK2 inhibitor Fedratinib analysed with antibodies detecting phosphorylated and total STAT3. GAPDH served as a loading control. Data shown are representative of at least three independent biological repeats.

3.2.5 Functionally redundant MAPK proteins mediate STAT3 S727 phosphorylation in HPV18-containing keratinocytes

In addition to the well-studied tyrosine phosphorylation of STAT3, the protein can also be phosphorylated at a serine residue in its transactivation domain. The precise role of this additional phosphorylation event is contentious; however, it has been postulated to be required for the maximal transcriptional activity of STAT3. A number of candidate STAT3 S727 kinases have emerged including; CDK5 (293), mTOR (292) and several PKC isoforms (290,291). However, the strongest evidence indicates that MAPK members mediate the serine phosphorylation of STAT3, since it is embedded within a strong MAPK consensus sequence (^{725}PM<u>S</u>P^{728}) (191). To identify the kinase(s) responsible for STAT3 serine phosphorylation, the activation status of each of the canonical MAPK members was first assessed in differentiating keratinocytes. In these studies, levels of total ERK1/2 were increased in HPV18-containing keratinocytes compared to NHK controls (Fig 3.6A; compare lanes 1–3 and 4–6). As expected, both basal and differentiation-induced ERK1/2 phosphorylation was greater in HPV positive cells (Fig 3.6; compare lanes 1 and 4, and lanes 3 and 6). Whereas total p38 protein expression did not alter in the presence of HPV18, the levels of p38 phosphorylation were greater in both undifferentiated and differentiated HPV18-containing keratinocytes (Fig 3.6A; compare lanes 1 and 4, 3 and 6). In contrast with ERK1/2 and p38, less is known of JNK1/2 regulation by HPV18; however, studies demonstrate that JNK1/2 signalling can prevent keratinocyte differentiation (384). In keeping with this role, levels of JNK1/2 phosphorylation were highest in undifferentiated NHKs,and decreased rapidly upon differentiation in high calcium media (Fig 3.6A; compare lanes 1 and 3). JNK1/2 phosphorylation also declined in differentiating HPV18 positive keratinocytes, but overall levels were noticeably higher

than in NHK (compare lanes 1 and 4, lanes 3 and 6). Together, these data demonstrate the presence of active MAPK members in HPV18 genome-containing cells. To confirm that MAPK activation was dependent on the actions of E6, transient transfection experiments were performed, and these demonstrated that the phosphorylation of all three MAPK members was increased in C33A cells expressing GFP-18E6 compared to a GFP control (Fig 3.6B).

To test the roles of endogenous MAPK in the phosphorylation of STAT3, the levels of STAT3 S727 phosphorylation in undifferentiated HPV18-containing cells was assessed after treatment with the p38 inhibitor VX-702 (385), the MEK1/2 inhibitor UO126 (386) and the JNK1/2 inhibitor JNK-IN-8 (387), alone or in combinations (Fig 3.6C and D). The STAT3 inhibitor cryptotanshinone served as a positive control in these experiments and the Mitogen and Stress activated protein Kinase (MSK) inhibitor SB-747651 acted as a negative control (388). As shown in Fig 6C, STAT3 S727 and Y705 phosphorylation were significantly ($p<0.001$) impaired by cryptotanshinone (lane 2) but unaffected by the MSK inhibitor SB-747651 (lane 3). STAT3 Y705 phosphorylation remained intact in cells treated with the MAPK inhibitors, indicating that tyrosine phosphorylation of STAT3 is not dependent on active MAPK in keratinocytes, in line with our previous data. In contrast, whilst STAT3 S727 phosphorylation was largely unaffected in cells treated with VX-702 (p38 inhibitor), JNK-IN-8, and only partially suppressed by the MEK1/2 inhibitor UO126 (lanes 5 ($p<0.05$) and 7 ($p<0.01$)), the combination of UO126, VX-702 and JNK-IN-8, blocking all three MAPK members, was required to significantly ($p<0.001$) reduce STAT3 S727 phosphorylation (lane 8) (Fig 3.6D). Western blot analysis of the phosphorylated forms of the MAPK substrates MAPKAP-K2 (p38), MSK (ERK1/2) and c-Jun (JNK1/2) were used to demonstrate the efficacy of inhibitor treatment. Together, these data indicate

that several MAPK family members can phosphorylate STAT3 S727 in HPV18-positive keratinocytes.

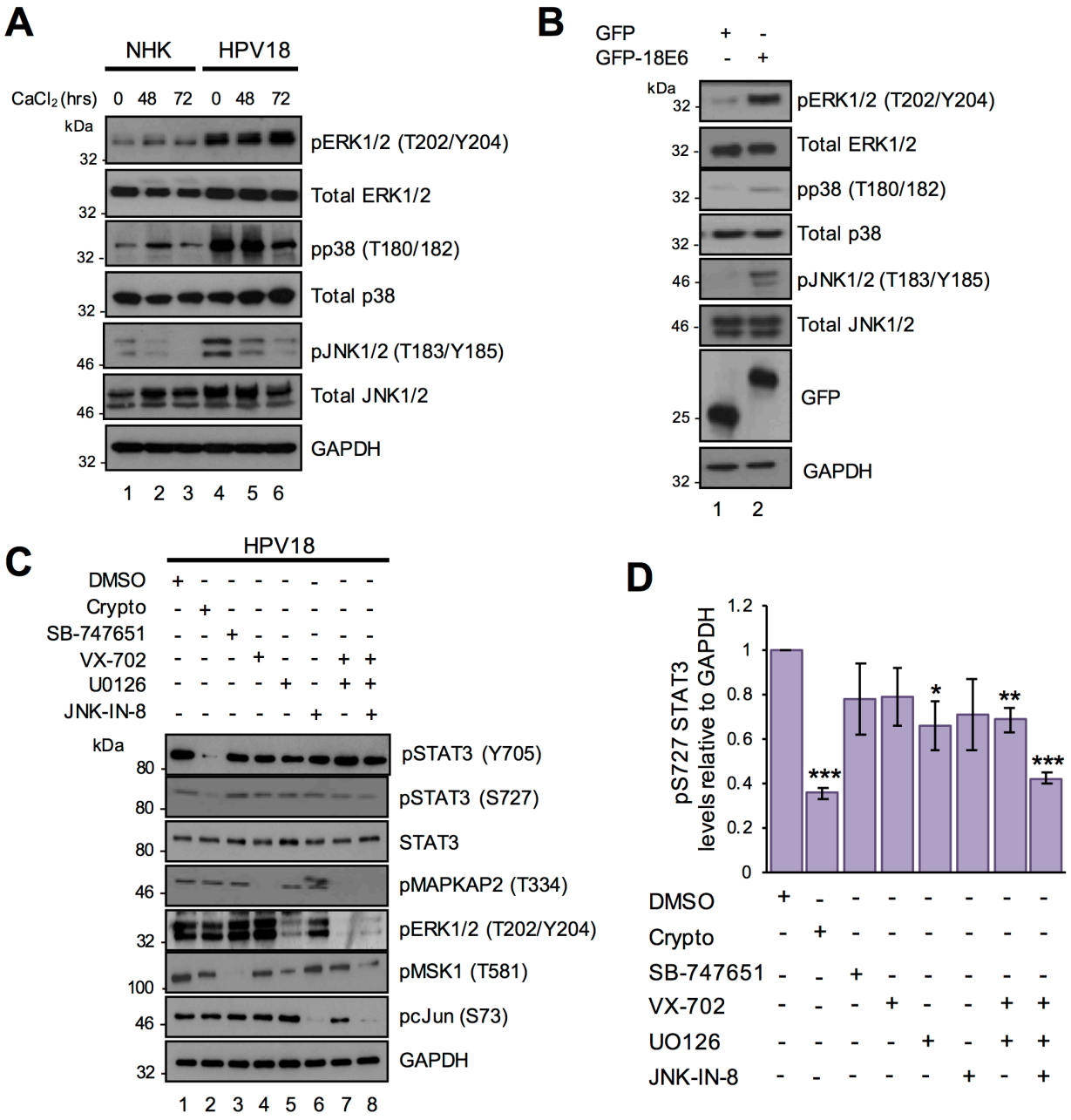

Figure 3.6. MAP kinases are responsible for serine phosphorylation of STAT3 in HPV18 containing keratinocytes. A) Representative western blot of normal human keratinocytes (NHK) and HPV18 containing keratinocytes subjected to high

calcium differentiation and analysed for total and phosphorylated forms of ERK1/2 (Thr202/Tyr204), p38 (Thr180/Tyr182) and JNK (Thr183/Tyr185). GAPDH served as a loading control. Data shown are representative of at least three independent biological repeats**. B)** Representative western blot of C33A cells transfected with GFP or GFP tagged HPV18 E6 analysed for the total and phosphorylated forms of ERK1/2 (Thr202/Tyr204), p38 (Thr180/Tyr182) and JNK (Thr183/Tyr185). GAPDH served as a loading control. **C)** Representative western blots of HPV18 containing keratinocytes treated with specific inhibitors of STAT3 (Crypto), MSK1 (SB-747651A**;** SB), p38 (VX-745; VX)), JNK (JNK-IN-8), Mek1/2 (UO126) or in combination as described in the methods and materials and examined with antibodies specific for phosphorylated and total STAT3. The phosphorylation status of substrate proteins pMSK1 (T581), p-cJun (S63), pMAPKAPK2 (T334), and ERK1/2 (T202/Y204) demonstrated inhibitor efficacy and specificity. **D)** Quantification of the protein band intensities of (C) standardised to GAPDH and shown relative to the DMSO control. Bars represent the means ± standard deviation from at least three independent biological repeats. *P<0.05, **P<0.01, ***P<0.001 (Student's t-test).

3.2.6 Active STAT3 is required for viral gene expression in undifferentiated primary keratinocytes

The data thus far suggests that STAT3 is activated in HPV18-containing keratinocytes; it was then important to investigate if STAT3 was necessary for the virus life cycle. For this, STAT3 was depleted from HPV18-containing keratinocytes using a panel of four commercially-validated siRNAs. Each siRNA produced a reproducible depletion of STAT3 by an average of 38% compared to a scrambled control (Fig 3.7A). Despite the relatively modest depletion of STAT3, expression of the HPV18 E6 and E7 proteins was significantly reduced compared to the scrambled control (Fig 3.7A). To assess if the inhibition of HPV18 oncoprotein expression occurred at the transcriptional level, HPV18 containing keratinocytes were transfected with a pool of STAT3 siRNA, and mRNA expression was assessed by qRT-PCR for the levels of STAT3, E6 and E7 transcripts. STAT3 depletion ($p<0.05$) caused a significant decrease in early oncogene expression (E6 $p<0.05$, E7 $p<0.05$), indicating that STAT3 has a role in HPV gene expression in undifferentiated cells (Fig 3.7B).

In combination with our knock down strategy, small molecule inhibitors were used to specifically block STAT3 phosphorylation and activation. HPV protein expression in undifferentiated HPV18-containing keratinocytes treated with increasing concentrations of the STAT3 inhibitor cryptotanshinone was then analysed by western blot. As shown in Fig 3.7C, inhibitor treatment reduced STAT3 phosphorylation at both sites in a dose-dependent manner, whilst having no impact upon keratinocyte viability during the experiment (Fig 3.7D). Concentrations of cryptotanshinone that blocked STAT3 phosphorylation also decreased HPV E6 and E7 protein expression (Fig 3.7C) and transcript levels ($p<0.05$) (Fig 3.7E).

Next, the importance of the individual phosphorylation sites was investigated, as there is debate about the role of serine phosphorylated STAT3 (280,286). For this, dominant negative forms of STAT3 were used in which Y705 was replaced with a phenylalanine or S727 substituted with an alanine, generating mutants with a single un-phosphorylatable site (389,390). The STAT3 mutants were expressed in HPV18-containing keratinocytes and the effect of STAT3 phosphorylation was assessed by western blot. Importantly, expression of the Y705F mutant abolished tyrosine phosphorylation without affecting serine phosphorylation; similarly, expression of S727A abolished serine phosphorylation without affecting tyrosine phosphorylation (Fig 3.7F compare lanes 3 and 4). Notably, expression of either of the phosphorylation site mutants led to a substantial reduction in HPV18 E6 and E7 protein expression (Fig 3.7F). Taken together, these data demonstrate that dual STAT3 phosphorylation is essential for HPV oncogene expression in undifferentiated keratinocytes.

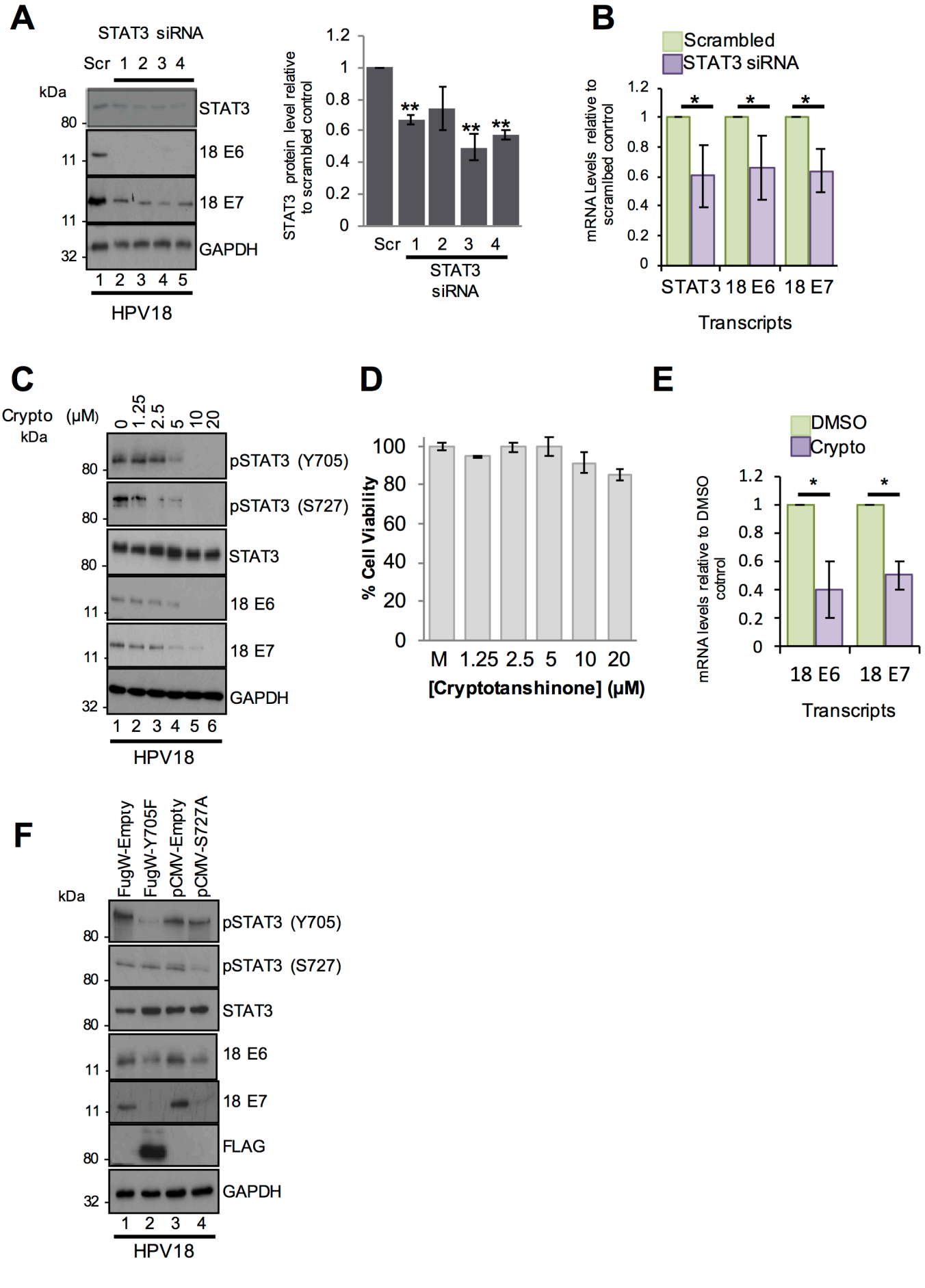
A
STAT3 siRNA
Scr 1 2 3 4
kDa
80
11
11
32
STAT3
18 E6
18 E7
GAPDH
1 2 3 4 5
HPV18
STAT3 protein level relative to scrambled control
1.2
1
0.8
0.6
0.4
0.2
0
**
**
**
Scr 1 2 3 4
STAT3 siRNA
B
Scrambled
STAT3 siRNA
mRNA Levels relative to scramlbed conrtrol
1.2
1
0.8
0.6
0.4
0.2
0
*
*
*
STAT3 18 E6 18 E7
Transcripts
C
Crypto (μM)
0 1.25 2.5 5 10 20
kDa
80
80
80
11
11
32
pSTAT3 (Y705)
pSTAT3 (S727)
STAT3
18 E6
18 E7
GAPDH
1 2 3 4 5 6
HPV18
D
% Cell Viability
100
80
60
40
20
0
M 1.25 2.5 5 10 20
[Cryptotanshinone] (μM)
E
DMSO
Crypto
mRNA levels relative to DMSO cotnrol
1.2
1
0.8
0.6
0.4
0.2
0
*
*
18 E6 18 E7
Transcripts
F
FugW-Empty
FugW-Y705F
pCMV-Empty
pCMV-S727A
kDa
80
80
80
11
11
80
32
pSTAT3 (Y705)
pSTAT3 (S727)
STAT3
18 E6
18 E7
FLAG
GAPDH
1 2 3 4
HPV18

Figure 3.7. STAT3 is required for viral gene expression in undifferentiated keratinocytes. **A)** Left: Representative western blot of HPV18 containing keratinocytes transfected with a panel of 4 STAT3 specific siRNA and a scrambled control and analysed for total STAT3 antibody and HPV18 E6 and E7. GAPDH served as loading control. Right: Quantification of the STAT3 protein band intensities standardised to GAPDH levels. Data are expressed as fold reduced compared to scramble siRNA treated cells. Bars represent the means ± standard deviation of at least three biological repeats. **p <0.01 (Student's t-test). **B)** RNA was extracted from HPV18 containing keratinocytes after transfection with a pool of four STAT3 specific siRNA and qRT-PCR analysis was performed for expression of the *stat3* and HPV early genes. Samples were normalized against U6 mRNA levels and data are presented relative to the scrambled control. Bars represent means ± standard deviation of at least three biological repeats. *P<0.05 (Student's t-test). **C)** Representative western blot from HPV18 containing keratinocytes treated with increasing doses of the STAT3 inhibitor cryptotanshinone and analysed with antibodies specific for phosphorylated and total STAT3, and HPV18 E6 and E7. GAPDH served as a loading control. Data are representative of at least three biological repeats. **D)** MTT assay was performed in HPV18 containing keratinocytes treated with increasing doses of the STAT3 inhibitor cryptotanshinone. **E)** RNA was extracted from HPV18 containing keratinocytes treated with 10 μM cryptotanshinone and qRT-PCR analysis performed for levels of HPV E6 and E7 mRNA. Samples were normalized against the U6 mRNA levels and expressed relative to the DMSO control. Bars represent means ± standard deviation of at least three biological repeats. *P<0.05 (Student's t-test). **F)** Representative western blot from HPV18 containing keratinocytes transduced with a lentivirus encoding a dominant negative Y705F

phospho-site mutant or transiently transfected with a dominant negative STAT3 S727A mutant and analysed for phosphorylated and total STAT3 and HPV18 E6 and E7. An antibody detecting the FLAG epitope confirmed expression of the Y705F STAT3 mutant and GAPDH served as a loading control. Data shown are representative of at least three biological repeats.

3.2.7 Suppression of STAT3 impairs cell cycle progression and results in loss of HPV18 genome maintenance in undifferentiated keratinocytes

As STAT3 is an important mediator of cell proliferation, the impact of STAT3 inhibition on the proliferation of HPV containing keratinocytes was assessed. Western blot analyses were performed to determine the expression of the STAT3-dependent gene product and key cell cycle regulator cyclin D1, in undifferentiated HPV-positive keratinocytes after 24 hours of cryptotanshinone treatment. Treatment with cryptotanshinone decreased the expression of cyclin D1 in a dose-dependent manner (Figure 3.8A). Lower levels of cyclin D1 protein expression correlated with significantly ($p<0.01$) lower levels of cyclin D1 mRNA in these cells as confirmed by qRT-PCR (Fig 3.8B). In addition to our inhibitor data, depletion of total STAT3 protein by siRNA (Fig 3.8C) or expression of dominant negative forms of STAT3 (Fig 3.8D) also resulted in reduced cyclin D1 expression in HPV containing keratinocytes. STAT3 also contributes to cell cycle progression through regulation of the cyclin dependent kinase (CDK) inhibitor $p21^{WAF1/CIP1}$. Inhibition of STAT3 activity, or loss of STAT3 protein expression, led to an up-regulation of $p21^{WAF1/CIP1}$ expression at both the protein and transcript level (Fig 3.8A–D).

As cell cycle progression depends on the temporal expression of cyclins, the effect of STAT3 inhibition or loss of STAT3 expression on the cell cycle was analysed by flow cytometry. When HPV18-containing keratinocytes were treated with cryptotanshione, there was an accompanying increase of cells in S phase ($p<0.05$), with a decrease of cells in the G2/M phases ($p<0.001$) (Fig 3.8E). This is in contrast to normal keratinocytes, in which cryptotanshinone treatment had no significant impact on the cell cycle profile (Fig 3.8F). Similar results were achieved after depletion of STAT3 by

siRNA ($p<0.001$) (Fig 8G), together suggesting that STAT3 is essential for cell cycle progression and the proliferative ability of HPV containing keratinocytes.

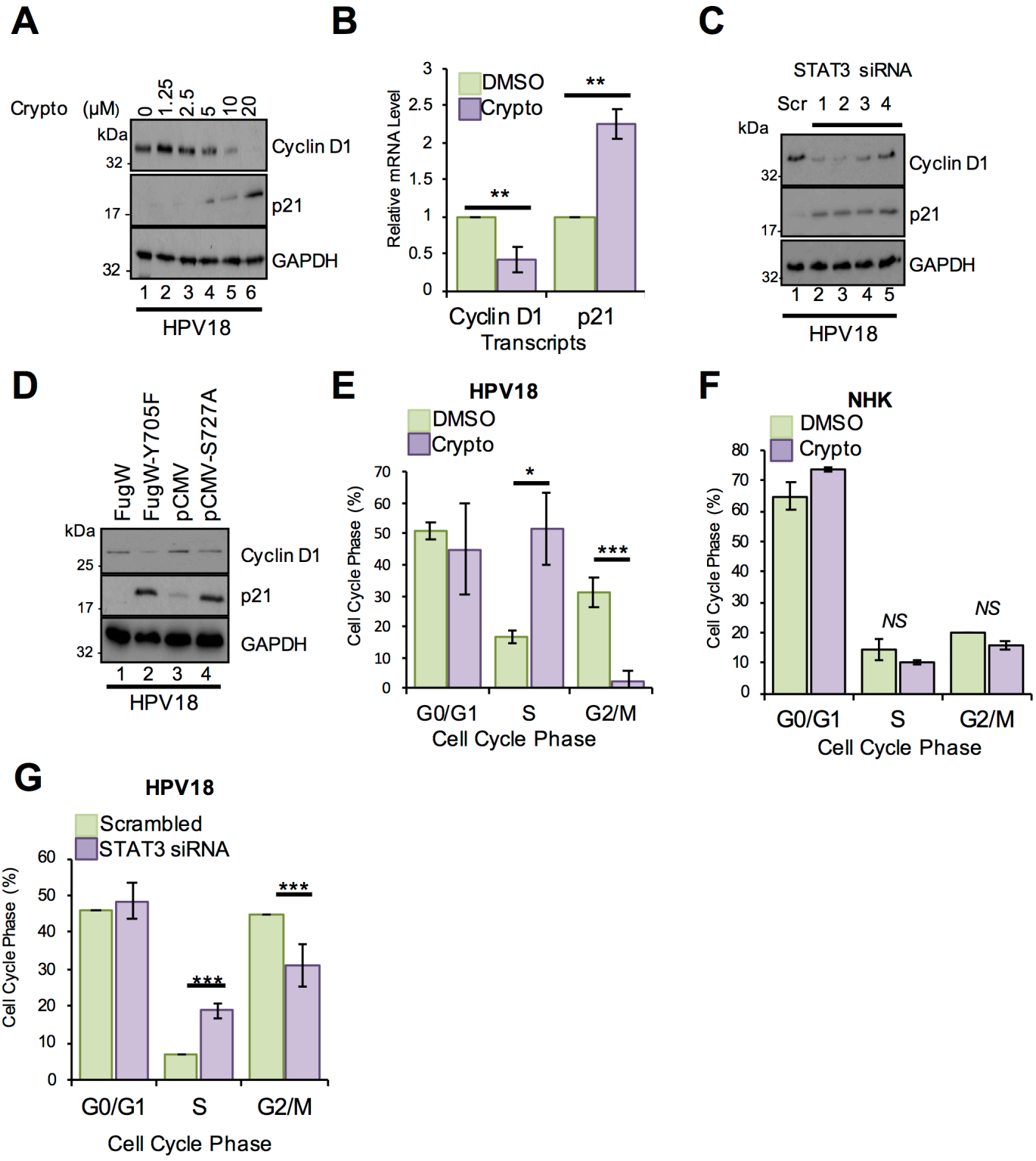
A
Crypto (μM) 0 1.25 2.5 5 10 20
kDa
32
Cyclin D1
17
p21
32
GAPDH
1 2 3 4 5 6
HPV18
B
DMSO
Crypto
Relative mRNA Level
3
2.5
2
1.5
1
0.5
0
**
**
Cyclin D1
p21
Transcripts
C
STAT3 siRNA
Scr 1 2 3 4
kDa
32
Cyclin D1
17
p21
32
GAPDH
1 2 3 4 5
HPV18
D
FugW
FugW-Y705F
pCMV
pCMV-S727A
kDa
25
Cyclin D1
17
p21
32
GAPDH
1 2 3 4
HPV18
E
HPV18
DMSO
Crypto
Cell Cycle Phase (%)
70
60
50
40
30
20
10
0
*
***
G0/G1
S
G2/M
Cell Cycle Phase
F
NHK
DMSO
Crypto
Cell Cycle Phase (%)
80
70
60
50
40
30
20
10
0
NS
NS
G0/G1
S
G2/M
Cell Cycle Phase
G
HPV18
Scrambled
STAT3 siRNA
Cell Cycle Phase (%)
60
50
40
30
20
10
0
***
***
G0/G1
S
G2/M
Cell Cycle Phase

Figure 3.8. Suppression of STAT3 impairs cell cycle progression and HPV genome maintenance in undifferentiated keratinocytes. A) Representative western blot from HPV18-containing keratinocytes treated with increasing doses of the STAT3 inhibitor cryptotanshinone and analysed for cyclin D1 and p21 expression. GAPDH served as loading control. **B)** RNA was extracted from HPV18 containing keratinocytes incubated with 10 μM cryptotanshinone and analysed by qRT-PCR for levels of *ccnd1* and *p21* mRNA. Samples were normalised against U6 mRNA levels and presented relative to the DMSO control. Bars represent means ± standard deviation of at least three biological repeats. **P<0.01 (Student's t-test). **C)** Representative western blot of HPV18 -containing keratinocytes transfected with a panel of 4 STAT3 specific siRNA and a scrambled control and analysed by western blotting using antibodies specific for cyclin D1 and p21. GAPDH served as loading control. **D)** Representative western blot from HPV18 containing keratinocytes transduced with a lentivirus encoding a dominant negative Y705F phospho-site mutant or transiently transfected with a dominant negative STAT3 S727A mutant and analysed by blotting with antibodies specific for cyclin D1 and p21. GAPDH served as loading control. Data are representative of at least three biological independent repeats. Representative flow cytometric analysis of the cell cycle in HPV18 containing keratinocytes treated with 10 μM cryptotanshione (**E**), NHKs treated with 10 μM cryptotanshinone (**F**) or a pool of four STAT3 specific siRNAs (**G**). All data are expressed as percentage of cells at each stage of the cell cycle. Bars represent means ± standard deviation of at least three biological repeats. *P<0.05, ***P<0.001 (Student's t-test) compared to DMSO or scrambled control cells.

3.2.8 STAT3 is necessary for delayed differentiation and increased keratinocyte proliferation in stratified epithelia

Given that levels of STAT3 phosphorylation were maintained upon keratinocyte differentiation, STAT3 may also be important during the differentiation-dependent stages of the HPV18 life cycle. HPV18-containing keratinocytes were co-cultured for 48 hours in media containing high calcium to induce differentiation and cryptotanshinone to block STAT3 activation. Phosphorylation of STAT3 and the expression of HPV E6 and E7 were reduced but maintained upon differentiation in control cells; however, they were suppressed by cryptotanshinone treatment (Fig 3.9A; compare lanes 2 and 3). High expression levels of cyclin proteins are required for HPV-containing cells to remain active in the cell cycle upon differentiation to allow for virus genome amplification. In accordance with this, upon differentiation high levels of cyclin D1 were maintained, and expression of the CDK inhibitor $p21^{WAF1/CIP1}$ was not elevated (Fig 3.9A; compare lanes 1 and 2). STAT3 inhibition led to a reduction in cyclin D1 levels in differentiated cells (Fig 3.9A; compare lanes 2 and 3), and an increase in $p21^{WAF1/CIP1}$ expression (Fig 3.9A; compare lanes 2 and 3).

The switch between keratinocyte proliferation and differentiation is tightly controlled and STAT3 has been identified as a regulator of this process(391). As STAT3 inhibition reduced the proliferative ability of HPV18-containing keratinocytes, the impact of STAT3 inhibition on keratinocyte differentiation was analysed. In untreated HPV18-containing keratinocytes, levels of the differentiation-specific proteins involucrin and filaggrin did not increase significantly upon incubation in high calcium media (Fig 3.9A; compare lanes 1 and 2), consistent with the ability of HPV to suppress keratinocyte differentiation. In contrast, cells treated with cryptotanshinone displayed enhanced expression of these differentiation-dependent proteins (Fig 3.9A;

compare lanes 2 and 3). These experiments indicate that STAT3 regulates keratinocyte differentiation and cell proliferation in differentiating HPV-positive keratinocytes.

The monolayer differentiation assay suggested that the ability of HPV to promote cell cycle re-entry and delay differentiation was dependent on active STAT3. To understand this in the context of the full HPV life cycle, we transduced HPV18-containing keratinocytes with a lentivirus expressing the dominant negative STAT3 Y705F or an empty vector control (pFugW). The Y705F mutant was utilised as it appeared marginally more effective at impairing HPV gene expression compared to the S727A mutant (Fig 3.7D and 7E). After transduction, cells were seeded onto collagen plugs and grown as organotypic raft cultures, and sections stained with haematoxylin and eosin (Fig 3.9B). In comparison to NHK epithelium, the presence of HPV18 genomes was associated with a thickening of the supra and parabasal cell layers as previously show (381). Over-expression of the dominant negative STAT3 had no overall effect on raft morphology of NHK or HPV containing keratinocytes (Fig 3.9B); however, the thickness of the HPV containing keratinocytes was consistently and drastically reduced, with an appearance more closely resembling an NHK raft.

Viral amplification occurs in suprabasal cell that have an elongated G2 phase of the cell cycle. In G2, cyclin B accumulates in the cytoplasm; therefore, cells that have cytoplasmic cyclin B are likely to be cells where viral genome amplification is occurring (392). The raft cultures were therefore stained for the expression of cyclin B; in NHK rafts, cyclin B1 was only observed in the basal layers of the raft and this was unaffected by transduction with the Y705F STAT3 mutant (Fig 3.9C). In contrast, we observed a significant ($p<0.001$) decrease in the population of cyclin B1 positive suprabasal cells following staining of the Y705F transduced HPV18 rafts, relative to empty vector

transduced HPV18 rafts (Fig 3.9E and H). These data demonstrate that STAT3 inhibition leads to a failure of cells to maintain cell cycle activity in the suprabasal layers of the epithelia.

To investigate the impact of STAT3 inhibition on keratinocyte differentiation, rafts were stained for expression of the differentiation marker involucrin, an intermediate stage differentiation marker found in the suprabasal layer of the epithelia. In control transduced HPV18 rafts, involucrin expression is confined to the upper suprabasal layers (Fig 3.9F). In contrast, abundant involucrin staining was noted throughout the spinuous layers of the epithelium in rafts transduced with the dominant negative Y705F phosphorylation mutant. Finally, the effect of STAT3 activity on late viral function was assessed. Sections were also stained for the viral protein E1^E4, a marker of productive infection (70,378). E1^E4 staining was observed in the mid and upper suprabasal layers of HPV18 control rafts but was significantly ($p<0.001$) reduced in rafts expressing STAT3 Y705F (Fig 3.9G and H). Taken together, these data indicate that active STAT3 is not required for the formation of a stratified epithelium in NHK but is necessary for increased suprabasal cellular proliferation and cell cycle progression in cells harbouring HPV18 genomes. STAT3 function also contributes to the delay in differentiation and expression virus proteins observed in HPV-positive cells.

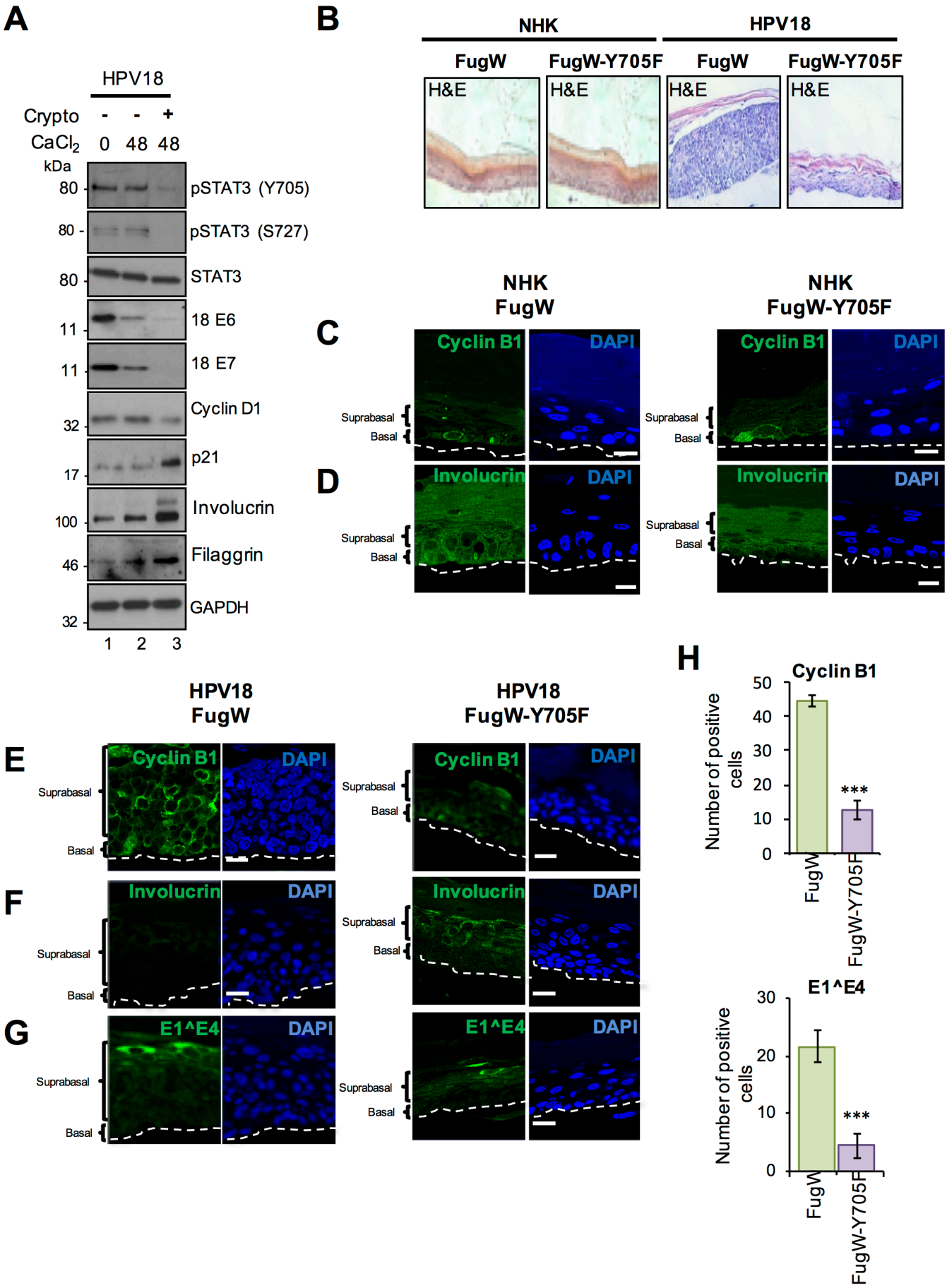
A
HPV18
Crypto - - +
CaCl2 0 48 48
kDa
80 pSTAT3 (Y705)
80 pSTAT3 (S727)
80 STAT3
11 18 E6
11 18 E7
32 Cyclin D1
17 p21
100 Involucrin
46 Filaggrin
32 GAPDH
1 2 3
B
NHK
HPV18
FugW
FugW-Y705F
FugW
FugW-Y705F
H&E
H&E
H&E
H&E
C
NHK FugW
NHK FugW-Y705F
Cyclin B1
DAPI
Suprabasal
Basal
D
Involucrin
E
HPV18 FugW
HPV18 FugW-Y705F
F
G
E1^E4
H
Cyclin B1
Number of positive cells
50
40
30
20
10
0
***
FugW
FugW-Y705F
E1^E4
30
20
10
0

Figure 3.9. STAT3 is necessary for delayed differentiation and increased keratinocyte proliferation in a stratified epithelium containing HPV. A) Representative western blots of phosphorylated and total STAT3, HPV18 E6 and E7, cyclin D1, p21, involucrin and filaggrin in differentiated HPV18 containing keratinocytes in the presence or absence of 10 μM cryptotanshione. Data shown represent at least three biological repeats. **B)** Representative organotypic raft cultures of NHK and HPV18 containing keratinocytes transduced with empty lentivirus and lentivirus expressing a dominant negative phosphorylation null Y705F mutant STAT3 fixed at day 14 and stained with haematoxylin and eosin (H&E) to assess morphology. **C-D)** Representative organotypic raft cultures of NHKs transduced with empty lentivirus and lentivirus expressing a dominant negative phosphorylation null Y705F mutant STAT3 fixed at day 14 and stained **C)** cyclin B1 and **D)** involucrin. Nuclei are visualised with DAPI (blue) and white dotted lines indicate the basal cell layer.

E-G) Representative organotypic raft cultures of HPV18 containing keratinocytes transduced with empty lentivirus and lentivirus expressing a dominant negative phosphorylation null Y705F mutant STAT3 fixed at day 14. Sections from HPV18 containing keratinocyte rafts were stained with antibodies against **E)** cyclin B1, **F)** involucrin and **G)** E1^E4. Nuclei are visualised with DAPI (blue) and white dotted lines indicate the basal cell layer. **H)** The number of cells positive for cyclin B1 and E1^E4 in the empty vector and Y705F STAT3 transduced HPV18 containing keratinocyte sections was counted in 5 fields of vision from sections of three independent raft cultures from two donor lines. Bars represent means ± standard deviation. ***P<0.001 (Student's t-test) compared to empty vector control.

3.2.9 STAT3 expression and phosphorylation positively correlate with disease state in cervical biopsies

Having demonstrated that STAT3 phosphorylation was increased in primary keratinocytes containing HPV18, the role of STAT3 phosphorylation in cervical cancer initiation and progression was assessed. Initially, the W12 *in vitro* cervical cancer progression model system was utilised (393). The W12 system was developed from a polyclonal culture of cervical squamous cells infected with HPV16, derived from a low-grade squamous intraepithelial lesion (LSIL). At early passages, these cells recapitulate an LSIL in organotypic raft cultures. However, following long-term culture these cells mirror the events associated with cervical cancer progression, with phenotypic progression to high-grade intraepithelial lesions (HSIL) and squamous cell carcinoma. Organotypic raft cultures were generated from NHK cells and a W12 clone representing a HSIL phenotype and stained for serine phosphorylated STAT3. In contrast to the NHKs, high levels of S727 phosphorylation was observed in the nuclei of cells throughout the basal and suprabasal layers of the HSIL raft (Fig 3.10A). These data confirm that STAT3 S727 phosphorylation is greater in a high-grade lesion compared to normal keratinocytes. They also confirm that increased STAT3 S727 phosphorylation is observed in the context of a high-risk HPV16 infection.

Next, cervical liquid-based cytology samples from a cohort of HPV16 positive patients representing the progression of disease development (CIN1-CIN3) and HPV negative normal cervical tissues were collected from the Scottish HPV archive and examined for phosphorylated and total STAT3 by western blot. In normal cervical tissue, STAT3 expression and phosphorylation was low (Fig 3.10B). However, STAT3 expression and phosphorylation at both tyrosine and serine residues increased in the disease samples and this correlated with cervical disease severity (Fig 3.10C-E). Finally,

immunofluorescence analysis was used to examine the levels of STAT3 S727 phosphorylation in human cervical sections classified as LSIL (CIN1), LSIL with foci of HSIL (CIN1/CIN2) and HSIL (CIN3). An analysis of the staining pattern showed a clear difference between the three groups (Fig 3.10F), with abundant STAT3 S727 phosphorylation in the high-grade neoplasia compared with lower grade lesions. Together, these findings demonstrate that STAT3 phosphorylation is increased in HPV positive keratinocytes including those of a natural HPV infection and these correlate with cervical disease progression.

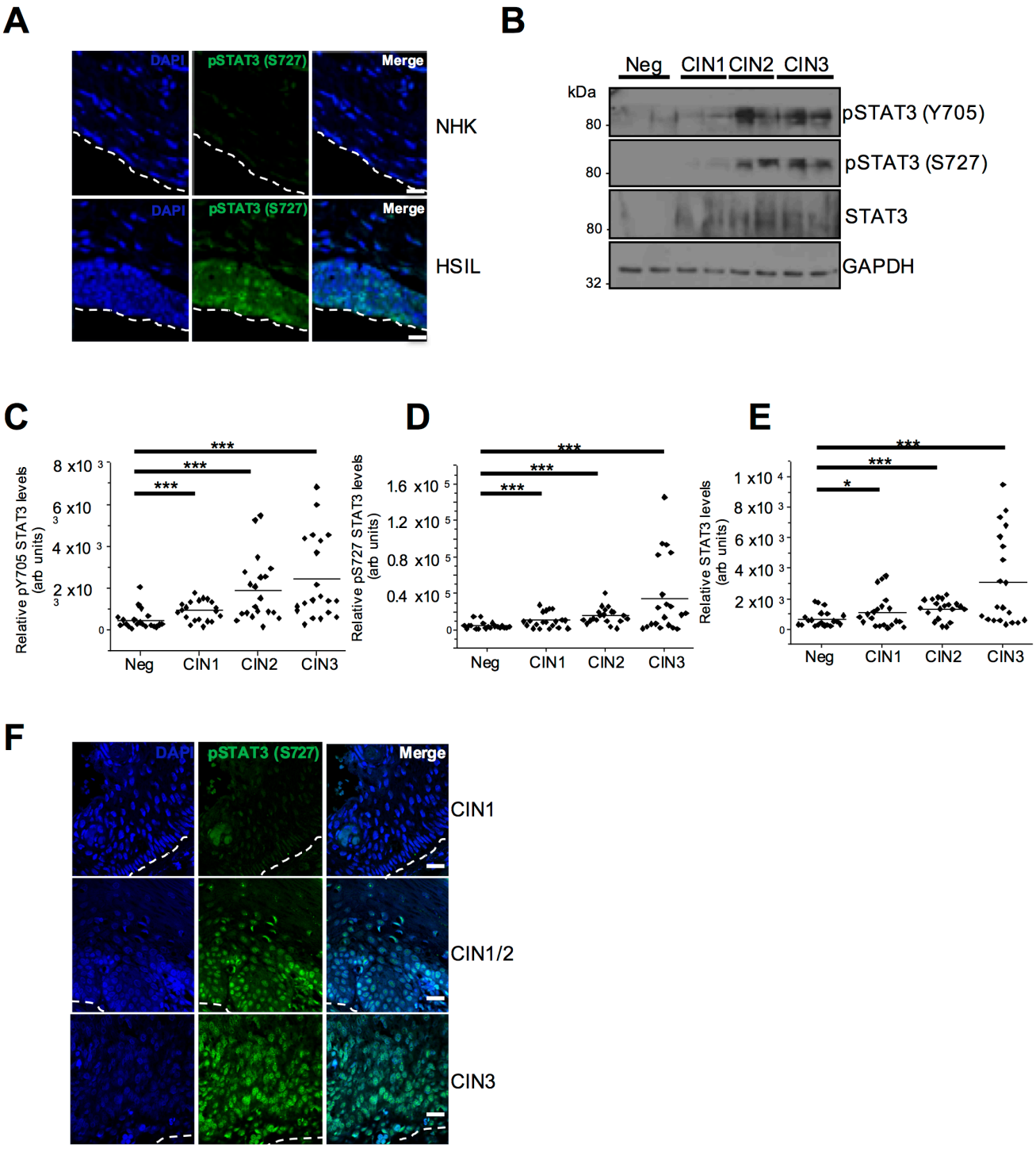
A
DAPI
pSTAT3 (S727)
Merge
NHK
HSIL
B
Neg
CIN1
CIN2
CIN3
kDa
80
80
80
32
pSTAT3 (Y705)
pSTAT3 (S727)
STAT3
GAPDH
C
Relative pY705 STAT3 levels (arb units)
8 x10 3
6 x10 3
4 x10 3
2 x10 3
0
***
***
***
Neg
CIN1
CIN2
CIN3
D
Relative pS727 STAT3 levels (arb units)
1.6 x10 5
1.2 x10 5
0.8 x10 5
0.4 x10 5
0
***
***
***
Neg
CIN1
CIN2
CIN3
E
Relative STAT3 levels (arb units)
1 x10 4
8 x10 3
6 x10 3
4 x10 3
2 x10 3
0
***
***
*
Neg
CIN1
CIN2
CIN3
F
DAPI
pSTAT3 (S727)
Merge
CIN1
CIN1/2
CIN3

Figure 3.10. STAT3 expression and phosphorylation is increased in HPV-associated cervical diseases A) Representative immunofluorescence analysis of sections from organotypic raft cultures of NHK and a W12 cell line presenting with HSIL morphology detecting pS727 STAT3 levels (green). Nuclei were visualized with DAPI (blue) and the white dotted line indicates the basal layer. Images were acquired with identical exposure times. **B)** Representative western blots from cytology samples of CIN lesions of increasing grade analysed with antibodies specific for phosphorylated (Y705 and S727) and total STAT3 levels. GAPDH served as a loading control. **C-E)** Scatter dot plot of densitometry analysis of a panel of cytology samples. 20 samples from each clinical grade (neg, CIN I-III) were analysed by western blot and densitometry analysis was performed using ImageJ. Phosphorylated STAT3 levels were first normalised against total STAT3 levels before normalising against protein levels using GAPDH as a loading control. **F)** Representative immunofluorescence analysis of tissue sections from cervical lesions of increasing CIN grade. Sections were stained for pS727 STAT3 levels (green) and nuclei were visualized with DAPI (blue). Images were acquired with identical exposure times. Scale bar, 20 μm. Bars represent the means ± standard deviation from at least three independent biological repeats. *P<0.05, **P<0.01, ***P<0.001 (Student's t-test).

3.3 Discussion

This study identifies the STAT3 transcription factor as a critical regulator of the HPV18 life cycle. Using calcium differentiation in monolayer, and organotypic raft culture models of primary human keratinocytes harbouring HPV18 episomes, this study demonstrates that STAT3 is necessary for cell cycle progression and HPV gene expression in both undifferentiated cells and in stratified epithelium. In undifferentiated cells, inhibition of STAT3 activity, either by small molecule inhibitors or expression of dominant negative STAT3 phosphorylation mutants, led to a reduction in HPV oncogene expression. Using ChIP-Seq, previous studied have demonstrated that STAT3 binds to the viral URR in HPV18-positive HeLa cervical cancer cells (370). Further studied will be required to identify if STAT3 controls viral transcription directly by binding to the viral URR, or indirectly by controlling the expression of host factors such as cyclin D1. This is one possible mechanism that HPV mediated up-regulation of STAT3 activity may drive viral transcription – by generating a cellular milieu favourable for virus transcription. In this regard, STAT3 is a driver of cell cycle progression and keratinocyte proliferation. Our results show that HPV-containing keratinocytes express cyclin D1 and this is largely STAT3-dependent as STAT3 inhibitor treatment, or depletion by siRNA, resulted in a loss of cyclin D1 expression and an increase in expression of the cell cycle arrest protein $p21^{WAF1/CIP1}$. Furthermore, these changes correlated with induction of S phase arrest of the cell cycle. This likely results from the reduced expression of cyclin D1, which in actively-cycling cells must be increased in expression in order for cells to transition into G2. A similar S-phase arrest is observed in Epstein Barr virus infected lymphoblastoid cell lines (LCLs), where STAT3 is required to relax the intra-S phase checkpoint (394). Intriguingly,

STAT3 inhibition had no discernable impact on the cell cycle profile of normal human keratinocytes, indicating that STAT3 is non-essential in HPV negative cells.

As STAT3 inhibition leads to an S phase accumulation in the cell cycle and a decrease in cells in G2, it is likely that STAT3 has a role in viral replication in HPV18-containing keratinocytes. Viral genome amplification occurs in the G2 phase of the cell cycle in the suprabasal layers of the epithelia (79); in these cells, G2 phase is identified by cytoplasmic cyclin B expression. As cyclin B expression is decreased in HPV18 raft expressing dominant negative STAT3 Y705F, it is likely that these cells have lost the ability to support viral genome amplification. Additionally, the viral protein E1^E4 is a mark of productive infection; as dominant negative STAT3 Y705F leads to a reduction in E1^E4 expression, viral genome amplification is likely to be impaired. Although these data collectively suggest that viral replication is likely to be disrupted, further work will assess the impact of STAT3 inhibition on viral episome maintenance in undifferentiated keratinocytes and on viral genome amplification in differentiating keratinocytes. Again, it should also be assessed whether or not this effect is direct – due to binding of STAT3 to the viral URR – or indirect, due to change the cellular milieu to favour viral replication.

Our studies show that HPV infection leads to enhanced STAT3 Y705 and S727 phosphorylation that are maintained at high levels during keratinocyte differentiation. Interestingly, all three HPV oncoproteins could induce STAT3 phosphorylation to a degree, but only E6 was sufficient to induce the dual phosphorylation and activation of STAT3. This is consistent with previous observations showing increased STAT3 Y705 phosphorylation in HPV-positive cancer cell lines and leading to increased levels of STAT3-dependent gene products {Shukla:2010kg, Shukla:2013hs}. A number of

cellular pathways converge to phosphorylate and activate STAT3 {Johnson:2018gu}. The role of serine STAT3 phosphorylation has been contentious; it has been demonstrated to be important for maximal transcriptional activity (286) or to inhibit tyrosine phosphorylated STAT3 (191). Using dominant negative STAT3 mutants that blocked phosphorylation at the specific tyrosine or serine residues, the results clearly demonstrate that in HPV containing keratinocytes, mono-phosphorylation of either site is insufficient to activate the STAT3-dependent genes analysed in this study. The data also demonstrate that phosphorylation of both sites in STAT3 is required for viral gene expression, suggesting that dual phosphorylated STAT3 is critical during the HPV life cycle. Moreover, our work does not support previous findings that S727 phosphorylation is detrimental to Y705 phosphorylation.

In addition to analysing the requirement for both STAT3 phosphorylation sites for the HPV life cycle, this study also identified the kinases involved in that phosphorylation in HPV18-containing keratinocytes. Using clinically available small molecule inhibitors, Y705 phosphorylation was demonstrated to be critically dependent on JAK2 activity in HPV containing keratinocytes. Whilst JAK kinases are the best characterised mediators of Y705 phosphorylation in other cellular systems, to the best of our knowledge no study has shown that E6 increases their activity. Since they function downstream of growth factor and gp130 cytokine receptor pathways, it is possible that E6 up-regulates an upstream component which subsequently activates JAK2 to phosphorylate STAT3 Y705. In this regard, E6 activates the EGF receptor and increases IL-6 and oncostatin-M expression, which mediate their effects via gp130 receptors (164,395,396).

The mechanisms that mediate S727 phosphorylation are less clear due to a wider field

of potential candidate kinases. As a first step we focused on MAPK proteins, given the presence of a strong MAPK consensus motif adjacent to S727. Phosphorylation and activation of all three canonical MAPK proteins (ERK1/2, p38 and JNK1/2) was found to be dysregulated in HPV containing keratinocytes (397). This study showed that inhibition of all three MAPK members was necessary to fully impair STAT3 S727 phosphorylation, suggesting functional redundancy between the kinases. To begin to deduce the mechanism by which E6 up-regulates STAT3 phosphorylation, we initially focused on the key functions of E6, which are p53 degradation and PDZ domain binding. Surprisingly, whilst E6AP-mediated p53 degradation and PDZ domain binding are well-characterised attributes of high-risk E6 proteins, neither of these functions was required for the increase in STAT3 phosphorylation. Further studies will be needed to investigate whether STAT3 phosphorylation and activation is conserves amongst HPV E6 proteins, or whether it is specific for the high-risk types and which domains in E6 are required for this function.

Together, this study has identified that the transcription factor STAT3 is phosphorylated on both Y705 and S727 during the HPV differentiation-dependent life cycle. It has also shown that HPV E6 protein mediates the dual phosphorylation of STAT3 via JAK2 and MAP kinase activation. Finally, STAT3 activation is essential for viral gene expression and for cell cycle progression and proliferation in HPV raft culture. Further studies will identify how STAT3 is activated by HPV E6 (Chapter 4) and the role of STAT3 in HPV mediated cervical disease and cervical cancer progression (Chapter 5).

Chapter 4. Mechanistic investigation of STAT3 activation in cervical cancer

4.1 Introduction

Human papillomaviruses (HPV) are the leading etiological cause of cervical cancer and a number of other cancers, including Head and Neck cancer and other anogenital cancers. High risk HPVs (hrHPV), including HPV16 and 18, are responsible for >99% of cervical cancers and there is currently an epidemic of HPV positive oropharyngeal carcinomas (398,399). HPV encodes three oncoproteins, E5, E6 and E7, which have previously been shown to modulate signalling pathways related to cellular transformation, including EGFR (164), Wnt (400,401) and Hippo signalling (402). The E5 oncoprotein has been shown to modulate EGFR signalling (116,129) and its viroporin activity may be required for induction of mitogenic signalling (121). HPV E6 induces the proteosomal degradation of the tumour suppressor p53 and increases the activity of telomerase, leading to the prevention of apoptosis and the immortalisation of infected cells, respectively (158,167,380). Additionally, the E7 oncoprotein activates the DNA damage response, driving viral replication and genomic instability, and promotes the progression of cells through the S phase of the cell cycle (403,404).

Signal transducer and activator of transcription (STAT) 3 is a transcription factor and an important regulator of proliferation, differentiation and cell survival(283,405). STAT3 activation is mediated by extracellular stimuli and requires the phosphorylation of tyrosine 705 (Y705) and serine 727 (S727), resulting in its nuclear translocation (406). A number of cytokines and growth factors can induce STAT3 signalling. The

cytokine IL-6 is key mediator of STAT3 activation through its receptors IL-6R and gp130 (407), leading to a signalling cascade resulting in STAT3 phosphorylation and nuclear translocation (187).

Importantly, STAT3 has been shown to be a *bona fide* oncogene, implicated in several cancers (283).

Most oncogenic viruses activate STAT3 to drive cellular proliferation, and tumourigenesis (327,333,408,409). A common mechanism used by other oncogenic viruses to activate STAT3 is to increase expression of the pro-inflammatory cytokine IL-6, a key regulator of STAT3 activation (410). This can be achieved via activation of the transcription factor NF-κB. In the canonical NF-κB pathway, a signalling cascade results in the phosphorylation of IκBα, a negative regulator of the NF-κB pathway, by IκB kinases (IKKs) (411). This leads to the proteosomal degradation of IκBα and the nuclear translocation of the NFκB p65 and p50 sub-units (Fig 4.1).

Kaposi's Sarcoma associated Herpesvirus (KSHV) down regulates IκBα via the viral miRNA miR-K12-1, leading to enhanced IL-6 expression and STAT3 activation [23]. Both Hepatitis C virus (HCV) core protein and Human Cytomegalovirus (HCMV) US28 protein induce STAT3 phosphorylation and nuclear translocation in an autocrine manner via up regulation of IL-6 (327,329,330,412).

Previous studies have provided conflicting data on HPV mediated activation of NF-κB; HPV E6 has been shown to induce expression of NF-κB dependent genes and the anti-apoptotic gene cIAP2 (413,414), whilst another study showed it can activate NF-κB under hypoxic conditions (173).

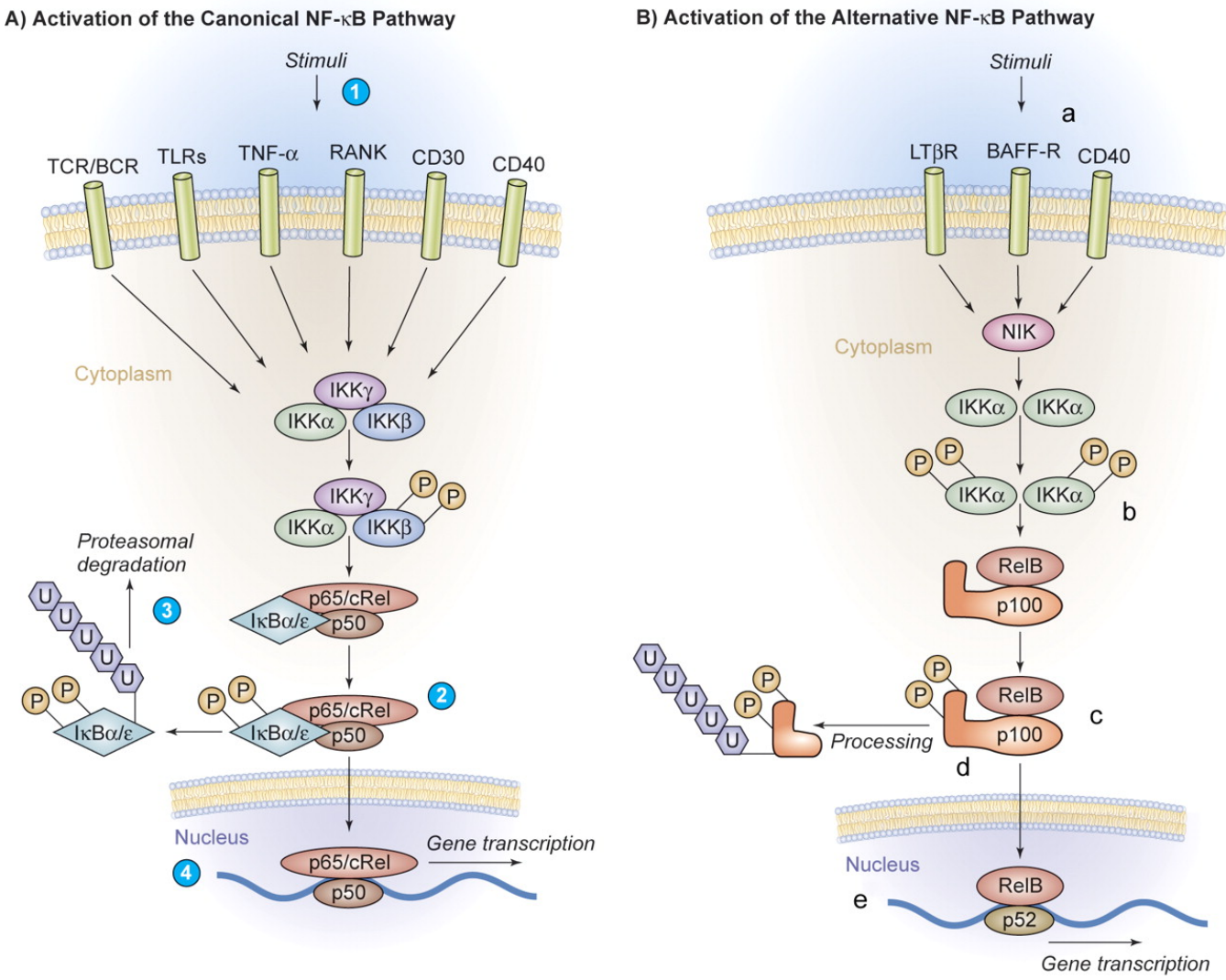

Figure 4.1. The canonical and alternative NF-κB signalling patwhways. A) The activation of the canonical NF-κB pathway. Diverse stimuli induce the activation of the IκB kinase (IKK) complex (1). This results in the phosphorylation and activation of IκB proteins, in particular IκBα at serine 32/62 (2). This induces the polyubiquitination of IκBα and its subsequent degradation by the proteasome (3). Following IκBα degradation, the p65/p50 complex is released and translocations to the nucleus to drive gene transcription (4). This pathway is inhibited by small molecule inhibitors of the IKK proteins, or a mutant IκBα which cannot be phosphorylated at S32/26 (S32/36A). **B)** The activation of the NF-κB alternative pathway. Activation of this

pathway occurs through stimuli distinct to that of the canonical pathway and results in the specific activation of IKKα, mostly through the kinase NF-κB inducing kinase (NIK) (a, b). IKKα then phosphorylates NF-κB2/p100 (c) inducing its partial proteolysis, converting it to p52 (d). This allows p52 to preferentially bind to the NF-κB protein RelB and translocate to the nucleus to drive a gene transcription profile different to canonical NF-κB signalling. Image modified from(415).

In contrast, others have demonstrated that HPV E7 attenuates NF-κB activity, whilst the impact of E6 on NF-κB is cell type dependent {Vandermark:2012kf}. Ultimately, a definitive role for the NF-κB pathway in HPV mediated malignancies and in the HPV lifecycle is still lacking.

The data in the previous chapter identified a critical role for STAT3 in the HPV life cycle; however, the role STAT3 plays in cervical cancer is currently poorly understood. Additionally, the mechanism of STAT3 phosphorylation utilised by HPV E6 is unknown; therefore, in this chapter, the mechanism of STAT3 activation by HPV E6 in cervical cancer cells is investigated.

4.2 Results

4.2.1 STAT3 protein expression and phosphorylation is higher in HPV+ cervical cancer cells compared with HPV- cancer cells.

To begin to decipher the mechanism by which HPV augments STAT phosphorylation, the level of STAT3 phosphorylation was analysed in a panel of six cervical cancer cell lines. These included two HPV negative (HPV-) lines (C33A and DoTc2 4510), two HPV16 positive (HPV16+; SiHa and CaSKi) and two HPV18 positive (HPV18+; SW756 and HeLa) lines. Both HPV16+ and HPV18+ cancer cells displayed higher levels of STAT3 phosphorylation at both (Y705 and S727) sites compared to the HPV- cell lines (significant in CaSKi and HeLa, $p<0.05$). Additionally, the levels of total STAT3 were also increased in the HPV+ cervical cancer cells compared with HPV- cervical cancer cells (Fig 4.2A and B). Together, these data demonstrate that STAT3 expression and phosphorylation is increased in HPV+ cervical cancer cells.

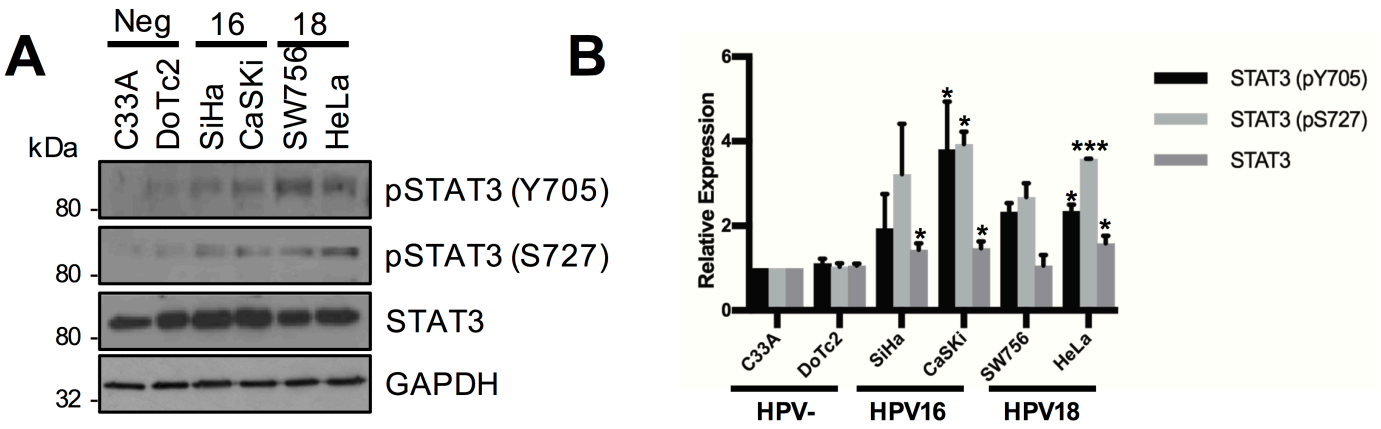

Figure 4.2. STAT3 phosphorylation is higher in HPV+ verses HPV- cervical cancer cells. A) Representative western blot of from six cervical cancer cell lines – two HPV- (C33A and Dotc2 4510), two HPV16+ (SiHa and CaSKi) and HPV18+ (SW756 and HeLa) – for the expression of phosphorylated (Y705 and S727) and total STAT3. GAPDH served as a loading control. Data are representative of at least three biological independent repeats. **B)** Quantification of the protein band intensities in **A)** standardised to GAPDH levels. Bars represent the means ± standard deviation from at least three independent biological repeats. *P<0.05, **P<0.01, ***P<0.001 (Student's t-test).

4.2.2 A factor in the media from HPV+ cancer cells induces STAT3 phosphorylation in C33A cells.

STAT3 is primarily activated by a number of growth factors and cytokines {Johnson:2018gu}. To identify if HPV stimulates the secretion of factors that can induce STAT3 phosphorylation, we incubated C33A cells (HPV-) with conditioned media from HeLa cells (HPV18+) (Fig 4.3A). Incubation with the conditioned media induced phosphorylation of STAT3 on both Y705 and S727 residues in C33A cells, reaching a peak between 30 minutes and 1 hour. Similar results were observed when conditioned media from CaSKi cells (HPV16+) was used (Fig 4.3B). Additionally, the conditioned media from either HeLa or CaSKi cells caused STAT3 nuclear translocation in C33A cells (Fig 4.3C and D). These data indicate that a secreted factor in the media from HPV+ cells can induce STAT3 phosphorylation through paracrine signalling.

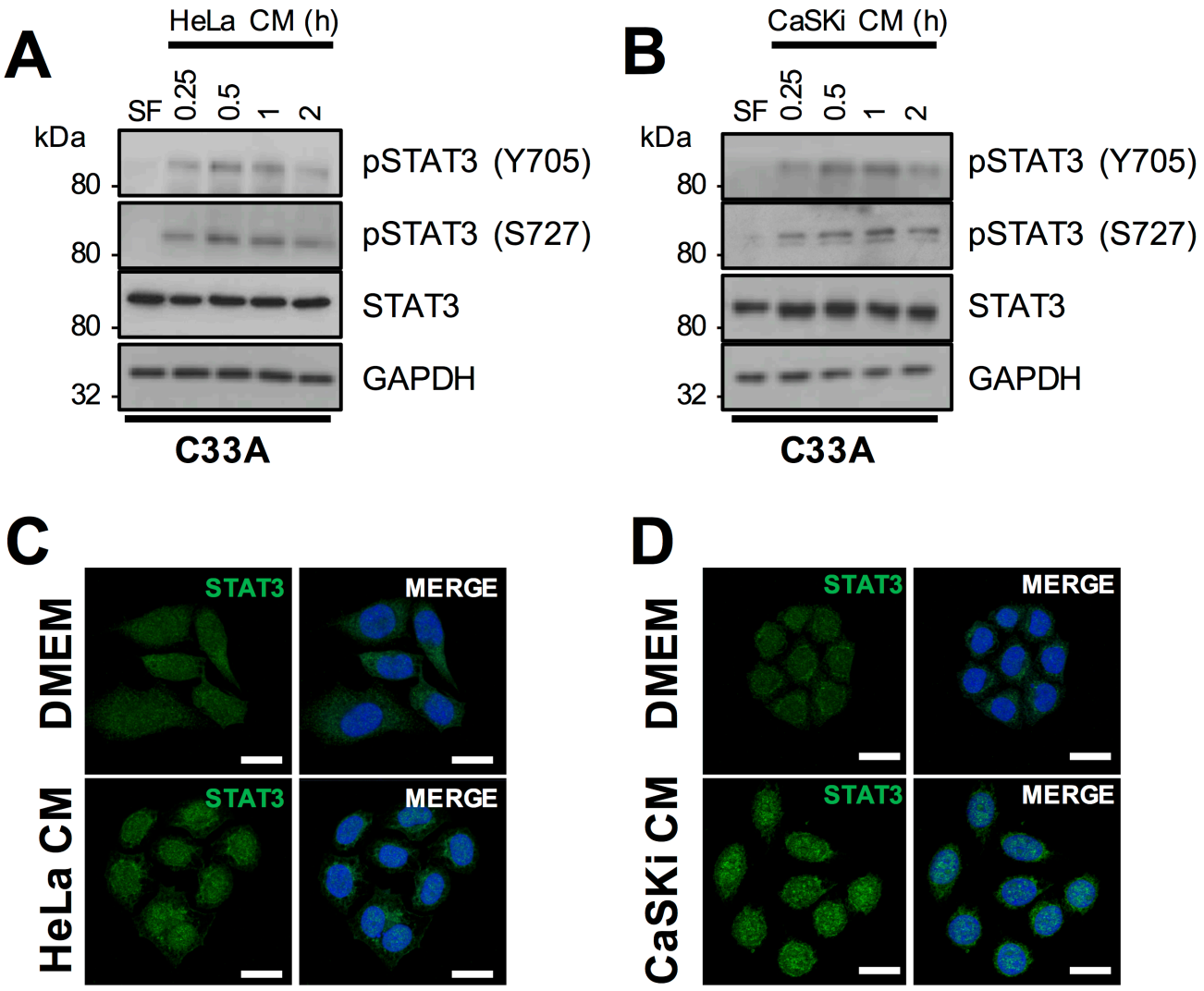

Figure 4.3. A secreted factor from HPV+ cervical cancer cells can induce STAT3 phosphorylation in HPV- cervical cancer cells. A-B) C33A cells were serum starved for 24 hours and conditioned media from **A)** HeLa or **B)** CaSKi cells was added for the indicated time points. Represented western blot shows cell lysates analysed for the expression of phosphorylated and total STAT3. GAPDH served as a loading control. Data are representative of at least three biological independent repeats. **C-D)** C33A cells were serum starved for 24 hours and incubated with conditioned media from **C)** HeLa or **D)** CaSKi cells for 2 hours. Cells were analysed by immunofluorescence staining for total STAT3 (green) and counterstained with DAPI to highlight the nuclei (blue in the merged panels). Scale bar, 20 μm.

4.2.3 IL-6 secretion is increased in HPV+ cervical cancer cells

To identify the soluble factor responsible for inducing STAT3 phosphorylation, we focused on members of the IL-6 family of pro-inflammatory cytokines, as these are well studied mediators of STAT3 activation {Kitamura:2017cr}. Firstly, the expression levels of key members of the family were analysed. In both HeLa and CaSKi cells, *IL6, IL10*, *LIF* (Leukemia inhibitory factor) and *OSM* (Oncostatin M) mRNA levels were significantly higher than in C33A cells (Fig 4.4A); however, *IL*-6 showed the greatest increase. To confirm this result, we looked at *IL-6* mRNA expression in all six cervical cancer cells. In both HPV16+ and HPV18+ cervical cancer cells, a significantly higher level of *IL-6* mRNA expression was observed compared with HPV- cervical cancer cells (Fig 4.4B). Importantly, this result correlated to IL-6 protein expression when analysed by western blot (Fig 4.4C). Finally, to confirm that the IL-6 protein detected was capable of being secreted, an IL-6 specific ELISA was performed. IL-6 was undetectable in the culture medium of HPV- cells; in contrast a significant quantity of IL-6 could be detected the culture medium of both HPV16+ and HPV18+ cells. These data suggest that IL-6 is a likely candidate for the secreted factor responsible for activation of STAT3 in HPV+ cervical cancer cells.

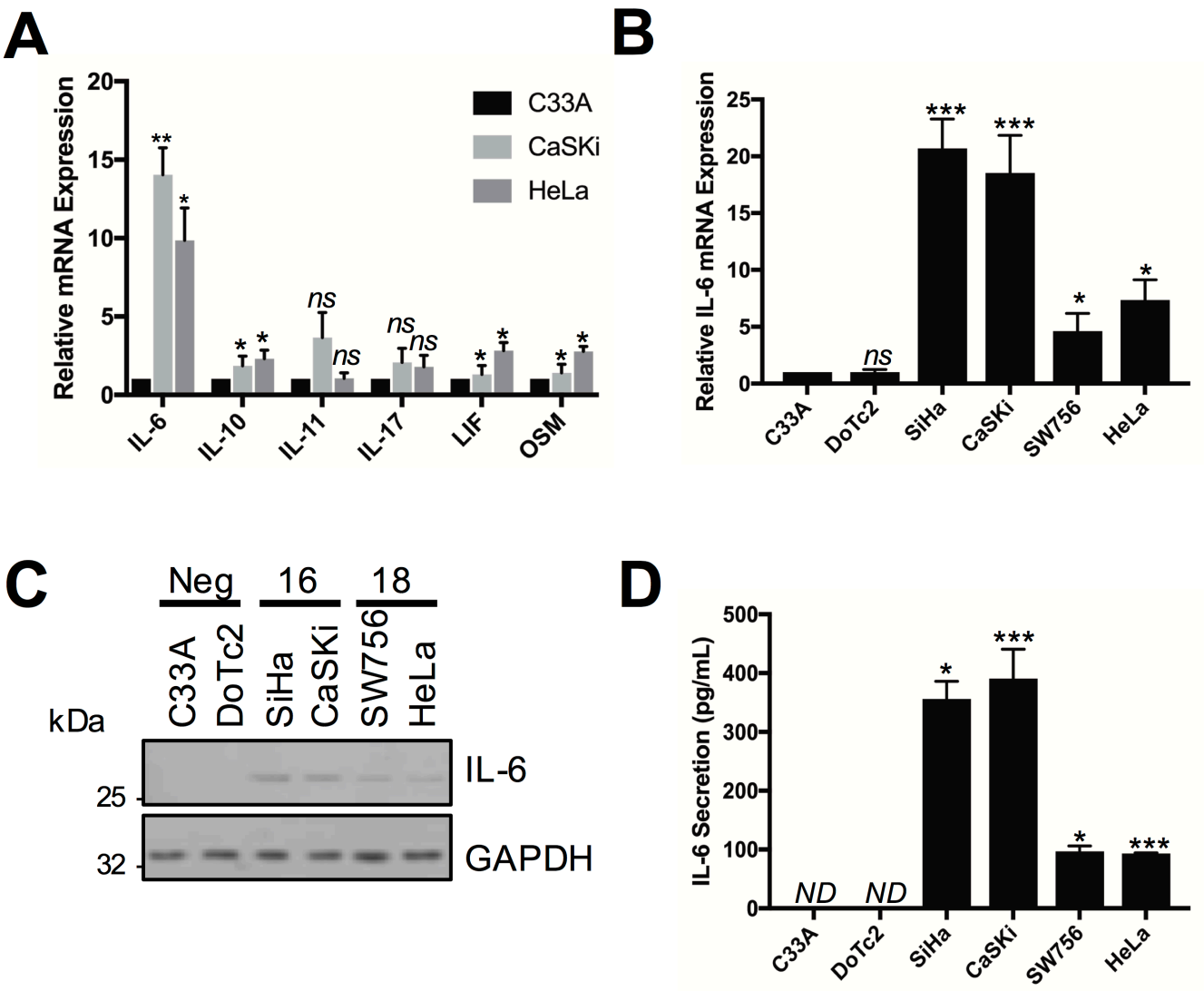

Figure 4.4. Interleukin-6 (IL-6) is up regulated in HPV+ cervical cancer cells. A) The expression level of cytokines from the IL-6 family were analysed in HPV-, HPV16+ and HPV18+ cervical cancer cells by qRT-PCR. Samples were normalized against U6 mRNA levels. Representative data are presented relative to the HPV- cervical cancer cells. Bars are the means ± standard deviation from at least three biological repeats. *P<0.05, **P<0.01, ***P<0.001 (Student's t-test). **B)** The expression of IL-6 from six cervical cancer cell lines – two HPV- (C33A and Dotc2 4510), two HPV16+ (SiHa and CaSKi) and HPV18+ (SW756 and HeLa) – was analysed by qRT-PCR. Samples were normalized against U6 mRNA levels. Representative data are presented relative to the HPV- cervical cancer cells. Bars are the means ± standard deviation from at least

three biological repeats. *P<0.05, **P<0.01, ***P<0.001 (Student's t-test). **C)** Representative western blot of from six cervical cancer cell lines – two HPV- (C33A and Dotc2 4510), two HPV16+ (SiHa and CaSKi) and HPV18+ (SW756 and HeLa) – for the expression of IL-6. GAPDH served as a loading control. Data are representative of at least three biological independent repeats. **D)** ELISA analysis from the culture medium from six cervical cancer cell lines – two HPV- (C33A and Dotc2 4510), two HPV16+ (SiHa and CaSKi) and HPV18+ (SW756 and HeLa) – for secreted IL-6 protein. Error bars represent the mean +/- standard deviation of a minimum of three biological repeats. ND = not determined (below the detection threshold). *P<0.05, **P<0.01, ***P<0.001 (Student's t-test).

4.2.4 IL-6 induces STAT3 phosphorylation and activation in cervical cancer cell lines

Next, the role of IL-6 in the activation of STAT3 in cervical cell lines was interrogated. HeLa, CaSKi and C33A cells were serum starved for 24 hours and then treated with increasing doses of recombinant IL-6 protein (Fig 4.5A, D and G). IL-6 induced robust STAT3 phosphorylation at both Y705 and S727 residues, without affecting total STAT3 levels, in both HPV+ and HPV- cell lines. Additionally, time of addition studies showed that IL-6 mediated STAT3 phosphorylation peaked around 30 minutes after IL-6 addition (Figure 4.5B, E and H). Furthermore, IL-6 treatment induced STAT3 nuclear translocation in all three cell lines (Fig 4.5C, F and I). Taken together, these data indicate that IL-6 is able to induce STAT3 phosphorylation and nuclear translocation in cervical cancer cells.

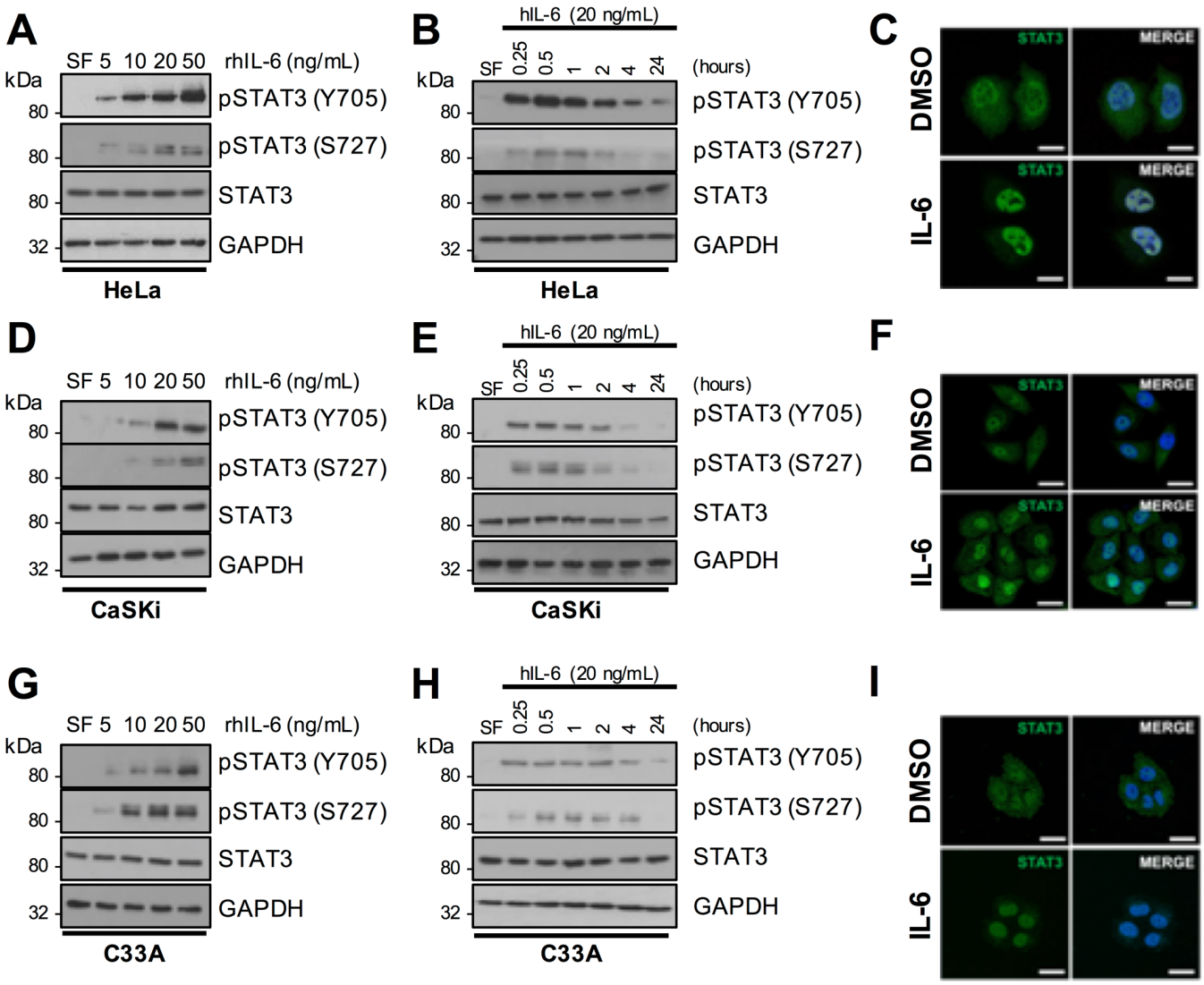

Figure 4.5. Exogenous IL-6 induces STAT3 phosphorylation and nuclear translocation in cervical cancer cells. Representative western blot of HeLa **(A)**, CaSKi **(D)** and C33A **(G)** cells treated with increasing doses of recombinant human IL-6. Cell lysates were analysed for phosphorylated and total STAT3 expression. GAPDH served as a loading control. Data are representative of at least three biological independent repeats. Representative western blot of HeLa **(B)**, CaSKi **(E)** and C33A **(H)** cells treated with 20 ng/mL recombinant human IL-6 for the indicated time points. Cell lysates were analysed for phosphorylated and total STAT3 expression. GAPDH served as a loading control. Data are representative of at least three biological independent repeats. HeLa **(C)**, CaSKi **(F)** and C33A **(I)** cells treated with 20 ng/mL

recombinant human IL-6 for 30 mins were fixed and were analysed by immunofluorescence staining for total STAT3 (green) and counterstained with DAPI to highlight the nuclei (blue in the merged panels). SF indicates cells incubated in serume free media with C33A conditioned media added as a control. Scale bar, 20 μm.

4.2.5 STAT3 phosphorylation requires IL-6/gp130 signalling in cervical cancer cells

IL-6 signalling is initiated by an interaction between IL-6 and the IL-6 receptor (IL-6R) and the glycoprotein 130 (gp130) co-receptor (407). In order to confirm that IL-6 was required for STAT3 phosphorylation in cervical cancer cells, neutralizing antibodies against IL-6 and the IL-6 co-receptor gp130 were utilised. C33A cells were incubated with either antibody for 4 hours before being treated with recombinant IL-6 for 30 minutes. As shown in Figure 4.6A, phosphorylation of both sites on STAT3 was induced by recombinant IL-6. Pre-incubation with neutralizing antibodies against either IL-6 or gp130 led to a loss of Y705 and S727 phosphorylated STAT3 (Fig 4.6A). To confirm that IL-6 was the mediator secreted by HPV+ cells to induce STAT3 phosphorylation, we pre-incubated C33A cells with the gp130 neutralising antibodies before treating them with conditioned media from HeLa and CaSKi cells. Separately, we added the neutralising IL-6 antibody with the conditioned media before addition to cells. As before, conditioned media from HPV+ cells induced STAT3 phosphorylation in HPV- cells; however, pre-incubation of C33A cells gp130 neutralising antibody, or the addition of the conditioned media containing the neutralising IL-6 antibody, blocked the ability of HPV+ conditioned media to induce STAT3 phosphorylation (Fig 4.6B) and nuclear translocation (Fig 4.6C). This suggests that IL-6 secretion from HPV+ cervical cancer cells is able to induce the paracrine activation of STAT3 in HPV- cervical cancer cells.

Finally, to confirm that IL-6/gp130 signalling was required for the autocrine activation of STAT3 in HPV+ cervical cancer cells, HeLa cells were pre-incubated with IL-6 and g130 neutralizing antibodies. Incubation with either neutralising antibody led to a

reduction in STAT3 phosphorylation on both sites accompanied by a block in STAT3 nuclear translocation, suggesting that IL-6 is required for the autocrine activation of STAT3 (Fig 4.6D and E). Taken together, HPV induces autocrine and paracrine IL-6/STAT3 signalling in cervical cancer.

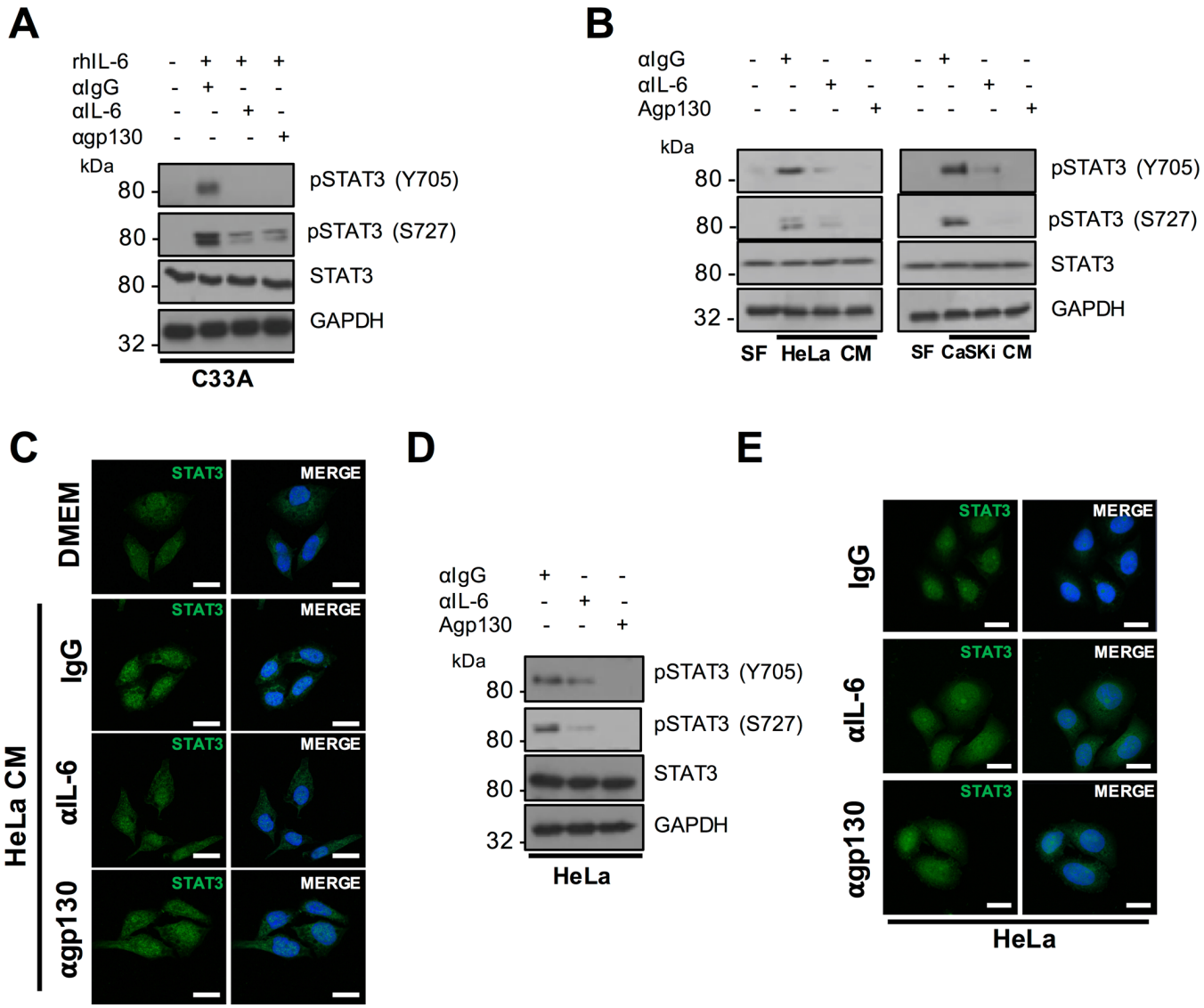

Figure 4.6. STAT3 phosphorylation requires IL-6/gp130 signalling in cervical cancer cells. A) Representative western blot of C33A cells treated with 20 ng/mL recombinant human IL-6 for 30 mins. Cells were pre-treated with IgG, anti-IL6 or anti-gp130 antibody for 4 hours before IL-6 addition. Cell lysates were analysed for phosphorylated and total STAT3 expression. GAPDH served as a loading control. Data are representative of at least three biological independent repeats. **B)** Representative western blot of C33A cells treated with conditioned medium (CM) from HeLa and CaSKi cells for 2 hours. Cells were pre-treated with IgG, anti-IL6 or anti-gp130 antibody for 4 hours before CM addition. Cell lysates were analysed for

phosphorylated and total STAT3 expression. GAPDH served as a loading control. Data are representative of at least three biological independent repeats. **C)** C33A cells treated with conditioned medium (CM) from HeLa and CaSKi cells for 2 hours. Cells were pre-treated with IgG, anti-IL6 or anti-gp130 antibody for 4 hours before CM addition. Cells were then analysed by immunofluorescence staining for total STAT3 (green) and counterstained with DAPI to highlight the nuclei (blue in the merged panels). Scale bar, 20 μm. **D)** HeLa cells were treated with IgG, anti-IL6 or anti-gp130 for 4 hours. Cell lysates were analysed for phosphorylated and total STAT3 expression. GAPDH served as a loading control. Data are representative of at least three biological independent repeats. **E)** HeLa cells were treated with IgG, anti-IL6 or anti-gp130 for 4 hours. Cells were then analysed by immunofluorescence staining for total STAT3 (green) and counterstained with DAPI to highlight the nuclei (blue in the merged panels). Scale bar, 20 μm.

4.2.6 HPV E6 induction of IL-6 expression is required for the induction of STAT3 phosphorylation

The data from chapter 3 demonstrated that the increased STAT3 phosphorylation observed in HPV containing keratinocytes was dependent on the E6 oncoprotein. Additionally, HPV16 E6 has been previously demonstrated to induce IL-6 secretion in non-small cell lung cancer (NSCLC) cells (416,417). Therefore, the ability of E6 to induce IL-6 expression in cervical cancer cells was assessed. To this end, we firstly utilised an IL-6 promoter luciferase reporter. In C33A cells, expression of HPV18 E6 significantly increased IL-6 promoter activity by ~4-fold compared with the GFP control (Fig 4.7A; p= 0.002). This corresponded to a ~4-fold increase in endogenous *IL-6* mRNA expression (Fig 4.7B; p= 0.01) and IL-6 protein expression (Fig 4.7C). Finally, E6 expression resulted in a significant increase in IL-6 secretion, measured by ELISA (Fig 4.7D; p= 0.0245). To demonstrate that the E6 protein expressed in HPV+ cancer cells could induce IL-6 expression, HeLa cells were treated with an E6 specific siRNA. Knockdown of E6 expression led to a significant reduction in *IL-6* mRNA expression (Fig 4.7E; p= 0.046), IL-6 protein expression (Fig 4.7F) and secretion (Fig 4.7G; p= 0.003). Together, these data demonstrate that HPV E6 increases the expression and secretion of IL-6.

To confirm if IL-6 expression was necessary for E6-mediated STAT3 phosphorylation, E6 was expressed in C33A cells which were then treated with neutralising antibodies against either IL-6 or the gp130 co-receptor. As previously shown in chapter 3, the presence of HPV E6 induced the phosphorylation of both Y705 and S727 residues in STAT3. However, treatment of E6 expressing cells with neutralising antibodies against IL-6 or gp130 inhibited of STAT3 phosphorylation (Fig 4.7H). This suggests that the E6 induction of IL-6 expression is essential for the autocrine phosphorylation

and activation of STAT3 in cervical cancer cells.

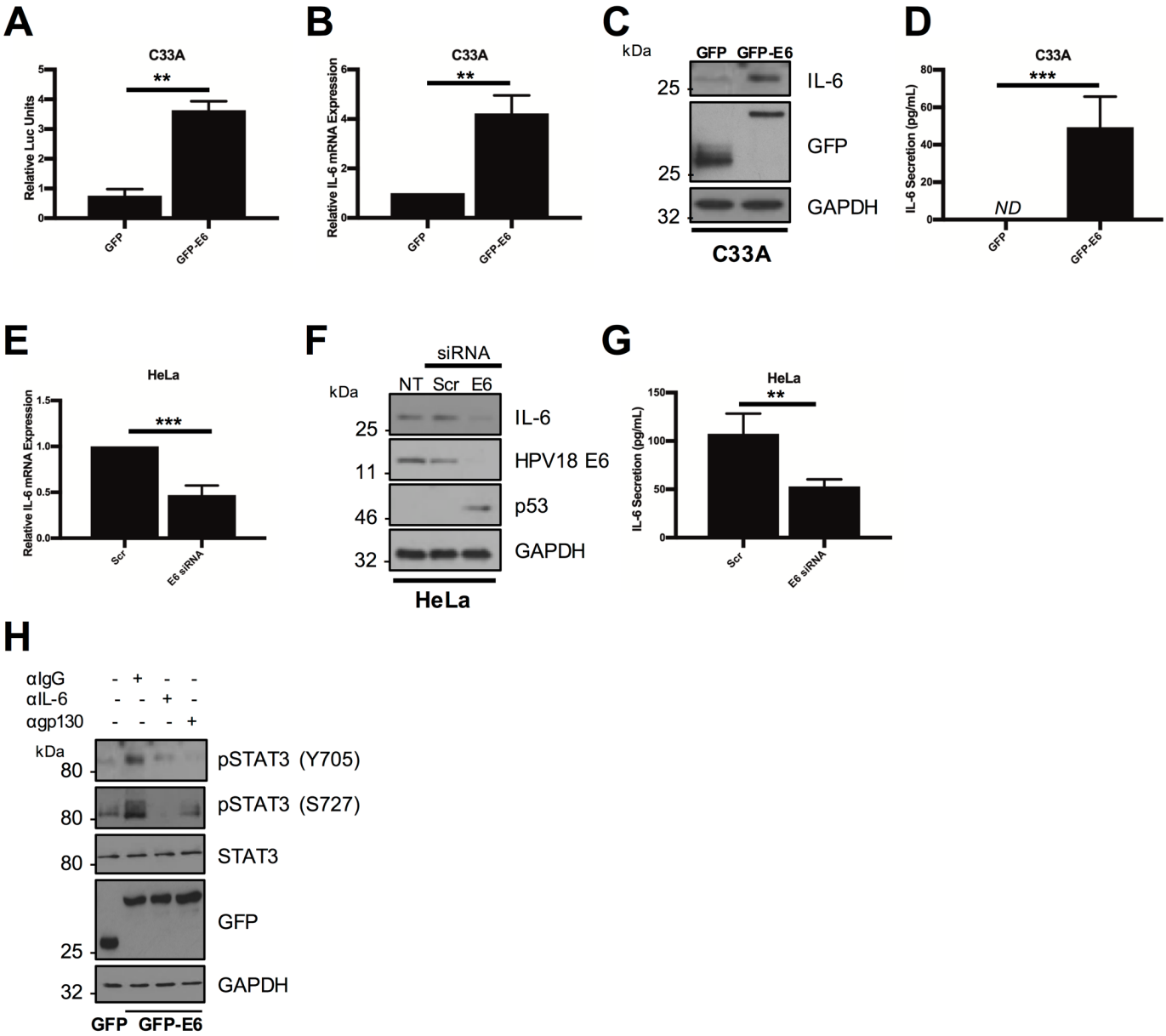

Figure 4.7. HPV E6 induced IL-6 expression is required for STAT3 phosphorylation. A) Representative luciferase reporter assay from C33A cells co-transfected with GFP tagged E6 and an IL-6 promoter reporter. Promoter activity was measured using a dual-luciferase system. Data are presented as relative to the GFP transfected control. **B)** C33A cells were transiently transfected with GFP or GFP

tagged HPV18 E6 and RNA was extracted for qRT-PCR analysis of IL-6 expression. Samples were normalized against U6 mRNA levels. Representative data are presented relative to the GFP control. **C)** Representative western blot of C33A cells transiently transfected with GFP or GFP tagged HPV18 E6 and analysed for IL-6 expression. Expression of HPV E6 was confirmed using a GFP antibody and GAPDH served as a loading control. **D)** C33A cells were transiently transfected with GFP or GFP tagged HPV18 E6. The culture medium was analysed for IL-6 protein by ELISA. **E)** HeLa cells were transfected with a pool of two specific siRNAs against HPV18 E6 and analysed for IL-6 mRNA expression by qRT-PCR. Samples were normalized against U6 mRNA levels. Representative data are presented relative to the GFP control. **F)** Representative western blot of HeLa cells transfected with a pool of two specific siRNAs against HPV18 E6 and analysed for the expression of IL-6. Knockdown of HPV18 E6 was confirmed using an antibody against HPV18 E6 and p53. GAPDH served as a loading control. **G)** HeLa cells were transfected with a pool of two specific siRNAs against HPV18 E6. The culture medium was analysed for IL-6 protein by ELISA. **H)** Representative western blot of C33A cells transiently transfected with GFP or GFP tagged HPV18 E6 and treated with IgG, anti-IL6 or anti-gp130 for 4 hours before harvest. Cell lysates were then analysed for phosphorylated and total STAT3. Expression of HPV E6 was confirmed using a GFP antibody and GAPDH served as a loading control. Bars represent the means ± standard deviation from at least three independent biological repeats. *P<0.05, **P<0.01 (Student's t-test).

4.2.7 HPV E6 activates NFκB to increase IL-6 expression

Several signalling pathways can induce IL-6 expression (352). One key host factor is the transcription factor NFκB, which is activated in response to a range of extracellular ligands including TNFα (418). HPV E6 has previously been shown to activate NFκB signalling, particularly in hypoxia (173,413). To assess if NFκB was required for E6-mediated IL-6 expression, we firstly tested whether expression of E6 in isolation could activate NFκB in C33A cells. Using an NFκB driven luciferase reporter plasmid, overexpression of E6 induced NFκB activity ~3-fold compared to a GFP control (Fig 4.8A; p= 0.001).

Canonical NFκB signalling results in the phosphorylation of the p65 subunit and its nuclear translocation where it is transcriptionally active in complex with other NFκB subunits including p50 (Fig 4.1). Over expression of E6 in C33A cells induced robust p65 phosphorylation (Fig 4.8B). In contrast, siRNA mediated knockdown of E6 in HeLa cells led to a reduction in p65 phosphorylation (Fig 4.8C), together suggesting that HPV E6 activates the NFκB signalling pathway.

To assess if NFκB activity was required for the increase in IL-6 production observed in E6 expressing cells, we firstly employed a dual approach to prevent NFκB activation in C33A overexpressing E6 cells. For this, cells were treated either with a small molecule inhibitor targeting the IKKα/β (IKKi) complex, which is required to phosphorylate and activate NFκB, or transfected with a plasmid encoding a mutant IκBα protein (IkBm), which cannot be degraded and as such retains NFκB in the cytosol in an inactive conformation. As previously shown, expression of E6 increased *IL-6* mRNA production, and significantly inhibition of NFκB using either IKKi or IkBm led to a reduction in *IL-6* mRNA expression (Fig 4.8D; IKKi, p=0.00001; IkBm, 0.04). Importantly, inhibition of NFκB by either strategy led to a reduction in IL-6 protein levels

(Fig 4.8E) and secretion (Fig 4.8F; IKKi, p= 0.02; IκBm, p=0.007). To confirm if NFκB activity was also required for mediating the increased IL-6 levels observed in the context of HPV+ cancer cells, NFκB activity was blocked in HeLa cells. Inhibition of NFκB led to a reduction in *IL-6* mRNA expression (Fig 4.8F; IKKi, p= 0.03; IκBm, p =0.02), IL-6 protein levels (Fig 4.8H) and secretion (Fig 4.8I; IKKi, p= 0.007; IκBm, p=0.007). Collectively, these data demonstrate that HPV E6 mediated IL-6 expression is dependent on an active NFκB transcription factor in cervical cancer cells.

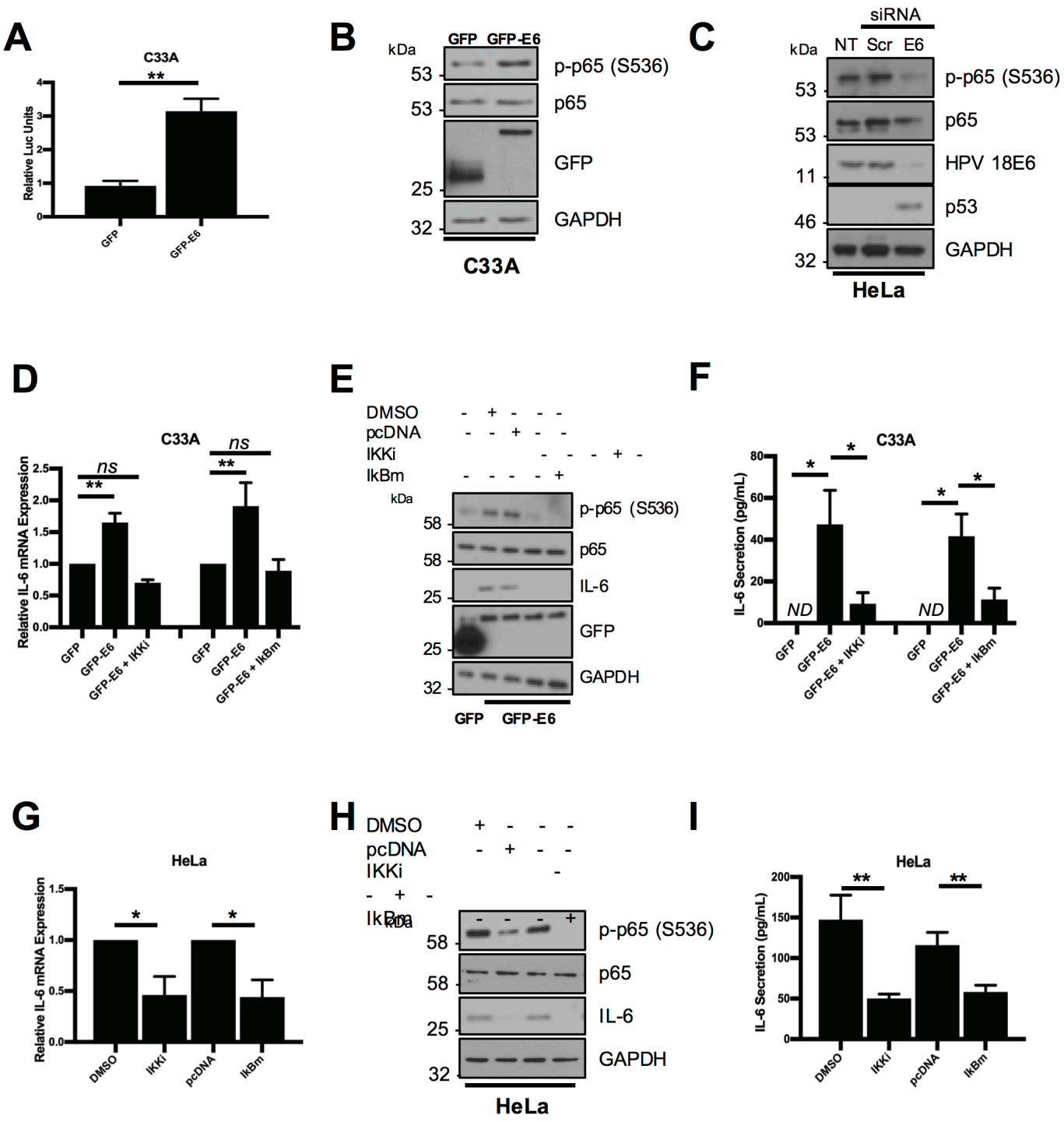

Figure 4.8. HPV E6 mediated IL-6 expression requires NF-κB activity. A) Representative luciferase reporter assay from C33A cells co-transfected with GFP tagged E6 and a ConA reporter, which contains tandem κB binding sites (419). Promoter activity was measured using a dual-luciferase system. Data are presented as relative to the GFP transfected control. **B)** Representative western blot of C33A

cells transiently transfected with GFP or GFP tagged HPV18 E6 and analysed for phosphorylated and total p65 expression. Expression of HPV E6 was confirmed using a GFP antibody and GAPDH served as a loading control. **C)** Representative western blot of HeLa cells transfected with a pool of two specific siRNAs against HPV18 E6 and analysed for the expression of phosphorylated and total p65. Knockdown of HPV18 E6 was confirmed using an antibody against HPV18 E6 and p53. GAPDH served as a loading control. **D-F)** C33A cells were co-transfected with GFP, GFP tagged HPV18 E6 or GFP tagged HPV18 E6 and mutant IκBα (IkBm). Cells were then either left untreated or treated with IKK inhibitor VII (IKKi). **E)** Total RNA was extracted for qRT-PCR analysis of IL-6 expression. Samples were normalized against U6 mRNA levels. Representative data are presented relative to the GFP control. **F)** Cell lysates were analysed for the expression of phosphorylated and total p65 and IL-6. Expression of HPV E6 was confirmed using a GFP antibody and GAPDH served as a loading control. **G)** The culture medium was analysed for IL-6 protein by ELISA **G-I)** HeLa cells transfected with a pool of two specific siRNAs against HPV18 E6. **H)**Total RNA was extracted for qRT-PCR analysis of IL-6 expression. Samples were normalized against U6 mRNA levels. Representative data are presented relative to the GFP control. **I)** Cell lysates were analysed for the expression of phosphorylated and total p65 and IL-6. Expression of HPV E6 was confirmed using a GFP antibody and GAPDH served as a loading control. **J)** The culture medium was analysed for IL-6 protein by ELISA. Bars represent the means ± standard deviation from at least three independent biological repeats. *P<0.05, **P<0.01, ***P<0.001 (Student's t-test).

4.2.8 NFκB is required for STAT3 phosphorylation in HPV E6 expressing cells

As NFκB was absolutely required for the increase in IL-6 expression observed in HPV+ cancer cell lines, it was necessary to next test whether NFκB was also required for the activation of STAT3. First, we tested the ability of an inducer of NFκB activation, TNFα, to cause STAT3 phosphorylation. Treatment of serum starved C33A cells with TNFα led to an increase in p65 phosphorylation, which peaked at 0.5 hours after treatment (Fig 4.9A; lane 3). TNFα treatment also induced IL-6 expression; starting at 0.5 hours post treatment and remaining high up to 24 hours post treatment. Interestingly, TNFα treatment also led to an increase in STAT3 phosphorylation at both Y705 and S727 residues; however, this peaked much later, at 2 hours (Fig 4.9A; lane 5). TNFα treatment also led to the nuclear translocation of STAT3, 2 hours post treatment (Fig 4.9B).

To assess the importance of NFκB activation for STAT3 phosphorylation in cervical cancer cells, HPV E6 was firstly overexpressed in C33A cells, with or without treatment with the NFκB inhibitor IKKi, or co-expression of IkBm. E6 overexpression noticeably increased p65 and STAT3 phosphorylation and inhibition of NFκB using either approach led to a loss of STAT3 phosphorylation (Fig 4.9C), Additionally, blockade of NFκB also led to a reduction in STAT3 phosphorylation in HeLa cells (Fig 4.9D and E), suggesting that E6 mediated STAT3 phosphorylation is depended on NFκB. Finally, to ascertain if NFκB was essential for the paracrine activation of STAT3 in C33A cells, we took conditioned media from HeLa cells in which NFκB was inhibited and added this to C33A cells. This conditioned media failed to induce STAT3 phosphorylation (Fig 4.9F) and nuclear translocation (Fig 4.9G). Importantly, inhibition of NFκB activity had no effect on STAT3 phosphorylation or nuclear translocation

mediated by treatment with exogenous IL-6 (Fig 4.10A and 9B), demonstrating that NFκB is upstream of IL-6 secretion. Together, the data suggests that NFκB activity is required for the autocrine and paracrine activation of STAT3 in HPV+ cervical cancer cells.

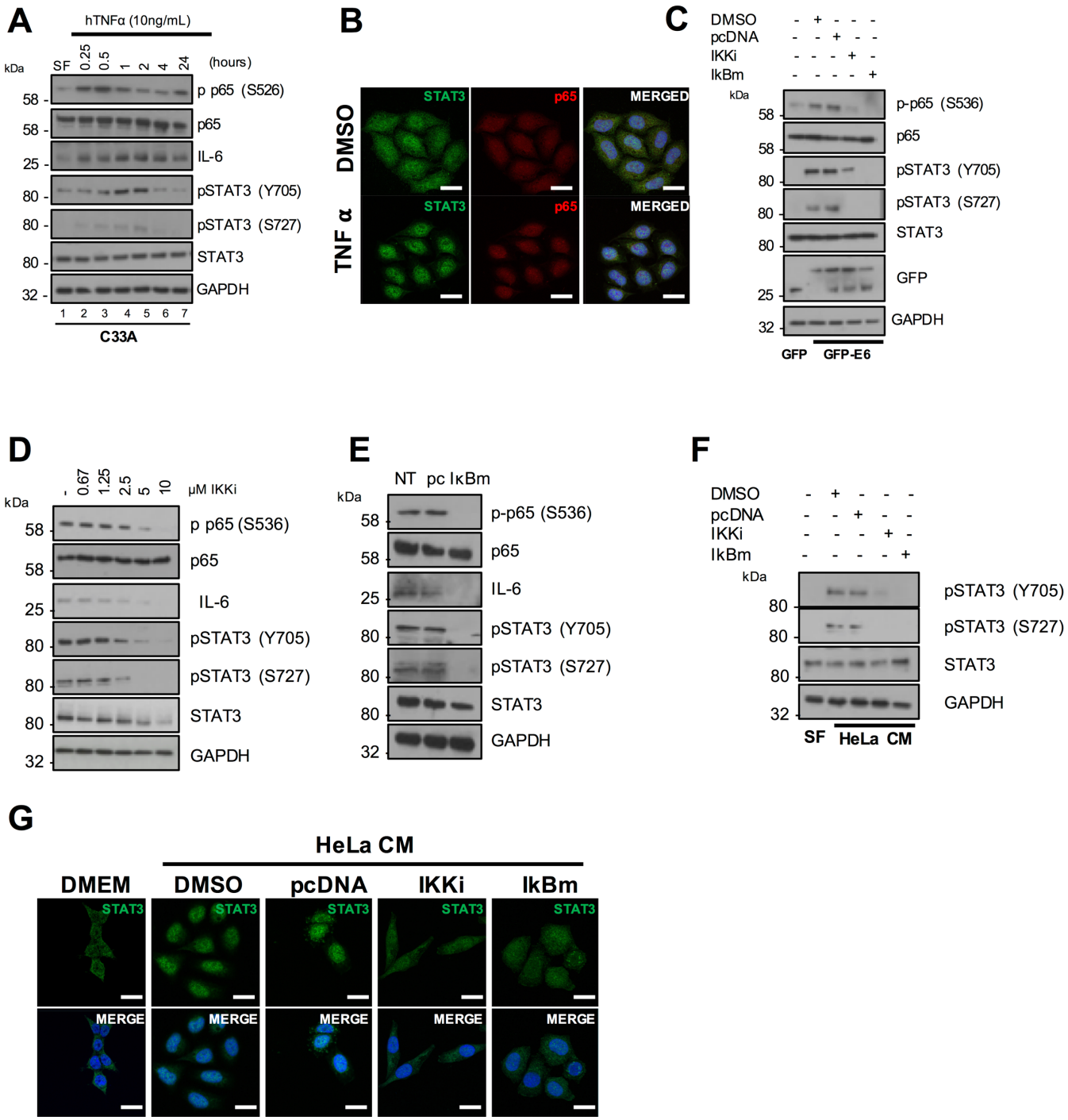

Figure 4.9. NF-κB activity is required for HPV E6 mediated STAT3 signalling. A) Representative western blot of C33A cells treated with 20 ng/mL recombinant human TNFα for the indicated time points. Cell lysates were analysed for phosphorylated and total p65, phosphorylated and total STAT3 and IL-6 expression. GAPDH served as a loading control. Data are representative of at least three biological independent

repeats. **B)** C33A cells treated with 20 ng/mL recombinant human TNFα for 60 mins were fixed and were analysed by immunofluorescence staining for total STAT3 (green) and total p65 (red) and counterstained with DAPI to highlight the nuclei (blue in the merged panels). Scale bar, 20 μm. **C)** C33A cells were co-transfected with GFP, GFP tagged HPV18 E6 or GFP tagged HPV18 E6 and mutant IκBα (IkBm). Cells were then either left untreated or treated with IKK inhibitor VII (IKKi). Cell lysates were then analysed for phosphorylated and total p65, phosphorylated and total STAT3 expression. Expression of HPV E6 was confirmed using a GFP antibody and GAPDH served as a loading control. **D)** Representative western blot from HeLa cells treated with increasing doses of the IKKα/β inhibitor IKK inhibitor VII (IKKi). Cell lysates were analysed for the expression of phosphorylated and total p65, phosphorylated and total STAT3 and IL-6 expression. GAPDH served as a loading control. **E)** Representative western blot from HeLa cells transfected with mutant IκBα (IkBm). Cell lysates were analysed as in **D). F)** C33A cells were serum starved for 24 hours. Cells were then treated with HeLa condition media from HeLa cells treated with DMSO or IKKi, or transfected with pcDNA or IkBm. Cell lysates were analysed for phosphorylated and total STAT3 expression. GAPDH served as a loading control. **G)** C33A cells were serum starved for 24 hours. Cells were then treated with HeLa condition media from HeLa cells treated with DMSO or IKKi, or transfected with pcDNA or IkBm. Cells were analysed by immunofluorescence staining for total STAT3 (green) and counterstained with DAPI to highlight the nuclei (blue in the merged panels). Scale bar, 20 μm.

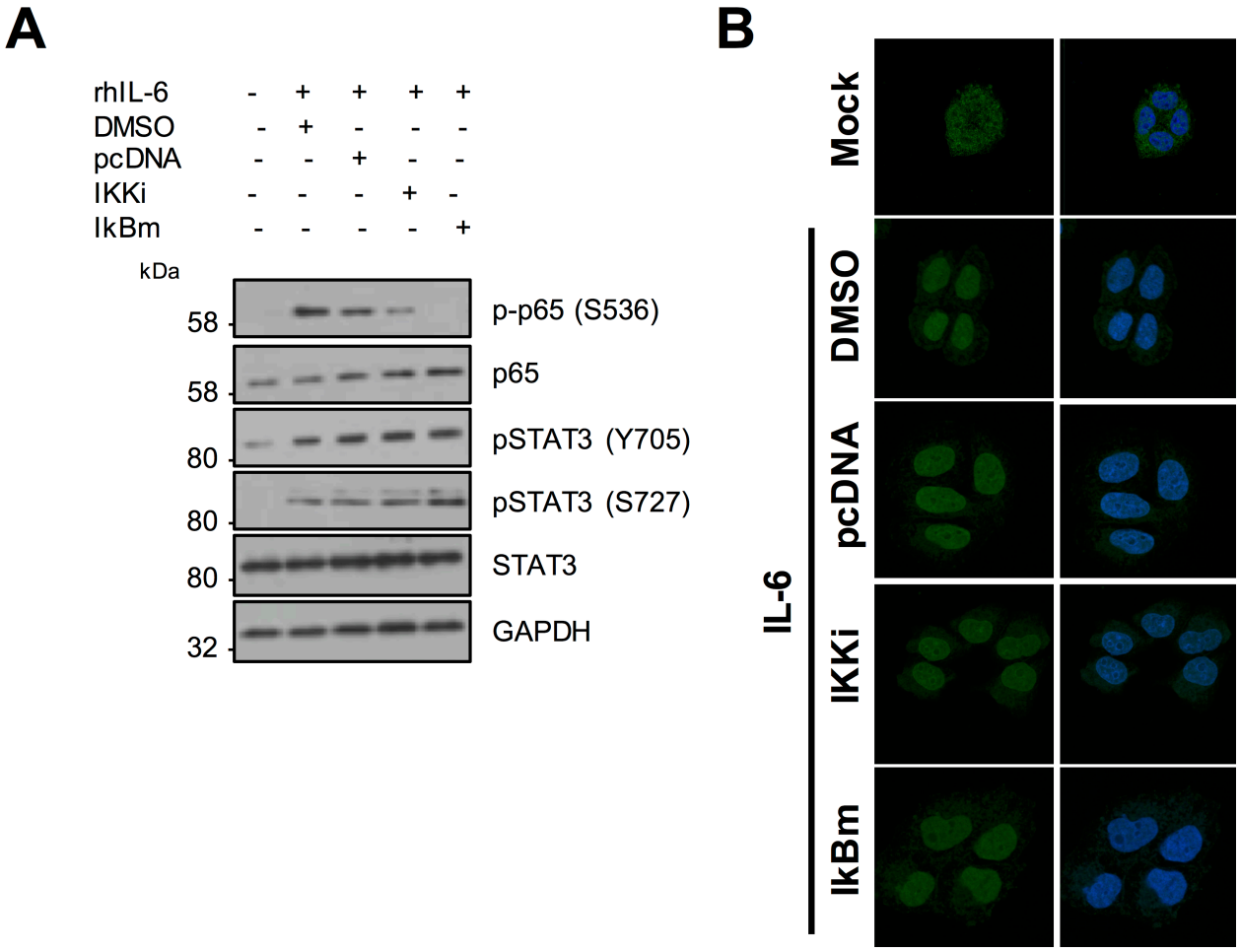

Figure 4.10. NF-κB inhibition does not affect exogenous IL-6 mediated STAT3 signalling. A) C33A were treated with DMSO or IKKi or transfected with pcDNA or IkBm before treatment with 20 ng/mL recombinant human IL-6 for 30 mins. Cell lystaes were analysed for phosphorylated and total p65 and phosphorylated and total STAT3 expression. GAPDH served as a loading control. Data are representative of at least three biological independent repeats. **B)** C33A were treated with DMSO or IKKi or transfected with pcDNA or IkBm before treatment with 20 ng/mL recombinant human IL-6 for 30 mins. Cells were analysed by immunofluorescence staining for total STAT3 (green) and counterstained with DAPI to highlight the nuclei (blue in the merged panels). Scale bar, 20 μm.

4.2.9 IL-6 expression correlates with disease progression in cervical cancer

The IL-6/STAT3 signalling axis is deregulated in several cancers (420-422). Additionally, IL-6 is over expressed in lung cancer and head and neck cancers (423,424). We analysed cervical liquid-based cytology samples from a cohort of HPV16+ patients representing the progression of disease development (CIN1-CIN3) and HPV negative normal cervical tissue controls. Levels of *IL-6* mRNA significantly correlated with disease progression through CIN1-CIN3 (Fig 4.11A; CIN1, p= 0.01; CIN2, p= 0.004; CIN3, p=0.00005), with the greatest increase observed in CIN3 samples when compared with normal cervical tissue. Additionally, IL-6 protein levels also correlated with disease progression (Fig 4.11B and C; CIN1, p= NS; CIN2, p= 0.0003; CIN3, p=0.04), again showing the largest increase in CIN3. Finally, we mined a publicly available database of microarray data of normal cervical samples against cervical cancer samples(425). There was a statistically significant increase in *IL-6* mRNA expression in the cervical cancer samples (Fig 4.11D; p=0.03). Together, these data demonstrated that *IL-6* levels are regulated at the mRNA level in HPV+ cervical cancer.

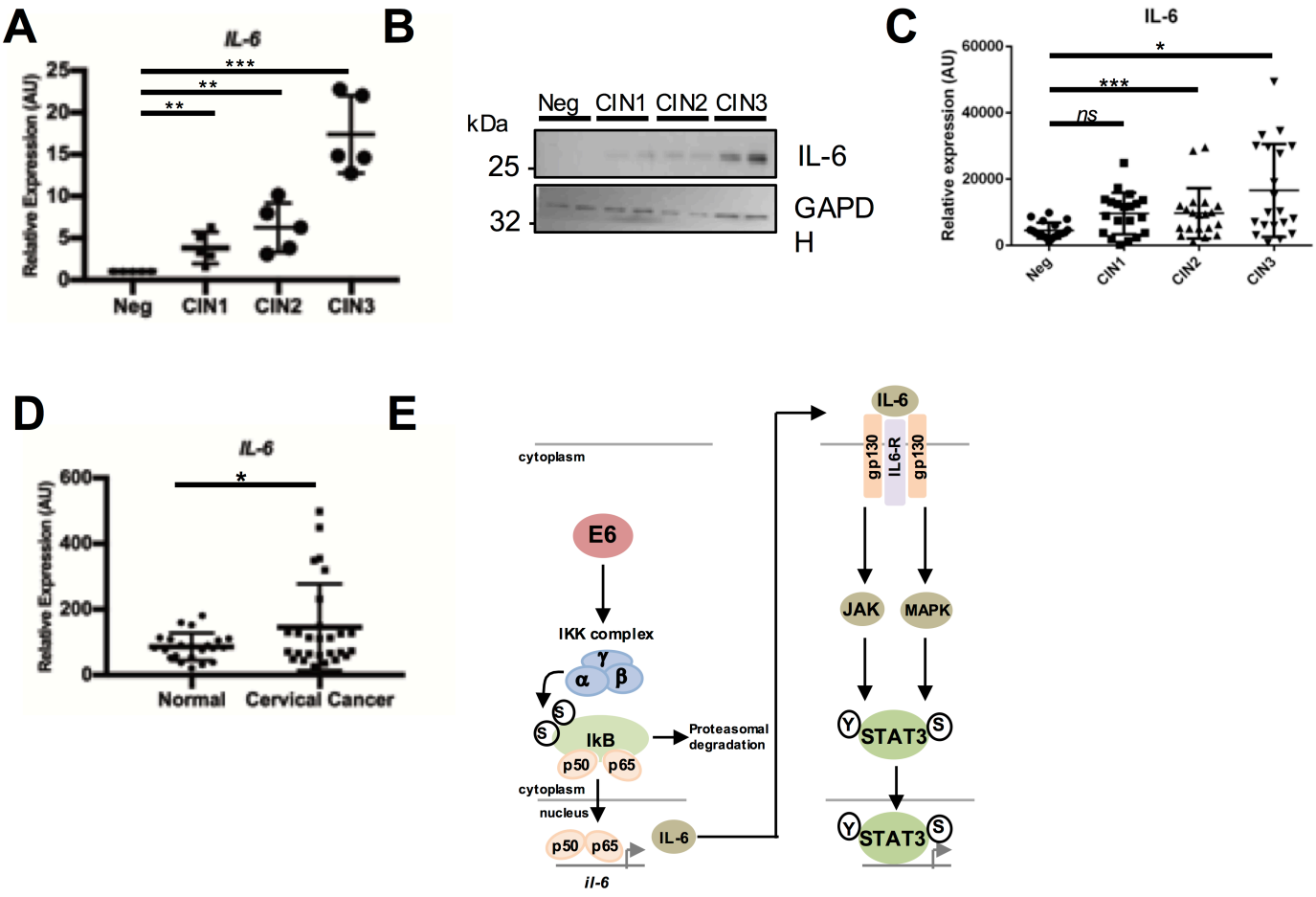

Figure 4.11. IL-6 expression correlates with cervical disease progression and is up regulated in cervical cancer. A) Scatter dot plot of qRT-PCR analysis of RNA extracted from a panel of cytology samples of CIN lesions of increasing grade. Five samples from each clinical grade (neg, CIN I-III) were analysed and mRNA levels were normalized to neg samples. Samples were normalized against U6 mRNA levels. Representative data are presented relative to the HPV- cervical cancer cells. Bars are the means ± standard deviation from at least three biological repeats. *P<0.05, **P<0.01, ***P<0.001 (Student's t-test). **B)** Representative western blots from cytology samples of CIN lesions of increasing grade analysed IL-6 expression. GAPDH served as a loading control. **C)** Scatter dot plot of densitometry analysis of a panel of cytology samples. Twenty samples from each clinical grade (neg, CIN I-III) were analysed by

western blot and densitometry analysis was performed using ImageJ. GAPDH was used as a loading control. **D)** Scatter dot plot of data acquired from the dataset GSE9750 on the GEO database. Arbitrary values for the mRNA expression of IL-6 in normal cervix (n=23) and cervical cancer (n=28) samples were plotted. Error bars represent the mean +/- standard deviation of a minimum of three biological repeats. *P<0.05, **P<0.01, ***P<0.001 (Student's t-test). **E)** Schematic diagram of E6 mediated NF-κB/IL-6/STAT3 signalling in HPV+ cervical cancer cells.

4.3 Discussion

The cytokine IL-6 is over-expressed in diverse cancers and is often correlated with activation of STAT3 (410). IL-6 displays many pleiotropic functions, being both pro-inflammatory and immunosuppressive by interacting with the surrounding stroma of tumours (426). In HNSCC and oral squamous cell carcinoma, serum levels of IL-6 level are significantly higher than control patients and serum IL-6 is a potential biomarker for these cancers (355). Additionally, targeting IL-6 in combination with EGFR inhibitors such as Erlotinib is currently being investigated as a potential therapy for HNSCC due to the resistance to EGFR inhibition seen in many tumours (427). In cervical cancer, IL-6 expression promotes tumour proliferation by inducing VEGF-dependent angiogenesis in a STAT3 dependent manner (428) and has also been suggested as a potential biomarker for cervical cancer (429) Here, STAT3 phosphorylation and IL-6 expression has been shown to be increased in HPV+ cervical cancer cell lines when compared with normal keratinocytes and HPV- cervical cancer cells (Figure 4.1). Additionally, IL-6 expression correlates with cervical disease progression and is increased in cervical cancer (Figure 4.11). This surplus of IL-6 expression may contribute to the increased level of immune suppressive T_h17 cells and T_{reg} seen in the stroma of cervical cancer tumours (430).

The HPV E6 oncoprotein has been demonstrated to be required for the expression and secretion of IL-6 NSCLC cells (416); however, the role of E6 in driving IL-6 expression in cervical cancer is unknown. Furthermore, the contribution of IL-6 to STAT3 activation in cervical cancer is poorly defined. In this chapter, the increased phosphorylation of STAT3 in HPV cervical cancer cells was attributed to an increase in IL-6 expression by HPV E6 and the induction of autocrine/paracrine IL-6/gp130/STAT3 signalling (Figure 4.11E). In cervical cancer cells, EGFR signalling

can induce STAT3 activation (431) However, the data here identified that blockade of IL-6 or gp130 signalling using neutralising antibodies abolished STAT3 phosphorylation (Figure 4.6), suggesting that IL-6/gp130 is required for STAT3 phosphorylation in HPV+ cervical cancer cells.

To further investigate the regulation of IL-6 by E6 in HPV+ cervical cancer, the transcription factor NFκB was identified as an essential upstream mediator of IL-6 expression. NFκB is a key component of the inflammatory response, which is a key hallmark of cancer (283,352,418). The induction of inflammation by diverse mechanisms contributes to around 20% of cancers, including the role of inflammatory bowel disease in the development of colorectal cancer (CRC) (432). Importantly, infection also plays an important role in inflammation-driven cancer; *H. pylori* can lead to the induction of stomach cancers, whilst Hepatitis B and C infection can lead to hepatocellular carcinoma development (433-435). Previous data suggests that inflammation induced by HPV infection may contribute to HPV induced cervical cancers (436,437). Indeed, several genes known to be induced by the inflammatory response, including COX-2 (438), are up-regulated in cervical cancer.

The role of NFκB in cervical remains controversial, with HPV implicated in both activation and inhibition of the transcription factor (173,413,439). HPV E6 was demonstrated to increase the expression of NFκB components and induce NFκB DNA binding activity, increasing pro-inflammatory cytokine expression (413). Additionally, E6 reduces the expression of the deubiquitinase CYLD, a known negative regulator of NFκB signalling, in hypoxic cells (173). In contrast, E6 has been shown to inhibit NFκB transcriptional activity, whilst HPV E7 can attenuate p65 nuclear translocation (439). The data presented here demonstrates that HPV18 E6 increases the phosphorylation of p65, essential for its nuclear translocation and transactivation. Additionally, NFκB is

essential for IL-6 expression in HPV+ cervical cancer cells.

The link between NFκB and STAT3 has been observed in many cancers. STAT3 and NFκB share many target genes implicated in cancer progression, including cyclin D1 and Bcl xL (440). In addition, STAT3 and NFκB can interact directly, resulting in the retention of NFκB in the nucleus and the binding of unique DNA target sites (440). Furthermore, STAT3 activation can also induce NFκB activation (441). In glioblastoma, the activation of STAT3 by an NFκB/IL-6 signalling axis is required for cancer aggressiveness (442). The data presented here demonstrates that NFκB is essential for the induction of IL-6 and the autocrine/paracrine induction of STAT3 phosphorylation in HPV+ cervical cancer cells. Therefore, the IL-6/STAT3 signalling axis may be an attractive therapeutic target in HPV+ cervical cancer.

Chapter 5. The role of STAT3 signalling in cervical cancer

5.1 Introduction

As an oncogenic virus, HPV infection accounts for 5% of human cancer cases worldwide (398). Despite the availability of vaccines against HPV infection, these are preventative and not therapeutic (39). There is currently no direct acting anti-viral that targets HPV, with the most common treatment for cervical cancer being with platinum-based chemotherapeutics such as cisplatin (443). Additionally, many cancers develop resistance to such chemotherapeutics (444). Therefore, there is a need to identify novel therapeutic targets for the treatment of HPV-mediated cervical cancer.

The transcription factor STAT3 has been demonstrated to be an attractive therapeutic target in a diverse range of cancers, including bladder (345), ovarian (445) and head and neck squamous cell carcinoma (HNSCC) (446). In bladder cancer, STAT3 is essential for cell proliferation and survival, whereas in pancreatic cancer it also is required for angiogenesis and metastasis (347).

In cervical cancer, inhibition of STAT3 has been shown to be detrimental to cervical cancer cell proliferation and to increase the expression of the tumour suppressor proteins p53 and pRb (369). In another study, knockdown of STAT3 using siRNA led to a similar reduction in cervical cancer cell proliferation (370). However, a detailed investigation in to the role of STAT3 in cervical cancer is currently lacking.

In this chapter, the effect of STAT3 inhibition and depletion on cervical cancer cell proliferation, migration and invasion was investigated. Additionally, the role of STAT3 in epithelial-to-mesenchymal transition (EMT) was investigated.

5.2 Results

5.2.1 STAT3 is required for the proliferation of HPV+ cervical cancer cells

To investigate the role of STAT3 during HPV+ cervical cancer cell proliferation, STAT3 was inhibited using the specific small molecule inhibitor cryptotanshinone. In both HPV18+ HeLa and HPV16+ CaSKi cells, inhibition of STAT3 activation led to a significant reduction in cell proliferation (Fig 5.1A; HeLa, $p = 0.0009$ for crypto, $p = 0.0009$ for S3I-201 at day 5; CaSKi, $p = 0.002$ for crypto, $p = 0.002$ for S3I-201 at day 5). To confirm that this effect was due to the specific inhibition of STAT3, STAT3 protein expression was next depleted using a pool of four validated STAT3 specific siRNAs. Depletion of STAT3 also led to a reduction in cell proliferation (Fig 5.1B; HeLa, $p = 0.009$ at day 5; CaSKi, $p = 0.01$ at day 5.), indicating that the observed effects on cell proliferation were specific to STAT3. Next, the effect of STAT3 inhibition on the expression of key mediators of cell proliferation was examined. Treatment of cells with increasing doses of cryptotanshinone led to a gradual decrease in appearance of the phosphorylated forms of STAT3 at both Y705 and S727 without affecting the total levels of STAT3 protein (Fig 5.1C). Additionally, inhibition of STAT3 led to a reduction in cyclin D1 protein expression, a key mediator of cell cycle progression, and the appearance of the p21 protein, a cyclin dependent kinase inhibitor. STAT3 inhibition also led to the reduction of HPV E6 and E7 expression, which are important virus coded regulators of proliferation in HPV+ cervical cancer cells (Fig 5.1C). In line with this, depletion of STAT3 led to a similar reduction in cyclin D1, HPV E6 and E7, and a corresponding increase in p21 (Fig 5.1D).

To confirm these findings, the effect of STAT3 inhibition using two STAT3 small molecule inhibitors, cryptotanshinone and S3I-201, or the depletion of STAT3 using

siRNA on the clonogenicity of HPV+ cervical cancer cells was assessed. In both HeLa and CaSKi cells, there was a significant decrease in anchorage-dependent colony formation ability after STAT3 inhibition (Fig 5.1E; HeLa, $p = 5x10^{-11}$ for crypto, $p = 1x10^{-6}$ for S3I-201; CaSKi, $p = 7x10^{-5}$ for crypto, $p = 9x10^{-6}$ for S3I-201) or STAT3 depletion (Fig 5.1F; HeLa, p = 0.02; CaSKi, p = 0.004). Additionally, STAT3 activity (Fig 5.1G; HeLa, p = 0.002 for crypto, p = 0.003 for S3I-201; CaSKi, p = 0.002 for crypto, p = 0.003 for S3I-201) and protein expression (Fig 5.1H; HeLa, p = 0.001; CaSKi, p = 0.0003) was also required for the ability of HPV+ cervical cancer cells to form colonies in an anchorage-independent manner in a soft agar assay). Together, these data show that STAT3 is required for cell proliferation and the ability of HPV+ cervical cancer cells to form colonies in an anchorage dependent or independent manner.

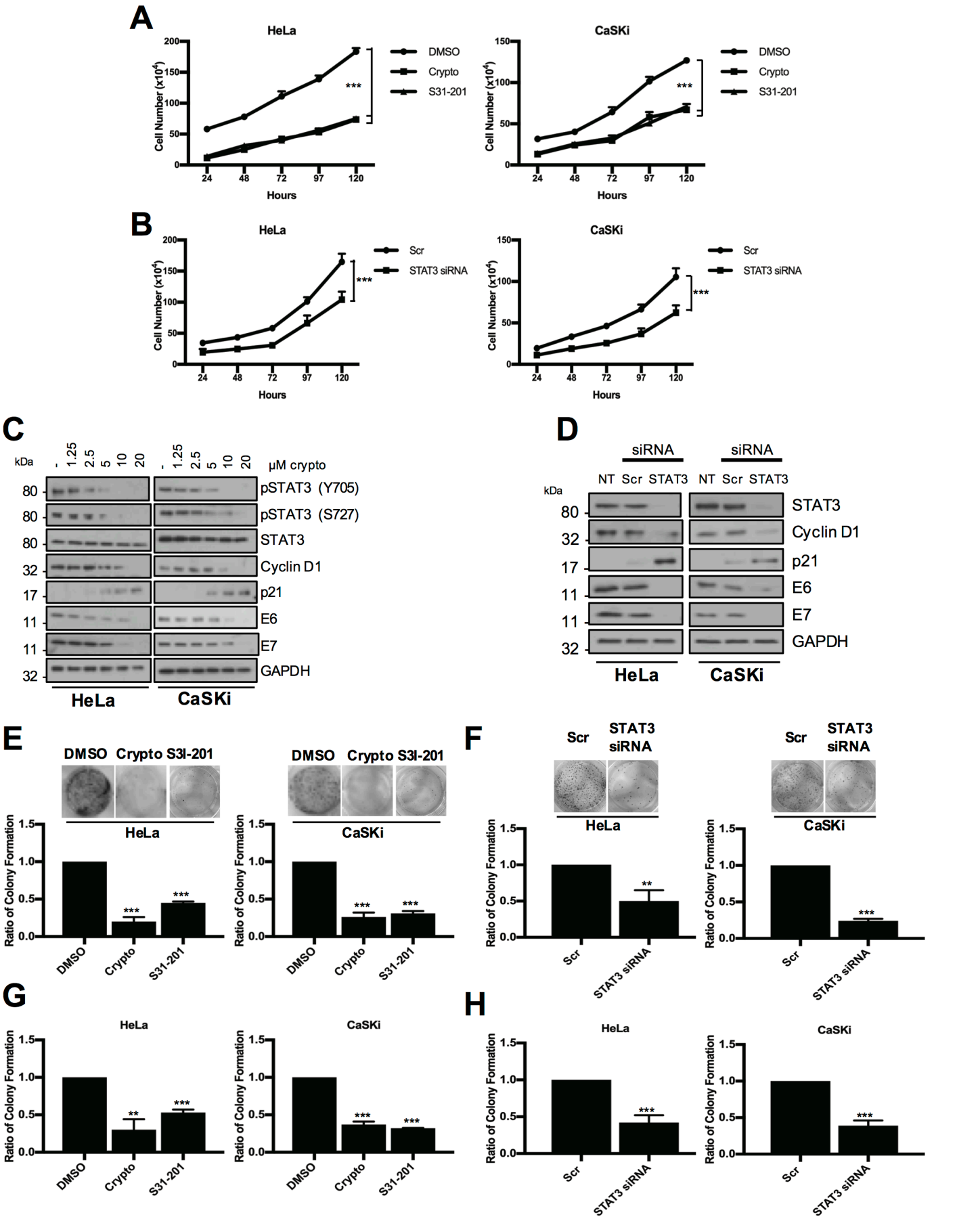
A
HeLa
CaSKi
Cell Number (x10⁴)
Hours
DMSO
Crypto
S31-201
***
B
Scr
STAT3 siRNA
C
kDa
μM crypto
pSTAT3 (Y705)
pSTAT3 (S727)
STAT3
Cyclin D1
p21
E6
E7
GAPDH
D
siRNA
NT Scr STAT3
E
DMSO Crypto S3I-201
Ratio of Colony Formation
F
Scr
STAT3 siRNA
G
H

Fig 5.1. STAT3 is required for the proliferation of HPV+ cervical cancer cells. A) Growth curve analysis of HeLa and CaSKi cells after addition of inhibitors for 24 hours. **B)** Growth curve analysis of HeLa (left) and CaSKi (right) cells after transfection of a pool of four specific STAT3 siRNA for 72 hours. **C)** Representative western blot of cryptotanshinone dose response after 24 hours. **D)** Representative western blot after transfection of a pool of four specific STAT3 siRNA for 72 hours. **E)** Colony formation assay (anchorage dependent growth) of HeLa and CaSKi cells after addition of inhibitors for 24 hours. **E)** Colony formation assay (anchorage dependent growth) of HeLa and CaSKi cells after transfection of a pool of four specific STAT3 siRNA for 72 hours. **G)** Soft agar assay (anchorage independent growth) of HeLa and CaSKi cells after addition of inhibitors for 24 hours. **H)** Soft agar assay (anchorage independent growth) of HeLa and CaSKi cells after transfection of a pool of four specific STAT3 siRNA for 72 hours. Error bars represent the mean +/- standard deviation of a minimum of three biological repeats. *P<0.05, **P<0.01, ***P<0.001 (Student's t-test).

5.2.2 STAT3 inhibition or depletion results in cell cycle arrest in HPV+ cervical cancer cells

Cyclin D1 is a key cell cycle regulator that is over-expressed in several cancers (351). As the inhibition of STAT3 activation or depletion of total STAT3 protein both led to a reduction in cyclin D1 expression, the role of STAT3 in regulation of the cell cycle was analysed by flow cytometry. Treatment with cryptotanshinone led to a significant increase in the number of cells in the S phase of the cell cycle (Fig 5.2A: HeLa, $p = 0.05$ for crypto, $p = 0.027$ for S3I-201; CaSKi, $p = 0.03$ for crypto, $p = 0.02$ for S3I-201) with a concomitant decrease in cells in G2/M (Fig 5.2A; not significant) A similar effect was seen upon depletion of STAT3 protein levels by siRNA treatment (Fig 5.2B; HeLa S phase, $p = 0.003$; CaSKi S phase, $p = 0.002$), indicating that STAT3 is required for cell cycle progression from S phase to G2/M, potentially through the regulation of cyclin D1 expression.

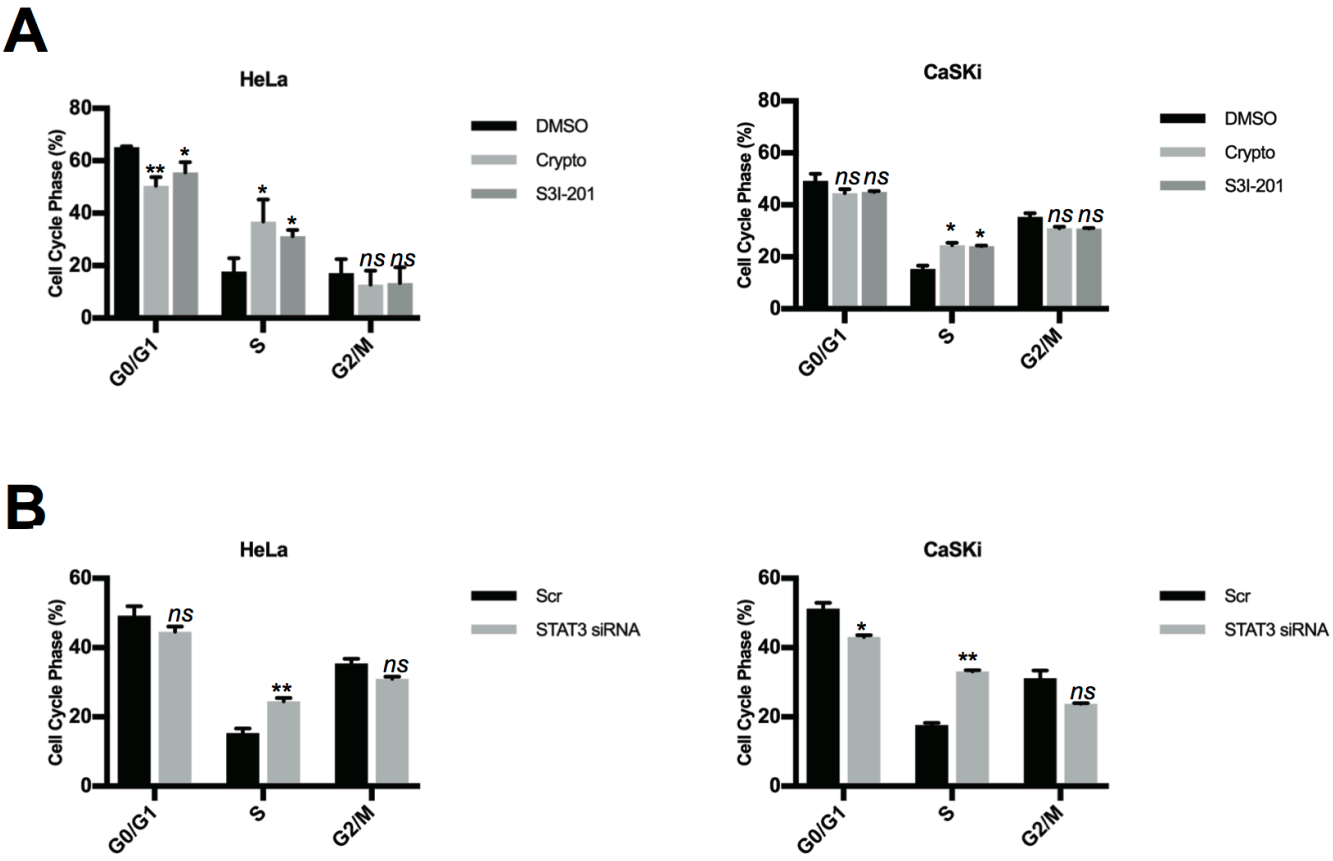

Fig 5.2. STAT3 inhibition or depletion results in cell cycle arrest in HPV+ cervical cancer cells. A) Flow cytometric analysis of cell cycle profile of HeLa and CaSKi cells after addition of inhibitors for 24 hours. **B)** Flow cytometric analysis of cell cycle profile of HeLa and CaSKi cells after transfection of a pool of four specific STAT3 siRNA for 72 hours. Error bars represent the mean +/- standard deviation of a minimum of three biological repeats. *P<0.05, **P<0.01, ***P<0.001 (Student's t-test).

5.2.3 STAT3 regulates apoptosis through the expression of the pro-survival genes, Bcl xL and Survivn in HPV+ cervical cancer

As well as being a driver of cancer cell proliferation, in some circumstances STAT3 is also required for cell survival (345). In cervical cancer cells, inhibition of STAT3 has been shown to induce caspase activation and PARP cleavage (370). Therefore, the effect of STAT3 inhibition or depletion on apoptosis of HPV+ cervical cancer cells was assessed. To look at the early stages of apoptosis, an Annexin V assay was performed, which measures phospholipid flipping in the cell membrane, an early indicator for cell apoptosis (447). In both HeLa and CaSKi cells, the percentage of early apoptotic cells significantly increased after STAT3 inhibition for 6 hours (Fig 5.3A; HeLa, $p = 0.02$ for crypto, $p = 0.003$ for S3I-201; CaSKi, $p = 0.01$ for crypto, $p = 0.005$ for S3I-201). By 24 hours, the percentage of cells in late apoptosis increased significantly (HeLa, $p = 0.0001$ for crypto, $p = 0.001$ for S3I-201; CaSKi, $p = 0.0007$ for crypto, $p = 7x10^{-5}$ for S3I-201), whilst there was also a significant percentage of necrotic cells (HeLa, $p = 0.002$ for crypto, $p = 0.005$ for S3I-201; CaSKi, $p = 0.00006$ for crypto, $p = 0.0004$ for S3I-201). Depletion of STAT3 had a similar, although less pronounced effect on cell apoptosis (Fig 5.3B).

To further investigate the role of STAT3 in cell survival, an assay to measure DNA condensation, another hallmark of apoptosis, was performed. STAT3 inhibition or depletion resulted in a significant percentage of apoptotic and necrotic cells in both HeLa and CaSKi cells (Fig 5.3C and D). To investigate the molecular mechanism involved in the induction of apoptosis due to STAT3 inhibition or depletion, immunofluorescence staining was performed to measure the activity of caspase 3, a key caspase involved in the initiation of apoptosis(448). At 6 hours post STAT3 inhibition, cleaved caspase 3, indicative of the active form of the caspase enzyme,

was detected in cells that displayed rounded up or fragmented nuclei (Fig 5.3E). A similar effect was seen after STAT3 depletion at 24 hours (Fig 5.3F), indicating that STAT3 inhibition or depletion results in the activation of caspase dependent apoptosis. To confirm this, the activity of caspase 3 was analysed by western blotting for the presence of the cleaved form of the caspase 3 substrate PARP-1. After 24 hours inhibition (Fig 5.3G), or 48 hours of STAT3 depletion (Fig 5.3H), PARP-1 cleavage was readily detectable, indicating that caspase 3 was activated.

Several pro-survival genes are known to be direct STAT3 targets, including Bcl xL and Survivin. Therefore, the expression of these genes was analysed by RT-qPCR and western blot. In both HeLa and CaSKi cells, inhibition or depletion of STAT3 led to a reduction in Bcl xL protein expression as indicated by western blotting (Fig 5.3G and H). Furthermore, the mRNA expression of both Bcl xL and Survivin was decreased (Fig 5.3I and J). Together, these data suggest that STAT3 is essential for the survival of HPV+ cervical cancer cells, potential through the regulation of pro-survival genes such as Bcl xL and Survivin.

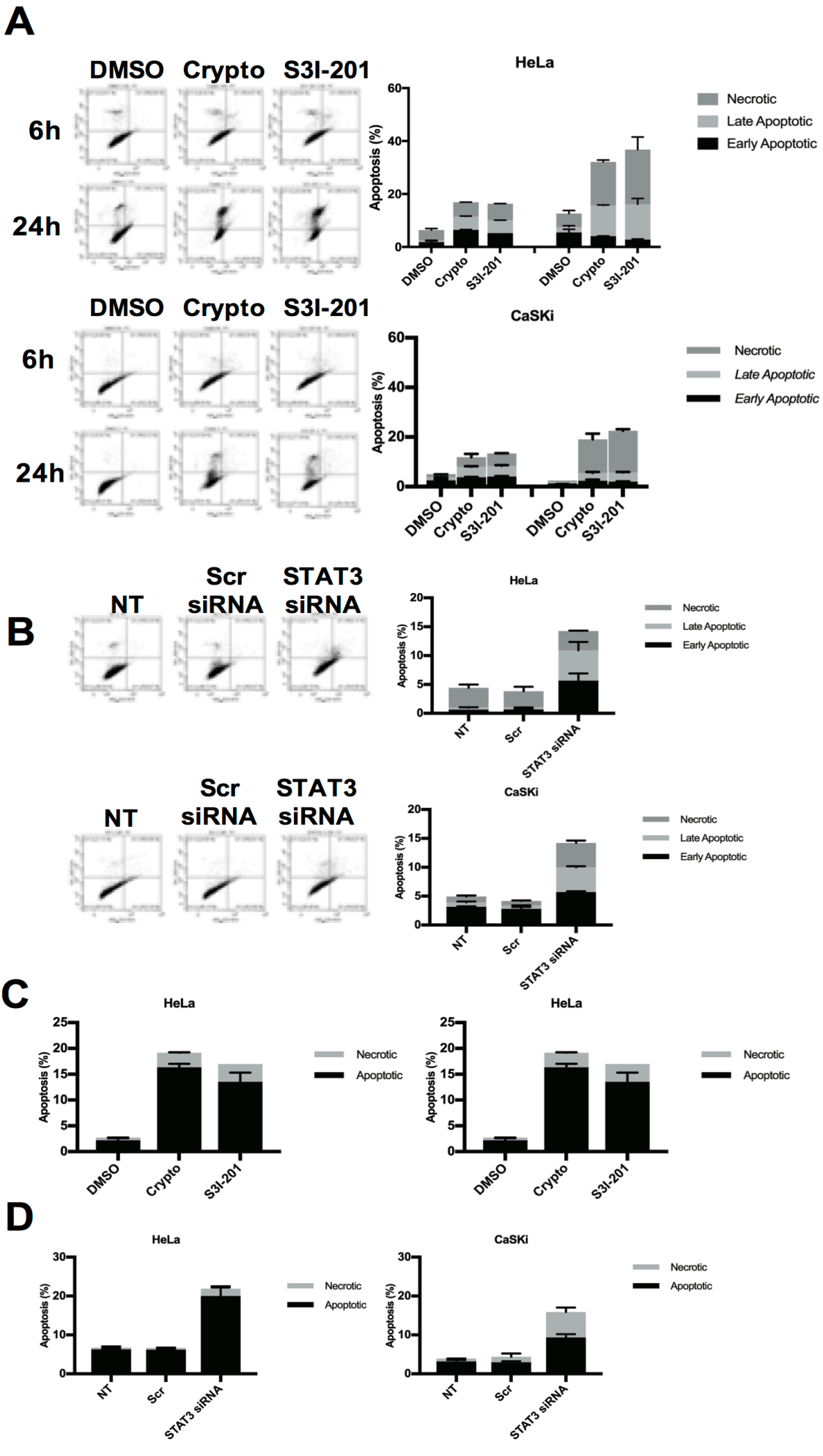
A
DMSO
Crypto
S3I-201
6h
24h
HeLa
Apoptosis (%)
Necrotic
Late Apoptotic
Early Apoptotic
CaSKi
B
NT
Scr siRNA
STAT3 siRNA
C
Apoptotic
D

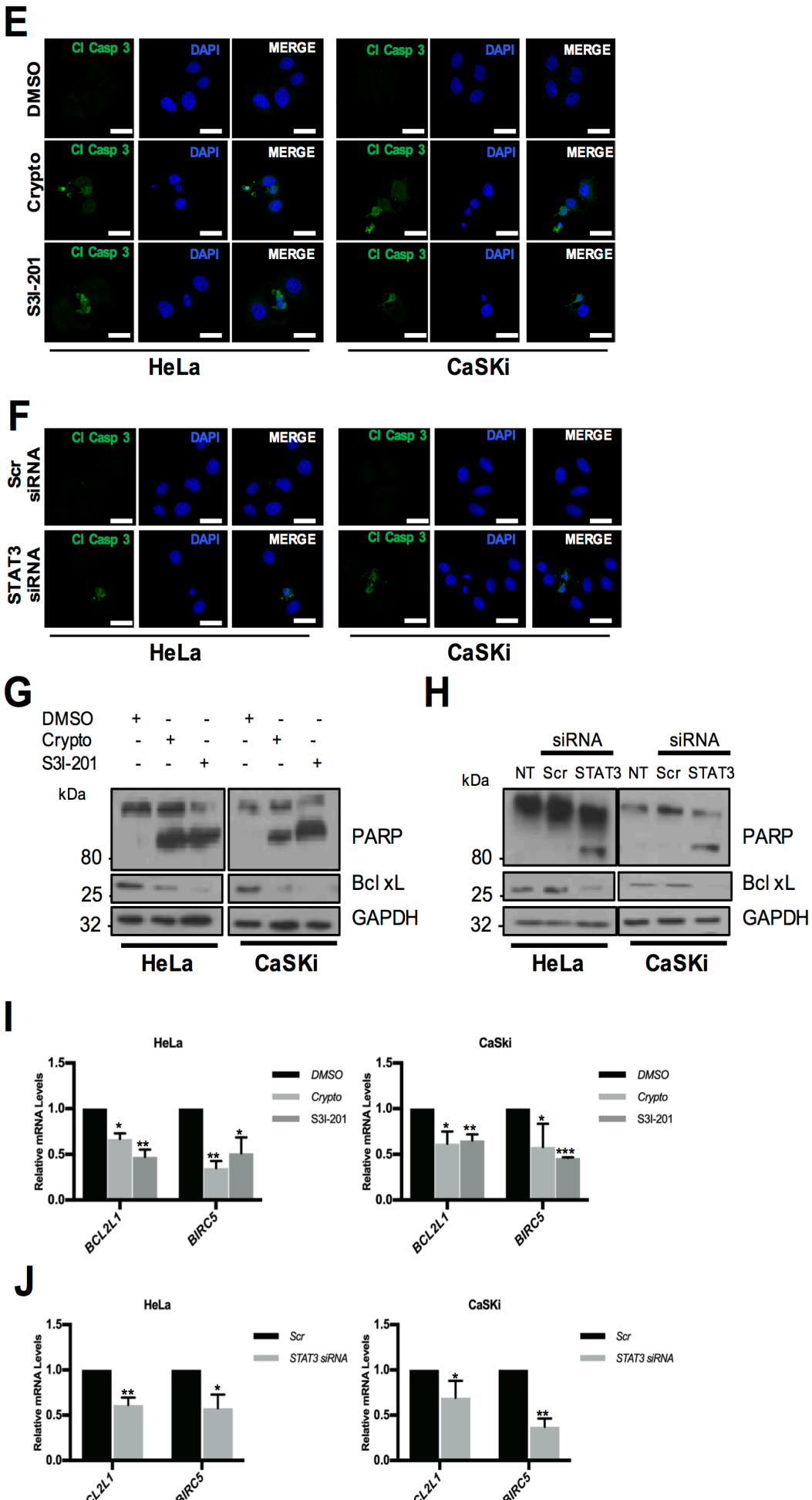
E
Cl Casp 3
DAPI
MERGE
DMSO
Crypto
S3I-201
HeLa
CaSKi
F
Scr siRNA
STAT3 siRNA
G
DMSO
Crypto
S3I-201
kDa
80
25
32
PARP
Bcl xL
GAPDH
H
siRNA
NT Scr STAT3 NT Scr STAT3
I
Relative mRNA Levels
BCL2L1
BIRC5
J
Scr
STAT3 siRNA

Fig 5.3. STAT3 regulates apoptosis through the expression of the pro-survival genes, Bcl xL and Survivn in HPV+ cervical cancer. A) Flow cytometric analysis of Annexin V assay in HeLa and CaSKi cells after addition of inhibitors for 6 and 24 hours. **B)** Flow cytometric analysis of Annexin V assay in HeLa and CaSKi cells after transfection of a pool of four specific STAT3 siRNA for 24 hours. **C)** Flow cytometric analysis of Vybrant™ DyeCycle™ Violet/SYTOX™ AADvanced™ apoptosis kit assay in HeLa and CaSKi cells after addition of inhibitors for 24 hours. **D)** Flow cytometric analysis of Vybrant™ DyeCycle™ Violet/SYTOX™ AADvanced™ apoptosis kit assay in HeLa and CaSKi cells after transfection of a pool of four specific STAT3 siRNA for 24 hours. **E)** Immunofluorescence analysis of HeLa and CaSKi cells after addition of inhibitors for 6 hours. Cover slips were stained for Cleaved caspase 3 (green). Nuclei were visualised using DAPI (blue). **F)** Immunofluorescence analysis of HeLa and CaSKi cells after transfection of a pool of four specific STAT3 siRNA for 24 hours. Cover slips were stained for Cleaved caspase 3 (green). Nuclei were visualised using DAPI (blue). Images were acquired using identical exposure times. Scale bar, 20 μm. **G)** Representative western blot of HeLa and CaSKi cells after addition of inhibitors for 24 hours and analysed for PARP cleavage and Bcl xL expression. GAPDH served as the loading control. **H)** Representative western blot of HeLa and CaSKi cells after transfection of a pool of four specific STAT3 siRNA for 72 hours. **I)** Quantitative PCR analysis of HeLa and CaSKi cells after addition of inhibitors for 24 hours and analysed for PARP cleavage and Bcl xL expression. GAPDH served as the loading control. Cells were analysed for the pro-survival genes *BCL2L1 and BIRC5*. *U6* served as a loading control. Error bars represent the mean +/- standard deviation of a minimum of three biological repeats. *P<0.05, **P<0.01, ***P<0.001 (Student's t-test). **J)** Quantitative PCR analysis of HeLa and CaSKi cells after transfection of a pool of four

specific STAT3 siRNA for 72 hours. Cells were analysed for the pro-survival genes *BCL2L1 and BIRC5*. *U6* served as a loading control. Error bars represent the mean +/- standard deviation of a minimum of three biological repeats. *P<0.05, **P<0.01, ***P<0.001 (Student's t-test).

5.2.4 STAT3 is required for the migration and invasion of HPV+ cervical cancer cells

STAT3 activity has been demonstrated to be essential for the migration and invasion of hepatocellular carcinoma cells (449). Additionally, STAT3 knockout mice have a compromised wound healing response (315). Therefore, the role of STAT3 in the migration and invasion of HPV+ cervical cancer cells was investigated. Using a standard wound healing assay, chemical inhibition of STAT3 or depletion of total STAT3 protein levels both led to a significant reduction in would closure in either HeLa or CaSKi cells (Fig 5.4A and B; HeLa, $p < 5x10^{-5}$ for all conditions; CaSKi, $p < 0.006$ for all conditions). To build on these findings, the migration and invasion properties of HPV+ cervical cancer cells were tested after STAT3 inhibition or depletion using a Transwell® Assay. STAT3 inhibition or depletion led to a significant reduction in the number of migrated cells through the uncoated Transwell® membrane (Fig 5.4C; HeLa, $p < 2x10^{-7}$ for all conditions; CaSKi, $p < 2x10^{-7}$ for all conditions). In addition, STAT3 was also required for the invasion of HPV+ cervical cancer cells through Matrigel® coated Transwell® membranes (Fig 5.4D; HeLa, $p < 2x10^{-7}$ for all conditions; CaSKi, $p < 2x10^{-7}$ for all conditions). These data demonstrate that STAT3 is required for the migration and invasion of HPV+ cervical cancer cells.

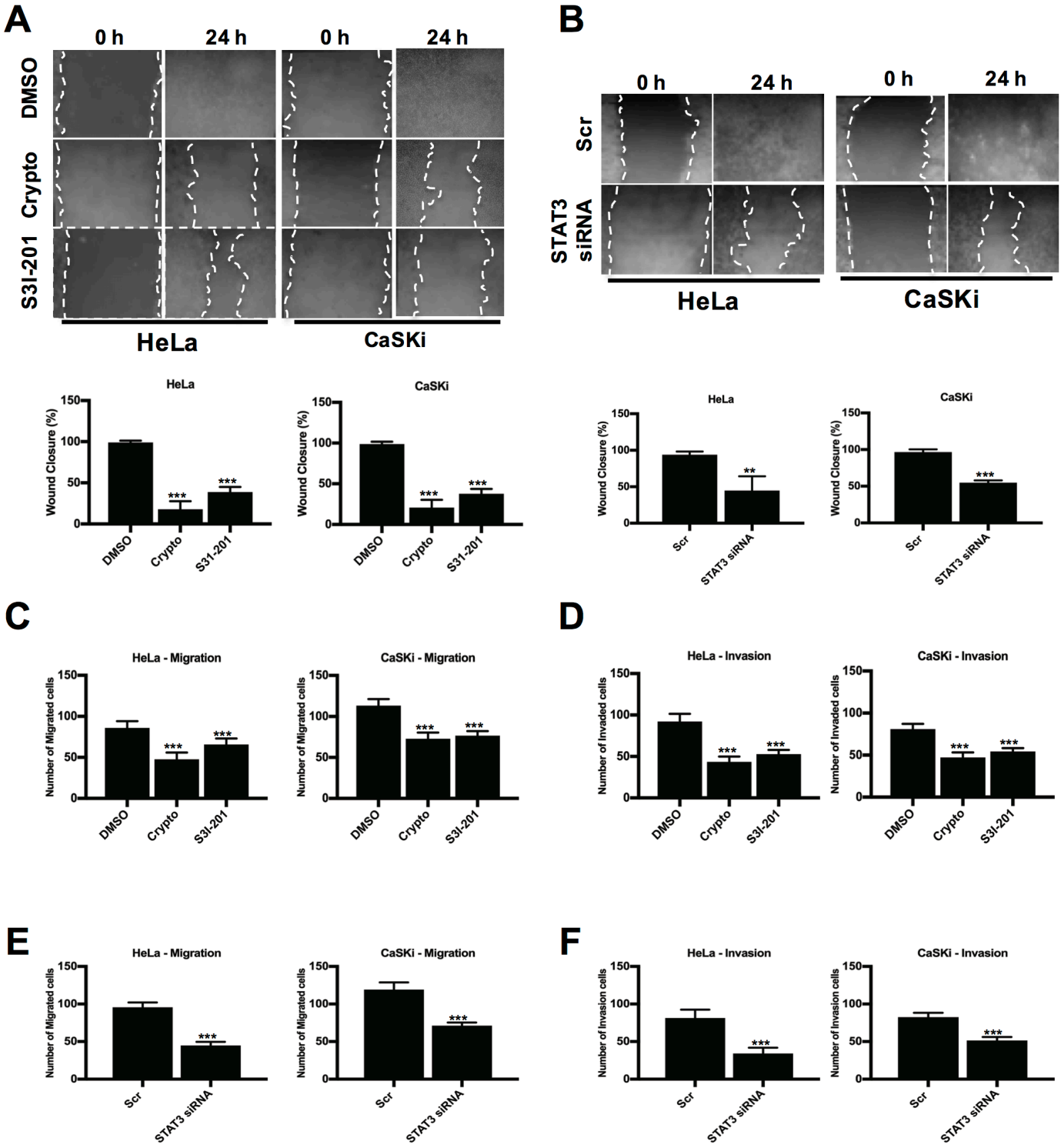

Fig 5.4. STAT3 is required for the migration and invasion of HPV+ cervical cancer cells. A) Wound healing assay in HeLa and CaSKi cells after addition of inhibitors for 24 hours. Confluent cells were then wounded and imaged immediately and after 24 hours. **B)** Wound healing assay in HeLa and CaSKi cells after transfection

of a pool of four specific STAT3 siRNA for 72 hours. Confluent cells were then wounded and imaged immediately and after 24 hours. **C)** Quantification of the migration of HeLa and CaSKi cells over expressing after addition of inhibitors for 24 hours by Transwell® migration assay. The average number of invaded cells per field was calculated from five representative fields per experiment. **D)** Quantification of the invasion of HeLa and CaSKi cells after transfection of a pool of four specific STAT3 siRNA for 72 hours by Transwell® invasion assay. The average number of invaded cells per field was calculated from five representative fields per experiment. Error bars represent the mean +/- standard deviation of a minimum of three biological repeats. *P<0.05, **P<0.01, ***P<0.001 (Student's t-test).

5.2.5 STAT3 is essential for epithelial to mesenchymal transition (EMT) through the regulation of the EMT associated transcription factors Snail and Slug in HPV+ cervical cancer cells

In oesophageal cancers and HNSCC, STAT3 is required to drive EMT and cancer cell metastasis (346,450). Additionally, IL-6 mediated STAT3 signalling has been shown to induce the expression of the key EMT related transcription factors Snail and Slug, as well as the mesenchymal gene vimentin (451).

To investigate if STAT3 was required for the EMT observed in HPV+ cervical cancer cells, the expression of key genes involved in EMT was first analysed by RT-qPCR. Chemical inhibition of STAT3 activation reduced the mRNA expression of the Snail and Slug transcription factors, as well as the mesenchymal markers vimentin and ZEB-1 (Fig 5.5A). Additionally, mRNA expression of the epithelial marker ZO-1 was increased upon STAT3 inhibition. Similar results were obtained by STAT3 siRNA depletion (Fig 5.5B). Western blotting confirmed that STAT3 also regulated the protein expression of these EMT markers (Fig 5.5C and D). Additionally, the expression and localisation of vimentin was assessed by immunofluorescence. Vimentin is highly expressed in HeLa and CaSKi control cells, with a filamentous cytosolic expression pattern throughout a cell. Inhibition or depletion of STAT3 led to a reduced expression of vimentin, with a reduction in visible fibrous vimentin structures (Fig 5.5F).

A key characteristic of EMT is cadherin switching, in which cancer cells lose expression of E-cadherin and instead preferentially express N-cadherin (452). Blockade of STAT3 activity, either by inhibition or siRNA depletion led to an increase in E-cadherin expression and a reduction in N-cadherin expression, indicating that STAT3 is required for cadherin switching in HPV+ cervical cancer cells. Western

blotting or immunofluorescence staining could not confirm the expression of E-cadherin and N-cadherin protein after STAT3 inhibition or depletion. Therefore, flow cytometry was used to analyse the expression of cell surface E-cadherin. After STAT3 inhibition, the surface expression of E-cadherin increased by an average of 72% in HeLa cells and 44% in CaSKi cells (Fig 5.5E).

Together, these data demonstrate that STAT3 is essential for EMT in HPV+ cervical cancer cells.

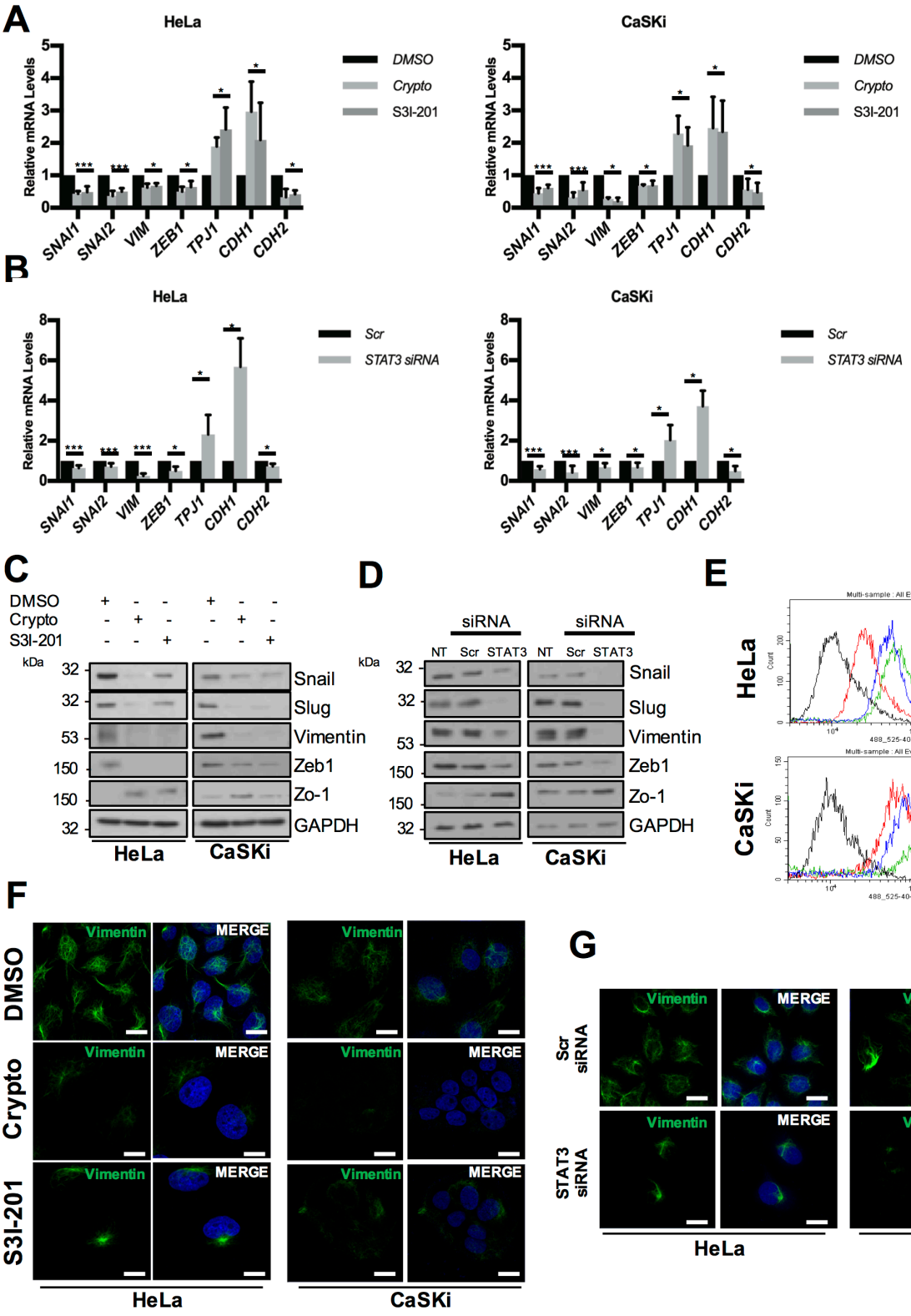
A
HeLa
CaSKi
Relative mRNA Levels
DMSO
Crypto
S3I-201
SNAI1
SNAI2
VIM
ZEB1
TPJ1
CDH1
CDH2
B
Scr
STAT3 siRNA
C
DMSO
Crypto
S3I-201
kDa
Snail
Slug
Vimentin
Zeb1
Zo-1
GAPDH
D
siRNA
NT
Scr
STAT3
E
Multi-sample : All Events
HeLa DMSO
HeLa Crypto
HeLa S3I-201
HeLa IgG
CaSKi DMSO
CaSKi Crypto
CaSKi S3I-201
CaSKi IgG
F
Vimentin
MERGE
G
Scr siRNA
STAT3 siRNA

Fig 5.5. STAT3 is essential for epithelial to mesenchymal transition (EMT) through the regulation of the EMT associated transcription factors Snail and Slug in HPV+ cervical cancer cells. A) Quantitative PCR analysis of HeLa and CaSKi cells after addition of inhibitors for 24 hours. Cells were analysed for the EMT marker expression. *U6* served as a loading control. **B)** Quantitative PCR analysis of HeLa and CaSKi cells after transfection of a pool of four specific STAT3 siRNA for 72 hours. Cells were analysed for the EMT marker expression. *U6* served as a loading control. **C)** Representative western blot of HeLa and CaSKi cells after addition of inhibitors for 24 hours. Cells were analysed for the EMT marker expression. GAPDH served as a loading control. **D)** Representative western blot of HeLa and CaSKi cells after transfection of a pool of four specific STAT3 siRNA for 72 hours. Cells were analysed for the EMT marker expression. GAPDH served as a loading control. **E)** Flow cytometric analysis of E-cadherin expression in HeLa and CaSKi cells after addition of inhibitors for 24 hours. **F)** Immunofluorescence analysis of vimentin expression in HeLa and CaSKi cells after addition of inhibitors for 24 hours. Cover slips were stained for vimentin (green). Nuclei were visualised using DAPI (blue). **G)** Immunofluorescence analysis of vimentin expression in HeLa and CaSKi cells after transfection of a pool of four specific STAT3 siRNA for 72 hours. Cover slips were stained for vimentin (green). Nuclei were visualised using DAPI (blue). Error bars represent the mean +/- standard deviation of a minimum of three biological repeats. *P<0.05, **P<0.01, ***P<0.001 (Student's t-test).

5.2.6 Inhibition of JAK2 reduces STAT3 phosphorylation and impairs HPV+ cervical cancer cell proliferation, migration and invasion

Although there is substantial evidence that STAT3 transactivation function is activate in many cancers, there are currently no clinically available STAT3 inhibitors. The main issue preventing development of such inhibitors has been toxicity in early stage animal models (350); therefore, targeting other components in the core STAT3 signalling pathway is an attractive alternative. The data presented in Chapter 3 demonstrated that HPV E6 induces STAT3 tyrosine phosphorylation by activating Janus Kinase 2 (JAK2). Therefore, the effect of JAK2 inhibition in HPV+ cervical cancer cells was also investigated. Ruxolitinib is a clinically available JAK1/2 inhibitor for the treatment of high-risk myelofibrosis and Fedratinib is a JAK2 specific inhibitor currently in Phase III trials for high-risk myelofibrosis (382,383). In both HPV18+ Hela and HPV16+ CaSKi cells, inhibition of JAK2 activation, as judged by its phosphorylation, resulted in a significant reduction in cell proliferation (Fig 5.6A; HeLa, $p = 0.0007$ for ruxo, $p = 0.001$ for fed at day 5; CaSKi, $p = 0.001$ for ruxo, $p = 0.005$ for fed at day 5), which was comparable to that observed with the STAT3 small molecule inhibitors (Fig 1A). To confirm that treatment with the JAK2 inhibitors reduced STAT3 phosphorylation, western blotting was performed. In these experiments, treatment with the inhibitor led to a dose-dependent reduction in JAK2 phosphorylation, confirming the action of ruxolitinib (Fig 5.6B). Importantly, inhibition of JAK2 also led to a dose-dependent reduction in STAT3 tyrosine phosphorylation, whilst having only a minimal effect on STAT3 serine phosphorylation at the higher doses. The inhibition of JAK2 also resulted in a reduction in cyclin D1 expression and an increase in p21 expression, consistent with the results obtained upon STAT3 inhibition. Furthermore, JAK2 inhibition resulted in a significant decrease in anchorage-dependent (Fig 5.6C; HeLa,

p = 0.0002 for ruxo, p = $2x10^{-5}$ for fed; CaSKi, p = 0.003 for ruxo, p = 0.01 for fed) and anchorage independent colony formation (Fig 5.6D; HeLa, p = $6x10^{-6}$ for ruxo, p = 0.03 for fed; CaSKi, p = $2x10^{-5}$ for ruxo, p = 0.07 for fed).

JAK2 has been demonstrated to be required for the migration and invasion of glioblastoma cells (453). Therefore, a Transwell® Assay was performed, and in this assay the inhibition of JAK2 led to a significant reduction in the number of migrated cells through the uncoated Transwell® membrane (Fig 5.6E; HeLa, p < $2x10^{-7}$ for all conditions; CaSKi, p < $2x10^{-6}$ for all conditions) and the invasion of HPV+ cervical cancer cells through Matrigel® coated Transwell® membranes (Fig 5.6F; HeLa, p < $2x10^{-7}$ for all conditions; CaSKi, p < $2x10^{-9}$ for all conditions). Together, these data demonstrate that targeting JAK2 generates a similar phenotype to that observed when STAT3 is inhibited in HPV+ cervical cancer cells.

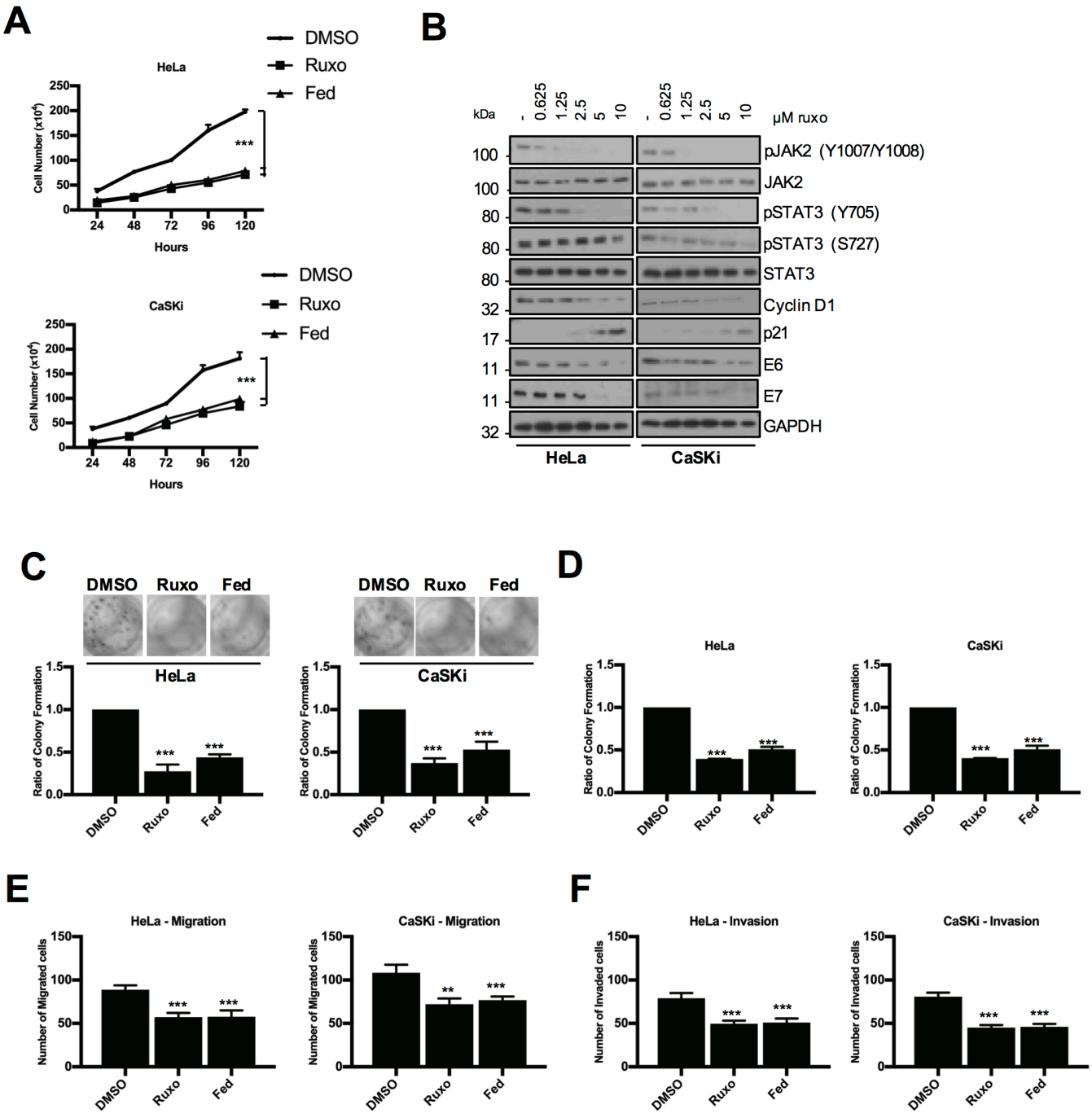

Fig 5.6. Inhibition of JAK2 inhibits STAT3 phosphorylation and impairs cell proliferation, migration and invasion in HPV+ cervical cancer cells. A) Growth curve analysis of HeLa and CaSKi cells after addition of inhibitors for 48 hours. **B)** Representative western blot of ruxolitinib dose response after 48 hours. **C)** Colony formation assay (anchorage dependent growth) of HeLa and CaSKi cells after addition

of inhibitors for 48 hours. **D)** Soft agar assay (anchorage independent growth) of HeLa and CaSKi cells after addition of inhibitors for 48 hours. **E)** Quantification of the migration and invasion of HeLa and CaSKi cells after addition of inhibitors for 48 hours by Transwell® invasion assay. The average number of invaded cells per field was calculated from five representative fields per experiment. Error bars represent the mean +/- standard deviation of a minimum of three biological repeats. *P<0.05, **P<0.01, ***P<0.001 (Student's t-test).

5.2.7 JAK2 inhibitors induce cell cycle arrest and apoptosis in HPV+ cervical cancer cells

JAK2 is involved in the regulation of the cell cycle in cancer cells through the direct phosphorylation of the cyclin-dependent kinase inhibitor p27 (454). In contrast to the effect of role of STAT3 on the cell cycle, JAK2 inhibition resulted in a decrease in cells in the S and G2/M phase of the cell cycle and a significant increase of cells in G0/G1 (Fig 5.7A; HeLa G0/G1, $p = 0.017$ for ruxo, $p = 0.03$ for fed; CaSKi G0/G1, $p = 0.035$ for ruxo, $p = 0.027$ for fed).

To identify if this accumulation of cells in G0/G1 resulted in apoptosis, cells treated with the JAK2 inhibitors were analysed by Annexin V staining and flow cytometry. In both HeLa and CaSKi cells, the percentage of early apoptotic cells significantly increased after STAT3 inhibition for 6 hours (Fig 5.7B; HeLa, $p = 0.09$ for ruxo, $p = 0.001$ for fed; CaSKi, $p = 8x10^{-5}$ for ruxo, $p = .003$ for fed). By 24 hours, the percentage of cells in late apoptosis increased significantly (HeLa, $p = 0.05$ for ruxo, $p = 0.03$ for fed; CaSKi, $p = 0.03$ for ruxo, $p = 0.05$ for fed), whilst there was also an increase in necrotic cells (HeLa, $p = 0.009$ for ruxo, $p = 0.32$ for fed; CaSKi, $p = 0.19$ for ruxo, $p = 0.03$ for fed). Inhibition of JAK2 also resulted in a significant increase in apoptotic and necrotic cells as detected in the DNA condensation assay (Fig 5.7C).

As demonstrated for STAT3 inhibition or depletion, the induction of apoptosis upon JAK2 inhibition involved the activation of caspase 3, as determined by the induction of cleaved caspase 3 (Fig 5.7D) and PARP cleavage (Fig 5.7E). JAK2 inhibition also resulted in the reduction in Bcl xL protein expression, suggesting that the inhibition JAK2 reduced the ability of STAT3 induce the expression of pro-survival genes.

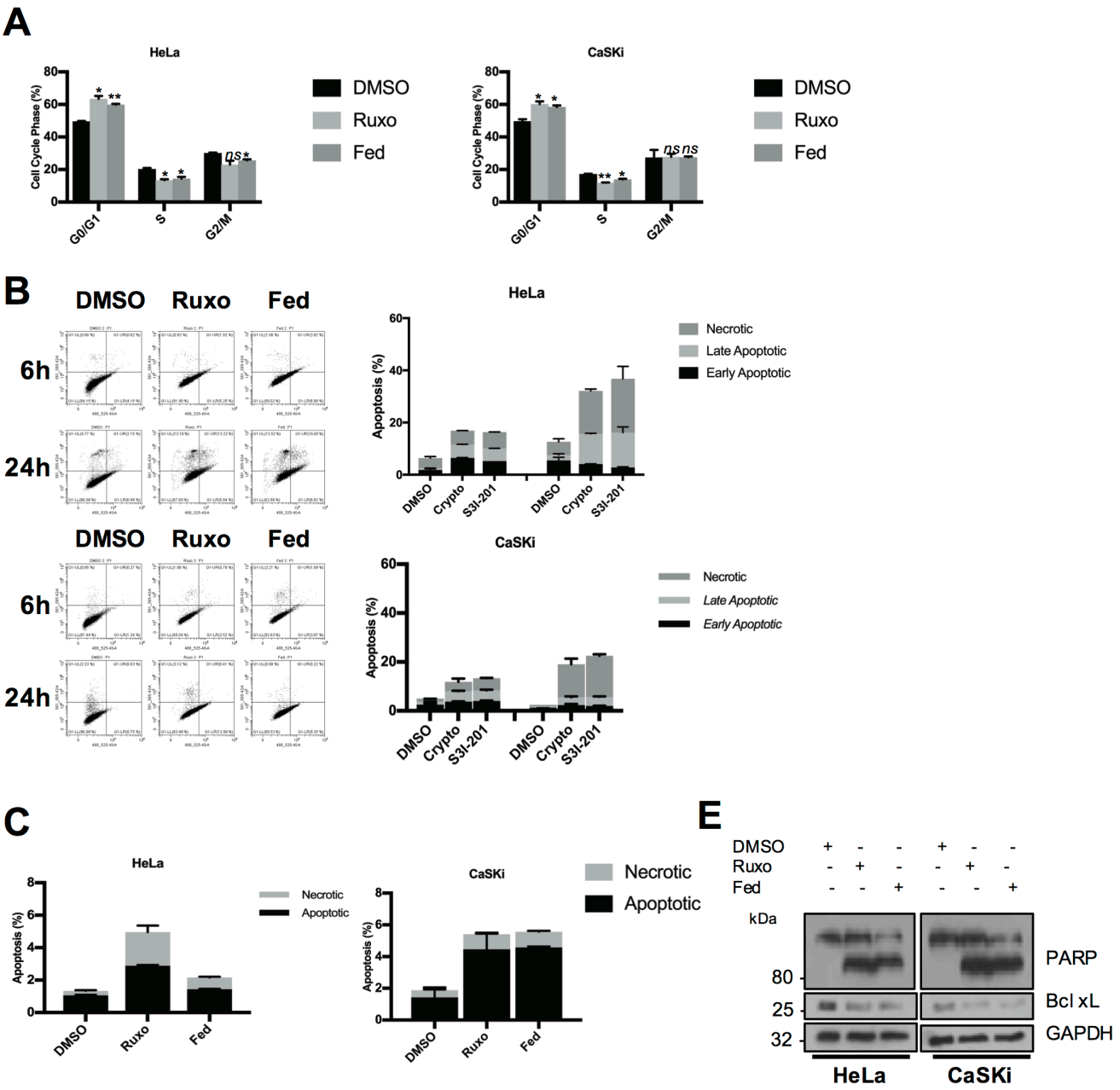

Fig 5.7. JAK2 inhibitors induce cell cycle arrest and apoptosis in HPV+ cervical cancer cells. A) Flow cytometric analysis of cell cycle profile of HeLa and CaSKi cells after addition of inhibitors for 24 hours. **A)** Flow cytometric analysis of Annexin V assay in HeLa and CaSKi cells after addition of inhibitors for 6 and 24 hours. **C)** Flow cytometric analysis of Vybrant™ DyeCycle™ Violet/SYTOX™ AADvanced™ apoptosis kit assay in HeLa and CaSKi cells after addition of inhibitors for 24 hours.

D) Immunofluorescence analysis of HeLa and CaSKi cells after addition of inhibitors for 6 hours. Cover slips were stained for Cleaved caspase 3 (green). Nuclei were visualised using DAPI (blue). **E)** Representative western blot of HeLa and CaSKi cells after addition of inhibitors for 24 hours and analysed for PARP cleavage and Bcl xL expression. GAPDH served as the loading control. Error bars represent the mean +/- standard deviation of a minimum of three biological repeats. *P<0.05, **P<0.01, ***P<0.001 (Student's t-test).

5.2.8 JAK2 phosphorylation correlates with cervical disease severity and is increased in HPV+ cervical cancer cells

JAK2 phosphorylation is increased in several haematological cancers (455). As the data suggests that JAK2 activity is critical for HPV+ cervical cancer cell proliferation and survival, the phosphorylation status of JAK2 in cervical disease was analysed. Cervical liquid-based cytology samples representing pre-cancerous cervical disease progression (CIN1-3) and normal cervical tissue were analysed for phosphorylated and total JAK2 expression by western blot. JAK2 phosphorylation increased in line with cervical disease grade from CIN1 to CIN3, whilst total JAK2 levels remained confirming that JAK2 phosphorylation significantly increases upon cervical disease grade (Fig 5.8B; CIN1, $p = 6.5x10^{-5}$; CIN2, $p = 6.6x10^{-6}$; CIN3, $p = 8.1x10^{-6}$).

Finally, to confirm if JAK2 phosphorylation was elevated in cervical cancer cells, the phosphorylation status in cervical cancer cell lines was also assessed. Increased JAK2 phosphorylation was observed in both HPV16+ and HPV18+ cervical cancer cell lines when compared to HPV- cervical cancer cells. These data suggest that JAK2 phosphorylation correlates with cervical disease severity and JAK2 is aberrantly phosphorylated in HPV+ cervical cancer cells.

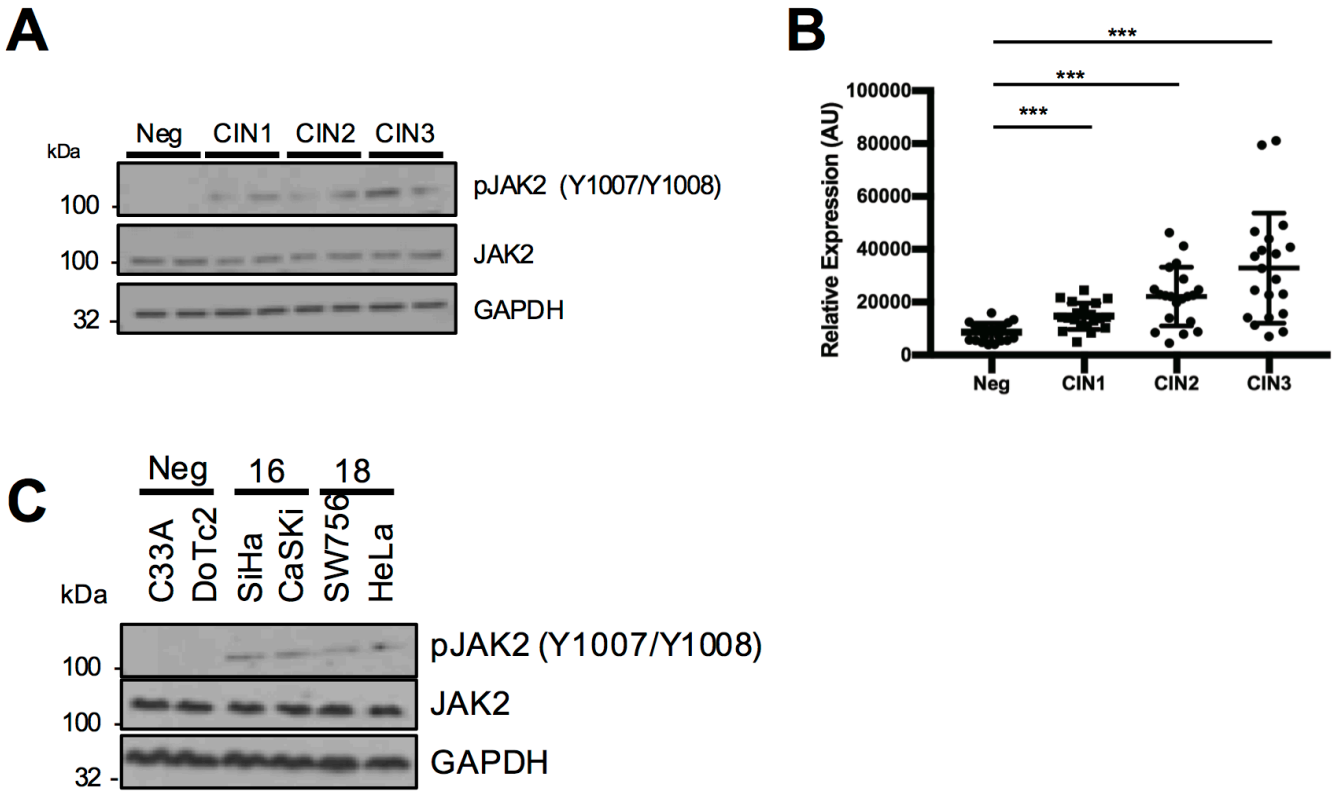

Fig 5.8. JAK2 phosphorylation correlates with cervical disease severity and is increased in HPV+ cervical cancer cells. A) Representative western blots from cytology samples of CIN lesions of increasing grade analysed IL-6 expression. GAPDH served as a loading control. **B)** Scatter dot plot of densitometry analysis of a panel of cytology samples. Twenty samples from each clinical grade (neg, CIN I-III) were analysed by western blot and densitometry analysis was performed using ImageJ. GAPDH was used as a loading control. **C)** Representative western blot of from six cervical cancer cell lines – two HPV- (C33A and Dotc2 4510), two HPV16+ (SiHa and CaSKi) and HPV18+ (SW756 and HeLa) – for the expression of phosphorylated and total JAK2. GAPDH served as a loading control. Data are representative of at least three biological independent repeats. Error bars represent the mean +/- standard deviation of a minimum of three biological repeats. *P<0.05, **P<0.01, ***P<0.001 (Student's t-test).

5.3 Discussion

The transcription factor STAT3 is activated in many haemopoietic and solid cancers, including HNSCC, glioblastoma and pancreatic cancer (347,442,446). STAT3 controls the expression of genes that contribute to the hallmarks of cancer, including proliferation, survival, angiogenesis, immune evasion and inflammation(283). In cervical cancer, STAT3 has previously been shown to be required for viral gene expression and for cell growth (370). However, these studies were undertaken using the plant metabolite curcumin that has broad effects on a multitude of signalling pathways. Therefore, data gained from this study must be further validated using a more targeted approach using specific small molecule inhibitors. Both of the small molecule inhibitors used in this study, cryptotanshinone and S3I-201, bind to the SH2 domain of STAT3 to inhibit its dimerisation and nuclear translocation (456,457); these compounds offer higher levels of specificity in inhibiting the STAT3 signalling pathway. Additionally, the authors used a STAT3 siRNA to study the role of STAT3 in viral oncogene expression and cell growth (370). Whilst their results using STAT3 siRNA correlate with the pharmacological data, they did not extend the siRNA studies to look at other cancer phenotypes after STAT3 depletion, limiting the scope of their study.

In this study, the role of STAT3 in cervical cancer proliferation, survival migration, invasion and EMT was investigated using two highly specific small molecule inhibitors and a pool of STAT3 specific siRNA. The results demonstrate that STAT3 is essential for cell proliferation and cell cycle progression in HPV+ cervical cancer cells and inhibition or depletion of STAT3 resulted in caspase-mediated apoptosis. Additionally, STAT3 is required for the migration and invasion of HPV+ cervical cancer cells and the expression of key transcription factors and cellular markers involved in EMT.

A number of validated STAT3 target genes are key drivers of cell proliferation. Cyclin

D1 is an important oncogenic driver of cell cycle progression and its expression is up-regulated in many cancers, often in a STAT3 dependent manner (458). Additionally, STAT3 signalling can repress the expression of p53 and its downstream target p21, proteins that are essential in modulation of the cell cycle and inducing growth arrest (458). The data here demonstrates that in HPV+ cervical cancer cells, STAT3 is required for the expression of cyclin D1 and repression of p21 (Fig 5.1C and D), and this could be one of the mechanisms utilised by STAT3 to drive cells proliferation and cell cycle progression (Fig 5.2). However, as both HPV E6/E7 expression up-regulates cyclin D1 to drive transformation (ref), studies in which cyclin D1 is overexpressed in STAT3 silenced cells would be required in order to confirm that cyclin D1 is required for the proliferative effects associated with aberrant STAT3 activation.

A key hallmark of cancer is the ability to avoid apoptosis (459). As p53 is important in inducing apoptosis after genotoxic stress (460) and STAT3 regulates a number of pro-survival genes, the role of STAT3 in cell survival in HPV+ cervical cancer was assessed. Short term inhibition or depletion of STAT3 resulted in the induction of caspase 3 activation (Fig 5.3E and F) and an increase in early apoptosis as indicated by Annexin V assay (Fig 5.3A and B). After 24 hours, cells underwent the later stages of apoptosis (Fig 5.3A-D), PARP-1 cleavage (Fig 5.3G and H) and necrotic cell death. At the molecular level, STAT3 was required for the expression of the pro-survival genes Bcl xL and Survivin (Fig 5.3G-H), suggesting that STAT3 may confer cell survival through the regulation of key proteins involved in cell survival.

The ability of cancer cells to migrate and invade into the lumen of blood vessel is critical for cancer metastasis (459). STAT3 controls several key genes involved in these processes, such as matrix metallopeptidase family members (280). In HPV+ cervical cancer cells, STAT3 is required for the migration of cells (Fig 5.4A-C) and the

invasion of cells through a Matrigel® membrane (Fig 5.4D). To identify if this is due to the regulation of genes involved in these process, further experiments will be required to look at the expression of such genes.

Another key component of cell metastasis is epithelial to mesenchymal transition (EMT). This process is controlled by the expression of key transcription factors, including Snail, Slug and Twist, that act to activate or repress key epithelia or mesenchymal genes (452). Snail, Slug and Twist have all been demonstrated to be involved in EGF-stimulated EMT in cervical cancer cells (461). Additionally, IL-6 stimulated EMT has been shown to be STAT3 dependent in cervical cancer cells (462). The data presented here showed that STAT3 is required for the expression of the EMT transcription factors Snail and slug, the mesenchymal markers vimentin and ZEB-1 and the repression of the epithelial tight junction protein ZO-1 (Fig 5.5A-D). STAT3 inhibition or depletion also resulted in 'cadherin switching', where N-cadherin expression is decreased and E-cadherin expression is increased (Fig 5.5A-B). Additionally, surface expression of these cadherin markers is altered upon STAT3 inhibition or depletion (Fig 5.5E), together suggesting that STAT3 is essential for the EMT program in HPV+ cervical cancer cells. Further experiments would be required to demonstrate if STAT3 contributes to EMT driven by key cytokine and growth factor stimulations, such as EGF, IL-6 or TGF-β.

STAT3 as a target for cancer therapeutics has been of wide interest for the last 15 years, due to the ability to generate potent, specific inhibitors and the number of cancers that have deregulated STAT3 signalling. However, the main issue with developing a clinically available STAT3 inhibitor has been toxicity in early stage clinical trials. Therefore, a better approach in targeting the STAT3 signalling pathway may be to target upstream components in the hope of reducing toxicities associated with

STAT3 inhibition. The tyrosine kinase JAK2 is key for STAT3 tyrosine phosphorylation and consequent activation. JAK2 is phosphorylated in many cancers, particularly those of a haematopoietic origin (455). Several of these cancers harbour the JAK2 V617F mutant, which is able to drive cell proliferation and enable immune escape (362,463). Inhibition of JAK2 using the non-selective compound AG490 has demonstrated that JAK2 activity is required for STAT3 phosphorylation and viral oncogene expression in HPV+ cervical cancer cells (370). Here, the well-characterised JAK1/2 inhibitor Ruxolitinib, which has been approved for the treatment of Polycythemia Vera (PV), and the JAK2 inhibitor Fedratinib, which is currently in Phase III trials for myeloproliferative disorders, were utilised to specifically inhibit JAK2 in HPV+ cervical cancer. In these cells, use of either inhibitor resulted in a significant inhibition in cell proliferation (Fig 5.6A) and colony formation potential (Fig 5.6C-D). JAK2 inhibition also decreased STAT3 tyrosine phosphorylation, and reduced expression of the STAT3 target cyclin D1, with a corresponding increase in p21 expression. JAK2 inhibition also resulted in an arrest of the cell cycle and the induction of apoptosis in HPV+ cervical cancer cells. However, whereas STAT3 inhibition or depletion resulted in an accumulation of cells in the S phase of the cell cycle (Fig 5.2), JAK2 inhibition resulted in an accumulation of cells in G0/G1 (Fig 5.7A). This is likely due to the fact that JAK2 feeds into other signalling pathways besides STAT3, including STAT5, MAPK and PI3K/AKT (464). JAK2 inhibition also resulted in apoptosis with the induction of caspase 3 activation (Fig 5.7B-D) and PARP-1 cleavage (Fig 5.7E). As JAK2 inhibition also resulted in the reduced expression of Bcl xL (Fig 5.7E), the mechanism of apoptosis induction upon JAK2 inhibition may be due to the reduction in STAT3 dependent Bcl xL expression. Further work would need to demonstrate that STAT3 is the essential downstream target of JAK2 inhibition Finally,

JAK2 phosphorylation correlated with disease severity in liquid biopsy samples of cervical disease and was shown to be in aberrantly phosphorylated in HPV+ cervical cancer cells.

In conclusion, the data presented here demonstrates that STAT3 is essential for the proliferation, migration and invasion of HPV+ cervical cancer cells. Additionally, inhibition or depletion of STAT3 results in the induction of apoptosis. Furthermore, the upstream kinase JAK2 is aberrantly phosphorylated in HPV+ cervical cancer cells and targeting JAK2 using clinically available inhibitors results in a similar phenotype to STAT3 inhibition, identifying JAK2 a potential therapeutic target in HPV+ cervical cancer.

Chapter 6. Final Discussion and Summary

The work presented in this thesis represents the most detailed characterised of the role of the STAT3 transcription factor both during the differentiation-dependent HPV life cycle and in HPV+ cervical cancer. It identifies STAT3 as an essential host factor in both in the HPV life cycle and in HPV-mediated transformation.

As an obligate intracellular pathogen, HPV must manipulate host cell factor and signalling pathways in order to drive is own replication (375). Previous work has identified several transcription factors and signalling pathway modulated by HPV to drive viral replication and persistence. For example, the transcription factor KLF4 has been shown to regulate keratinocyte differentiation and cell cycle progression and is upregulated by HPV to drive viral transcription (55). Furthermore, the MAP kinase p38 and its downstream target MAPKAP2 have been identified as critical for viral genome amplification(397). Extensive studies have also elucidated a critical role for the DNA damage response (DDR) in driving viral genome amplification (404). Both the E6 and E7 proteins can activate the ATM and ATR arms of the DDR (465), with several key genes involved in this response activated by HPV. One of these genes involved in HPV mediated activation of the DDR is the transcription factor STAT5. STAT5 activation is essential for HPV induced ATM phosphorylation (150) and the acetyltransferase Tip60 is a key regulator of STAT5 mediated ATM activation (466). The activation of the ATR arm of the DDR is also dependent on STAT5, through the regulation of Topoisomerase IIβ-Binding protein 1 (TopBP1) (264).

In this study, the transcription factor STAT3 was identified as a host cell factor that is essential for the productive HPV life cycle (Chapter 3). The activation of STAT3 by HPV E6 is required for viral transcription and oncogene expression and is critical for cell cycle progression in keratinocytes. Additionally, a phosphorylation null STAT3

mutant displayed a profound reduction in the suprabasal hyperplasia seen in HPV-containing organotypic rafts, demonstrating the requirement of STAT3 for the full, productive HPV life cycle.

STAT3 is a *bona fide* oncogene that can induce tumours in nude mice (272). Of the STAT proteins, STAT3 is most strongly associated with tumour formation and is the only STAT family member that is embryonic lethal upon genetic deletion (273). Aberrantly phosphorylated STAT3 is found in several cancers of diverse origin (345,347,449,456) and the targeting of constitutive STAT3 signalling is a promising therapeutic target in oncology (194). The activation of STAT3 occurs primarily through cytokine and growth factor signalling, resulting in the activation of JAK proteins (194,467). The data shows that JAK2 phosphorylation is increased in HPV containing keratinocytes and this is induced by the E6 oncogene. Use of the two well characterised small molecule inhibitors of JAK1/2 (ruxolitinib) and JAK2 (Fedratinib) demonstrated that the tyrosine phosphorylation of STAT3 in HPV containing keratinocytes is primarily mediated by JAK2. Importantly, Ruxolitinib is a clinically approved inhibitor of JAK1/2 in the treatment of myeloproliferative disorders; therefore, the use of Ruxolitinib or other JAK inhibitors may have therapeutic potential in treating HPV infection and this line of research warrants further investigation.

Additionally, the identification of the kinase responsible for STAT3 serine phosphorylation was identified. Many candidate kinase have been shown to induce the serine phosphorylation of STAT3 and this appears to be tissue-specific (191). In T cells, the kinase CDK5 phosphorylates STAT3 at S727 and this is required to supress the development of T_{reg} cells(293), whereas in the liver cancer cell line HepG2, Protein Kinase C (PKC) induces STAT3 S727 phosphorylation in an IL-6 dependent manner (290,291) However, the serine 727 residue of STAT3 sits in a strong MAP kinase

consensus sequence (^{725}PMSP^{728}), suggesting that MAP kinase may play an important role in serine phosphorylation of STAT3. Indeed, the three canonical MAP kinases p38, ERK and JNK have all been demonstrated to induce STAT3 S727 (287-289)Using specific small molecule inhibitors, all three canonical MAP kinases were identified to be important in the serine phosphorylation of STAT3 in HPV containing keratinocytes. Interestingly, S727 phosphorylation was only abolished upon inhibition of all three MAP kinases, suggesting a level of redundancy between the kinases and demonstrating the critical important of this post-translational modification of STAT3.

The upregulation of STAT3 phosphorylation during the primary life cycle of HPV suggests that this pathway may play an important role in HPV-driven tumourigenesis. In order to target the pathways that are required for the proliferative environment that HPV induces in order to drive its own replication, it is essential that the mechanism HPV uses to regulate these pathways is understood. STAT3 is activated in response to receptor mediated signalling. The most well-studied signalling axis leading to the downstream activation of STAT3 is IL-6/gp130 signalling (194). This pathway is deregulated in many cancers such as lung cancer (423), chronic lymphocytic leukaemia (CLL) (276) and glioblastoma (468). In these cancers, STAT3 activation is often mediated by autocrine IL-6 signalling. The constitutive activation of IL-6/STAT3 signalling is mostly due to over-production of IL-6; this is primarily due to the loss of key negative regulators of the pathway, such as SOCS3, PIAS3 and members of the protein tyrosine phosphatase (PTPs) family (304,469,470). Additionally, constitutive activation of receptor tyrosine kinases, such as EGFR, or tyrosine kinases, such as c-SRC, can induce STAT3 activation in certain cancers (365). Interestingly, gain-of-function mutations in STAT3 are relatively rare (471,472). Recently, a number of

mutations in the SH2 domain were identified in Granular Lymphocytic Leukaemia (GLL) and these were suggested to promote STAT3 phosphorylation (473).

In HPV associated cancers, it is well studied that the EGFR is over expressed and can result in the activation of key tumourigenic signalling pathways, such as MEK-ERK signalling. Additionally, treatment of cervical cancers with EGF can induce STAT3 phosphorylation (431). However, the data here suggests that IL-6 is the main driver of STAT3 phosphorylation in HPV+ cervical cancers.

The up-regulation of IL-6 and autocrine IL-6 signalling in cancer cells is often involved in constitutive activation of STAT3 (474). IL-6 is regulated at the transcriptional level and contains transcription factors binding sites for AP-1, NF-κB CREB and SP-1 (475). The activity of the transcription factor NF-κB often coincides with STAT3 activity in cancer(440). Both pathways are involved in promoting a pro-inflammatory environment and this has been demonstrate to promote the development of cancers, including cervical cancer (173,370). Like STAT3, the deregulated activation of NF-κB is attributed to several mechanisms. The loss of negative regulators of NF-κB, such as the deubiquitinases CYLD and A20, allow uncontrolled NF-κB signalling, and this results in the expression of pro-inflammatory and pro-proliferative genes that can drive tumourigenesis (476,477). Indeed, reduced CYLD expression in cervical cancer by the over expression of miR-501 promotes cell proliferation by the activation of NF-κB (478). The regulation of IL-6 by NF-κB occurs in many cancer and this can drive an inflammatory state and induce the autocrine/paracrine activation of STAT3 (442,479). In cervical cancer, the E6 oncoprotein has previously been demonstrated to induce STAT3 phosphorylation (369) and can induce IL-6 expression and secretion in non-small cell lung cancer (NSCLC) cells (416). However, whether or not IL-6 directly contributes to STAT3 phosphorylation in cervical cancer cells is currently unknown.

The data presented in Chapter 4 demonstrates that IL-6 is the key mediator of STAT3 phosphorylation in HPV+ cervical cancer cells. Additionally, the data showed that NF-κB is essential for IL-6 production induced by E6.

The exact mechanism used by HPV E6 to drive this is signalling axis is still currently unknown. E6 has been demonstrated to induce the proteosomal degradation of the deubiquitinase CYLD, resulting in the activation of NF-κB in hypoxic cells (173). This may contribute to the increased expression and secretion of IL-6 and the subsequent activation of STAT3. Further studies will be needed to identify if CYLD plays a significant role in this pathway. Additionally, the tumour suppressor PTEN has been demonstrated to be down regulated in cervical cancers (480). HPV E6 has also been shown to induce PTEN phosphorylation, thus reducing the ability of PTEN to inhibit AKT signalling (481). Again, whether PTEN is involved in this pathway requires further studies.

Currently, there is still no targeted therapeutic for the virus. Despite the availability of vaccines for HPV, the efficacy of these vaccines in reducing HPV-mediated cancers is only just becoming apparent (39). In addition, men and women who reached adolescence before the vaccine was available and are thus unlikely to be given the opportunity to receive the vaccine are still susceptible to several HPV induced cancers. Thus, there is still a requirement for novel therapeutics to treat HPV mediated disease. Whilst a number of studies have shown a dependence on STAT3 for cervical cancer proliferation and survival (369,370), whether STAT3 is also needed for cell migration, invasion and EMT induction is lacking. The data in chapter 5 demonstrated that STAT3 essential for cell proliferation and survival, as well as being required for the migration and invasion of HPV+ cervical cancer cells. Additionally, STAT3 was essential for the

expression of key genes involved in EMT. The mesenchymal protein vimentin has previously been demonstrated to be over expressed in cervical cancers and correlates with an invasive phenotype (482). Furthermore, nuclear localisation of the transcription factor Snail is associated with the downregulation for E-Cadherin, an essential part of EMT (483). As STAT3 regulates the expression of these key genes involved in the initiation of EMT and the maintenance of the EMT phenotype, the therapeutic targeting of STAT3 may result in the reversal of EMT and a less metastatic phenotype.

A current problem in developing targeted therapies for STAT3 is the high level of toxicity seen in pre-clinical trials (350). Due to the availability of clinically available therapies to other components of the IL-6/STAT3 signalling pathway, one option to target STAT3 in cervical cancer may be to target JAK2. There are currently clinically available drugs targeting JAK2, such as Ruxolitinib, and others such as Fedratinib, in late stage clinical trials (484). The targeting of JAK2 resulted in a similar phenotype to the inhibition or depletion of STAT3, suggesting that JAK2 may be a viable target for HPV+ cervical cancer. However, further is required to identify if this effect is seen *in vivo*, for example in a mouse model using cervical cancer cell xenografts.

In conclusion, STAT3 is essential for the productive virus life cycle and the activation of STAT3 by HPV E6 is essential for the tumorigenesis of HPV+ cervical cancer cells. Further research should focus on the feasibility of targeting STAT3 or its upstream components as a therapeutic avenue for cervical cancer.

References

1. Bravo IG, Félez-Sánchez M. Papillomaviruses: Viral evolution, cancer and evolutionary medicine. Evol Med Public Health. 2015 Jan 28;2015(1):32–51.

2. Gupta S, Kumar P, Das BC. HPV: Molecular pathways and targets. Curr Probl Cancer. 2018 Apr;42(2):161–74.

3. Shope RE, Hurst EW. INFECTIOUS PAPILLOMATOSIS OF RABBITS : WITH A NOTE ON THE HISTOPATHOLOGY. J Exp Med. The Rockefeller University Press; 1933 Oct 31;58(5):607–24.

4. Latsuzbaia A, Arbyn M, Dutta S, Fischer M, Gheit T, Tapp J, et al. Complete Genome Sequence of a Novel Human Gammapapillomavirus Isolated from a Cervical Swab in Luxembourg. Genome Announc. American Society for Microbiology; 2018 Mar 15;6(11):1.

5. de Villiers E-M, Fauquet C, Broker TR, Bernard H-U, Hausen zur H. Classification of papillomaviruses. Virology. 2004 2004/06/20/;324(1):17–27.

6. Van Doorslaer K, Chen Z, Bernard H-U, Chan PKS, DeSalle R, Dillner J, et al. ICTV Virus Taxonomy Profile: Papillomaviridae. J Gen Virol. 2018 Jun 21.

7. Zheng Z-M, Baker CC. Papillomavirus genome structure, expression, and post-transcriptional regulation. Front Biosci. NIH Public Access; 2006;11:2286–302.

8. Ghittoni R, Accardi R, Chiocca S, Tommasino M. Role of human papillomaviruses in carcinogenesis. Ecancermedicalscience. 2015;9:526.

9. Ghittoni R, Accardi R, Hasan U, Gheit T, Sylla B, Tommasino M. The biological properties of E6 and E7 oncoproteins from human papillomaviruses. Virus Genes. 2010 Feb;40(1):1–13.

10. Egawa N, Egawa K, Griffin H, Doorbar J. Human Papillomaviruses; Epithelial Tropisms, and the Development of Neoplasia. Viruses. Multidisciplinary Digital Publishing Institute; 2015 Jul 16;7(7):3863–90.

11. Sabeena S, Bhat P, Kamath V, Arunkumar G. Possible non-sexual modes of transmission of human papilloma virus. J Obstet Gynaecol Res. 2017 Mar;43(3):429–35.

12. Lee SM, Park JS, Norwitz ER, Koo JN, Oh IH, Park JW, et al. Risk of vertical transmission of human papillomavirus throughout pregnancy: a prospective study. Burk RD, editor. PLoS ONE. Public Library of Science; 2013;8(6):e66368.

13. Syrjänen S, Puranen M. Human papillomavirus infections in children: the potential role of maternal transmission. Crit Rev Oral Biol Med. 2000;11(2):259–74.

14. Bruggink SC, de Koning MNC, Gussekloo J, Egberts PF, Schegget Ter J, Feltkamp MCW, et al. Cutaneous wart-associated HPV types: prevalence and relation with patient characteristics. J Clin Virol. 2012 Nov;55(3):250–5.

15. Kalińska-Bienias A, Kowalewski C, Majewski S. The EVER genes - the genetic etiology of carcinogenesis in epidermodysplasia verruciformis and a possible role in non-epidermodysplasia verruciformis patients. Postepy Dermatol Alergol. Termedia; 2016 Apr;33(2):75–80.

16. Patel AS, Karagas MR, Pawlita M, Waterboer T, Nelson HH. Cutaneous human papillomavirus infection, the EVER2 gene and incidence of squamous cell carcinoma: a case-control study. Int J Cancer. 2008 May 15;122(10):2377–9.

17. Vuillier F, Gaud G, Guillemot D, Commere P-H, Pons C, Favre M. Loss of the HPV-infection resistance EVER2 protein impairs NF-κB signaling pathways in keratinocytes. Hotchin NA, editor. PLoS ONE. 2014;9(2):e89479.

18. Cornet I, Bouvard V, Campo MS, Thomas M, Banks L, Gissmann L, et al. Comparative analysis of transforming properties of E6 and E7 from different beta human papillomavirus types. J Virol. 2012 Feb;86(4):2366–70.

19. Viarisio D, Müller-Decker K, Zanna P, Kloz U, Aengeneyndt B, Accardi R, et al. Novel ß-HPV49 Transgenic Mouse Model of Upper Digestive Tract Cancer. Cancer Res. 2016 Jul 15;76(14):4216–25.

20. Viarisio D, Mueller-Decker K, Kloz U, Aengeneyndt B, Kopp-Schneider A, Gröne H-J, et al. E6 and E7 from beta HPV38 cooperate with ultraviolet light in the development of actinic keratosis-like lesions and squamous cell carcinoma in mice. Lambert P, editor. PLoS Pathog. 2011 Jul;7(7):e1002125.

21. Yanofsky VR, Patel RV, Goldenberg G. Genital warts: a comprehensive review. J Clin Aesthet Dermatol. Matrix Medical Communications; 2012 Jun;5(6):25–36.

22. Omland T, Akre H, Lie KA, Jebsen P, Sandvik L, Brøndbo K. Risk factors for aggressive recurrent respiratory papillomatosis in adults and juveniles. Angeletti PC, editor. PLoS ONE. Public Library of Science; 2014;9(11):e113584.

23. Kanazawa T, Fukushima N, Imayoshi S, Nagatomo T, Kawada K, Nishino H, et al. Rare case of malignant transformation of recurrent respiratory papillomatosis associated with human papillomavirus type 6 infection and p53 overexpression. Springerplus. Nature Publishing Group; 2013 Dec;2(1):153.

24. Bascones-Martínez A, Cok S, Bascones-Ilundáin C, Arias-Herrera S, Gomez-Font R, Bascones-Ilundáin J. Multifocal epithelial hyperplasia: A potentially precancerous disease? (Review). Oncol Lett. 2012 Feb;3(2):255–8.

25. Nour NM. Cervical cancer: a preventable death. Rev Obstet Gynecol. MedReviews, LLC; 2009;2(4):240–4.

26. Crosbie EJ, Einstein MH, Franceschi S, Kitchener HC. Human papillomavirus and cervical cancer. Lancet. 2013 Sep 7;382(9895):889–99.

27. Dürst M, Gissmann L, Ikenberg H, Hausen zur H. A papillomavirus DNA from a cervical carcinoma and its prevalence in cancer biopsy samples from different geographic regions. Proc Natl Acad Sci USA. National Academy of Sciences; 1983 Jun;80(12):3812–5.

28. Moore KA, Mehta V. The Growing Epidemic of HPV-Positive Oropharyngeal Carcinoma: A Clinical Review for Primary Care Providers. J Am Board Fam Med. American Board of Family Medicine; 2015 Jul;28(4):498–503.

29. Leemans CR, Braakhuis BJM, Brakenhoff RH. The molecular biology of head and neck cancer. Nat Rev Cancer. Nature Publishing Group; 2011 Jan;11(1):9–22.

30. Karimi Zarchi M, Behtash N, Chiti Z, Kargar S. Cervical cancer and HPV vaccines in developing countries. Asian Pac J Cancer Prev. 2009;10(6):969–74.

31. Bosch FX, Tsu V, Vorsters A, Van Damme P, Kane MA. Reframing cervical cancer prevention. Expanding the field towards prevention of human papillomavirus infections and related diseases. Vaccine. 2012 Nov 20;30 Suppl 5:F1–11.

32. de Sanjosé S, Diaz M, Castellsagué X, Clifford G, Bruni L, Muñoz N, et al. Worldwide prevalence and genotype distribution of cervical human papillomavirus DNA in women with normal cytology: a meta-analysis. Lancet Infect Dis. 2007 Jul;7(7):453–9.

33. Thapa N, Maharjan M, Xiong Y, Jiang D, Nguyen T-P, Petrini MA, et al. Impact of cervical cancer on quality of life of women in Hubei, China. Sci Rep. Nature Publishing Group; 2018 Aug 10;8(1):11993.

34. Wieland U, Kreuter A. The importance of HPV16 in anal cancer prevention. Lancet Infect Dis. 2018 Feb;18(2):131–2.

35. Lowy DR, Schiller JT. Reducing HPV-associated cancer globally. Cancer Prev Res (Phila). American Association for Cancer Research; 2012 Jan;5(1):18–23.

36. Kidd LC, Chaing S, Chipollini J, Giuliano AR, Spiess PE, Sharma P. Relationship between human papillomavirus and penile cancer-implications for prevention and treatment. Transl Androl Urol. 2017 Oct;6(5):791–802.

37. Mirghani H, Leroy C, Chekourry Y, Casiraghi O, Aupérin A, Tao Y, et al. Smoking impact on HPV driven head and neck cancer's oncological outcomes? Oral Oncol. 2018 Jul;82:131–7.

38. Gillison ML, Chaturvedi AK, Anderson WF, Fakhry C. Epidemiology of Human Papillomavirus-Positive Head and Neck Squamous Cell Carcinoma. J Clin Oncol. 2015 Oct 10;33(29):3235–42.

39. Harper DM, DeMars LR. HPV vaccines - A review of the first decade. Gynecol Oncol. 2017 Jul;146(1):196–204.

40. Cuzick J. Gardasil 9 joins the fight against cervix cancer. Expert Rev Vaccines. Informa Healthcare; 2015;14(8):1047–9.

41. Audrey S, Batista Ferrer H, Ferrie J, Evans K, Bell M, Yates J, et al. Impact and acceptability of self-consent procedures for the school-based human papillomavirus vaccine: a mixed-methods study protocol. BMJ Open. 2018 Mar 3;8(3):e021321.

42. Kmietowicz Z. Boys in England to get HPV vaccine from next year. BMJ. 2018 Jul 24;362:k3237.

43. Muthumariappan M, Raj GA. Cost and financing issues limit access to the HPV vaccine. Asian Pac J Cancer Prev. 2010;11(2):573–4.

44. Lind H, Waldenström A-C, Dunberger G, al-Abany M, Alevronta E, Johansson K-A, et al. Late symptoms in long-term gynaecological cancer survivors after radiation therapy: a population-based cohort study. Br J Cancer. Nature Publishing Group; 2011 Sep 6;105(6):737–45.

45. Khan MJ, Smith-McCune KK. Treatment of cervical precancers: back to basics. Obstet Gynecol. 2014 Jun;123(6):1339–43.

46. Peralta-Zaragoza O, Bermúdez-Morales VH, Pérez-Plasencia C, Salazar-León J, Gómez-Cerón C, Madrid-Marina V. Targeted treatments for cervical cancer: a review. Onco Targets Ther. Dove Press; 2012;5:315–28.

47. Mirghani H, Blanchard P. Treatment de-escalation for HPV-driven oropharyngeal cancer: Where do we stand? Clin Transl Radiat Oncol. 2018 Jan;8:4–11.

48. Christensen ND, Cladel NM, Hu J, Balogh KK. Formulation of cidofovir improves the anti-papillomaviral activity of topical treatments in the CRPV/rabbit model. Antiviral Res. 2014 Aug;108:148–55.

49. Rasi A, Soltani-Arabshahi R, Khatami A. Cryotherapy for anogenital warts: factors affecting therapeutic response. Dermatol Online J. 2007 Oct 13;13(4):2.

50. Castanon A, Landy R, Pesola F, Windridge P, Sasieni P. Prediction of cervical cancer incidence in England, UK, up to 2040, under four scenarios: a modelling study. Lancet Public Health. 2018 Jan;3(1):e34–e43.

51. Santesso N, Mustafa RA, Schünemann HJ, Arbyn M, Blumenthal PD, Cain J, et al. World Health Organization Guidelines for treatment of cervical intraepithelial neoplasia 2-3 and screen-and-treat strategies to prevent cervical cancer. Vol. 132,

International journal of gynaecology and obstetrics: the official organ of the International Federation of Gynaecology and Obstetrics. 2016. pp. 252–8.

52. Catarino R, Petignat P, Dongui G, Vassilakos P. Cervical cancer screening in developing countries at a crossroad: Emerging technologies and policy choices. World J Clin Oncol. Baishideng Publishing Group Inc; 2015 Dec 10;6(6):281–90.

53. Lace MJ, Anson JR, Thomas GS, Turek LP, Haugen TH. The E8--E2 gene product of human papillomavirus type 16 represses early transcription and replication but is dispensable for viral plasmid persistence in keratinocytes. J Virol. American Society for Microbiology Journals; 2008 Nov;82(21):10841–53.

54. Wang X, Liu H, Ge H, Ajiro M, Sharma NR, Meyers C, et al. Viral DNA Replication Orientation and hnRNPs Regulate Transcription of the Human Papillomavirus 18 Late Promoter. Palese P, editor. MBio. American Society for Microbiology; 2017 May 30;8(3):12.

55. Gunasekharan VK, Li Y, Andrade J, Laimins LA. Post-Transcriptional Regulation of KLF4 by High-Risk Human Papillomaviruses Is Necessary for the Differentiation-Dependent Viral Life Cycle. Meyers C, editor. PLoS Pathog. Public Library of Science; 2016 Jul;12(7):e1005747.

56. Doorbar J. The papillomavirus life cycle. J Clin Virol. 2005 Mar;32 Suppl 1:S7–15.

57. Drobni P, Mistry N, McMillan N, Evander M. Carboxy-fluorescein diacetate, succinimidyl ester labeled papillomavirus virus-like particles fluoresce after internalization and interact with heparan sulfate for binding and entry. Virology. 2003 May 25;310(1):163–72.

58. Joyce JG, Tung JS, Przysiecki CT, Cook JC, Lehman ED, Sands JA, et al. The L1 major capsid protein of human papillomavirus type 11 recombinant virus-like particles

interacts with heparin and cell-surface glycosaminoglycans on human keratinocytes. J Biol Chem. 1999 Feb 26;274(9):5810–22.

59. Day PM, Lowy DR, Schiller JT. Heparan sulfate-independent cell binding and infection with furin-precleaved papillomavirus capsids. J Virol. American Society for Microbiology; 2008 Dec;82(24):12565–8.

60. Bronnimann MP, Calton CM, Chiquette SF, Li S, Lu M, Chapman JA, et al. Furin Cleavage of L2 during Papillomavirus Infection: Minimal Dependence on Cyclophilins. Banks L, editor. J Virol. 2016 Jul 15;90(14):6224–34.

61. Richards RM, Lowy DR, Schiller JT, Day PM. Cleavage of the papillomavirus minor capsid protein, L2, at a furin consensus site is necessary for infection. Proc Natl Acad Sci USA. 2006 Jan 31;103(5):1522–7.

62. Day PM, Schelhaas M. Concepts of papillomavirus entry into host cells. Curr Opin Virol. 2014 Feb;4:24–31.

63. Scheffer KD, Gawlitza A, Spoden GA, Zhang XA, Lambert C, Berditchevski F, et al. Tetraspanin CD151 mediates papillomavirus type 16 endocytosis. J Virol. 2013 Mar;87(6):3435–46.

64. Schelhaas M, Shah B, Holzer M, Blattmann P, Kühling L, Day PM, et al. Entry of human papillomavirus type 16 by actin-dependent, clathrin- and lipid raft-independent endocytosis. Meyers C, editor. PLoS Pathog. 2012;8(4):e1002657.

65. Lipovsky A, Popa A, Pimienta G, Wyler M, Bhan A, Kuruvilla L, et al. Genome-wide siRNA screen identifies the retromer as a cellular entry factor for human papillomavirus. Proc Natl Acad Sci USA. 2013 Apr 30;110(18):7452–7.

66. Popa A, Zhang W, Harrison MS, Goodner K, Kazakov T, Goodwin EC, et al. Direct binding of retromer to human papillomavirus type 16 minor capsid protein L2 mediates

endosome exit during viral infection. McBride AA, editor. PLoS Pathog. Public Library of Science; 2015 Feb;11(2):e1004699.

67. Heino P, Zhou J, Lambert PF. Interaction of the papillomavirus transcription/replication factor, E2, and the viral capsid protein, L2. Virology. 2000 Oct 25;276(2):304–14.

68. Day PM, Roden RB, Lowy DR, Schiller JT. The papillomavirus minor capsid protein, L2, induces localization of the major capsid protein, L1, and the viral transcription/replication protein, E2, to PML oncogenic domains. J Virol. American Society for Microbiology (ASM); 1998 Jan;72(1):142–50.

69. McBride AA, Jang MK. Current understanding of the role of the Brd4 protein in the papillomavirus lifecycle. Viruses. Multidisciplinary Digital Publishing Institute; 2013 Jun;5(6):1374–94.

70. Doorbar J, Egawa N, Griffin H, Kranjec C, Murakami I. Human papillomavirus molecular biology and disease association. Rev Med Virol. 2015 Mar;25 Suppl 1:2–23.

71. Sedman J, Stenlund A. The papillomavirus E1 protein forms a DNA-dependent hexameric complex with ATPase and DNA helicase activities. J Virol. American Society for Microbiology (ASM); 1998 Aug;72(8):6893–7.

72. Bergvall M, Melendy T, Archambault J. The E1 proteins. Virology. 2013 Oct;445(1-2):35–56.

73. Sanders CM, Kovalevskiy OV, Sizov D, Lebedev AA, Isupov MN, Antson AA. Papillomavirus E1 helicase assembly maintains an asymmetric state in the absence of DNA and nucleotide cofactors. Nucleic Acids Res. 2007;35(19):6451–7.

74. Wilson VG, West M, Woytek K, Rangasamy D. Papillomavirus E1 proteins: form, function, and features. Virus Genes. 2002 Jun;24(3):275–90.

75. Fradet-Turcotte A, Moody C, Laimins LA, Archambault J. Nuclear export of human papillomavirus type 31 E1 is regulated by Cdk2 phosphorylation and required for viral genome maintenance. J Virol. 2010 Nov;84(22):11747–60.

76. Yu J-H, Lin BY, Deng W, Broker TR, Chow LT. Mitogen-activated protein kinases activate the nuclear localization sequence of human papillomavirus type 11 E1 DNA helicase to promote efficient nuclear import. J Virol. American Society for Microbiology Journals; 2007 May;81(10):5066–78.

77. Schuck S, Stenlund A. Role of papillomavirus E1 initiator dimerization in DNA replication. J Virol. American Society for Microbiology Journals; 2005 Jul;79(13):8661–4.

78. Hughes FJ, Romanos MA. E1 protein of human papillomavirus is a DNA helicase/ATPase. Nucleic Acids Res. Oxford University Press; 1993 Dec 25;21(25):5817–23.

79. Moody CA, Fradet-Turcotte A, Archambault J, Laimins LA. Human papillomaviruses activate caspases upon epithelial differentiation to induce viral genome amplification. Proc Natl Acad Sci USA. National Acad Sciences; 2007 Dec 4;104(49):19541–6.

80. Hernandez-Ramon EE, Burns JE, Zhang W, Walker HF, Allen S, Antson AA, et al. Dimerization of the human papillomavirus type 16 E2 N terminus results in DNA looping within the upstream regulatory region. J Virol. American Society for Microbiology Journals; 2008 May;82(10):4853–61.

81. Wu Y-C, Bian X-L, Heaton PR, Deyrieux AF, Wilson VG. Host cell sumoylation level influences papillomavirus E2 protein stability. Virology. 2009 Apr 25;387(1):176–83.

82. Graham SV. Human Papillomavirus E2 Protein: Linking Replication, Transcription, and RNA Processing. Sullivan CS, editor. J Virol. American Society for Microbiology Journals; 2016 Oct 1;90(19):8384–8.

83. Ozbun MA, Meyers C. Human papillomavirus type 31b E1 and E2 transcript expression correlates with vegetative viral genome amplification. Virology. NIH Public Access; 1998 Sep 1;248(2):218–30.

84. Zou N, Lin BY, Duan F, Lee KY, Jin G, Guan R, et al. The hinge of the human papillomavirus type 11 E2 protein contains major determinants for nuclear localization and nuclear matrix association. J Virol. American Society for Microbiology (ASM); 2000 Apr;74(8):3761–70.

85. Holmgren SC, Patterson NA, Ozbun MA, Lambert PF. The minor capsid protein L2 contributes to two steps in the human papillomavirus type 31 life cycle. J Virol. 2005 Apr;79(7):3938–48.

86. Chang S-W, Liu W-C, Liao K-Y, Tsao Y-P, Hsu P-H, Chen S-L. Phosphorylation of HPV-16 E2 at serine 243 enables binding to Brd4 and mitotic chromosomes. Banks L, editor. PLoS ONE. 2014;9(10):e110882.

87. Jang MK, Kwon D, McBride AA. Papillomavirus E2 proteins and the host BRD4 protein associate with transcriptionally active cellular chromatin. J Virol. American Society for Microbiology Journals; 2009 Mar;83(6):2592–600.

88. Abbate EA, Voitenleitner C, Botchan MR. Structure of the papillomavirus DNA-tethering complex E2:Brd4 and a peptide that ablates HPV chromosomal association. Mol Cell. 2006 Dec 28;24(6):877–89.

89. Baxter MK, McPhillips MG, Ozato K, McBride AA. The mitotic chromosome binding activity of the papillomavirus E2 protein correlates with interaction with the cellular

chromosomal protein, Brd4. J Virol. American Society for Microbiology Journals; 2005 Apr;79(8):4806–18.

90. Parish JL, Bean AM, Park RB, Androphy EJ. ChlR1 is required for loading papillomavirus E2 onto mitotic chromosomes and viral genome maintenance. Mol Cell. 2006 Dec 28;24(6):867–76.

91. Collins SI, Constandinou-Williams C, Wen K, Young LS, Roberts S, Murray PG, et al. Disruption of the E2 gene is a common and early event in the natural history of cervical human papillomavirus infection: a longitudinal cohort study. Cancer Res. American Association for Cancer Research; 2009 May 1;69(9):3828–32.

92. Van Tine BA, Dao LD, Wu S-Y, Sonbuchner TM, Lin BY, Zou N, et al. Human papillomavirus (HPV) origin-binding protein associates with mitotic spindles to enable viral DNA partitioning. Proc Natl Acad Sci USA. 2004 Mar 23;101(12):4030–5.

93. Schiffman M, Doorbar J, Wentzensen N, de Sanjosé S, Fakhry C, Monk BJ, et al. Carcinogenic human papillomavirus infection. Nat Rev Dis Primers. Nature Publishing Group; 2016 Dec 1;2:16086.

94. Buck CB, Day PM, Trus BL. The papillomavirus major capsid protein L1. Virology. 2013 Oct;445(1-2):169–74.

95. Letian T, Tianyu Z. Cellular receptor binding and entry of human papillomavirus. Virol J. BioMed Central; 2010;7(1):2.

96. Raff AB, Woodham AW, Raff LM, Skeate JG, Yan L, Da Silva DM, et al. The evolving field of human papillomavirus receptor research: a review of binding and entry. J Virol. 2013 Jun;87(11):6062–72.

97. Broniarczyk J, Massimi P, Bergant M, Banks L. Human Papillomavirus Infectious Entry and Trafficking Is a Rapid Process. Imperiale MJ, editor. J Virol. American Society for Microbiology Journals; 2015 Sep;89(17):8727–32.

98. Bergant Marušič M, Ozbun MA, Campos SK, Myers MP, Banks L. Human papillomavirus L2 facilitates viral escape from late endosomes via sorting nexin 17. Traffic. Wiley/Blackwell (10.1111); 2012 Mar;13(3):455–67.

99. Schneider MA, Spoden GA, Florin L, Lambert C. Identification of the dynein light chains required for human papillomavirus infection. Cell Microbiol. Wiley/Blackwell (10.1111); 2011 Jan;13(1):32–46.

100. Calton CM, Bronnimann MP, Manson AR, Li S, Chapman JA, Suarez-Berumen M, et al. Translocation of the papillomavirus L2/vDNA complex across the limiting membrane requires the onset of mitosis. Meyers C, editor. PLoS Pathog. 2017 May;13(5):e1006200.

101. Aydin I, Villalonga-Planells R, Greune L, Bronnimann MP, Calton CM, Becker M, et al. A central region in the minor capsid protein of papillomaviruses facilitates viral genome tethering and membrane penetration for mitotic nuclear entry. Meyers C, editor. PLoS Pathog. Public Library of Science; 2017 May;13(5):e1006308.

102. Schwartz S. Regulation of human papillomavirus late gene expression. Ups J Med Sci. 2000;105(3):171–92.

103. Doorbar J. The E4 protein; structure, function and patterns of expression. Virology. 2013 Oct;445(1-2):80–98.

104. McIntosh PB, Martin SR, Jackson DJ, Khan J, Isaacson ER, Calder L, et al. Structural analysis reveals an amyloid form of the human papillomavirus type 16 E1--E4 protein

and provides a molecular basis for its accumulation. J Virol. 2008 Aug;82(16):8196–203.

105. Nasseri M, Hirochika R, Broker TR, Chow LT. A human papilloma virus type 11 transcript encoding an E1--E4 protein. Virology. 1987 Aug;159(2):433–9.

106. Wang Q, Kennedy A, Das P, McIntosh PB, Howell SA, Isaacson ER, et al. Phosphorylation of the human papillomavirus type 16 E1--E4 protein at T57 by ERK triggers a structural change that enhances keratin binding and protein stability. J Virol. American Society for Microbiology Journals; 2009 Apr;83(8):3668–83.

107. Davy CE, Jackson DJ, Wang Q, Raj K, Masterson PJ, Fenner NF, et al. Identification of a G(2) arrest domain in the E1 wedge E4 protein of human papillomavirus type 16. J Virol. American Society for Microbiology (ASM); 2002 Oct;76(19):9806–18.

108. Egawa N, Wang Q, Griffin HM, Murakami I, Jackson D, Mahmood R, et al. HPV16 and 18 genome amplification show different E4-dependence, with 16E4 enhancing E1 nuclear accumulation and replicative efficiency via its cell cycle arrest and kinase activation functions. Lambert PF, editor. PLoS Pathog. Public Library of Science; 2017 Mar;13(3):e1006282.

109. Biryukov J, Myers JC, McLaughlin-Drubin ME, Griffin HM, Milici J, Doorbar J, et al. Mutations in HPV18 E1^E4 Impact Virus Capsid Assembly, Infectivity Competence, and Maturation. Viruses. Multidisciplinary Digital Publishing Institute; 2017 Dec 19;9(12):385.

110. Goldstein DJ, Andresson T, Sparkowski JJ, Schlegel R. The BPV-1 E5 protein, the 16 kDa membrane pore-forming protein and the PDGF receptor exist in a complex that is dependent on hydrophobic transmembrane interactions. EMBO J. European Molecular Biology Organization; 1992 Dec;11(13):4851–9.

111. Venuti A, Paolini F, Nasir L, Corteggio A, Roperto S, Campo MS, et al. Papillomavirus E5: the smallest oncoprotein with many functions. Mol Cancer. BioMed Central; 2011 Nov 11;10(1):140.

112. Genther SM, Sterling S, Duensing S, Münger K, Sattler C, Lambert PF. Quantitative role of the human papillomavirus type 16 E5 gene during the productive stage of the viral life cycle. J Virol. American Society for Microbiology (ASM); 2003 Mar;77(5):2832–42.

113. Fehrmann F, Klumpp DJ, Laimins LA. Human papillomavirus type 31 E5 protein supports cell cycle progression and activates late viral functions upon epithelial differentiation. J Virol. American Society for Microbiology (ASM); 2003 Mar;77(5):2819–31.

114. Conrad M, Bubb VJ, Schlegel R. The human papillomavirus type 6 and 16 E5 proteins are membrane-associated proteins which associate with the 16-kilodalton pore-forming protein. J Virol. American Society for Microbiology (ASM); 1993 Oct;67(10):6170–8.

115. Disbrow GL, Hanover JA, Schlegel R. Endoplasmic reticulum-localized human papillomavirus type 16 E5 protein alters endosomal pH but not trans-Golgi pH. J Virol. American Society for Microbiology Journals; 2005 May;79(9):5839–46.

116. Pim D, Collins M, Banks L. Human papillomavirus type 16 E5 gene stimulates the transforming activity of the epidermal growth factor receptor. Oncogene. 1992 Jan;7(1):27–32.

117. Genther Williams SM, Disbrow GL, Schlegel R, Lee D, Threadgill DW, Lambert PF. Requirement of epidermal growth factor receptor for hyperplasia induced by E5, a high-risk human papillomavirus oncogene. Cancer Res. 2005 Aug 1;65(15):6534–42.

118. Rodríguez MI, Finbow ME, Alonso A. Binding of human papillomavirus 16 E5 to the 16 kDa subunit c (proteolipid) of the vacuolar H+-ATPase can be dissociated from the E5-mediated epidermal growth factor receptor overactivation. Oncogene. Nature Publishing Group; 2000 Aug 3;19(33):3727–32.

119. Zhang B, Srirangam A, Potter DA, Roman A. HPV16 E5 protein disrupts the c-Cbl-EGFR interaction and EGFR ubiquitination in human foreskin keratinocytes. Oncogene. Nature Publishing Group; 2005 Apr 7;24(15):2585–8.

120. Crusius K, Auvinen E, Alonso A. Enhancement of EGF- and PMA-mediated MAP kinase activation in cells expressing the human papillomavirus type 16 E5 protein. Oncogene. Nature Publishing Group; 1997 Sep 18;15(12):1437–44.

121. Wetherill LF, Holmes KK, Verow M, Müller M, Howell G, Harris M, et al. High-risk human papillomavirus E5 oncoprotein displays channel-forming activity sensitive to small-molecule inhibitors. J Virol. American Society for Microbiology; 2012 May;86(9):5341–51.

122. Wetherill LF, Wasson CW, Swinscoe G, Kealy D, Foster R, Griffin S, et al. Alkyl-imino sugars inhibit the pro-oncogenic ion channel function of human papillomavirus (HPV) E5. Antiviral Res. 2018 Oct;158:113–21.

123. Ashrafi GH, Haghshenas M, Marchetti B, Campo MS. E5 protein of human papillomavirus 16 downregulates HLA class I and interacts with the heavy chain via its first hydrophobic domain. Int J Cancer. Wiley Subscription Services, Inc., A Wiley Company; 2006 Nov 1;119(9):2105–12.

124. Campo MS, Graham SV, Cortese MS, Ashrafi GH, Araibi EH, Dornan ES, et al. HPV-16 E5 down-regulates expression of surface HLA class I and reduces recognition by CD8 T cells. Virology. 2010 Nov 10;407(1):137–42.

125. Ashrafi GH, Haghshenas MR, Marchetti B, O'Brien PM, Campo MS. E5 protein of human papillomavirus type 16 selectively downregulates surface HLA class I. Int J Cancer. Wiley-Blackwell; 2005 Jan 10;113(2):276–83.

126. Regan JA, Laimins LA. Bap31 is a novel target of the human papillomavirus E5 protein. J Virol. American Society for Microbiology; 2008 Oct;82(20):10042–51.

127. Kotnik Halavaty K, Regan J, Mehta K, Laimins L. Human papillomavirus E5 oncoproteins bind the A4 endoplasmic reticulum protein to regulate proliferative ability upon differentiation. Virology. 2014 Mar;452-453:223–30.

128. Talbert-Slagle K, DiMaio D. The bovine papillomavirus E5 protein and the PDGF beta receptor: it takes two to tango. Virology. 2009 Feb 20;384(2):345–51.

129. Wasson CW, Morgan EL, Müller M, Ross RL, Hartley M, Roberts S, et al. Human papillomavirus type 18 E5 oncogene supports cell cycle progression and impairs epithelial differentiation by modulating growth factor receptor signalling during the virus life cycle. Oncotarget. Impact Journals LLC; 2017 10/06

07/26/received

08/16/accepted;8(61):103581–600.

130. McLaughlin-Drubin ME, Münger K. The human papillomavirus E7 oncoprotein. Virology. 2009 Feb 20;384(2):335–44.

131. Knapp AA, McManus PM, Bockstall K, Moroianu J. Identification of the nuclear localization and export signals of high risk HPV16 E7 oncoprotein. Virology. 2009 Jan 5;383(1):60–8.

132. Roman A, Münger K. The papillomavirus E7 proteins. Virology. 2013 Oct;445(1-2):138–68.

133. Gulliver GA, Herber RL, Liem A, Lambert PF. Both conserved region 1 (CR1) and CR2 of the human papillomavirus type 16 E7 oncogene are required for induction of epidermal hyperplasia and tumor formation in transgenic mice. J Virol. American Society for Microbiology (ASM); 1997 Aug;71(8):5905–14.

134. White EA, Kramer RE, Hwang JH, Pores Fernando AT, Naetar N, Hahn WC, et al. Papillomavirus E7 oncoproteins share functions with polyomavirus small T antigens. Imperiale MJ, editor. J Virol. 6 ed. 2015 Mar;89(5):2857–65.

135. Dahiya A, Gavin MR, Luo RX, Dean DC. Role of the LXCXE Binding Site in Rb Function. Mol Cell Biol. American Society for Microbiology; 2000;20(18):6799–805.

136. Todorovic B, Hung K, Massimi P, Avvakumov N, Dick FA, Shaw GS, et al. Conserved region 3 of human papillomavirus 16 E7 contributes to deregulation of the retinoblastoma tumor suppressor. J Virol. American Society for Microbiology Journals; 2012 Dec;86(24):13313–23.

137. Boyer SN, Wazer DE, Band V. E7 protein of human papilloma virus-16 induces degradation of retinoblastoma protein through the ubiquitin-proteasome pathway. Cancer Res. 1996 Oct 15;56(20):4620–4.

138. Chien WM, Parker JN, Schmidt-Grimminger DC, Broker TR, Chow LT. Casein kinase II phosphorylation of the human papillomavirus-18 E7 protein is critical for promoting S-phase entry. Cell Growth Differ. 2000 Aug;11(8):425–35.

139. Liang Y-J, Chang H-S, Wang C-Y, Yu WCY. DYRK1A stabilizes HPV16E7 oncoprotein through phosphorylation of the threonine 5 and threonine 7 residues. Int J Biochem Cell Biol. 2008;40(11):2431–41.

140. Shin M-K, Balsitis S, Brake T, Lambert PF. Human papillomavirus E7 oncoprotein overrides the tumor suppressor activity of p21Cip1 in cervical carcinogenesis. Cancer Res. American Association for Cancer Research; 2009 Jul 15;69(14):5656–63.

141. Zerfass-Thome K, Zwerschke W, Mannhardt B, Tindle R, Botz JW, Jansen-Dürr P. Inactivation of the cdk inhibitor p27KIP1 by the human papillomavirus type 16 E7 oncoprotein. Oncogene. 1996 Dec 5;13(11):2323–30.

142. Huh K-W, DeMasi J, Ogawa H, Nakatani Y, Howley PM, Münger K. Association of the human papillomavirus type 16 E7 oncoprotein with the 600-kDa retinoblastoma protein-associated factor, p600. Proc Natl Acad Sci USA. National Acad Sciences; 2005 Aug 9;102(32):11492–7.

143. Yoshida K, Inoue I. Regulation of Geminin and Cdt1 expression by E2F transcription factors. Oncogene. Nature Publishing Group; 2004 May 6;23(21):3802–12.

144. Hasan UA, Zannetti C, Parroche P, Goutagny N, Malfroy M, Roblot G, et al. The human papillomavirus type 16 E7 oncoprotein induces a transcriptional repressor complex on the Toll-like receptor 9 promoter. J Exp Med. Rockefeller University Press; 2013 Jul 1;210(7):1369–87.

145. Barnard P, McMillan NA. The human papillomavirus E7 oncoprotein abrogates signaling mediated by interferon-alpha. Virology. 1999 Jul 5;259(2):305–13.

146. Um S-J, Rhyu J-W, Kim E-J, Jeon K-C, Hwang E-S, Park J-S. Abrogation of IRF-1 response by high-risk HPV E7 protein in vivo. Cancer Lett. 2002 May 28;179(2):205–12.

147. Bottley G, Watherston OG, Hiew Y-L, Norrild B, Cook GP, Blair GE. High-risk human papillomavirus E7 expression reduces cell-surface MHC class I molecules and

increases susceptibility to natural killer cells. Oncogene. Nature Publishing Group; 2008 Mar 13;27(12):1794–9.

148. Graham SV. Keratinocyte Differentiation-Dependent Human Papillomavirus Gene Regulation. Viruses. Multidisciplinary Digital Publishing Institute; 2017 Aug 30;9(9):245.

149. Hong S, Mehta KP, Laimins LA. Suppression of STAT-1 expression by human papillomaviruses is necessary for differentiation-dependent genome amplification and plasmid maintenance. J Virol. 2011 Sep;85(18):9486–94.

150. Hong S, Laimins LA. The JAK-STAT transcriptional regulator, STAT-5, activates the ATM DNA damage pathway to induce HPV 31 genome amplification upon epithelial differentiation. McBride AA, editor. PLoS Pathog. Public Library of Science; 2013;9(4):e1003295.

151. Wallace NA, Galloway DA. Novel Functions of the Human Papillomavirus E6 Oncoproteins. Annu Rev Virol. Annual Reviews; 2015 Nov;2(1):403–23.

152. Stewart D, Ghosh A, Matlashewski G. Involvement of nuclear export in human papillomavirus type 18 E6-mediated ubiquitination and degradation of p53. J Virol. American Society for Microbiology Journals; 2005 Jul;79(14):8773–83.

153. Martinez-Zapien D, Ruiz FX, Poirson J, Mitschler A, Ramirez J, Forster A, et al. Structure of the E6/E6AP/p53 complex required for HPV-mediated degradation of p53. Nature. 2016 Jan 28;529(7587):541–5.

154. Thomas M, Myers MP, Massimi P, Guarnaccia C, Banks L. Analysis of Multiple HPV E6 PDZ Interactions Defines Type-Specific PDZ Fingerprints That Predict Oncogenic Potential. Lambert PF, editor. PLoS Pathog. 2016 Aug;12(8):e1005766.

155. Song S, Pitot HC, Lambert PF. The human papillomavirus type 16 E6 gene alone is sufficient to induce carcinomas in transgenic animals. J Virol. American Society for Microbiology (ASM); 1999 Jul;73(7):5887–93.

156. Zanier K, Charbonnier S, Sidi AOMO, McEwen AG, Ferrario MG, Poussin-Courmontagne P, et al. Structural basis for hijacking of cellular LxxLL motifs by papillomavirus E6 oncoproteins. Science. 2013 Feb 8;339(6120):694–8.

157. Vande Pol S. Papillomavirus E6 Oncoproteins Take Common Structural Approaches to Solve Different Biological Problems. Condit RC, editor. PLoS Pathog. Public Library of Science; 2015 Oct;11(10):e1005138.

158. Scheffner M, Huibregtse JM, Vierstra RD, Howley PM. The HPV-16 E6 and E6-AP complex functions as a ubiquitin-protein ligase in the ubiquitination of p53. Cell. 1993 Nov 5;75(3):495–505.

159. Zimmermann H, Degenkolbe R, Bernard HU, O'Connor MJ. The human papillomavirus type 16 E6 oncoprotein can down-regulate p53 activity by targeting the transcriptional coactivator CBP/p300. J Virol. American Society for Microbiology (ASM); 1999 Aug;73(8):6209–19.

160. Pietsch EC, Murphy ME. Low risk HPV-E6 traps p53 in the cytoplasm and induces p53-dependent apoptosis. Cancer Biol Ther. NIH Public Access; 2008 Dec;7(12):1916–8.

161. Thomas MC, Chiang C-M. E6 oncoprotein represses p53-dependent gene activation via inhibition of protein acetylation independently of inducing p53 degradation. Mol Cell. 2005 Jan 21;17(2):251–64.

162. Li X, Coffino P. High-risk human papillomavirus E6 protein has two distinct binding sites within p53, of which only one determines degradation. J Virol. American Society for Microbiology (ASM); 1996 Jul;70(7):4509–16.

163. Camus S, Menéndez S, Cheok CF, Stevenson LF, Laín S, Lane DP. Ubiquitin-independent degradation of p53 mediated by high-risk human papillomavirus protein E6. Oncogene. 2007 Jun 14;26(28):4059–70.

164. Spangle JM, Münger K. The HPV16 E6 oncoprotein causes prolonged receptor protein tyrosine kinase signaling and enhances internalization of phosphorylated receptor species. Roman A, editor. PLoS Pathog. Public Library of Science; 2013 Mar;9(3):e1003237.

165. Wang S, Pang T, Gao M, Kang H, Ding W, Sun X, et al. HPV E6 induces eIF4E transcription to promote the proliferation and migration of cervical cancer. FEBS Lett. Wiley-Blackwell; 2013 Mar 18;587(6):690–7.

166. McCormack SJ, Brazinski SE, Moore JL, Werness BA, Goldstein DJ. Activation of the focal adhesion kinase signal transduction pathway in cervical carcinoma cell lines and human genital epithelial cells immortalized with human papillomavirus type 18. Oncogene. Nature Publishing Group; 1997 Jul 17;15(3):265–74.

167. Klingelhutz AJ, Foster SA, McDougall JK. Telomerase activation by the E6 gene product of human papillomavirus type 16. Nature. Nature Publishing Group; 1996 Mar 7;380(6569):79–82.

168. Katzenellenbogen RA, Vliet-Gregg P, Xu M, Galloway DA. NFX1-123 increases hTERT expression and telomerase activity posttranscriptionally in human papillomavirus type 16 E6 keratinocytes. J Virol. American Society for Microbiology Journals; 2009 Jul;83(13):6446–56.

169. Webb Strickland S, Brimer N, Lyons C, Vande Pol SB. Human Papillomavirus E6 interaction with cellular PDZ domain proteins modulates YAP nuclear localization. Virology. 2018 Mar;516:127–38.

170. Nguyen ML, Nguyen MM, Lee D, Griep AE, Lambert PF. The PDZ ligand domain of the human papillomavirus type 16 E6 protein is required for E6's induction of epithelial hyperplasia in vivo. J Virol. American Society for Microbiology (ASM); 2003 Jun;77(12):6957–64.

171. Thomas M, Banks L. Human papillomavirus (HPV) E6 interactions with Bak are conserved amongst E6 proteins from high and low risk HPV types. J Gen Virol. Microbiology Society; 1999 Jun;80 (Pt 6)(6):1513–7.

172. Garnett TO, Filippova M, Duerksen-Hughes PJ. Accelerated degradation of FADD and procaspase 8 in cells expressing human papilloma virus 16 E6 impairs TRAIL-mediated apoptosis. Cell Death Differ. Nature Publishing Group; 2006 Nov;13(11):1915–26.

173. An J, Mo D, Liu H, Veena MS, Srivatsan ES, Massoumi R, et al. Inactivation of the CYLD deubiquitinase by HPV E6 mediates hypoxia-induced NF-kappaB activation. Cancer Cell. 2008 Nov 4;14(5):394–407.

174. Shostak K, Zhang X, Hubert P, Göktuna SI, Jiang Z, Klevernic I, et al. NF-κB-induced KIAA1199 promotes survival through EGFR signalling. Nat Commun. Nature Publishing Group; 2014 Nov 4;5(1):5232.

175. Shah M, Anwar MA, Park S, Jafri SS, Choi S. In silico mechanistic analysis of IRF3 inactivation and high-risk HPV E6 species-dependent drug response. Sci Rep. Nature Publishing Group; 2015 Aug 20;5(1):13446.

176. Li S, Labrecque S, Gauzzi MC, Cuddihy AR, Wong AH, Pellegrini S, et al. The human papilloma virus (HPV)-18 E6 oncoprotein physically associates with Tyk2 and impairs Jak-STAT activation by interferon-alpha. Oncogene. Nature Publishing Group; 1999 Oct 14;18(42):5727–37.

177. Chiang C, Pauli E-K, Biryukov J, Feister KF, Meng M, White EA, et al. The Human Papillomavirus E6 Oncoprotein Targets USP15 and TRIM25 To Suppress RIG-I-Mediated Innate Immune Signaling. Jung JU, editor. J Virol. American Society for Microbiology Journals; 2018 Mar 15;92(6):1.

178. Marsh EK, Delury CP, Davies NJ, Weston CJ, Miah MAL, Banks L, et al. Mitotic control of human papillomavirus genome-containing cells is regulated by the function of the PDZ-binding motif of the E6 oncoprotein. Oncotarget. 2017 Mar 21;8(12):19491–506.

179. Dong W, Arpin C, Accardi R, Gissmann L, Sylla BS, Marvel J, et al. Loss of p53 or p73 in human papillomavirus type 38 E6 and E7 transgenic mice partially restores the UV-activated cell cycle checkpoints. Oncogene. 2008 May 1;27(20):2923–8.

180. Accardi R, Scalise M, Gheit T, Hussain I, Yue J, Carreira C, et al. IkappaB kinase beta promotes cell survival by antagonizing p53 functions through DeltaNp73alpha phosphorylation and stabilization. Mol Cell Biol. 2011 Jun;31(11):2210–26.

181. White EA, Walther J, Javanbakht H, Howley PM. Genus beta human papillomavirus E6 proteins vary in their effects on the transactivation of p53 target genes. J Virol. 6 ed. 2014 Aug;88(15):8201–12.

182. Wallace NA, Robinson K, Galloway DA. Beta human papillomavirus E6 expression inhibits stabilization of p53 and increases tolerance of genomic instability. J Virol. 2014 Jun;88(11):6112–27.

183. Brimer N, Drews CM, Vande Pol SB. Association of papillomavirus E6 proteins with either MAML1 or E6AP clusters E6 proteins by structure, function, and evolutionary relatedness. Lambert PF, editor. PLoS Pathog. 2017 Dec;13(12):e1006781.

184. Meyers JM, Uberoi A, Grace M, Lambert PF, Münger K. Cutaneous HPV8 and MmuPV1 E6 Proteins Target the NOTCH and TGF-β Tumor Suppressors to Inhibit Differentiation and Sustain Keratinocyte Proliferation. Galloway DA, editor. PLoS Pathog. 2017 Jan;13(1):e1006171.

185. Wallace NA, Robinson K, Howie HL, Galloway DA. β-HPV 5 and 8 E6 disrupt homology dependent double strand break repair by attenuating BRCA1 and BRCA2 expression and foci formation. McBride AA, editor. PLoS Pathog. 2015 Mar;11(3):e1004687.

186. Darnell JE, Kerr IM, Stark GR. Jak-STAT pathways and transcriptional activation in response to IFNs and other extracellular signaling proteins. Science. 1994 Jun 3;264(5164):1415–21.

187. Yu H, Lee H, Herrmann A, Buettner R, Jove R. Revisiting STAT3 signalling in cancer: new and unexpected biological functions. Nat Rev Cancer. 2014 Nov;14(11):736–46.

188. Lim CP, Cao X. Structure, function, and regulation of STAT proteins. Mol Biosyst. The Royal Society of Chemistry; 2006 Nov;2(11):536–50.

189. Sgrignani J, Garofalo M, Matkovic M, Merulla J, Catapano CV, Cavalli A. Structural Biology of STAT3 and Its Implications for Anticancer Therapies Development. Int J Mol Sci. Multidisciplinary Digital Publishing Institute; 2018 May 28;19(6):1591.

190. Tripathi SK, Chen Z, Larjo A, Kanduri K, Nousiainen K, Äijo T, et al. Genome-wide Analysis of STAT3-Mediated Transcription during Early Human Th17 Cell Differentiation. Cell Rep. 2017 May 30;19(9):1888–901.

191. Decker T, Kovarik P. Serine phosphorylation of STATs. Oncogene. Nature Publishing Group; 2000 May 15;19(21):2628–37.

192. Zong CS, Chan J, Levy DE, Horvath C, Sadowski HB, Wang LH. Mechanism of STAT3 activation by insulin-like growth factor I receptor. J Biol Chem. 2000 May 19;275(20):15099–105.

193. Trevino JG, Gray MJ, Nawrocki ST, Summy JM, Lesslie DP, Evans DB, et al. Src activation of Stat3 is an independent requirement from NF-kappaB activation for constitutive IL-8 expression in human pancreatic adenocarcinoma cells. Angiogenesis. Springer Netherlands; 2006;9(2):101–10.

194. Johnson DE, O'Keefe RA, Grandis JR. Targeting the IL-6/JAK/STAT3 signalling axis in cancer. Nat Rev Clin Oncol. Nature Publishing Group; 2018 Apr;15(4):234–48.

195. Park OK, Schaefer TS, Nathans D. In vitro activation of Stat3 by epidermal growth factor receptor kinase. Proc Natl Acad Sci USA. National Academy of Sciences; 1996 Nov 26;93(24):13704–8.

196. Wang YZ, Wharton W, Garcia R, Kraker A, Jove R, Pledger WJ. Activation of Stat3 preassembled with platelet-derived growth factor beta receptors requires Src kinase activity. Oncogene. Nature Publishing Group; 2000 Apr 20;19(17):2075–85.

197. Oda K, Oda T, Matoba Y, Sato M, Irie T, Sakaguchi T. Structural analysis of the STAT1:STAT2 heterodimer revealed the mechanism of Sendai virus C protein-mediated blockade of type 1 interferon signaling. J Biol Chem. 2017 Dec 1;292(48):19752–66.

198. Ivashkiv LB. IFNγ: signalling, epigenetics and roles in immunity, metabolism, disease and cancer immunotherapy. Nat Rev Immunol. Nature Publishing Group; 2018 Jun 19;18(9):545–58.

199. Chang TL, Peng X, Fu XY. Interleukin-4 mediates cell growth inhibition through activation of Stat1. J Biol Chem. 2000 Apr 7;275(14):10212–7.

200. Kamiya S, Owaki T, Morishima N, Fukai F, Mizuguchi J, Yoshimoto T. An indispensable role for STAT1 in IL-27-induced T-bet expression but not proliferation of naive CD4+ T cells. J Immunol. 2004 Sep 15;173(6):3871–7.

201. Abdul-Sater AA, Majoros A, Plumlee CR, Perry S, Gu AD, Lee C, et al. Different STAT Transcription Complexes Drive Early and Delayed Responses to Type I IFNs. J Immunol. American Association of Immunologists; 2015 Jul 1;195(1):210–6.

202. Chatterjee-Kishore M, Wright KL, Ting JP, Stark GR. How Stat1 mediates constitutive gene expression: a complex of unphosphorylated Stat1 and IRF1 supports transcription of the LMP2 gene. EMBO J. 2000 Aug 1;19(15):4111–22.

203. Meissl K, Macho-Maschler S, Müller M, Strobl B. The good and the bad faces of STAT1 in solid tumours. Cytokine. 2017 Jan;89:12–20.

204. Youlyouz-Marfak I, Gachard N, Le Clorennec C, Najjar I, Baran-Marszak F, Reminieras L, et al. Identification of a novel p53-dependent activation pathway of STAT1 by antitumour genotoxic agents. Cell Death Differ. Nature Publishing Group; 2008 Feb;15(2):376–85.

205. Xu X, Fu XY, Plate J, Chong AS. IFN-gamma induces cell growth inhibition by Fas-mediated apoptosis: requirement of STAT1 protein for up-regulation of Fas and FasL expression. Cancer Res. 1998 Jul 1;58(13):2832–7.

206. de Prati AC, Ciampa AR, Cavalieri E, Zaffini R, Darra E, Menegazzi M, et al. STAT1 as a new molecular target of anti-inflammatory treatment. Curr Med Chem. 2005;12(16):1819–28.

207. Xi S, Dyer KF, Kimak M, Zhang Q, Gooding WE, Chaillet JR, et al. Decreased STAT1 expression by promoter methylation in squamous cell carcinogenesis. J Natl Cancer Inst. 2006 Feb 1;98(3):181–9.

208. Zhang Y, Chen Y, Liu Z, Lai R. ERK is a negative feedback regulator for IFN-γ/STAT1 signaling by promoting STAT1 ubiquitination. BMC Cancer. BioMed Central; 2018 May 31;18(1):613.

209. Leibowitz MS, Srivastava RM, Andrade Filho PA, Egloff AM, Wang L, Seethala RR, et al. SHP2 is overexpressed and inhibits pSTAT1-mediated APM component expression, T-cell attracting chemokine secretion, and CTL recognition in head and neck cancer cells. Clin Cancer Res. 2013 Feb 15;19(4):798–808.

210. Xie H, Huang S, Li W, Zhao H, Zhang T, Zhang D. Upregulation of Src homology phosphotyrosyl phosphatase 2 (Shp2) expression in oral cancer and knockdown of Shp2 expression inhibit tumor cell viability and invasion in vitro. Oral Surg Oral Med Oral Pathol Oral Radiol. 2014 Feb;117(2):234–42.

211. Shim S-H, Sung M-W, Park S-W, Heo DS. Absence of STAT1 disturbs the anticancer effect induced by STAT3 inhibition in head and neck carcinoma cell lines. Int J Mol Med. 2009 Jun;23(6):805–10.

212. Blaszczyk K, Nowicka H, Kostyrko K, Antonczyk A, Wesoly J, Bluyssen HAR. The unique role of STAT2 in constitutive and IFN-induced transcription and antiviral responses. Cytokine Growth Factor Rev. 2016 Jun;29:71–81.

213. Meraz MA, White JM, Sheehan KC, Bach EA, Rodig SJ, Dighe AS, et al. Targeted disruption of the Stat1 gene in mice reveals unexpected physiologic specificity in the JAK-STAT signaling pathway. Cell. 1996 Feb 9;84(3):431–42.

214. Fu XY, Kessler DS, Veals SA, Levy DE, Darnell JE. ISGF3, the transcriptional activator induced by interferon alpha, consists of multiple interacting polypeptide chains. Proc Natl Acad Sci USA. National Academy of Sciences; 1990 Nov;87(21):8555–9.

215. Rengachari S, Groiss S, Devos JM, Caron E, Grandvaux N, Panne D. Structural basis of STAT2 recognition by IRF9 reveals molecular insights into ISGF3 function. Proc Natl Acad Sci USA. 2018 Jan 23;115(4):E601–9.

216. Kadota S, Nagata K. pp32, an INHAT component, is a transcription machinery recruiter for maximal induction of IFN-stimulated genes. J Cell Sci. 2011 Mar 15;124(Pt 6):892–9.

217. Bhattacharya S, Eckner R, Grossman S, Oldread E, Arany Z, D'Andrea A, et al. Cooperation of Stat2 and p300/CBP in signalling induced by interferon-alpha. Nature. Nature Publishing Group; 1996 Sep 26;383(6598):344–7.

218. Park C, Li S, Cha E, Schindler C. Immune response in Stat2 knockout mice. Immunity. 2000 Dec;13(6):795–804.

219. Hambleton S, Goodbourn S, Young DF, Dickinson P, Mohamad SMB, Valappil M, et al. STAT2 deficiency and susceptibility to viral illness in humans. Proc Natl Acad Sci USA. 2013 Feb 19;110(8):3053–8.

220. Wang J, Pham-Mitchell N, Schindler C, Campbell IL. Dysregulated Sonic hedgehog signaling and medulloblastoma consequent to IFN-alpha-stimulated STAT2-independent production of IFN-gamma in the brain. J Clin Invest. American Society for Clinical Investigation; 2003 Aug;112(4):535–43.

221. Gamero AM, Young MR, Mentor-Marcel R, Bobe G, Scarzello AJ, Wise J, et al. STAT2 contributes to promotion of colorectal and skin carcinogenesis. Cancer Prev Res (Phila). 2010 Apr;3(4):495–504.

222. Kaplan MH. STAT4: a critical regulator of inflammation in vivo. Immunol Res. 2005;31(3):231–42.

223. O'Malley JT, Eri RD, Stritesky GL, Mathur AN, Chang H-C, Hogenesch H, et al. STAT4 isoforms differentially regulate Th1 cytokine production and the severity of inflammatory bowel disease. J Immunol. NIH Public Access; 2008 Oct 1;181(7):5062–70.

224. Wang Y, Feng D, Wang H, Xu M-J, Park O, Li Y, et al. STAT4 knockout mice are more susceptible to concanavalin A-induced T-cell hepatitis. Am J Pathol. 2014 Jun;184(6):1785–94.

225. Tarleton RL, Grusby MJ, Zhang L. Increased susceptibility of Stat4-deficient and enhanced resistance in Stat6-deficient mice to infection with Trypanosoma cruzi. J Immunol. 2000 Aug 1;165(3):1520–5.

226. Nguyen KB, Watford WT, Salomon R, Hofmann SR, Pien GC, Morinobu A, et al. Critical role for STAT4 activation by type 1 interferons in the interferon-gamma response to viral infection. Science. American Association for the Advancement of Science; 2002 Sep 20;297(5589):2063–6.

227. Ji JD, Lee WJ, Kong KA, Woo JH, Choi SJ, Lee YH, et al. Association of STAT4 polymorphism with rheumatoid arthritis and systemic lupus erythematosus: a meta-analysis. Mol Biol Rep. Springer Netherlands; 2010 Jan;37(1):141–7.

228. Beltrán Ramírez O, Mendoza Rincón JF, Barbosa Cobos RE, Alemán Ávila I, Ramírez Bello J. STAT4 confers risk for rheumatoid arthritis and systemic lupus erythematosus in Mexican patients. Immunol Lett. 2016 Jul;175:40–3.

229. Zhao L, Ji G, Le X, Luo Z, Wang C, Feng M, et al. An integrated analysis identifies STAT4 as a key regulator of ovarian cancer metastasis. Oncogene. Nature Publishing Group; 2017 Jun 15;36(24):3384–96.

230. Li J, Liang L, Liu Y, Luo Y, Liang X, Luo D, et al. Clinicopathological significance of STAT4 in hepatocellular carcinoma and its effect on cell growth and apoptosis. Onco Targets Ther. Dove Press; 2016;9:1721–34.

231. Able AA, Burrell JA, Stephens JM. STAT5-Interacting Proteins: A Synopsis of Proteins that Regulate STAT5 Activity. Biology (Basel). Multidisciplinary Digital Publishing Institute; 2017 Mar 11;6(1):20.

232. Heltemes-Harris LM, Farrar MA. The role of STAT5 in lymphocyte development and transformation. Curr Opin Immunol. 2012 Apr;24(2):146–52.

233. Novak U, Mui A, Miyajima A, Paradiso L. Formation of STAT5-containing DNA binding complexes in response to colony-stimulating factor-1 and platelet-derived growth factor. J Biol Chem. 1996 Aug 2;271(31):18350–4.

234. Pfitzner E, Jähne R, Wissler M, Stoecklin E, Groner B. p300/CREB-binding protein enhances the prolactin-mediated transcriptional induction through direct interaction with the transactivation domain of Stat5, but does not participate in the Stat5-mediated suppression of the glucocorticoid response. Mol Endocrinol. 1998 Oct;12(10):1582–93.

235. Nakajima H, Brindle PK, Handa M, Ihle JN. Functional interaction of STAT5 and nuclear receptor co-repressor SMRT: implications in negative regulation of STAT5-dependent transcription. EMBO J. 2001 Dec 3;20(23):6836–44.

236. Yao Z, Cui Y, Watford WT, Bream JH, Yamaoka K, Hissong BD, et al. Stat5a/b are essential for normal lymphoid development and differentiation. Proc Natl Acad Sci USA. National Academy of Sciences; 2006 Jan 24;103(4):1000–5.

237. Moriggl R, Topham DJ, Teglund S, Sexl V, McKay C, Wang D, et al. Stat5 is required for IL-2-induced cell cycle progression of peripheral T cells. Immunity. 1999 Feb;10(2):249–59.

238. Burchill MA, Goetz CA, Prlic M, O'Neil JJ, Harmon IR, Bensinger SJ, et al. Distinct effects of STAT5 activation on CD4+ and CD8+ T cell homeostasis: development of CD4+CD25+ regulatory T cells versus CD8+ memory T cells. J Immunol. 2003 Dec 1;171(11):5853–64.

239. Zhu J, Cote-Sierra J, Guo L, Paul WE. Stat5 activation plays a critical role in Th2 differentiation. Immunity. 2003 Nov;19(5):739–48.

240. Tripathi P, Kurtulus S, Wojciechowski S, Sholl A, Hoebe K, Morris SC, et al. STAT5 is critical to maintain effector CD8+ T cell responses. J Immunol. American Association of Immunologists; 2010 Aug 15;185(4):2116–24.

241. Meinke A, Barahmand-Pour F, Wöhrl S, Stoiber D, Decker T. Activation of different Stat5 isoforms contributes to cell-type-restricted signaling in response to interferons. Mol Cell Biol. American Society for Microbiology (ASM); 1996 Dec;16(12):6937–44.

242. Rani A, Murphy JJ. STAT5 in Cancer and Immunity. J Interferon Cytokine Res. Mary Ann Liebert, Inc. 140 Huguenot Street, 3rd Floor New Rochelle, NY 10801 USA; 2016 Apr;36(4):226–37.

243. Ghanem S, Friedbichler K, Boudot C, Bourgeais J, Gouilleux-Gruart V, Régnier A, et al. STAT5A/5B-specific expansion and transformation of hematopoietic stem cells. Blood Cancer J. Nature Publishing Group; 2017 Jan 6;7(1):e514–4.

244. Lacronique V, Boureux A, Monni R, Dumon S, Mauchauffé M, Mayeux P, et al. Transforming properties of chimeric TEL-JAK proteins in Ba/F3 cells. Blood. 2000 Mar 15;95(6):2076–83.

245. Warsch W, Walz C, Sexl V. JAK of all trades: JAK2-STAT5 as novel therapeutic targets in BCR-ABL1+ chronic myeloid leukemia. Blood. 2013 Sep 26;122(13):2167–75.

246. Lai SY, Johnson FM. Defining the role of the JAK-STAT pathway in head and neck and thoracic malignancies: implications for future therapeutic approaches. Drug Resist Updat. 2010 Jun;13(3):67–78.

247. Gu L, Vogiatzi P, Puhr M, Dagvadorj A, Lutz J, Ryder A, et al. Stat5 promotes metastatic behavior of human prostate cancer cells in vitro and in vivo. Endocr Relat Cancer. Society for Endocrinology; 2010 Jun;17(2):481–93.

248. Koppikar P, Lui VWY, Man D, Xi S, Chai RL, Nelson E, et al. Constitutive activation of signal transducer and activator of transcription 5 contributes to tumor growth, epithelial-mesenchymal transition, and resistance to epidermal growth factor receptor targeting. Clin Cancer Res. 2008 Dec 1;14(23):7682–90.

249. Leek JP, Hamlin PJ, Bell SM, Lench NJ. Assignment of the STAT6 gene (STAT6) to human chromosome band 12q13 by in situ hybridization. Cytogenet Cell Genet. Karger Publishers; 1997;79(3-4):208–9.

250. Li J, Rodriguez JP, Niu F, Pu M, Wang J, Hung L-W, et al. Structural basis for DNA recognition by STAT6. Proc Natl Acad Sci USA. National Academy of Sciences; 2016 Nov 15;113(46):13015–20.

251. Schroder AJ, Pavlidis P, Arimura A, Capece D, Rothman PB. Cutting edge: STAT6 serves as a positive and negative regulator of gene expression in IL-4-stimulated B lymphocytes. J Immunol. 2002 Feb 1;168(3):996–1000.

252. Patel BK, Wang LM, Lee CC, Taylor WG, Pierce JH, LaRochelle WJ. Stat6 and Jak1 are common elements in platelet-derived growth factor and interleukin-4 signal transduction pathways in NIH 3T3 fibroblasts. J Biol Chem. 1996 Sep 6;271(36):22175–82.

253. Masuda A, Matsuguchi T, Yamaki K, Hayakawa T, Kubo M, LaRochelle WJ, et al. Interleukin-15 induces rapid tyrosine phosphorylation of STAT6 and the expression of interleukin-4 in mouse mast cells. J Biol Chem. 2000 Sep 22;275(38):29331–7.

254. Yang J, Aittomäki S, Pesu M, Carter K, Saarinen J, Kalkkinen N, et al. Identification of p100 as a coactivator for STAT6 that bridges STAT6 with RNA polymerase II. EMBO J. European Molecular Biology Organization; 2002 Sep 16;21(18):4950–8.

255. Mikita T, Kurama M, Schindler U. Synergistic activation of the germline epsilon promoter mediated by Stat6 and C/EBP beta. J Immunol. 1998 Aug 15;161(4):1822–8.

256. Zhu J, Guo L, Watson CJ, Hu-Li J, Paul WE. Stat6 is necessary and sufficient for IL-4's role in Th2 differentiation and cell expansion. J Immunol. 2001 Jun 15;166(12):7276–81.

257. Takeda K, Tanaka T, Shi W, Matsumoto M, Minami M, Kashiwamura S, et al. Essential role of Stat6 in IL-4 signalling. Nature. Nature Publishing Group; 1996 Apr 18;380(6575):627–30.

258. Chen H, Sun H, You F, Sun W, Zhou X, Chen L, et al. Activation of STAT6 by STING is critical for antiviral innate immunity. Cell. 2011 Oct 14;147(2):436–46.

259. Wang N, Tao L, Zhong H, Zhao S, Yu Y, Yu B, et al. miR-135b inhibits tumour metastasis in prostate cancer by targeting STAT6. Oncol Lett. 2016 Jan;11(1):543–50.

260. Yildiz M, Li H, Bernard D, Amin NA, Ouillette P, Jones S, et al. Activating STAT6 mutations in follicular lymphoma. Blood. 2015 Jan 22;125(4):668–79.

261. Bruns HA, Kaplan MH. The role of constitutively active Stat6 in leukemia and lymphoma. Crit Rev Oncol Hematol. 2006 Mar;57(3):245–53.

262. Chang YE, Laimins LA. Microarray analysis identifies interferon-inducible genes and Stat-1 as major transcriptional targets of human papillomavirus type 31. J Virol. American Society for Microbiology (ASM); 2000 May;74(9):4174–82.

263. Ma W, Tummers B, van Esch EMG, Goedemans R, Melief CJM, Meyers C, et al. Human Papillomavirus Downregulates the Expression of IFITM1 and RIPK3 to Escape from IFNγ- and TNFα-Mediated Antiproliferative Effects and Necroptosis. Front Immunol. 2016;7(5):496.

264. Hong S, Cheng S, Iovane A, Laimins LA. STAT-5 Regulates Transcription of the Topoisomerase IIβ-Binding Protein 1 (TopBP1) Gene To Activate the ATR Pathway and Promote Human Papillomavirus Replication. MBio. 2015 Dec 22;6(6):e02006–15.

265. Zhang W, Hong S, Maniar KP, Cheng S, Jie C, Rademaker AW, et al. KLF13 regulates the differentiation-dependent human papillomavirus life cycle in keratinocytes through STAT5 and IL-8. Oncogene. Nature Publishing Group; 2016 Oct 20;35(42):5565–75.

266. Liu L-B, Xie F, Chang K-K, Shang W-Q, Meng Y-H, Yu J-J, et al. Chemokine CCL17 induced by hypoxia promotes the proliferation of cervical cancer cell. Am J Cancer Res. e-Century Publishing Corporation; 2015;5(10):3072–84.

267. Valle-Mendiola A, Weiss-Steider B, Rocha-Zavaleta L, Soto-Cruz I. IL-2 enhances cervical cancer cells proliferation and JAK3/STAT5 phosphorylation at low doses, while at high doses IL-2 has opposite effects. Cancer Invest. Taylor & Francis; 2014 May;32(4):115–25.

268. Akira S, Nishio Y, Inoue M, Wang XJ, Wei S, Matsusaka T, et al. Molecular cloning of APRF, a novel IFN-stimulated gene factor 3 p91-related transcription factor involved in the gp130-mediated signaling pathway. Cell. 1994 Apr 8;77(1):63–71.

269. Ren Z, Mao X, Mertens C, Krishnaraj R, Qin J, Mandal PK, et al. Crystal structure of unphosphorylated STAT3 core fragment. Biochem Biophys Res Commun. 2008 Sep 12;374(1):1–5.

270. Shao H, Xu X, Jing N, Tweardy DJ. Unique structural determinants for Stat3 recruitment and activation by the granulocyte colony-stimulating factor receptor at phosphotyrosine ligands 704 and 744. J Immunol. 2006 Mar 1;176(5):2933–41.

271. Caldenhoven E, van Dijk TB, Solari R, Armstrong J, Raaijmakers JA, Lammers JW, et al. STAT3beta, a splice variant of transcription factor STAT3, is a dominant negative regulator of transcription. J Biol Chem. 1996 May 31;271(22):13221–7.

272. Bromberg JF, Wrzeszczynska MH, Devgan G, Zhao Y, Pestell RG, Albanese C, et al. Stat3 as an oncogene. Cell. 1999 Aug 6;98(3):295–303.

273. Takeda K, Noguchi K, Shi W, Tanaka T, Matsumoto M, Yoshida N, et al. Targeted disruption of the mouse Stat3 gene leads to early embryonic lethality. Proc Natl Acad Sci USA. National Academy of Sciences; 1997 Apr 15;94(8):3801–4.

274. Silver JS, Hunter CA. gp130 at the nexus of inflammation, autoimmunity, and cancer. J Leukoc Biol. 2010 Dec;88(6):1145–56.

275. Wegiel B, Bjartell A, Culig Z, Persson JL. Interleukin-6 activates PI3K/Akt pathway and regulates cyclin A1 to promote prostate cancer cell survival. Int J Cancer. Wiley-Blackwell; 2008 Apr 1;122(7):1521–9.

276. Robak T, Wierzbowska A, Błasińska-Morawiec M, Korycka A, Błoński JZ. Serum levels of IL-6 type cytokines and soluble IL-6 receptors in active B-cell chronic lymphocytic leukemia and in cladribine induced remission. Mediators Inflamm. Hindawi; 1999;8(6):277–86.

277. Jones SA, Horiuchi S, Topley N, Yamamoto N, Fuller GM. The soluble interleukin 6 receptor: mechanisms of production and implications in disease. FASEB J. Federation of American Societies for Experimental Biology; 2001 Jan;15(1):43–58.

278. Jostock T, Müllberg J, Ozbek S, Atreya R, Blinn G, Voltz N, et al. Soluble gp130 is the natural inhibitor of soluble interleukin-6 receptor transsignaling responses. Eur J Biochem. 2001 Jan;268(1):160–7.

279. Buchert M, Burns CJ, Ernst M. Targeting JAK kinase in solid tumors: emerging opportunities and challenges. Oncogene. Nature Publishing Group; 2016 Feb 25;35(8):939–51.

280. Carpenter RL, Lo H-W. STAT3 Target Genes Relevant to Human Cancers. Cancers (Basel). Multidisciplinary Digital Publishing Institute; 2014;6(2):897–925.

281. Liu L, McBride KM, Reich NC. STAT3 nuclear import is independent of tyrosine phosphorylation and mediated by importin-alpha3. Proc Natl Acad Sci USA. National Academy of Sciences; 2005 Jun 7;102(23):8150–5.

282. Yang J, Liao X, Agarwal MK, Barnes L, Auron PE, Stark GR. Unphosphorylated STAT3 accumulates in response to IL-6 and activates transcription by binding to NFkappaB. Genes Dev. Cold Spring Harbor Lab; 2007 Jun 1;21(11):1396–408.

283. Yu H, Pardoll D, Jove R. STATs in cancer inflammation and immunity: a leading role for STAT3. Nat Rev Cancer. 2009 Nov;9(11):798–809.

284. Coppo P, Dusanter-Fourt I, Millot G, Nogueira MM, Dugray A, Bonnet ML, et al. Constitutive and specific activation of STAT3 by BCR-ABL in embryonic stem cells. Oncogene. 2003 Jun 26;22(26):4102–10.

285. Mori R, Wauman J, Icardi L, Van der Heyden J, De Cauwer L, Peelman F, et al. TYK2-induced phosphorylation of Y640 suppresses STAT3 transcriptional activity. Sci Rep. Nature Publishing Group; 2017 Nov 21;7(1):15919.

286. Wen Z, Zhong Z, Darnell JE. Maximal activation of transcription by Stat1 and Stat3 requires both tyrosine and serine phosphorylation. Cell. 1995 Jul 28;82(2):241–50.

287. Lim CP, Cao X. Serine phosphorylation and negative regulation of Stat3 by JNK. J Biol Chem. 1999 Oct 22;274(43):31055–61.

288. Lee HK, Jung J, Lee SH, Seo S-Y, Suh DJ, Park HT. Extracellular Signal-regulated Kinase Activation Is Required for Serine 727 Phosphorylation of STAT3 in Schwann Cells in vitro and in vivo. Korean J Physiol Pharmacol. 2009 Jun;13(3):161–8.

289. Riebe C, Pries R, Schroeder KN, Wollenberg B. Phosphorylation of STAT3 in head and neck cancer requires p38 MAPKinase, whereas phosphorylation of STAT1 occurs via a different signaling pathway. Anticancer Res. 2011 Nov;31(11):3819–25.

290. Jain N, Zhang T, Kee WH, Li W, Cao X. Protein kinase C delta associates with and phosphorylates Stat3 in an interleukin-6-dependent manner. J Biol Chem. 1999 Aug 20;274(34):24392–400.

291. Aziz MH, Manoharan HT, Sand JM, Verma AK. Protein kinase Cepsilon interacts with Stat3 and regulates its activation that is essential for the development of skin cancer. Mol Carcinog. 2007 Aug;46(8):646–53.

292. Busch S, Renaud SJ, Schleussner E, Graham CH, Markert UR. mTOR mediates human trophoblast invasion through regulation of matrix-remodeling enzymes and is associated with serine phosphorylation of STAT3. Exp Cell Res. 2009 Jun 10;315(10):1724–33.

293. Lam E, Choi SH, Pareek TK, Kim B-G, Letterio JJ. Cyclin-dependent kinase 5 represses Foxp3 gene expression and Treg development through specific phosphorylation of Stat3 at Serine 727. Mol Immunol. 2015 Oct;67(2 Pt B):317–24.

294. Waitkus MS, Chandrasekharan UM, Willard B, Tee TL, Hsieh JK, Przybycin CG, et al. Signal integration and gene induction by a functionally distinct STAT3 phosphoform. Mol Cell Biol. 2014 May;34(10):1800–11.

295. Lee H, Zhang P, Herrmann A, Yang C, Xin H, Wang Z, et al. Acetylated STAT3 is crucial for methylation of tumor-suppressor gene promoters and inhibition by resveratrol results in demethylation. Proc Natl Acad Sci USA. 2012 May 15;109(20):7765–9.

296. Dasgupta M, Dermawan JKT, Willard B, Stark GR. STAT3-driven transcription depends upon the dimethylation of K49 by EZH2. Proc Natl Acad Sci USA. 2015 Mar 31;112(13):3985–90.

297. Ray S, Zhao Y, Jamaluddin M, Edeh CB, Lee C, Brasier AR. Inducible STAT3 NH2 terminal mono-ubiquitination promotes BRD4 complex formation to regulate apoptosis. Cell Signal. 2014 Jul;26(7):1445–55.

298. Nishanth G, Deckert M, Wex K, Massoumi R, Schweitzer K, Naumann M, et al. CYLD enhances severe listeriosis by impairing IL-6/STAT3-dependent fibrin production. DeLeo FR, editor. PLoS Pathog. Public Library of Science; 2013;9(6):e1003455.

299. Zhou Z, Wang M, Li J, Xiao M, Chin YE, Cheng J, et al. SUMOylation and SENP3 regulate STAT3 activation in head and neck cancer. Oncogene. Nature Publishing Group; 2016 Nov 10;35(45):5826–38.

300. Peyser ND, Du Y, Li H, Lui V, Xiao X, Chan TA, et al. Loss-of-Function PTPRD Mutations Lead to Increased STAT3 Activation and Sensitivity to STAT3 Inhibition in Head and Neck Cancer. Tao Q, editor. PLoS ONE. Public Library of Science; 2015;10(8):e0135750.

301. Porcu M, Kleppe M, Gianfelici V, Geerdens E, De Keersmaecker K, Tartaglia M, et al. Mutation of the receptor tyrosine phosphatase PTPRC (CD45) in T-cell acute lymphoblastic leukemia. Blood. American Society of Hematology; 2012 May 10;119(19):4476–9.

302. Li J-P, Yang C-Y, Chuang H-C, Lan J-L, Chen D-Y, Chen Y-M, et al. The phosphatase JKAP/DUSP22 inhibits T-cell receptor signalling and autoimmunity by inactivating Lck. Nat Commun. Nature Publishing Group; 2014 Apr 9;5(1):3618.

303. Zehender A, Huang J, Györfi A-H, Matei A-E, Trinh-Minh T, Xu X, et al. The tyrosine phosphatase SHP2 controls TGFβ-induced STAT3 signaling to regulate fibroblast activation and fibrosis. Nat Commun. Nature Publishing Group; 2018 Aug 14;9(1):3259.

304. Inagaki-Ohara K, Kondo T, Ito M, Yoshimura A. SOCS, inflammation, and cancer. JAKSTAT. 2013 Jul 1;2(3):e24053.

305. Dabir S, Kluge A, Dowlati A. The association and nuclear translocation of the PIAS3-STAT3 complex is ligand and time dependent. Mol Cancer Res. 2009 Nov;7(11):1854–60.

306. Tsuruma R, Ohbayashi N, Kamitani S, Ikeda O, Sato N, Muromoto R, et al. Physical and functional interactions between STAT3 and KAP1. Oncogene. Nature Publishing Group; 2008 May 8;27(21):3054–9.

307. Li Y, Zhang Z, Xiao Z, Lin Y, Luo T, Zhou Q, et al. Chemotherapy-mediated miR-29b expression inhibits the invasion and angiogenesis of cervical cancer. Oncotarget. Impact Journals; 2017 Jan 19;5(0).

308. Cheng Y, Li Y, Nian Y, Liu D, Dai F, Zhang J. STAT3 is involved in miR-124-mediated suppressive effects on esophageal cancer cells. BMC Cancer. BioMed Central; 2015 Apr 19;15(1):306.

309. Xue F, Liu Y, Zhang H, Wen Y, Yan L, Tang Q, et al. Let-7a enhances the sensitivity of hepatocellular carcinoma cells to cetuximab by regulating STAT3 expression. Onco Targets Ther. Dove Press; 2016;9:7253–61.

310. Patel K, Kollory A, Takashima A, Sarkar S, Faller DV, Ghosh SK. MicroRNA let-7 downregulates STAT3 phosphorylation in pancreatic cancer cells by increasing SOCS3 expression. Cancer Lett. 2014 May 28;347(1):54–64.

311. Rokavec M, Öner MG, Li H, Jackstadt R, Jiang L, Lodygin D, et al. IL-6R/STAT3/miR-34a feedback loop promotes EMT-mediated colorectal cancer invasion and metastasis. J Clin Invest. American Society for Clinical Investigation; 2014 Apr;124(4):1853–67.

312. Li F, Gu C, Tian F, Jia Z, Meng Z, Ding Y, et al. MiR-218 impedes IL-6-induced prostate cancer cell proliferation and invasion via suppression of LGR4 expression. Oncol Rep. Spandidos Publications; 2016 May;35(5):2859–65.

313. Wu W, Takanashi M, Borjigin N, Ohno S-I, Fujita K, Hoshino S, et al. MicroRNA-18a modulates STAT3 activity through negative regulation of PIAS3 during gastric adenocarcinogenesis. Br J Cancer. Nature Publishing Group; 2013 Feb 19;108(3):653–61.

314. Liu S, Sun X, Wang M, Hou Y, Zhan Y, Jiang Y, et al. A microRNA 221- and 222-mediated feedback loop maintains constitutive activation of NFκB and STAT3 in colorectal cancer cells. Gastroenterology. 2014 Oct;147(4):847–859.e11.

315. Sano S, Itami S, Takeda K, Tarutani M, Yamaguchi Y, Miura H, et al. Keratinocyte-specific ablation of Stat3 exhibits impaired skin remodeling, but does not affect skin morphogenesis. EMBO J. EMBO Press; 1999 Sep 1;18(17):4657–68.

316. Wang Y, Shen Y, Wang S, Shen Q, Zhou X. The role of STAT3 in leading the crosstalk between human cancers and the immune system. Cancer Lett. 2018 Feb 28;415:117–28.

317. Lee H, Pal SK, Reckamp K, Figlin RA, Yu H. STAT3: a target to enhance antitumor immune response. Curr Top Microbiol Immunol. Berlin, Heidelberg: Springer Berlin Heidelberg; 2011;344(Chapter 51):41–59.

318. Mogensen TH. STAT3 and the Hyper-IgE syndrome: Clinical presentation, genetic origin, pathogenesis, novel findings and remaining uncertainties. JAKSTAT. 2013 Apr 1;2(2):e23435.

319. Xu L, Ji J-J, Le W, Xu YS, Dou D, Pan J, et al. The STAT3 HIES mutation is a gain-of-function mutation that activates genes via AGG-element carrying promoters. Nucleic Acids Res. 2015 Oct 15;43(18):8898–912.

320. Purvis HA, Anderson AE, Young DA, Isaacs JD, Hilkens CMU. A negative feedback loop mediated by STAT3 limits human Th17 responses. J Immunol. American Association of Immunologists; 2014 Aug 1;193(3):1142–50.

321. Flanagan SE, Haapaniemi E, Russell MA, Caswell R, Allen HL, De Franco E, et al. Activating germline mutations in STAT3 cause early-onset multi-organ autoimmune disease. Nat Genet. 2014 Aug;46(8):812–4.

322. Hedrich CM, Bream JH. Cell type-specific regulation of IL-10 expression in inflammation and disease. Immunol Res. Humana Press Inc; 2010 Jul;47(1-3):185–206.

323. Hösel M, Quasdorff M, Ringelhan M, Kashkar H, Debey-Pascher S, Sprinzl MF, et al. Hepatitis B Virus Activates Signal Transducer and Activator of Transcription 3 Supporting Hepatocyte Survival and Virus Replication. Cell Mol Gastroenterol Hepatol. 2017 Nov;4(3):339–63.

324. Lee YH, Yun Y. HBx protein of hepatitis B virus activates Jak1-STAT signaling. J Biol Chem. 1998 Sep 25;273(39):25510–5.

325. Wang Y, Lu Y, Toh ST, Sung W-K, Tan P, Chow P, et al. Lethal-7 is down-regulated by the hepatitis B virus x protein and targets signal transducer and activator of transcription 3. J Hepatol. 2010 Jul;53(1):57–66.

326. Yuan K, Lei Y, Chen H-N, Chen Y, Zhang T, Li K, et al. HBV-induced ROS accumulation promotes hepatocarcinogenesis through Snail-mediated epigenetic silencing of SOCS3. Cell Death Differ. Nature Publishing Group; 2016 Apr;23(4):616–27.

327. Yoshida T, Hanada T, Tokuhisa T, Kosai K-I, Sata M, Kohara M, et al. Activation of STAT3 by the hepatitis C virus core protein leads to cellular transformation. J Exp Med. The Rockefeller University Press; 2002 Sep 2;196(5):641–53.

328. Sarcar B, Ghosh AK, Steele R, Ray R, Ray RB. Hepatitis C virus NS5A mediated STAT3 activation requires co-operation of Jak1 kinase. Virology. 2004 Apr 25;322(1):51–60.

329. Lepiller Q, Abbas W, Kumar A, Tripathy MK, Herbein G. HCMV activates the IL-6-JAK-STAT3 axis in HepG2 cells and primary human hepatocytes. Mossman KL, editor. PLoS ONE. 2013;8(3):e59591.

330. Slinger E, Maussang D, Schreiber A, Siderius M, Rahbar A, Fraile-Ramos A, et al. HCMV-encoded chemokine receptor US28 mediates proliferative signaling through the IL-6-STAT3 axis. Sci Signal. 2010 Aug 3;3(133):ra58–8.

331. Kung C-P, Meckes DG, Raab-Traub N. Epstein-Barr virus LMP1 activates EGFR, STAT3, and ERK through effects on PKCdelta. J Virol. American Society for Microbiology; 2011 May;85(9):4399–408.

332. Koganti S, Clark C, Zhi J, Li X, Chen EI, Chakrabortty S, et al. Cellular STAT3 functions via PCBP2 to restrain Epstein-Barr Virus lytic activation in B lymphocytes. Longnecker RM, editor. J Virol. American Society for Microbiology; 2015 May;89(9):5002–11.

333. Punjabi AS, Carroll PA, Chen L, Lagunoff M. Persistent activation of STAT3 by latent Kaposi's sarcoma-associated herpesvirus infection of endothelial cells. J Virol. 2007 Mar;81(5):2449–58.

334. King CA, Li X, Barbachano-Guerrero A, Bhaduri-McIntosh S. STAT3 Regulates Lytic Activation of Kaposi's Sarcoma-Associated Herpesvirus. Longnecker RM, editor. J Virol. American Society for Microbiology; 2015 Nov;89(22):11347–55.

335. Wu J, Xu Y, Mo D, Huang P, Sun R, Huang L, et al. Kaposi's sarcoma-associated herpesvirus (KSHV) vIL-6 promotes cell proliferation and migration by upregulating DNMT1 via STAT3 activation. Gao S-J, editor. PLoS ONE. Public Library of Science; 2014;9(3):e93478.

336. Reitsma JM, Sato H, Nevels M, Terhune SS, Paulus C. Human cytomegalovirus IE1 protein disrupts interleukin-6 signaling by sequestering STAT3 in the nucleus. J Virol. 5 ed. 2013 Oct;87(19):10763–76.

337. Ramalingam D, Ziegelbauer JM. Viral microRNAs Target a Gene Network, Inhibit STAT Activation, and Suppress Interferon Responses. Sci Rep. Nature Publishing Group; 2017 Jan 19;7(1):40813.

338. Hui KPY, Li HS, Cheung MC, Chan RWY, Yuen KM, Mok CKP, et al. Highly pathogenic avian influenza H5N1 virus delays apoptotic responses via activation of STAT3. Sci Rep. Nature Publishing Group; 2016 Jun 27;6(1):28593.

339. Jia D, Rahbar R, Chan RWY, Lee SMY, Chan MCW, Wang BX, et al. Influenza virus non-structural protein 1 (NS1) disrupts interferon signaling. Zhang L, editor. PLoS ONE. 2010 Nov 10;5(11):e13927.

340. Ulane CM, Rodriguez JJ, Parisien J-P, Horvath CM. STAT3 ubiquitylation and degradation by mumps virus suppress cytokine and oncogene signaling. J Virol. American Society for Microbiology (ASM); 2003 Jun;77(11):6385–93.

341. Frank DA. STAT3 as a central mediator of neoplastic cellular transformation. Cancer Lett. 2007 Jun 28;251(2):199–210.

342. Hazan-Halevy I, Harris D, Liu Z, Liu J, Li P, Chen X, et al. STAT3 is constitutively phosphorylated on serine 727 residues, binds DNA, and activates transcription in CLL cells. Blood. 2010 Apr 8;115(14):2852–63.

343. Ding BB, Yu JJ, Yu RY-L, Mendez LM, Shaknovich R, Zhang Y, et al. Constitutively activated STAT3 promotes cell proliferation and survival in the activated B-cell subtype of diffuse large B-cell lymphomas. Blood. 2008 Feb 1;111(3):1515–23.

344. Bhardwaj A, Sethi G, Vadhan-Raj S, Bueso-Ramos C, Takada Y, Gaur U, et al. Resveratrol inhibits proliferation, induces apoptosis, and overcomes chemoresistance through down-regulation of STAT3 and nuclear factor-kappaB-regulated antiapoptotic and cell survival gene products in human multiple myeloma cells. Blood. American Society of Hematology; 2007 Mar 15;109(6):2293–302.

345. Tsujita Y, Horiguchi A, Tasaki S, Isono M, Asano T, Ito K, et al. STAT3 inhibition by WP1066 suppresses the growth and invasiveness of bladder cancer cells. Oncol Rep. Spandidos Publications; 2017 Oct;38(4):2197–204.

346. Cui Y, Li Y-Y, Li J, Zhang H-Y, Wang F, Bai X, et al. STAT3 regulates hypoxia-induced epithelial mesenchymal transition in oesophageal squamous cell cancer. Oncol Rep. Spandidos Publications; 2016 Jul;36(1):108–16.

347. Corcoran RB, Contino G, Deshpande V, Tzatsos A, Conrad C, Benes CH, et al. STAT3 plays a critical role in KRAS-induced pancreatic tumorigenesis. Cancer Res. American Association for Cancer Research; 2011 Jul 15;71(14):5020–9.

348. Macha MA, Matta A, Kaur J, Chauhan SS, Thakar A, Shukla NK, et al. Prognostic significance of nuclear pSTAT3 in oral cancer. Sturgis EM, editor. Head Neck. Wiley-Blackwell; 2011 Apr;33(4):482–9.

349. Kusaba T, Nakayama T, Yamazumi K, Yakata Y, Yoshizaki A, Inoue K, et al. Activation of STAT3 is a marker of poor prognosis in human colorectal cancer. Oncol Rep. 2006 Jun;15(6):1445–51.

350. Wong ALA, Hirpara JL, Pervaiz S, Eu J-Q, Sethi G, Goh B-C. Do STAT3 inhibitors have potential in the future for cancer therapy? Expert Opin Investig Drugs. Taylor & Francis; 2017 Aug;26(8):883–7.

351. Alao JP. The regulation of cyclin D1 degradation: roles in cancer development and the potential for therapeutic invention. Mol Cancer. BioMed Central; 2007 Apr 2;6(1):24.

352. Tanaka T, Narazaki M, Kishimoto T. IL-6 in inflammation, immunity, and disease. Cold Spring Harb Perspect Biol. 2014 Sep 4;6(10):a016295–5.

353. Jerez A, Clemente MJ, Makishima H, Koskela H, Leblanc F, Peng Ng K, et al. STAT3 mutations unify the pathogenesis of chronic lymphoproliferative disorders of NK cells and T-cell large granular lymphocyte leukemia. Blood. American Society of Hematology; 2012 Oct 11;120(15):3048–57.

354. Koskela HLM, Eldfors S, Ellonen P, van Adrichem AJ, Kuusanmäki H, Andersson EI, et al. Somatic STAT3 mutations in large granular lymphocytic leukemia. N Engl J Med. Massachusetts Medical Society; 2012 May 17;366(20):1905–13.

355. Gao J, Zhao S, Halstensen TS. Increased interleukin-6 expression is associated with poor prognosis and acquired cisplatin resistance in head and neck squamous cell carcinoma. Oncol Rep. Spandidos Publications; 2016 Jun;35(6):3265–74.

356. Sanguinete MMM, Oliveira PHD, Martins-Filho A, Micheli DC, Tavares-Murta BM, Murta EFC, et al. Serum IL-6 and IL-8 Correlate with Prognostic Factors in Ovarian Cancer. Immunol Invest. Taylor & Francis; 2017 Oct;46(7):677–88.

357. Kamińska K, Czarnecka AM, Escudier B, Lian F, Szczylik C. Interleukin-6 as an emerging regulator of renal cell cancer. Urol Oncol. 2015 Nov;33(11):476–85.

358. Sullivan NJ, Sasser AK, Axel AE, Vesuna F, Raman V, Ramirez N, et al. Interleukin-6 induces an epithelial-mesenchymal transition phenotype in human breast cancer cells. Oncogene. Nature Publishing Group; 2009 Aug 20;28(33):2940–7.

359. Yadav A, Kumar B, Datta J, Teknos TN, Kumar P. IL-6 promotes head and neck tumor metastasis by inducing epithelial-mesenchymal transition via the JAK-STAT3-SNAIL signaling pathway. Mol Cancer Res. 2011 Dec;9(12):1658–67.

360. Sommer J, Effenberger T, Volpi E, Waetzig GH, Bernhardt M, Suthaus J, et al. Constitutively active mutant gp130 receptor protein from inflammatory hepatocellular adenoma is inhibited by an anti-gp130 antibody that specifically neutralizes interleukin 11 signaling. J Biol Chem. American Society for Biochemistry and Molecular Biology; 2012 Apr 20;287(17):13743–51.

361. Fishman D, Faulds G, Jeffery R, Mohamed-Ali V, Yudkin JS, Humphries S, et al. The effect of novel polymorphisms in the interleukin-6 (IL-6) gene on IL-6 transcription and plasma IL-6 levels, and an association with systemic-onset juvenile chronic arthritis. J Clin Invest. American Society for Clinical Investigation; 1998 Oct 1;102(7):1369–76.

362. Oku S, Takenaka K, Kuriyama T, Shide K, Kumano T, Kikushige Y, et al. JAK2 V617F uses distinct signalling pathways to induce cell proliferation and neutrophil activation. Br J Haematol. Wiley/Blackwell (10.1111); 2010 Aug;150(3):334–44.

363. Steeghs EMP, Jerchel IS, de Goffau-Nobel W, Hoogkamer AQ, Boer JM, Boeree A, et al. JAK2 aberrations in childhood B-cell precursor acute lymphoblastic leukemia. Oncotarget. 2017 Oct 27;8(52):89923–38.

364. Liu KG, Verma A, Derman O, Kornblum N, Janakiram M, Braunschweig I, et al. JAK2 V617F mutation, multiple hematologic and non-hematologic processes: an association? Biomark Res. 4 ed. BioMed Central; 2016;4(1):19.

365. Abdelhamed S, Ogura K, Yokoyama S, Saiki I, Hayakawa Y. AKT-STAT3 Pathway as a Downstream Target of EGFR Signaling to Regulate PD-L1 Expression on NSCLC cells. J Cancer. 2016;7(12):1579–86.

366. Li Y, Deuring J, Peppelenbosch MP, Kuipers EJ, de Haar C, van der Woude CJ. IL-6-induced DNMT1 activity mediates SOCS3 promoter hypermethylation in ulcerative colitis-related colorectal cancer. Carcinogenesis. 2012 Oct;33(10):1889–96.

367. Huang L, Hu B, Ni J, Wu J, Jiang W, Chen C, et al. Transcriptional repression of SOCS3 mediated by IL-6/STAT3 signaling via DNMT1 promotes pancreatic cancer growth and metastasis. J Exp Clin Cancer Res. BioMed Central; 2016 Feb 4;35(1):27.

368. Lorenz U. SHP-1 and SHP-2 in T cells: two phosphatases functioning at many levels. Immunol Rev. Wiley/Blackwell (10.1111); 2009 Mar;228(1):342–59.

369. Shukla S, Shishodia G, Mahata S, Hedau S, Pandey A, Bhambhani S, et al. Aberrant expression and constitutive activation of STAT3 in cervical carcinogenesis: implications in high-risk human papillomavirus infection. Mol Cancer. BioMed Central; 2010;9(1):282.

370. Shukla S, Mahata S, Shishodia G, Pandey A, Tyagi A, Vishnoi K, et al. Functional regulatory role of STAT3 in HPV16-mediated cervical carcinogenesis. Williams BO, editor. PLoS ONE. Public Library of Science; 2013;8(7):e67849.

371. Sun S, Steinberg BM. PTEN is a negative regulator of STAT3 activation in human papillomavirus-infected cells. J Gen Virol. Microbiology Society; 2002 Jul;83(Pt 7):1651–8.

372. Orecchia V, Regis G, Tassone B, Valenti C, Avalle L, Saoncella S, et al. Constitutive STAT3 activation in epidermal keratinocytes enhances cell clonogenicity and favours spontaneous immortalization by opposing differentiation and senescence checkpoints. Exp Dermatol. 2015 Jan;24(1):29–34.

373. Macdonald A, Crowder K, Street A, McCormick C, Harris M. The hepatitis C virus NS5A protein binds to members of the Src family of tyrosine kinases and regulates kinase activity. J Gen Virol. Microbiology Society; 2004 Mar;85(Pt 3):721–9.

374. Kitamura T, Feng Y, Kitamura YI, Chua SC, Xu AW, Barsh GS, et al. Forkhead protein FoxO1 mediates Agrp-dependent effects of leptin on food intake. Nat Med. 2006 May;12(5):534–40.

375. Moody CA, Laimins LA. Human papillomavirus oncoproteins: pathways to transformation. Nat Rev Cancer. 2010 Aug;10(8):550–60.

376. Straight SW, Hinkle PM, Jewers RJ, McCance DJ. The E5 oncoprotein of human papillomavirus type 16 transforms fibroblasts and effects the downregulation of the epidermal growth factor receptor in keratinocytes. J Virol. American Society for Microbiology (ASM); 1993 Aug;67(8):4521–32.

377. Shin M-K, Sage J, Lambert PF. Inactivating all three rb family pocket proteins is insufficient to initiate cervical cancer. Cancer Res. American Association for Cancer Research; 2012 Oct 15;72(20):5418–27.

378. Knight GL, Pugh AG, Yates E, Bell I, Wilson R, Moody CA, et al. A cyclin-binding motif in human papillomavirus type 18 (HPV18) E1^E4 is necessary for association with CDK-cyclin complexes and G2/M cell cycle arrest of keratinocytes, but is not required for differentiation-dependent viral genome amplification or L1 capsid protein expression. Virology. 2011 Mar 30;412(1):196–210.

379. Kho E-Y, Wang H-K, Banerjee NS, Broker TR, Chow LT. HPV-18 E6 mutants reveal p53 modulation of viral DNA amplification in organotypic cultures. Proc Natl Acad Sci USA. 2013 May 7;110(19):7542–9.

380. Huibregtse JM, Scheffner M, Howley PM. E6-AP directs the HPV E6-dependent inactivation of p53 and is representative of a family of structurally and functionally related proteins. Cold Spring Harb Symp Quant Biol. 1994;59:237–45.

381. Delury CP, Marsh EK, James CD, Boon SS, Banks L, Knight GL, et al. The role of protein kinase A regulation of the E6 PDZ-binding domain during the differentiation-dependent life cycle of human papillomavirus type 18. J Virol. American Society for Microbiology; 2013 Sep;87(17):9463–72.

382. Quintás-Cardama A, Vaddi K, Liu P, Manshouri T, Li J, Scherle PA, et al. Preclinical characterization of the selective JAK1/2 inhibitor INCB018424: therapeutic implications for the treatment of myeloproliferative neoplasms. Blood. American Society of Hematology; 2010 Apr 15;115(15):3109–17.

383. Wernig G, Kharas MG, Okabe R, Moore SA, Leeman DS, Cullen DE, et al. Efficacy of TG101348, a selective JAK2 inhibitor, in treatment of a murine model of JAK2V617F-induced polycythemia vera. Cancer Cell. 2008 Apr;13(4):311–20.

384. Gazel A, Banno T, Walsh R, Blumenberg M. Inhibition of JNK promotes differentiation of epidermal keratinocytes. J Biol Chem. 2006 Jul 21;281(29):20530–41.

385. Damjanov N, Kauffman RS, Spencer-Green GT. Efficacy, pharmacodynamics, and safety of VX-702, a novel p38 MAPK inhibitor, in rheumatoid arthritis: results of two randomized, double-blind, placebo-controlled clinical studies. Arthritis Rheum. 2009 May;60(5):1232–41.

386. Dümmler BA, Hauge C, Silber J, Yntema HG, Kruse LS, Kofoed B, et al. Functional characterization of human RSK4, a new 90-kDa ribosomal S6 kinase, reveals constitutive activation in most cell types. J Biol Chem. 2005 Apr 8;280(14):13304–14.

387. Zhang T, Inesta-Vaquera F, Niepel M, Zhang J, Ficarro SB, Machleidt T, et al. Discovery of potent and selective covalent inhibitors of JNK. Chem Biol. 2012 Jan 27;19(1):140–54.

388. Naqvi S, Macdonald A, McCoy CE, Darragh J, Reith AD, Arthur JSC. Characterization of the cellular action of the MSK inhibitor SB-747651A. Biochem J. Portland Press Limited; 2012 Jan 1;441(1):347–57.

389. Wen Z, Darnell JE. Mapping of Stat3 serine phosphorylation to a single residue (727) and evidence that serine phosphorylation has no influence on DNA binding of Stat1 and Stat3. Nucleic Acids Res. Oxford University Press; 1997 Jun 1;25(11):2062–7.

390. Mohr A, Fahrenkamp D, Rinis N, Müller-Newen G. Dominant-negative activity of the STAT3-Y705F mutant depends on the N-terminal domain. Cell Commun Signal. BioMed Central; 2013;11(1):83.

391. Miyoshi K, Takaishi M, Nakajima K, Ikeda M, Kanda T, Tarutani M, et al. Stat3 as a therapeutic target for the treatment of psoriasis: a clinical feasibility study with STA-21, a Stat3 inhibitor. J Invest Dermatol. 2011 Jan;131(1):108–17.

392. Chow LT, Duffy AA, Wang H-K, Broker TR. A highly efficient system to produce infectious human papillomavirus: Elucidation of natural virus-host interactions. Cell Cycle. Taylor & Francis; 2009 May 1;8(9):1319–23.

393. Jeon S, Lambert PF. Integration of human papillomavirus type 16 DNA into the human genome leads to increased stability of E6 and E7 mRNAs: implications for cervical carcinogenesis. Proc Natl Acad Sci USA. National Academy of Sciences; 1995 Feb 28;92(5):1654–8.

394. Koganti S, Hui-Yuen J, McAllister S, Gardner B, Grasser F, Palendira U, et al. STAT3 interrupts ATR-Chk1 signaling to allow oncovirus-mediated cell proliferation. Proc Natl Acad Sci USA. 2014 Apr 1;111(13):4946–51.

395. Chuerduangphui J, Pientong C, Chaiyarit P, Patarapadungkit N, Chotiyano A, Kongyingyoes B, et al. Effect of human papillomavirus 16 oncoproteins on oncostatin M upregulation in oral squamous cell carcinoma. Med Oncol. Springer US; 2016 Aug;33(8):83.

396. Ren C, Cheng X, Lu B, Yang G. Activation of interleukin-6/signal transducer and activator of transcription 3 by human papillomavirus early proteins 6 induces fibroblast senescence to promote cervical tumourigenesis through autocrine and paracrine pathways in tumour microenvironment. Eur J Cancer. Elsevier; 2013 Dec;49(18):3889–99.

397. Satsuka A, Mehta K, Laimins L. p38MAPK and MK2 pathways are important for the differentiation-dependent human papillomavirus life cycle. Imperiale MJ, editor. J Virol. American Society for Microbiology Journals; 2015 Feb;89(3):1919–24.

398. Arbyn M, Castellsagué X, de Sanjosé S, Bruni L, Saraiya M, Bray F, et al. Worldwide burden of cervical cancer in 2008. Ann Oncol. 2011 Dec;22(12):2675–86.

399. Ajila V, Shetty H, Babu S, Shetty V, Hegde S. Human Papilloma Virus Associated Squamous Cell Carcinoma of the Head and Neck. J Sex Transm Dis. Hindawi; 2015;2015(3):791024–5.

400. Bello JOM, Nieva LO, Paredes AC, Gonzalez AMF, Zavaleta LR, Lizano M. Regulation of the Wnt/β-Catenin Signaling Pathway by Human Papillomavirus E6 and E7 Oncoproteins. Viruses. Multidisciplinary Digital Publishing Institute; 2015 Aug 19;7(8):4734–55.

401. Hu T, Li C. Convergence between Wnt-β-catenin and EGFR signaling in cancer. Mol Cancer. BioMed Central; 2010 Sep 9;9(1):236.

402. He C, Mao D, Hua G, Lv X, Chen X, Angeletti PC, et al. The Hippo/YAP pathway interacts with EGFR signaling and HPV oncoproteins to regulate cervical cancer progression. EMBO Mol Med. EMBO Press; 2015 Nov;7(11):1426–49.

403. Banerjee NS, Wang H-K, Broker TR, Chow LT. Human papillomavirus (HPV) E7 induces prolonged G2 following S phase reentry in differentiated human keratinocytes. J Biol Chem. 2011 Apr 29;286(17):15473–82.

404. Moody CA, Laimins LA. Human papillomaviruses activate the ATM DNA damage pathway for viral genome amplification upon differentiation. Galloway D, editor. PLoS Pathog. Public Library of Science; 2009 Oct;5(10):e1000605.

405. Yu H, Jove R. The STATs of cancer--new molecular targets come of age. Nat Rev Cancer. Nature Publishing Group; 2004 Feb;4(2):97–105.

406. Schindler C, Darnell JE. Transcriptional responses to polypeptide ligands: the JAK-STAT pathway. Annu Rev Biochem. 1995;64(1):621–51.

407. Hunter CA, Jones SA. IL-6 as a keystone cytokine in health and disease. Nat Immunol. 2015 May;16(5):448–57.

408. Shair KHY, Bendt KM, Edwards RH, Bedford EC, Nielsen JN, Raab-Traub N. EBV latent membrane protein 1 activates Akt, NFkappaB, and Stat3 in B cell lymphomas. PLoS Pathog. Public Library of Science; 2007 Nov;3(11):e166.

409. Morgan EL, Wasson CW, Hanson L, Kealy D, Pentland I, McGuire V, et al. STAT3 activation by E6 is essential for the differentiation-dependent HPV18 life cycle. Galloway DA, editor. PLoS Pathog. 2018 Apr;14(4):e1006975.

410. Mauer J, Denson JL, Brüning JC. Versatile functions for IL-6 in metabolism and cancer. Trends Immunol. 2015 Feb;36(2):92–101.

411. Hinz M, Scheidereit C. The IκB kinase complex in NF-κB regulation and beyond. EMBO Rep. 2014 Jan;15(1):46–61.

412. Chen M, Sun F, Han L, Qu Z. Kaposi's sarcoma herpesvirus (KSHV) microRNA K12-1 functions as an oncogene by activating NF-κB/IL-6/STAT3 signaling. Oncotarget. Impact Journals; 2016 May 7;7(22):33363–73.

413. James MA, Lee JH, Klingelhutz AJ. Human papillomavirus type 16 E6 activates NF-kappaB, induces cIAP-2 expression, and protects against apoptosis in a PDZ binding motif-dependent manner. J Virol. 2006 Jun;80(11):5301–7.

414. Nees M, Geoghegan JM, Hyman T, Frank S, Miller L, Woodworth CD. Papillomavirus type 16 oncogenes downregulate expression of interferon-responsive genes and upregulate proliferation-associated and NF-kappaB-responsive genes in cervical keratinocytes. J Virol. 2001 May;75(9):4283–96.

415. Jost PJ, Ruland J. Aberrant NF-kappaB signaling in lymphoma: mechanisms, consequences, and therapeutic implications. Blood. American Society of Hematology; 2007 Apr 1;109(7):2700–7.

416. Cheng Y-W, Lee H, Shiau M-Y, Wu T-C, Huang T-T, Chang Y-H. Human papillomavirus type 16/18 up-regulates the expression of interleukin-6 and antiapoptotic Mcl-1 in non-small cell lung cancer. Clin Cancer Res. 2008 Aug 1;14(15):4705–12.

417. Wu D-W, Tsai L-H, Chen P-M, Lee M-C, Wang L, Chen C-Y, et al. Loss of TIMP-3 promotes tumor invasion via elevated IL-6 production and predicts poor survival and relapse in HPV-infected non-small cell lung cancer. Am J Pathol. 2012 Nov;181(5):1796–806.

418. Hayden MS, Ghosh S. NF-κB, the first quarter-century: remarkable progress and outstanding questions. Genes Dev. 2012 Feb 1;26(3):203–34.

419. Kroll M, Margottin F, Kohl A, Renard P, Durand H, Concordet JP, et al. Inducible degradation of IkappaBalpha by the proteasome requires interaction with the F-box protein h-betaTrCP. J Biol Chem. 1999 Mar 19;274(12):7941–5.

420. Liu Y, Fuchs J, Li C, Lin J. IL-6, a risk factor for hepatocellular carcinoma: FLLL32 inhibits IL-6-induced STAT3 phosphorylation in human hepatocellular cancer cells. Cell Cycle. Taylor & Francis; 2010 Sep 1;9(17):3423–7.

421. Rojas A, Liu G, Coleman I, Nelson PS, Zhang M, Dash R, et al. IL-6 promotes prostate tumorigenesis and progression through autocrine cross-activation of IGF-IR. Oncogene. Nature Publishing Group; 2011 May 19;30(20):2345–55.

422. Voorzanger N, Touitou R, Garcia E, Delecluse HJ, Rousset F, Joab I, et al. Interleukin (IL)-10 and IL-6 are produced in vivo by non-Hodgkin's lymphoma cells and act as cooperative growth factors. Cancer Res. 1996 Dec 1;56(23):5499–505.

423. Ogawa H, Koyanagi-Aoi M, Otani K, Zen Y, Maniwa Y, Aoi T. Interleukin-6 blockade attenuates lung cancer tissue construction integrated by cancer stem cells. Sci Rep. Nature Publishing Group; 2017 Sep 26;7(1):12317.

424. Sriuranpong V, Park JI, Amornphimoltham P, Patel V, Nelkin BD, Gutkind JS. Epidermal growth factor receptor-independent constitutive activation of STAT3 in head and neck squamous cell carcinoma is mediated by the autocrine/paracrine stimulation of the interleukin 6/gp130 cytokine system. Cancer Res. 2003 Jun 1;63(11):2948–56.

425. Scotto L, Narayan G, Nandula SV, Arias-Pulido H, Subramaniyam S, Schneider A, et al. Identification of copy number gain and overexpressed genes on chromosome arm 20q by an integrative genomic approach in cervical cancer: potential role in progression. Genes Chromosomes Cancer. Wiley-Blackwell; 2008 Sep;47(9):755–65.

426. Fisher DT, Appenheimer MM, Evans SS. The two faces of IL-6 in the tumor microenvironment. Semin Immunol. 2014 Feb;26(1):38–47.

427. Stanam A, Love-Homan L, Joseph TS, Espinosa-Cotton M, Simons AL. Upregulated interleukin-6 expression contributes to erlotinib resistance in head and neck squamous cell carcinoma. Mol Oncol. 2015 Aug;9(7):1371–83.

428. Wei L-H, Kuo M-L, Chen C-A, Chou C-H, Lai K-B, Lee C-N, et al. Interleukin-6 promotes cervical tumor growth by VEGF-dependent angiogenesis via a STAT3 pathway. Oncogene. Nature Publishing Group; 2003 Mar 13;22(10):1517–27.

429. Song Z, Lin Y, Ye X, Feng C, Lu Y, Yang G, et al. Expression of IL-1α and IL-6 is Associated with Progression and Prognosis of Human Cervical Cancer. Med Sci Monit. International Scientific Information, Inc; 2016 Nov 20;22:4475–81.

430. Walch-Rückheim B, Mavrova R, Henning M, Vicinus B, Kim Y-J, Bohle RM, et al. Stromal Fibroblasts Induce CCL20 through IL6/C/EBPβ to Support the Recruitment of Th17 Cells during Cervical Cancer Progression. Cancer Res. American Association for Cancer Research; 2015 Dec 15;75(24):5248–59.

431. Li H, Lu Y, Pang Y, Li M, Cheng X, Chen J. Propofol enhances the cisplatin-induced apoptosis on cervical cancer cells via EGFR/JAK2/STAT3 pathway. Biomed Pharmacother. 2017 Feb;86:324–33.

432. Janakiram NB, Rao CV. The role of inflammation in colon cancer. Adv Exp Med Biol. Basel: Springer Basel; 2014;816(Chapter 2):25–52.

433. Polk DB, Peek RM. Helicobacter pylori: gastric cancer and beyond. Nat Rev Cancer. Nature Publishing Group; 2010 Jun;10(6):403–14.

434. Kremsdorf D, Soussan P, Paterlini-Brechot P, Brechot C. Hepatitis B virus-related hepatocellular carcinoma: paradigms for viral-related human carcinogenesis. Oncogene. 2006 Jun 26;25(27):3823–33.

435. Pecic V, Stankovic-Djordjevic D, Nestorovic M, Radojkovic M, Marjanovic H, Ilic B, et al. Hepatitis C virus-related hepatocellular carcinoma and liver cirrhosis. J BUON. 2011 Apr;16(2):277–81.

436. Fernandes JV, DE Medeiros Fernandes TAA, DE Azevedo JCV, Cobucci RNO, DE Carvalho MGF, Andrade VS, et al. Link between chronic inflammation and human papillomavirus-induced carcinogenesis (Review). Oncol Lett. 2015 Mar;9(3):1015–26.

437. Castle PE, Hillier SL, Rabe LK, Hildesheim A, Herrero R, Bratti MC, et al. An association of cervical inflammation with high-grade cervical neoplasia in women

infected with oncogenic human papillomavirus (HPV). Cancer Epidemiol Biomarkers Prev. 2001 Oct;10(10):1021–7.

438. Subbaramaiah K, Dannenberg AJ. Cyclooxygenase-2 transcription is regulated by human papillomavirus 16 E6 and E7 oncoproteins: evidence of a corepressor/coactivator exchange. Cancer Res. 2007 Apr 15;67(8):3976–85.

439. Vandermark ER, Deluca KA, Gardner CR, Marker DF, Schreiner CN, Strickland DA, et al. Human papillomavirus type 16 E6 and E 7 proteins alter NF-kB in cultured cervical epithelial cells and inhibition of NF-kB promotes cell growth and immortalization. Virology. 2012 Mar 30;425(1):53–60.

440. Grivennikov SI, Karin M. Dangerous liaisons: STAT3 and NF-kappaB collaboration and crosstalk in cancer. Cytokine Growth Factor Rev. 2010 Feb;21(1):11–9.

441. Hoentjen F, Sartor RB, Ozaki M, Jobin C. STAT3 regulates NF-kappaB recruitment to the IL-12p40 promoter in dendritic cells. Blood. American Society of Hematology; 2005 Jan 15;105(2):689–96.

442. McFarland BC, Hong SW, Rajbhandari R, Twitty GB, Gray GK, Yu H, et al. NF-κB-induced IL-6 ensures STAT3 activation and tumor aggressiveness in glioblastoma. Castro MG, editor. PLoS ONE. Public Library of Science; 2013;8(11):e78728.

443. Candelaria M, Garcia-Arias A, Cetina L, Dueñas-Gonzalez A. Radiosensitizers in cervical cancer. Cisplatin and beyond. Radiat Oncol. BioMed Central; 2006 May 8;1(1):15.

444. Zhu H, Luo H, Zhang W, Shen Z, Hu X, Zhu X. Molecular mechanisms of cisplatin resistance in cervical cancer. Drug Des Devel Ther. Dove Press; 2016;10:1885–95.

445. Dorayappan KDP, Wanner R, Wallbillich JJ, Saini U, Zingarelli R, Suarez AA, et al. Hypoxia-induced exosomes contribute to a more aggressive and chemoresistant

ovarian cancer phenotype: a novel mechanism linking STAT3/Rab proteins. Oncogene. Nature Publishing Group; 2018 Jul;37(28):3806–21.

446. Sun S, Wu Y, Guo W, Yu F, Kong L, Ren Y, et al. STAT3/HOTAIR Signaling Axis Regulates HNSCC Growth in an EZH2-dependent Manner. Clin Cancer Res. 2018 Jun 1;24(11):2665–77.

447. Schutte B, Nuydens R, Geerts H, Ramaekers F. Annexin V binding assay as a tool to measure apoptosis in differentiated neuronal cells. J Neurosci Methods. 1998 Dec 31;86(1):63–9.

448. Elmore S. Apoptosis: a review of programmed cell death. Toxicol Pathol. 6 ed. SAGE Publications; 2007 Jun;35(4):495–516.

449. Xie Y, Li J, Zhang C. STAT3 promotes the proliferation and migration of hepatocellular carcinoma cells by regulating AKT2. Oncol Lett. Spandidos Publications; 2018 Mar;15(3):3333–8.

450. Wang Y, Wu C, Zhang C, Li Z, Zhu T, Chen J, et al. TGF-β-induced STAT3 overexpression promotes human head and neck squamous cell carcinoma invasion and metastasis through malat1/miR-30a interactions. Cancer Lett. 2018 Nov 1;436:52–62.

451. Wendt MK, Balanis N, Carlin CR, Schiemann WP. STAT3 and epithelial-mesenchymal transitions in carcinomas. JAKSTAT. 2014 Jan 1;3(1):e28975.

452. Gheldof A, Berx G. Cadherins and epithelial-to-mesenchymal transition. Prog Mol Biol Transl Sci. Elsevier; 2013;116:317–36.

453. Senft C, Priester M, Polacin M, Schröder K, Seifert V, Kögel D, et al. Inhibition of the JAK-2/STAT3 signaling pathway impedes the migratory and invasive potential of human glioblastoma cells. J Neurooncol. 2011 Feb;101(3):393–403.

454. Jäkel H, Weinl C, Hengst L. Phosphorylation of p27Kip1 by JAK2 directly links cytokine receptor signaling to cell cycle control. Oncogene. 2011 Aug 11;30(32):3502–12.

455. Sayyah J, Sayeski PP. Jak2 inhibitors: rationale and role as therapeutic agents in hematologic malignancies. Curr Oncol Rep. NIH Public Access; 2009 Mar;11(2):117–24.

456. Shin D-S, Kim H-N, Shin KD, Yoon YJ, Kim S-J, Han DC, et al. Cryptotanshinone inhibits constitutive signal transducer and activator of transcription 3 function through blocking the dimerization in DU145 prostate cancer cells. Cancer Res. 2009 Jan 1;69(1):193–202.

457. Siddiquee K, Zhang S, Guida WC, Blaskovich MA, Greedy B, Lawrence HR, et al. Selective chemical probe inhibitor of Stat3, identified through structure-based virtual screening, induces antitumor activity. Proc Natl Acad Sci USA. 2007 May 1;104(18):7391–6.

458. Niu G, Wright KL, Ma Y, Wright GM, Huang M, Irby R, et al. Role of Stat3 in regulating p53 expression and function. Mol Cell Biol. 2005 Sep;25(17):7432–40.

459. Hanahan D, Weinberg RA. Hallmarks of cancer: the next generation. Cell. 2011 Mar 4;144(5):646–74.

460. Kumari R, Kohli S, Das S. p53 regulation upon genotoxic stress: intricacies and complexities. Mol Cell Oncol. Taylor & Francis; 2014 Jul;1(3):e969653.

461. Lamouille S, Xu J, Derynck R. Molecular mechanisms of epithelial-mesenchymal transition. Nat Rev Mol Cell Biol. Nature Publishing Group; 2014 Mar;15(3):178–96.

462. Miao J-W, Liu L-J, Huang J. Interleukin-6-induced epithelial-mesenchymal transition through signal transducer and activator of transcription 3 in human cervical carcinoma. Int J Oncol. Spandidos Publications; 2014 Jul;45(1):165–76.

463. Prestipino A, Emhardt AJ, Aumann K, O'Sullivan D, Gorantla SP, Duquesne S, et al. Oncogenic JAK2V617F causes PD-L1 expression, mediating immune escape in myeloproliferative neoplasms. Sci Transl Med. 2018 Feb 21;10(429):eaam7729.

464. Thomas SJ, Snowden JA, Zeidler MP, Danson SJ. The role of JAK/STAT signalling in the pathogenesis, prognosis and treatment of solid tumours. Br J Cancer. Nature Publishing Group; 2015 Jul 28;113(3):365–71.

465. Anacker DC, Moody CA. Modulation of the DNA damage response during the life cycle of human papillomaviruses. Virus Res. 2017 Mar 2;231:41–9.

466. Hong S, Dutta A, Laimins LA. The acetyltransferase Tip60 is a critical regulator of the differentiation-dependent amplification of human papillomaviruses. Imperiale MJ, editor. J Virol. 2015 Apr;89(8):4668–75.

467. Haan C, Kreis S, Margue C, Behrmann I. Jaks and cytokine receptors--an intimate relationship. Biochem Pharmacol. 2006 Nov 30;72(11):1538–46.

468. Shan Y, He X, Song W, Han D, Niu J, Wang J. Role of IL-6 in the invasiveness and prognosis of glioma. Int J Clin Exp Med. e-Century Publishing Corporation; 2015;8(6):9114–20.

469. Yagil Z, Nechushtan H, Kay G, Yang CM, Kemeny DM, Razin E. The enigma of the role of protein inhibitor of activated STAT3 (PIAS3) in the immune response. Trends Immunol. 2010 May;31(5):199–204.

470. Motiwala T, Jacob ST. Role of protein tyrosine phosphatases in cancer. Prog Nucleic Acid Res Mol Biol. Elsevier; 2006;81:297–329.

471. Nabhani S, Schipp C, Miskin H, Levin C, Postovsky S, Dujovny T, et al. STAT3 gain-of-function mutations associated with autoimmune lymphoproliferative syndrome like disease deregulate lymphocyte apoptosis and can be targeted by BH3 mimetic compounds. Clin Immunol. 2017 Aug;181:32–42.

472. Lorenzini T, Dotta L, Giacomelli M, Vairo D, Badolato R. STAT mutations as program switchers: turning primary immunodeficiencies into autoimmune diseases. J Leukoc Biol. 2017 Jan;101(1):29–38.

473. Walker S, Wang C, Walradt T, Hong BS, Tanner JR, Levinsohn JL, et al. Identification of a gain-of-function STAT3 mutation (p.Y640F) in lymphocytic variant hypereosinophilic syndrome. Blood. American Society of Hematology; 2016 Feb 18;127(7):948–51.

474. Grivennikov S, Karin M. Autocrine IL-6 signaling: a key event in tumorigenesis? Cancer Cell. 2008 Jan;13(1):7–9.

475. Luo Y, Zheng SG. Hall of Fame among Pro-inflammatory Cytokines: Interleukin-6 Gene and Its Transcriptional Regulation Mechanisms. Front Immunol. 2016;7(Pt 2):604.

476. Massoumi R. CYLD: a deubiquitination enzyme with multiple roles in cancer. Future Oncol. Future Medicine Ltd London, UK; 2011 Feb;7(2):285–97.

477. Hymowitz SG, Wertz IE. A20: from ubiquitin editing to tumour suppression. Nat Rev Cancer. Nature Publishing Group; 2010 May;10(5):332–41.

478. Sanches JGP, Xu Y, Yabasin IB, Li M, Lu Y, Xiu X, et al. miR-501 is upregulated in cervical cancer and promotes cell proliferation, migration and invasion by targeting CYLD. Chem Biol Interact. 2018 Apr 1;285:85–95.

479. Hendrayani S-F, Al-Harbi B, Al-Ansari MM, Silva G, Aboussekhra A. The inflammatory/cancer-related IL-6/STAT3/NF-κB positive feedback loop includes AUF1 and maintains the active state of breast myofibroblasts. Oncotarget. 2016 Jul 5;7(27):41974–85.

480. Qi Q, Ling Y, Zhu M, Zhou L, Wan M, Bao Y, et al. Promoter region methylation and loss of protein expression of PTEN and significance in cervical cancer. Biomed Rep. Spandidos Publications; 2014 Sep;2(5):653–8.

481. Contreras-Paredes A, la Cruz-Hernández De E, Martínez-Ramírez I, Dueñas-Gonzalez A, Lizano M. E6 variants of human papillomavirus 18 differentially modulate the protein kinase B/phosphatidylinositol 3-kinase (akt/PI3K) signaling pathway. Virology. 2009 Jan 5;383(1):78–85.

482. Yu J-Q, Zhou Q, Zheng Y-F, Bao Y. Expression of Vimentin and Ki-67 Proteins in Cervical Squamous Cell Carcinoma and their Relationships with Clinicopathological Features. Asian Pac J Cancer Prev. 2015;16(10):4271–5.

483. Zhao W, Zhou Y, Xu H, Cheng Y, Kong B. Snail family proteins in cervical squamous carcinoma: expression and significance. Clin Invest Med. 2013 Aug 1;36(4):E223–33.

484. Furumoto Y, Gadina M. The arrival of JAK inhibitors: advancing the treatment of immune and hematologic disorders. BioDrugs. Springer International Publishing; 2013 Oct;27(5):431–8.

Appendix

Table 1. Plasmids used in this study.

Plasmid Name	Plasmid Backbone	Expression Type	Source
pEGFP-c1	pEGFP-c1	Transient	Addgene
pEGFP-18E5	pEGFP-c1	Transient	Cloned by David Kealy, Macdonald lab
pEGFP-18E6	pEGFP-c1	Transient	
pEGFP-18E7	pEGFP-c1	Transient	
pEGFP-18E6ΔPDZ	pEGFP-c1	Transient	
pEGFP-18E6(F4V)	pEGFP-c1	Transient	
pEGFP-18E6(L52A)	pEGFP-c1	Transient	Genewiz®
β-casein luciferase reporter	pLucDSS	Transient	Lab of Kalle Saksela (University of Helsinki)
Pro-opiomelanocortin (Pom^C) luciferase reports	pGL3	Transient	Addgene
pcDNA3.1	pcDNA3.1	Transient	Addgene
pcDNA3-IκBα (S32/36A)	pcDNA3.1	Transient	Lab of Ronald T Hey (University of Dundee)
pRc/CMV	pRc/CMV	Transient	Addgene
pRc/CMV-STAT3 S727A	pRc/CMV	Transient	Addgene
pcFugW	pcFugW	Lentiviral	Addgene
pcFugW-EF.STAT3DN.Ubc.GFP	pcFugW	Lentiviral	Addgene
pCMV-VSV.G	pCMV	Lentiviral	Lab of Greg Towers (University College London (UCL))
pUMVC3-gag-pol	pUMVC	Lentiviral	

Table 2. Primer sequences used in this study for quantitative, reverse transcription PCR (qRT-PCR).

Gene Name	Forward Primer	Reverse Primer
VIM	GTTTCCCCTAAACCGCTAGG	AGCGAGAGTGGCAGAGGA
ZEB1	GCACCTGAAGAGGACCAGAG	TGCATCTGGTGTTCCATTTT
CDKN1A	CGGTCCTCTGAGCCTGTAAG	GGATCTACATGCGACGACAA
TPJ1		
CDH1	GCCGAGAGCTACACGTTCA	GACCGGTGCAATCTTCAAA
BCL2L1	GATTGCGGTACAGTGTAACTGGGAAG	CCCGAAACCGGGCTATCTGCTCG
CDH2		
U6	CTCGCTTCGGCAGCACA	AACGCTTCACGCATTTGC
CCND1	CCGCTGGCCATGAACTACCT	ACGAAGGTCTGCGCGTGTT
HIF1A	TGCATCTCCATCTTCTACCCAAGT	CCGACTGTGAGTGCCACTGT
BIRC5	TCCACTGCCCCACTGAGAAC	TGGCTCCCAGCCTTCCA
HPV18 *E6*	TGGCGCGCTTTGAGGA	TGTTCAGTTCCGTGCACAGAT
HPV18 *E7*	GACCTAAGGCAACATTGCA	GCTCGTGACATAGAAGGTCAA
IL6	GGCACTGGCAGAAAACAACC	GCAAGTCTCCTCATTGAATCC
IL10	GGCATGCACAGCTCAGCACTG	GTTTCGTATCTTCATTGTCATG
IL11	GACATGAACTGTGTTTGCCGC	CAGCCGAGTCTTCAGCAGCAG
IL17	CGCTGATGGGAACGTGGACTAC	GGTGGACAATCGGGGTGACA
LIF	CATAATGAAGGTCTTCGCGG	GAAGGCCTGGGCCAACACG
OSM	AGTACCGCGTGCTCCTTG	CCCTGCAGTGCTCTCTCAGT
SNAI1	TCGGAAGCCTAACTACAGCGA	AGATGAGCATTGGCAGCGAG
SNAI2	TGTTGCAGTGAGGGCAAGAA	GACCCTGGTTGCTTCAAGGA

Table 3. Primary and secondary antibodies used in this study for western blot (WB) and immunofluorescent analysis (IF).

Antibody Target	Manufacturer	Antibody Type	Antibody Use (dilution)
STAT3	CST (#9139)	Mouse mAb	WB (1:1000); IF (1:400)
pSTAT3 (Y705)	CST (#9131)	Mouse mAb	WB (1:1000)
pSTAT3 (S727)	Abcam (ab32143)	Mouse mAb	WB (1:1000); IF (1:400)
Involucrin	SCBT (sc-21748)	Mouse mAb	WB (1:500); IF (1:250)
Filaggrin	Abcam (ab81468)	Rabbit pAb	WB (1:1000)
HPV18 E7	Abcam (ab100953)	Mouse mAb	WB (1:1000)
HPV18 E6	SCBT (sc-365089)	Mouse mAb	WB (1:1000)
HPV16 E7	SCBT (sc-6981)	Mouse mAb	WB (1:500)
HPV16/18 E6	Abcam (ab70)	Mouse mAb	WB (1:500)
HPV18 E1^E4	Provided by Dr Sally Roberts (University of Birmingham)	Mouse mAb	IF (1:100)
GAPDH	SCBT (sc-365063)	Mouse mAb	WB (1:5000)
GFP	SCBT (sc-9996)	Mouse mAb	WB (1:2000)
p53	SCBT (sc-126)	Mouse mAB	WB (1:1000)
p21	CST (#2947)	Rabbit mAb	WB (1:1000)
Bcl xL	CST (#2764)	Rabbit mAb	WB (1:1000)
Cyclin D1	Abcam (ab134175)	Rabbit mAb	WB (1:1000)
Cyclin B1	SCBT (sc-594)	Rabbit pAb	IF (1:400)
FLAG	Sigma (F3165)	Mouse mAb	WB (1:1000)

Antibody Target	Manufacturer	Antibody Type	Antibody Use (dilution)
IL-6	Abcam (Ab6672)	Rabbit pAb	WB (1:1000), Neutralisation (1:250)
gp130	R&D Systems (MAB628)	Mouse mAb	Neutralisation (1:500)
pJAK2 (Y1007/Y1008)	CST (#3776)	Rabbit mAb	WB (1:500)
JAK2	CST (#3230)	Rabbit mAb	WB (1:1000)
pERK1/2 (T202/Y204)	CST (#43705)	Rabbit mAb	WB (1:1000)
ERK1/2	CST (#9102)	Rabbit mAb	WB (1:2000)
p-p38 (T180/Y182	CST (#9211)	Rabbit mAb	WB (1:1000)
p38	CST (#8690)	Rabbit mAb	WB (1:1000)
pJNK1/2 (T183/Y185)	CST (#4668)	Rabbit mAb	WB (1:1000)
JNK1/2	CST (#9252)	Rabbit mAb	WB (1:1000)
p-cJun (S73)	CST (#3270)	Rabbit mAb	WB (1:1000)
pMSK1 (T581)	CST (#9595)	Rabbit mAb	WB (1:1000)
pMK2 (T334)	CST (#3041)	Rabbit mAb	WB (1:1000)
p-p65 (S536)	CST (#3036)	Rabbit mAb	WB (1:1000)
p65	CST (#8242)	Rabbit mAb	WB (1:1000)
PARP-1	CST (#9542)	Rabbit mAb	WB (1:1000)

Snail	CST (#3879)	Rabbit mAb	WB (1:1000)
Slug	CST (#9585)	Rabbit mAb	WB (1:1000)
Vimentin	CST (#5741)	Rabbit mAb	WB (1:1000); IF (1:400)
ZEB-1	CST (#3396)	Rabbit pAb	WB (1:1000)
ZO-1	CST (#8193)	Rabbit mAb	WB (1:1000)
E-cadherin	CST (#3195)	Rabbit mAb	Flow cytometry (1:200)
α-mouse secondary	Sigma (A4416)	Goat pAb	WV (1:5000)
α-rabbit secondary	Sigma (A6154)	Goat pAb	WV (1:5000)

Table 4. Mammalian primary cells and cell lines used in this study.

Cells	Source	Cell Characteristics
Normal human keratinocytes (NHK)	Lab of Dr Sally Roberts (University of Birmingham)	Primary keratinocyte cell from human foreskin
3T3 J2 fibroblasts	Lab of Dr Sally Roberts (University of Birmingham)	Immortalised mouse fibroblasts used as feeder cells for NHKs
C33A	ATCC®	Epithelial cells, derived from cervical cancer biopsies; HPV-
DoTc2-4510	ATCC®	Epithelial cells, derived from cervical carcinoma; HPV-
SiHa	ATCC®	Epithelial cells of cervical SCC, reported to contain integrated HPV16 genomes (~1 - 2 copies per cell)
CaSki	ATCC®	Cervical epithelial cells from metastatic site: small intestine; epidermoid carcinoma, reported to contain integrated HPV16 (~600 copies per cell) as well as sequences related to HPV18
SW756	ATCC®	Epithelial cells, derived from cervical squamous cell carcinoma; HPV18+
HeLa	ATCC®	Epithelial cells from cervical adenocarcinoma, have been reported to contain HPV18 sequences
HEK293TT	Lab of Mathew Reeves (UCL)	Epithelial kidney cells expressing the transforming gene of adenovirus 5 and a SV40 Large T expression cassette